Fishery Bulletin 105(4) Contents

Click on page numbers to go to PDF version of article.

Articles

447–456
Katakura, Seiji, Hisatoshi Ikeda, Akira Nishimura, Tsuneo Nishiyama, and Yasunori Sakurai
An allometric smoothing function to describe the relation between otolith and somatic growth over the lifespan of walleye pollock (*Theragra chalcogramma*)

457–469
Able, Kenneth W., Peter J. Clarke, R. Christopher Chambers, and David A. Witting
Transitions in the morphological features, habitat use, and diet of young-of-the-year goosefish (*Lophius americanus*)

470–484
Stewart, Ian J.
Defining plausible migration rates based on historical tagging data: a Bayesian mark-recapture model applied to English sole (*Parophrys vetulus*)

485–492
Magel, Christopher, Kirstin Wakefield, Nancy Targett, and Richard Brill
Activity in the pallial nerve of knobbed (*Busycon carica*) and channeled (*Busycotypus canaliculatum*) whelks recorded during exposure of the osphradium to odorant solutions

493–508
Eveson, J. Paige, Tom Polacheck, and Geoff M. Laslett
Incorporating fishery observer data into an integrated catch-atage and multiyear tagging model for estimating mortality rates and abundance

509–526
Barlow, Jay, and Karin A. Forney
Abundance and population density of cetaceans in the California Current ecosystem

527–537
Tupper, Mark H.
Spillover of commercially valuable reef fishes from marine protected areas in Guam, Micronesia

538–547
Klibansky, Nikolai, and Francis Juanes
Species-specific effects of four preservative treatments on oocytes and ovarian material of Atlantic cod (*Gadus morhua*), haddock (*Melanogrammus aeglefinus*), and American plaice (*Hippoglossoides platessoides*)

548–559
Miller, Todd W., and Richard D. Brodeur

Diets of and trophic relationships among dominant marine nekton within the northern California Current ecosystem

Companion article and note

560–570
Lauth, Robert R, Jared Guthridge, Dan Nichol, Scott W. McEntire, and Nicola Hillgruber
Timing and duration of mating and brooding periods of Atka mackerel (*Pleurogrammus monopterygius*) in the North Pacific Ocean

571–576
Lauth, Robert R., and Deborah M. Blood
Description of embryonic development of Atka mackerel (*Pleurogrammus monopterygius*)

Notes

577–581
Kimura, Daniel K.
Using the empirical Bayes method to estimate and evaluate bycatch rates of seabirds from individual fishing vessels

582–587
DeVries, Douglas A.
No evidence of bias from fish behavior in the selectivity of size and sex of the protogynous red porgy (Pagrus pagrus, Sparidae) by hook-and-line gear

588
Acknowledgment of reviewers

590
List of titles

593
List of authors

595
Subject index

598
Guidelines for authors

Subscription form

U.S. Department of Commerce

Carlos M. Gutierrez
Secretary

National Oceanic and Atmospheric Administration

Vice Admiral
Conrad C. Lautenbacher Jr., USN (ret.)
Under Secretary for
Oceans and Atmosphere

National Marine Fisheries Service

William T. Hogarth
Assistant Administrator
for Fisheries

Scientific Editor
Adam Moles, Ph.D.

Associate Editor
Elizabeth Siddon

Ted Stevens Marine Research Institute
Auke Bay Laboratories
Alaska Fisheries Science Center
17109 Pt. Lena Loop Road
Juneau, Alaska 99801

Managing Editor
Sharyn Matriotti

National Marine Fisheries Service
Scientific Publications Office
7600 Sand Point Way NE, BIN C1570
Seattle, Washington 98115-0070

Editorial Committee

Jeffrey M. Leis	Australian Museum,
Thomas Shirley	Texas A&M Universit
David Somerton	National Marine Fish
Mark Terceiro	National Marine Fish

Abstract—We propose a new equation to describe the relation between otolith length (OL) and somatic length (fork length [FL]) of fish for the entire lifespan of the fish. The equation was developed by applying a mathematical smoothing method based on an allometric equation with a constant term for walleye pollock (*Theragra chalcogramma*)—a species that shows an extended longevity (>20 years). The most appropriate equation for defining the relation between OL and FL was a four-phase allometric smoothing function with three inflection points. The inflection points correspond to the timing of settlement of walleye pollock, changes in sexual maturity, and direction of otolith growth. Allometric smoothing functions describing the relation between short otolith radius and FL, long otolith radius and FL, and FL and body weight were also developed. The proposed allometric smoothing functions cover the entire lifespan of walleye pollock. We term these equations "allometric smoothing functions for otolith and somatic growth over the lifespan of walleye pollock."

An allometric smoothing function to describe the relation between otolith and somatic growth over the lifespan of walleye pollock (*Theragra chalcogramma*)

Seiji Katakura (contact author)[1]
Hisatoshi Ikeda[2]
Akira Nishimura[1]
Tsuneo Nishiyama[3]
Yasunori Sakurai[2]

Email address for S. Katakura: seijika@fra.affrc.go.jp

[1] Hokkaido National Fisheries Research Institute
116, Katsurakoi, Kushiro
Hokkaido 085-0802, Japan

[2] Graduate School of Fisheries Sciences
Hokkaido University, 3-1-1, Minato-cho, Hakodate
Hokkaido 041-8611, Japan

[3] Department of Marine Sciences and Technology
Hokkaido Tokai University, 5-1-1-1, Minamisawa, Minami-ku
Sapporo, Hokkaido 005-8601, Japan

The power function $y = ax^b$, used as an allometric equation (Huxley, 1924), is a useful tool for growth analysis of organisms. Equations that describe the relation between fish otolith length (OL: distance between the tip of rostrum and tip of postrostrum) and somatic length (e.g., fork length; FL: distance between the tip of head and fork of tail fin) have been widely used in fishery biology and ecological studies to estimate somatic length at younger ages with back-calculation methods. These methods are based on linear equations, log-transformed allometric equations, and quadratic equations (reviewed by Francis, 1990). However, these previous equations do not adequately reflect the complex changes in growth over the lifetime of a fish, especially for long-lived species.

Walleye pollock (*Theragra chalcogramma* (Pallas)) is the most abundant fish in the Bering Sea, constitutes the majority of the commercial catches from this area (Wespestad, 1993), and is a long-lived species. The oldest recorded age for this species is 28 years (McFarlane and Beamish, 1990). Juvenile walleye pollock serve as a substantial prey source for older walleye pollock, other fish species, marine mammals, and sea birds. Thus, the year-class strength and population dynamics of walleye pollock have a significant influence on the entire ecosystem (Springer, 1992; Hunt et al., 2002). Estimations of somatic length and growth analyses at particular ages or life stages are imperative for fishery biology and ecological studies of walleye pollock.

In studies of the growth of walleye pollock, the equation that describes the relation between OL and somatic length (i.e., fork length) (referred to as the "OL-FL equation" in this article) is required in order to reconstruct the size of walleye pollock from otoliths collected from the stomachs of predators. Frost and Lowry (1981) applied two linear equations, with an inflection point at 10 mm OL, corresponding to 220 mm FL, in a total size range of 60–570 mm FL. Nishimura and Yamada (1988) applied the log-transformed allometric equation of the three linear equations with log-transformed OL and total length (TL: distance between the tip of head and tip of tail fin; 4.6–

Manuscript submitted 21 August 2006 to the Scientific Editor's Office.

Manuscript approved for publication 30 March 2007 by the Scientific Editor.

Fish. Bull. 105:447–456 (2007).

680 mm) to data for three stages: larval stage (4.6–14.0 mm TL), juvenile stage (11–96 mm TL), and young-adult stage (88–680 mm TL). Zeppelin et al. (2004) adapted a quadratic equation for a fish size range of 49–530 mm FL. These previous equations allowed researchers to characterize the growth patterns of walleye pollock by regression analysis (the least-squares method), but they have several shortcomings because somatic length is not estimated across the whole life span of the fish. First, the equations, each of which represents a different life stage, do not facilitate comprehension of the continuity of each life stage. The equations are fitted to each segment of the data separately by inflection points that are derived from empirical data or visually from the scatter plots. Second, the quadratic equation has limitation in the shape of its curve which does not show the inflection point. The complex growth patterns are not adequately reflected in the equation. Third, the least-squares method does not allow for the incorporation of increasing variance with increasing fish length. When the sample distribution is biased, the calculated equation is largely influenced by the range of fish lengths from the largest number of samples. Fourth, previous OL-FL equations were not considered objectively in the selection of an adequate equation. No attempt has been made to apply information criteria such as Akaike's information criterion (AIC: Akaike, 1974), which is an operational way of trading off the complexity of an estimated equation against how well the equation fits the data.

To overcome these problems, we developed a new OL–FL equation for the whole lifespan of walleye pollock using a proposed allometric smoothing function to describe the relation between OL and FL. We also derived three distinctive allometric smoothing functions to establish the relationships between the short otolith radius (SOR: from core to the tip of rostrum) and FL, between the long otolith radius (LOR: from core to the tip of postrostrum) and FL, and between the FL and body weight (BW: wet body weight).

Materials and methods

General equations

The general equations in this analysis are linear equations (Eqs. 1 and 2), an allometric equation (Eq. 3), and an allometric equation with a constant term (Eq. 4):

$$y = ax \tag{1}$$

$$y = ax + c \tag{2}$$

$$y = ax^b \tag{3}$$

$$y = ax^b + c \tag{4}$$

where x = the independent variable;
y = the dependent variable; and
a, b, and c = parameters.

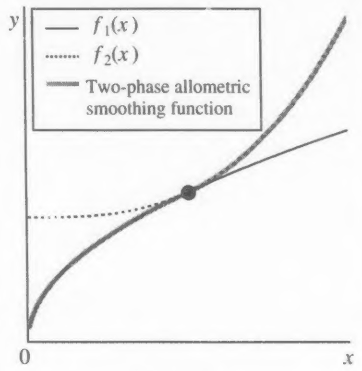

Figure 1

A two-phase allometric smoothing function connected smoothly from $f_1(x)$ to $f_2(x)$ at the inflection point (●) where there is a common tangent between $f_1(x)$ and $f_2(x)$. The coordinate (x, y) of the inflection point is $(q_1, f_1(q_1) = f_2(q_1))$.

Allometric smoothing function

A new OL-FL equation was developed by using a mathematical smoothing method based on an allometric equation with a constant term. The assumption of the allometric smoothing function was to have a common tangent at the inflection point to reflect the variable allometric growth smoothly. A composite of two or more allometric smoothing functions was defined as follows:

$$\delta_i(x) = \begin{cases} 1 & (q_{i-1} \le x \le q_i) \\ 0 & (x < q_{i-1}, q_i < x) \end{cases} \tag{5}$$

$$f_i(x) = \delta_i(x)(a_i x^{b_i} + c_i),$$

where $\delta_i(x)$ = switch function;
q_i = a value of x on the inflection point, here $q_0 = 0$;
$f_i(x)$ = a number i of function; and
a_i, b_i, and c_i = parameters for the function of i.

$f_i(x)$ is validated between the inflection points ($q_{i-1} \le x \le q_i$) which depend on the $\delta_i(x)$.

We assumed that for the smooth integration of $f_i(x)$ and $f_{i+1}(x)$ (the function on the next order of i), both functions must pass through the inflection point $(x, y) = (q_i, f_i(q_i) = f_{i+1}(q_i))$ and have a common tangent at this point (Fig. 1). To satisfy the above conditions, the following two equations must be equal.

$$f_i(q_i) = f_{i+1}(q_i) \tag{6}$$

Table 1

The size ranges (in terms of length and weight) of walleye pollock (*Theragra chalcogramma*) examined in the Bering Sea during 1983–2002 to describe the relation between x (the independent variable) and y (the dependent variable). OL = otolith length; FL = fork length; SOR = short otolith radius; LOR = long otolith radius; and BW = body weight.

The variables (x [left below] and y [right below])	Range of x		Range of y		Number of samples (n)
	Minimum	Maximum	Minimum	Maximum	
OL (mm) and FL (mm)	2.27×10^{-2}	25.98	4.56	803	2354
SOR (mm) and FL (mm)	9.22×10^{-3}	11.80	4.56	803	1752
LOR (mm) and FL (mm)	1.22×10^{-2}	14.50	4.56	803	1704
FL (mm) and BW (g)	35.88	803	0.24	3014	2891

$$f_i'(q_i)=f_{i+1}'(q_i). \tag{7}$$

When Equation 5 is substituted for Equations 6 and 7, the following equations are obtained:

$$a_iq_i^{b_i}+c_i=a_{i+1}q_i^{b_{i+1}}+c_{i+1} \tag{8}$$

$$a_ib_iq_i^{b_i-1}=a_{i+1}b_{i+1}q_i^{b_{i+1}-1}. \tag{9}$$

Solving Equations 8 and 9 simultaneously yields

$$a_{i+1}=\frac{a_ib_i}{b_{i+1}}\,q_i^{b_i-b_{i+1}} \tag{10}$$

$$c_{i+1}=a_iq_i^{b_i}\left(1-\frac{b_i}{b_{i+1}}\right)+c_i. \tag{11}$$

The functions of $f_i(x)$ and $f_{i+1}(x)$ can be smoothly connected at the inflection point if Equations 10 and 11 are equal. The formula of the allometric smoothing function y is shown as follows:

$$y=\sum_{i=1}^{n}f_i(x)=\sum_{i=1}^{n}\delta_i(x)(a_ix^{b_i}+c_i). \tag{12}$$

Fitting the OL-FL equations

The allometric smoothing function (Eq. 12) is fitted by using the maximum likelihood method. In the fitting, the sample distribution around the dependent variable was assumed to have a normal distribution. The estimated standard deviation (SD) for the dependent variable was used to calculate the weighted likelihood. The fitting procedure is shown as follows (see Appendix Table):

$$\hat{FL}=f_i(OL_j)=a_iOL_j^{b_i}+c_i+\varepsilon_j \qquad (q_{i-1}\le OL_j\le q_i), \tag{13}$$

where $\hat{FL}_j$ = the calculated FL for individual j;
OL_j = the measured OL of individual j; and
ε_j = the error for individual j.

Equation 13 is validated between the inflection points ($q_{i-1}\le OL_j\le q_i$).

The distribution of ε_j is assumed to have a normal distribution N (mean, variance) = $N\ (0, \hat{\sigma}_{FL_j}^2)$:

$$\hat{\sigma}_{FL_j}=dOL_j^e+f, \tag{14}$$

where $\hat{\sigma}_{FL_j}$ = the estimated SD of the FL of individual j; and
d, e, and f = parameters.

The variable $\hat{\sigma}_{FL_j}$ is assumed to fit the general equations (Eqs. 3 or 4).

To fit $\hat{FL}_j$ to the general equations (Eqs. 1–3), the following procedures are used. For Equation 1, the parameters in Equation 13 are fixed as $b_i = 1$ and $c_i = 0$; for Equation 2, the parameter is fixed as $b_i = 1$; and for Equation 3, the parameter is fixed as $c_i = 0$.

A likelihood of measured FL is calculated by the following equations:

$$L_j=\frac{1}{\sqrt{2\pi}\hat{\sigma}_{FL_j}}\exp\left\{-\frac{(FL_j-\hat{FL}_j)^2}{2\hat{\sigma}_{FL_j}^2}\right\} \tag{15}$$

and

$$LL=\sum_{j=1}^{n}\ln L_j, \tag{16}$$

where L_j = likelihood (the probability density) of FL_j;
FL_j = the measured FL of individual j; and
LL = a log-likelihood.

LL is maximized by changing the parameters.

Determination of the OL-FL equations

The equation with the minimum AIC was selected:

$$AIC = -2MLL + 2p \tag{17}$$

where MLL = the maximum LL and
p = the number of parameters.

In the composite of two or more functions, a_i and c_i of $i \geq 2$ are calculated by Equations 10 and 11. Therefore, these parameters are not included in the number of parameters needed to calculate the AIC (see Appendix Table).

The upper and lower 95% confidence intervals (CI_j) of $\hat{FL}_j$ were determined as follows:

$$CI_j = \hat{FL}_j \pm 1.96\hat{\sigma}_{FL_j}. \quad (18)$$

The equations for describing the relation between SOR and FL, LOR and FL, and FL and BW were calculated in the same way.

Application of equations to walleye pollock

Walleye pollock were collected and used as a model for long-lived species. The relevant biological data were collected, processed, and compiled from various cruise data conducted by Japanese and U.S. agencies at a total of 97 sampling stations in the Bering Sea (95 stations) and Chukchi Sea (northeastward extension of the Bering Sea; 2 stations) during 1983–2002 (Fig. 2).

In the central Bering Sea (Aleutian Basin), adult walleye pollock vary in age from 5 to >20 years (McFarlane and Beamish, 1990; Traynor et al., 1990). Young fish (0 to 4) are distributed on the continental shelf and slope and then migrate into the basin area beginning at age 5 (Traynor et al., 1990). In the present study, the samples of walleye pollock in the Bering Sea are presumed to have been collected from the same population of fish. Samples of juvenile walleye pollock at two discrete positions in the Chukchi Sea were also treated as originating from the Bering Sea. Larvae were sampled with a MOCNESS net, and juveniles and adults were captured with mid-water or bottom trawl nets. We measured the somatic length and BW of each fish and removed its otoliths (sagittae). For walleye pollock larger than 15 mm in somatic length, we measured FL, and for those smaller than 15 mm (with undeveloped fin rays), we measured TL. Difference in FL and TL was negligible in fish <15 mm; therefore TL is referred to as FL in the present analysis.

Specimens examined in the present study ranged from 4.56 mm to 803 mm FL. The number of samples used in the analysis of OL-FL equations is given in Table 1, as well as the size range of otolith measures and fish sizes. The approximate length of newly hatched larvae is 4.6 mm FL (=TL), 0.02 mm OL, and 0.01 mm SOR and LOR.

The relation between OL and FL was fitted to the general equations (Eqs. 1–4) and the allometric smoothing function (Eq. 12). The equations for describing the relation between SOR and FL, LOR and FL, and FL and BW were calculated in the same way.

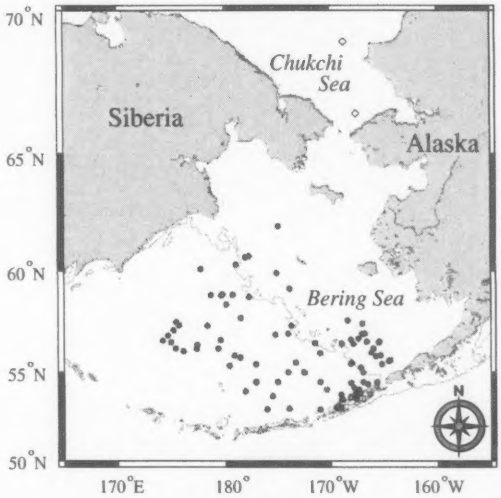

Figure 2

Map showing the sampling locations for walleye pollock (*Theragra chalcogramma*) in the present study. There were 97 total sampling stations: Bering Sea (●: 95 stations) and Chukchi Sea (○: 2 stations) in 1983–2002.

Otolith processing

For measurement of SOR and LOR, the left or right otolith was selected and processed as a frontal section to reveal the perpendicular structure of the proximal surface, including the tips of rostrum and postrostrum, and core (Fig. 3A). The procedure for otolith processing followed that of Secor et al. (1992).

Larval and juvenile otoliths were embedded in epoxy resin adhesive (Epoxy bond quick 5; Konishi Co., Ltd., Osaka, Japan) on a glass slide, and OL was measured under a microscope (SMZ-U or Labophot-2A; Nikon Co., Tokyo, Japan) by using an image analysis system (ARGUS-10; Hamamatsu Photonics K. K. Co., Shizuoka, Japan). The otolith was then carefully polished with wet sandpaper (no. 1200) and lapping paper (12–0.3 μ) as preparation for making the frontal section (Fig. 3B).

For the frontal section of large otoliths of postjuvenile and adult fish, the otolith proximal surface was placed facing up, and OL was measured. Then, the otolith proximal surface was marked at three points: the tip of the rostrum, the tip of the postrostrum, and the core region on the central concave area. The otolith was embedded in epoxy resin (Epoxicure; Buehler Ltd., Lake Bluff, IL) on a hardened epoxy bed about 3 mm deep in a plastic mold. The hardened epoxy block containing the otolith was cut and trimmed by a micro cutter (MC-201; Maruto Instrument Co., Ltd., Tokyo, Japan) to a 3-mm-wide section that included the three marks. The trimmed sample was fixed on a slide glass with hot wax (Stick wax; Maruto Instrument Co., Ltd., Tokyo, Japan) and polished with wet sandpaper (no. 400–800) on a polishing machine (ML-101; Maruto Instrument Co., Ltd., Tokyo, Japan and SBT900; South Bay Technology Inc., San Clemente, CA). Polishing was continued until the core and tips of the rostrum and postrostrum appeared. The polishing was also made on the opposite side of the

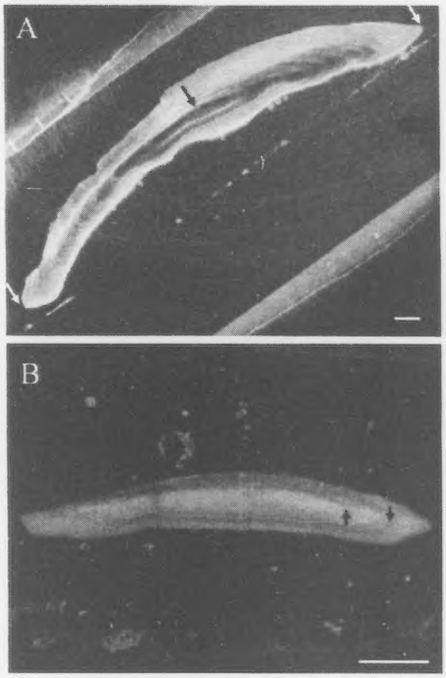

Figure 3

The frontal sections of an otolith from an adult walleye pollock (*Theragra chalcogramma*) (567 mm FL) viewed under transmitted light (A) and from a juvenile (138.8 mm FL) under reflected light (B). (A) The short otolith radius (SOR) was measured from the core (middle black arrow) to the tip of rostrum (right white arrow), and the long otolith radius (LOR) was measured from the core to the tip of postrostrum (left white arrow). The older annual rings are seen in the proximal surface region (the upper left side of the otolith, the clear white region). (B) The check-mark (left arrow) was observed inside of the first annual ring (right arrow). Scale bars = 1 mm

section. The section was finally polished by hand with wet sandpaper (no. 1200). The thickness of the polished frontal section (including the thickness of the wax) was 0.28 ±0.07 mm (mean ±SD, n=50). The OL in the frontal section shrank (98.7 ±2.5%, n=1775) after the polishing; however the decrease was not analyzed in this study.

Results

Relation between otolith length (OL) and fork length (FL)

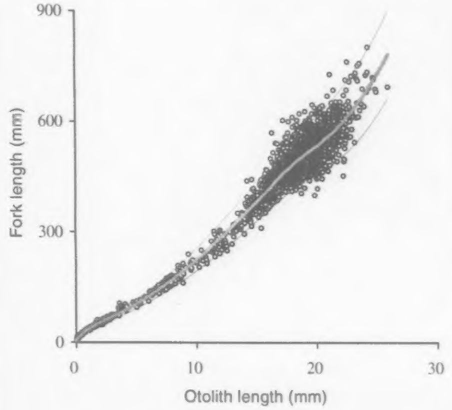

Figure 4

The equation that best describes the relation between otolith length (2.27×10^{-2}–25.98 mm) and fork length (4.56–803 mm) of walleye pollock (*Theragra chalcogramma*) in the Bering Sea (n=2354). Open circles (○) indicate individual samples of walleye pollock. The grey line represents a four-phase allometric smoothing function, and the dashed lines above and below are the 95% confidence intervals.

The most suitable equation to describe the OL (mm) and FL (mm) relationship chosen with the minimum AIC was the four-phase allometric smoothing function (Fig. 4). The minimum AIC in the general equations was an allometric equation with a constant term (Eq. 4). In the AIC, all allometric smoothing functions produced lower estimates than all of the general equations. In the allometric smoothing functions, the AIC decreased with the number of allometric smoothing functions, which increased from two to four. However, the AIC in the five-allometric smoothing function was higher than that in the four-phase allometric smoothing function (Table 2). The relation between OL (mm) and $\hat{\sigma}_{FL}$ (mm) is given as follows:

$$FL = 31.55\ OL^{0.67} + 4.05 \quad (0.00<OL<2.92) \quad (19.1)$$

$$FL = 5.64\ OL^{1.51} + 40.11 \quad (2.92\leq OL<16.48) \quad (19.2)$$

$$FL = -26083.56\ OL^{-1.49} + 831.85 \quad (16.48\leq OL<19.65) \quad (19.3)$$

$$FL = 1.28\times10^{-4}\ OL^{4.56} + 424.57 \quad (19.65\leq OL) \quad (19.4)$$

$$\hat{\sigma}_{FL} = 0.41\ OL^{1.52} + 1.80. \quad (20)$$

The coordinates (OL, FL) of the three inflection points were found at (2.92, 68.7), (16.48, 433.0), and (19.65, 525.0).

Relation between short otolith radius (SOR) and fork length (FL)

For the relation between SOR (mm) and FL (mm), we fitted the general equations (Eqs. 1–4) and the allometric

Table 2

Types of equations, range of otolith length (OL), inflection points, parameters, and Akaike's information criterion (AIC) for the equations used to describe the relation between OL (2.27×10^{-2} –25.98 mm) and fork length (FL: 4.56–803 mm) of walleye pollock (*Theragra chalcogramma*) in the Bering Sea (n= 2354). The minimum AIC was the four-phase allometric smoothing function. Estimated standard deviation of FL ($\hat{\sigma}_{FL}$) = $d\ OL^e + f$.

Relational	Range of OL		Inflection points		Parameter for equations			Parameter for $\hat{\sigma}_{FL}$			
equation types	Minimum	– Maximum	OL	FL	a	b	c	d	e	f	AIC
General equations											
$FL = a\ OL$	—	—	—	—	26.42	—	—	3.16	0.81	6.77	22,820
$FL = a\ OL + c$	—	—	—	—	25.94	—	7.02	5.66	0.68	1.27	22,573
$FL = a\ OL^b$	—	—	—	—	21.37	1.07	—	1.28	1.07	9.73	22,706
$FL = a\ OL^b + c$	—	—	—	—	15.18	1.18	15.14	0.74	1.31	4.61	22,016
Allometric smoothing functions											
$FL = a_1\ OL^{b1} + c_1$	0.00	– 2.25	—	—	32.41	0.64	3.34	0.41	1.54	1.76	21,194
$FL = a_2\ OL^{b2} + c_2$	2.25	–	2.25	57.7	8.33	1.37	32.40				
$FL = a_1\ OL^{b1} + c_1$	0.00	– 2.87	—	—	31.59	0.67	4.02	0.40	1.53	1.80	21,089
$FL = a_2\ OL^{b2} + c_2$	2.87	– 15.58	2.87	68.0	5.81	1.50	39.56				
$FL = a_3\ OL^{b3} + c_3$	15.58	–	15.58	400.7	3853.78	0.11	−4748.09				
$FL = a_1\ OL^{b1} + c_1$	0.00	– 2.92	—	—	31.55	0.67	4.05	0.41	1.52	1.80	21,066
$FL = a_2\ OL^{b2} + c_2$	2.92	– 16.48	2.92	68.7	5.64	1.51	40.11				
$FL = a_3\ OL^{b3} + c_3$	16.48	– 19.65	16.48	433.0	−26083.56	−1.49	831.85				
$FL = a_4\ OL^{b4} + c_4$	19.65	–	19.65	525.0	1.28×10^{-4}	4.56	424.57				
$FL = a_1\ OL^{b1} + c_1$	0.00	– 2.92	—	—	31.54	0.67	4.06	0.41	1.52	1.80	21,069
$FL = a_2\ OL^{b2} + c_2$	2.92	– 16.53	2.92	68.7	5.64	1.51	40.12				
$FL = a_3\ OL^{b3} + c_3$	16.53	– 19.97	16.53	434.8	−35709.22	−1.63	800.80				
$FL = a_4\ OL^{b4} + c_4$	19.97	– 20.42	19.97	532.0	9.28×10^{-17}	13.49	499.52				
$FL = a_5\ OL^{b5} + c_5$	20.42	–	20.42	543.3	2.40×10^{-3}	3.68	382.98				

smoothing function (Eq. 12). The minimum AIC was the four-phase allometric smoothing function. The relation between SOR (mm) and $\hat{\sigma}_{FL}$ (mm) was also shown as follows:

$$FL = 55.18\ SOR^{0.61} + 2.51 \quad (0.00<SOR<1.00) \quad (21.1)$$

$$FL = 24.22\ SOR^{1.39} + 33.47 \quad (1.00\leq SOR<7.55) \quad (21.2)$$

$$FL = -55349.12\ SOR^{-2.78} + 639.86 \quad (7.55\leq SOR<8.96) \quad (21.3)$$

$$FL = 6.68\times10^{-4}\ SOR^{5.25} + 447.65 \quad (8.96\leq SOR) \quad (21.4)$$

$$\hat{\sigma}_{FL} = 2.19\ SOR^{\ 1.37} + 1.91. \quad (22)$$

The coordinates (SOR, FL) of the three inflection points were found at (1.00, 57.8), (7.55, 437.3), and (8.96, 514.1).

Relation between long otolith radius (LOR) and fork length (FL)

In a similar way, the relationship between LOR (mm) and FL (mm) was derived, and the minimum AIC was a four-phase allometric smoothing function. The relation between LOR (mm) and $\hat{\sigma}_{FL}$ (mm) is also shown as follows:

$$FL = 48.98\ LOR^{0.65} + 3.26 \quad (0.00<LOR<1.54) \quad (23.1)$$

$$FL = 14.84\ LOR^{1.48} + 39.86 \quad (1.54\leq LOR<9.03) \quad (23.2)$$

$$FL = -16116.83\ LOR^{-1.77} + 754.41 \quad (9.03\leq LOR<11.30) \quad (23.3)$$

$$FL = 1.34\times10^{-4}\ LOR^{5.44} + 464.28 \quad (11.30\leq LOR) \quad (23.4)$$

$$\hat{\sigma}_{FL} = 1.77\ LOR^{1.32} + 1.85. \quad (24)$$

The coordinates (LOR, FL) of the three inflection points were found at (1.54, 68.1), (9.03, 428.8), and (11.30, 535.6).

Relation between fork length (FL) and body weight (BW) (g)

The relation between FL (mm) and BW (g) was fitted to the general equations (Eqs. 3 and 4), the allometric smoothing function (Eq. 12), and an allometric smoothing function without a constant term in the first function (c_1=0). The minimum AIC was the three-phase allometric smoothing function without c_1. The relation between FL (mm) and $\hat{\sigma}_{BW}$ (g) is shown as follows:

$$BW = 2.01\times10^{-5}\, FL^{2.77} \quad (0.00<FL<70.0) \quad (25.1)$$

$$BW = 6.61\times10^{-6}\, FL^{3.02} + 0.21 \quad (70.0\leq FL<431.2) \quad (25.2)$$

$$BW = 4.17\times10^{-6}\, FL^{3.09} + 13.89 \quad (431.2\leq FL) \quad (25.3)$$

$$\hat{\sigma}_{BW} = 1.06\times10^{-5}\, FL^{2.63}. \quad (26)$$

The coordinates (*FL*, *BW*) of the two inflection points were seen at (70.0, 2.6) and (431.2, 586.2).

Discussion

The allometric smoothing function

The best equation to describe the relation between OL and FL in walleye pollock throughout the entire lifespan of the fish was depicted by a four-phase allometric smoothing function with three inflection points. In our preliminary analysis, a quadratic equation was applied for the OL and FL relationship, and the resulting AIC was 21,743. This value was smaller than that derived from general equations, but was higher than the value derived from any of our allometric smoothing functions (see Table 2). The general equations and the quadratic equation do not adequately reflect the variable otolith and somatic allometric growth during the whole lifespan of the species.

Equations relating OL to somatic length have been developed to represent complex growth curves. Bervian et al. (2006) used an allometric equation transformed from the logistic function for the OL-TL relationship in whitemouth croaker (*Micropogonias furnieri*). Imai et al. (2002) applied a Gompertz model to the relation between otolith height and standard length in cyprinid fish "Ukekuchi-ugui" (*Tribolodon nakamurai*). However, these two models have limitations in both the shape of the curve and the number of inflection points. If the species in the model, such as walleye pollock in this study, has more than two inflection points in the derived curve, these models cannot represent the allometric growth patterns adequately. Our present allometric smoothing function has no such limitation in the number of inflection points or the shape of curve between inflection points and responds appropriately to the growth pattern of the fish.

Our allometric smoothing function has the ability to satisfy both the needs for mathematical continuity (see Fig. 1) and objectivity in the selection of an equation (see Table 2) while allowing for biological events. The allometric smoothing function was developed by using a mathematical smoothing method based on an allometric equation with a constant term. Among the smoothing methods available, the moving average, autoregression, and spline curve proved to be useful for fitting scatter sample plots, a type of plot that cannot be properly fitted in a single function. Nevertheless, the moving average requires that the modeler be subjective in determining the number of data points used to calculate the average. In contrast, the autoregression allows a measure of objectivity in selecting the equation; however steady growth conditions are assumed with this method. Finally, the spline curve is based on a multidimensional function developed by mathematical procedure where biological events were not taken into consideration.

Until recently, back-calculation models for individual fish growth have been developed to estimate past fish length and growth, under the assumption that fish growth is proportional to otolith growth (Francis, 1990). However, many studies have recognized that fish growth and otolith growth are uncoupled. "Growth rate effect" and "age effect" are two of the most important factors affecting uncoupling. The growth rate effect occurs when otoliths from slow growing fish are larger than those of fast growing fish, when these fish are compared at the same somatic length (Reznick, 1989; Campana, 1990; Secor and Dean, 1992). Adapting Campana's (1990) biological intercept method can reduce the error inherent in back-calculated somatic length from this growth-rate effect. Additionally, with the back-calculation model developed by Morita and Matsuishi (2001), the fact that age effect on otolith size increases continuously during nongrowth periods (Mugiya, 1990; Secor and Dean, 1992) can be taken into account. The inclusion of these growth and age effects of individual fish to our allometric smoothing function provides a more accurate analysis of growth at the individual level in the back-calculation model.

Application of the allometric smoothing function for walleye pollock

Our best equation to describe the relation between OL and FL was derived as a four-phase allometric smoothing function with three inflection points (Fig. 4). In Huxley's (1924) allometric equation ($y=ax^b$), relative growth rate was expressed by the relative growth coefficient (allometric coefficient, b). Our allometric smoothing function is based on the allometric equation with an added constant term ($y=ax^b + c$). The superscript b in our equation is not an allometric coefficient; it indicates the relative growth between x and y on the slope of the curve between inflection points.

The explicit changes in the shape of the curves and the appearance of inflection points in our equation imply that ecological and physiological changes are associated with unique aspects of life history of walleye pollock. In the first function (Eq. 19.1), somatic growth is slower than otolith growth, whereas in the second function (Eq. 19.2), somatic growth is faster than otolith growth. Concerning these contrasting outcomes, previous findings indicate that possible ecological changes may have occurred at a particular size range, as evidenced by otolith characters such as the check-mark. Nishimura (1993) reported that 32% of age-1 walleye pollock caught in the Bering Sea revealed check-marks inside the first annual ring of the otolith and he concluded that the check-mark would have been formed at 40–80 mm FL (mode: 70 mm) at an age of 4 months. This check-mark was frequently detected in our samples (Fig. 3B). Similarly, in Funka Bay, Japan, 58% of age-1 walleye pollock had check-marks inside the first annual ring (Katakura et al., 2003). The settlement of juvenile walleye pollock from pelagic to benthic habitat began from 70 mm TL and was completed when the fish reached >85 mm TL in Funka Bay (Nakatani and Maeda, 1987). Our calculated FL at the first inflection point was 68.7 mm, which is approximately the same size as that when settlement begins. The check-mark on the otoliths of walleye pollock appears to occur, irrespective of differences in geographic features of inhabited waters. Victor (1982) suggested that the check-mark occurs as a settlement mark and indicates the occurrence of physiological changes or biological processes associated with settlement. Thus, we conclude that the first inflection point at a particular size in our allometric growth curve shows the adaptive response of walleye pollock to physiological and environmental changes at the time of settlement.

The state of $b<0$ but $a<0$ in the third function (Eq. 19.3) also implies that somatic growth is slower than otolith growth. The allometric coefficient between OL and somatic length drastically changes in association with sexual maturity (Bervian et al., 2006). The Bogoslof area in the Aleutian Basin is known as one of the main spawning grounds of walleye pollock in winter. In this area, fish length at maturity was 360–570 mm FL (mean 464 mm) in males and 370–610 mm FL (482 mm) in females (Traynor et al., 1990). The second inflection point that appeared at 433.0 mm FL in our study is situated within the size range of maturing fish. We assume that the fish length around the second inflection point corresponds to the timing of an energy shift from somatic growth to gonad development, and to corresponding changes that occur in the shifts of the allometric growth curve.

Both the third inflection point at 525.0 mm FL and the fourth function (Eq. 19.4) indicate faster somatic growth than otolith growth. Otolith growth persists despite the cessation of body growth (Mugiya, 1990; Secor and Dean, 1992); therefore, the otolith is also assumed to grow throughout the lifetime of walleye pollock (McFarlane and Beamish, 1990). Older annual rings appear on the ventral proximal surface region, as evidenced in the transverse section (McFarlane and Beamish, 1990), similar to those seen in the proximal surface region of the frontal section (Fig. 3A). The shape of the large otolith is an arched curve connecting the tip of the rostrum, core, and tip of the postrostrum. Thus, the third inflection point is considered to be closely related to the slow growth phase of otoliths, accompanying the change in the direction of growth in otoliths from length (between the tips of rostrum and postrostrum) to width (proximal surface region increasing), and an increase in the slope of the curve.

The best equations that describe the relation of SOR to FL, and LOR to FL were also represented by the four-phase allometric smoothing function with three inflection points (Eqs. 21.1–21.4 and 23.1–23.4). The characteristics of the allometric otolith and somatic growth patterns are similar, as found in the OL and FL relation. These relationships can be useful for the analysis of growth of juvenile walleye pollock from the back-calculation of adult otoliths. The measurements of the SOR or LOR of fish at young ages allow one to convert these measurements to FL values. Similarly, our equations allow the conversion of FL from any otolith measurement (OL, SOR, and LOR) into BW.

The resultant coordinates of the two inflection points at FL of 70.0 mm and 431.2 mm derived from our FL and BW relationship (Eqs. 25.1–25.3) were very close to the first (68.7 mm FL) and second (433.0 mm FL) inflection points that emerged in the OL and FL relationship (Eqs. 19.1–19.4). Because settlement and sexual maturity are distinct biological events in the life history of this fish, the timing of these events will be clearly demonstrated in allometric growth.

The condition factor (CF) of fish is generally calculated by a formula ($CF=10^3 \times BW/FL^3$). However, our results indicate that the relation between FL and BW is not constant over the lifetime of walleye pollock, and probably for other fish species. In our equations, b increased as fish grew in association with life stages from $b_1=2.77$ to $b_2=3.02$ and $b_3=3.09$, and this inflation has potential implications for studies of fish growth.

The present equations can be applied to the reconstruction of size composition of fish from the remnant otoliths found in the digestive organs of predators. We expect that these reliable equations, with transformation of otolith measurement data into FL or BW values, are useful not only for fish growth analysis, but also for food habit and energetic studies (e.g., food conversion efficiency studies) because these studies rely substantially on the back-calculation method.

The samples of walleye pollock used in this study provided a range of fish lengths from 4.56 mm FL (=TL in larvae) to 803 mm FL. Newly hatched walleye pollock measure about 4.6 mm TL (Nishimura and Yamada, 1988), and the oldest fish reported from the Bering Sea was 28 years old and measured 530 mm FL (McFarlane and Beamish, 1990). Thus, the present data set can be regarded as including almost the entire size range of walleye pollock over the whole life span. Because the proposed allometric smoothing functions can be extensively applicable to all life stages of walleye pollock, we term these equations "allometric smoothing functions for otolith and somatic growth over the lifespan of walleye pollock."

Acknowledgments

We thank J. R. Bower, K. Morita, N. J. Williamson, and the anonymous referees for invaluable advice on the manuscript, T. Yanagimoto, K. Mito, T. Honkalehto, S. de Blois, N. Tanimata, R. Nanbu, and O. Sakai for assistance with the sampling and measurements of fish samples. We also thank the scientists of the following agencies for the offer of biological data and otolith samples: National Research Institute of Far Seas Fisheries, Fisheries Research Agency, Japan; Hokkaido National Fisheries Research Institute, Fisheries Research Agency, Japan; Graduate School of Fisheries Sciences, Hokkaido University, Japan; and Alaska Fisheries Science Center, National Marine Fisheries Service, National Oceanic and Atmospheric Administration, USA. We also thank the crews of the RV *Kaiyo Maru*, TS *Oshoro Maru*, RV *Miller Freeman*, and chartered fishing vessels.

Literature cited

Akaike, H.
1974. A new look at statistical model identification. IEEE (Institute of Electrical and Electronics Engineers, Inc.) Transactions on Automatic Control 19:716–723.

Bervian, G., N. F. Fontoura, and M. Haimovici.
2006. Statistical model of variable allometric growth: otolith growth in *Micropogonias furnieri* (Actinopterygii, Sciaenidae). J. Fish Biol. 68:196–208.

Campana, S. E.
1990. How reliable are growth back-calculations based on otoliths? Can. J. Fish. Aquat. Sci. 47:2219–2227.

Francis, R. I. C. C.
1990. Back-calculation of fish length: a critical review. J. Fish Biol. 36:883–902.

Frost, K. J., and L. F. Lowry.
1981. Trophic importance of some marine gadids in northern Alaska and their body-otolith size relationships. Fish. Bull. 79:187–192.

Hunt, G. L., P. Stabeno, G. Walters, E. Sinclair, R. D. Brodeur, J. M. Napp, and N. A. Bond.
2002. Climate change and control of the southeastern Bering Sea pelagic ecosystem. Deep-Sea Res. II 49:5821–5853.

Huxley, J. S.
1924. Constant differential growth-ratios and their significance. Nature 14:895–896.

Imai, C., H. Sakai, K. Katsura, W. Honto, Y. Hida, and T. Takazawa.
2002. Growth model for the endangered cyprinid fish *Tribolodon nakamurai* based on otolith analyses. Fish. Sci. 68:843–848.

Katakura, S., M. Ohta, M. Jin, and Y. Sakurai.
2003. Otolith-marking experiments of juvenile walleye pollock *Theragra chalcogramma* using oxytetracycline, alizarin complexone, and alizarin red S. Suisanzoshoku 51:327–335. [In Japanese with English summary.]

McFarlane, G. A., and R. J. Beamish.
1990. An examination of age determination structures of walleye pollock (*Theragra chalcogramma*) from five stocks in the northeast Pacific Ocean. Int. North Pac. Fish. Comm. Bull. 50:37–56.

Morita, K., and T. Matsuishi.
2001. A new model of growth back-calculation incorporating age effect based on otoliths. Can. J. Fish. Aquat. Sci. 58:1805–1811.

Mugiya, Y.
1990. Long-term effects of hypophysectomy on the growth and calcification of otoliths and scales in the goldfish *Carassius auratus*. Zool. Sci. 7:273–279.

Nakatani, T., and T. Maeda.
1987. Distribution and movement of walleye pollock larvae *Theragra chalcogramma* in Funka Bay and the adjacent waters, Hokkaido. Nippon Suisan Gakkaishi 53:1585–1591. [In Japanese with English summary.]

Nishimura, A.
1993. Age determination of walleye pollock based on the otoliths (Review). *In* Present status and prospects of research on the biology and fisheries resources of walleye pollock and other gadid species in the waters around Hokkaido—special edition of the "Hokkaido Suketoudara Kenkyu Group" (Hokkaido Walleye Pollock Research Group) for the 25th anniversary (H. Yoshida, ed.), p.37–49. Sci. Rep. Hokkaido Fish. Exp. Stn. 42. Hokkaido Central Fisheries Experimental Station, Yoichi, Hokkaido, Japan. [In Japanese with English summary.]

Nishimura, A., and J. Yamada.
1988. Geographical differences in early growth of walleye pollock *Theragra chalcogramma*, estimated by back-calculation of otolith daily growth increments. Mar. Biol. 97:459–465.

Reznick, D.
1989. Slower growth results in larger otoliths: an experimental test with guppies (*Poecilia reticulata*). Can. J. Fish. Aquat. Sci. 46:108–112.

Secor D. H., and J. M. Dean.
1992. Comparison of otolith-based back-calculation methods to determine individual growth histories of larval striped bass, *Morone saxatilis*. Can. J. Fish. Aquat. Sci. 49:1439–1454.

Secor D. H., J. M. Dean, and E. H. Laban.
1992. Otolith removal and preparation for microstructural examination. *In* Otolith microstructure examination and analysis (D. K. Stevenson, and S. E. Campana, eds.), p. 19–57. Can. Spec. Publ. Fish. Aquat. Sci. 117.

Springer, A. M.
1992. A review: walleye pollock in the North Pacific—how much difference do they really make? Fish. Oceanogr. 1:80–96.

Traynor, J. J., W. A. Karp, T. M. Sample, M. Furusawa, T. Sasaki, K. Teshima, N. J. Williamson, and T. Yoshimura.
1990. Methodology and biological results from surveys of walleye pollock (*Theragra chalcogramma*) in the eastern Bering Sea and Aleutian Basin in 1988. Int. North Pac. Fish. Comm. Bull. 50:69–100.

Victor, B. C.
1982. Daily otolith increments and recruitment in two coral-reef wrasses, *Thalassoma bifasciatum* and *Halichoeres bivittatus*. Mar. Biol. 71:203–208.

Wespestad, V. G.
1993. The status of Bering Sea pollock and effect of the "Donut Hole" fishery. Fisheries 18:18–25.

Zeppelin, T. K., D. J. Tollit, K. A. Call, T. J. Orchard, and C. J. Gudmundson.
2004. Sizes of walleye pollock (*Theragra chalcogramma*) and Atka mackerel (*Pleurogrammus monopterygius*) consumed by the western stock of sea lions (*Eumetopias jubatus*) in Alaska from 1998 to 2000. Fish. Bull. 102: 509–521.

Appendix

The spreadsheets of the computer application Microsoft Excel (Microsoft Co., Tokyo, Japan) were used as an analysis platform, and an add-in tool solver was used for the optimization of the present OL-FL equation. The solver has been standard add-in tool in Excel since the Excel 95 version. The optimized value of the parameters and the Akaike's information criterion (AIC) in the present equations were identical with the use of Excel 2003 and Excel 2007. The modified spreadsheet of a Microsoft Excel workbook shows how to fit the two-phase allometric smoothing function for the otolith length (OL) and fork length (FL) relationship (Appendix Table below). The most suitable equation to describe the relation between otolith length and somatic length was chosen if it accorded with the minimum AIC.

Appendix Table

The modified spreadsheet of a Microsoft Excel workbook is shown to fit the two-phase allometric smoothing function for the otolith length (OL, mm) and fork length (FL, mm) relationship in walleye pollock (*Theragra chalcogramma*) (n=2354). At the add-in tool of the Solver parameters dialog box in Excel, the Akaike's information criterion (AIC: cell B3) sits in the "target cell" and the parameters (cells B5 to B12) sit in the "changing cell." The optimization for the equation is a minimized AIC with adjusting parameters using solver constraints. $\hat{\sigma}_{FL_j}$ = estimated standard deviation of FL of individual j; $f_1(OL_j)$ = calculated FL for individual j in the first function; $f_2(OL_j)$ = calculated FL for individual j in the second function; $\hat{FL}_j$ = employed calculated FL for individual j; L_j = likelihood of individual j; ln L_j = log-likelihood of individual j; LL = a log-likelihood; d, e, f = parameters for $\hat{\sigma}_{FL_j}$; a_1, b_1, c_1 = parameters for $f_1(OL_j)$; and a_2, b_2, c_2 = parameters for $f_2(OL_j)$; and q_1 = a value of OL on the inflection point.

	A	B	C	D	E	F
1	Two-phase allometric smoothing function		OL	FL	$\hat{\sigma}_{FL_j}$	$f_1(OL_j)$
2	LL	`= SUM(J2:J2355)`	1.06	37.2	`= $B$5*C2^$B$6+$B$7`	`= $B$8*C2^$B$9+$B$10`
3	AIC	`= –2*B2+2*COUNT(B5:B12)`	1.09	38.1	`= $B$5*C3^$B$6+$B$7`	`= $B$8*C3^$B$9+$B$10`
4	Parameters		1.11	32.8	`= $B$5*C4^$B$6+$B$7`	`= $B$8*C4^$B$9+$B$10`
5	d	0.41	1.15	37.8	Copy down to row 2355, where n=2354	
6	e	1.54	1.16	36.8	2.281	38.973
7	f	1.76	1.17	36.9	2.288	39.169
8	a_1	32.41	1.18	35.5	2.295	39.364
9	b_1	0.64	1.23	40.8	2.329	40.332
10	c_1	3.34	1.25	39.4	2.344	40.715
11	q_1	2.25	13.73	308	24.734	175.993
12	b_2	1.37	13.51	351	24.173	174.222
13	a_2	`= B8*B9/B12*B11^(B9–B12)`	13.76	333	24.811	176.234
14	c_2	`= B8*B11^B9*(1–(B9/B12))+B10`	1.12	33.1	To row 2355	

	G	H	I	J
1	$f_2(OL_j)$	$\hat{FL}_j$	L_j	ln L_j
2	`= $B$13*C2^$B$12+$B$14`	`= IF(C2<$B$11,F2,G2)`	`= NORMDIST(D2,H2,E2,FALSE)`	`= IF(I2<=0,–10000,LN(I2))`
3	`= $B$13*C3^$B$12+$B$14`	`= IF(C3<$B$11,F3,G3)`	`= NORMDIST(D3,H3,E3,FALSE)`	`= IF(I3<=0,–10000,LN(I3))`
4	`= $B$13*C4^$B$12+$B$14`	`= IF(C4<$B$11,F4,G4)`	`= NORMDIST(D4,H4,E4,FALSE)`	`= IF(I4<=0,–10000,LN(I4))`
5	Copy down to row 2355, where n=2354			
6	42.563	38.973	0.111	–2.197
7	42.685	39.169	0.106	–2.238
8	42.807	39.364	0.042	–3.167
9	43.421	40.332	0.166	–1.793
10	43.671	40.715	0.147	–1.916
11	335.852	335.852	0.008	–4.761
12	329.204	329.204	0.011	–4.511
13	336.761	336.761	0.015	–4.141
14	To row 2355			

Transitions in the morphological features, habitat use, and diet of young-of-the-year goosefish (*Lophius americanus*)

Kenneth W. Able (contact author)[1]
Peter J. Clarke[1]
R. Christopher Chambers[2]
David A. Witting[3]
Email address for K. W. Able: able@marine.rutgers.edu

[1] Rutgers University, Institute of Marine and Coastal Sciences
Marine Field Station
800 c/o 132 Great Bay Boulevard
Tuckerton, New Jersey 08087-2004

[2] National Oceanic and Atmospheric Administration (NOAA)
National Marine Fisheries Service
Northeast Fisheries Science Center (NEFSC)
James J. Howard Marine Science Laboratory
74 Magruder Road, Highlands, New Jersey 07732

[3] NOAA/Montrose Settlements Restoration Program (MSRP)
501 West Ocean Blvd, Suite 4470
Long Beach, California 90802-4213

Abstract—This study was designed to improve our understanding of transitions in the early life history and the distribution, habitat use, and diets for young-of-the-year (YOY) goosefish (*Lophius americanus*) and, as a result, their role in northeastern U.S. continental shelf ecosystems. Pelagic juveniles (>12 to ca. 50 mm total length [TL]) were distributed over most portions of the continental shelf in the Middle Atlantic Bight, Georges Bank, and into the Gulf of Maine. Most individuals settled by 50–85 mm TL and reached approximately 60–120 mm TL by one year of age. Pelagic YOY fed on chaetognaths, hyperiid amphipods, calanoid copepods, and ostracods, and benthic YOY had a varied diet of fishes and benthic crustaceans. Goosefish are widely scattered on the continental shelf in the Middle Atlantic Bight during their early life history and once settled, are habitat generalists, and thus play a role in many continental shelf habitats.

Manuscript submitted 2 April 2004
to the Scientific Editor's Office.

Manuscript approved for publication
14 March 2007 by the Scientific Editor.

Fish. Bull. 105:457–469 (2007).

Our understanding of the life history and ecology of the goosefish (*Lophius americanus*) is incomplete. Much of what we believe to be true is drawn by analogy from European congeners (Caruso, 2002). This lack of knowledge is especially relevant given the development of an important fishery for goosefish since the 1980s (Caruso, 2002) and given the evidence that goosefish were overexploited in the 1990s (Almeida et al., 1995). Goosefish are found in the western North Atlantic from the Grand Banks off Newfoundland to the east coast of Florida (Wood, 1982; Caruso, 1983). Larval development, from hatching to completion of fin rays (up to 12 mm total length [TL]) has been described in detail (Everly, 2002). Little is known about pelagic and settled young-of-the-year (YOY) life stages and thus their role in continental shelf ecosystems. The smallest benthic individuals reported by Caruso (2002) were 76–114 mm TL (n=3).

Information on ages of YOY goosefish appears to be contradictory, but does indicate that sizes attained by the end of age 1 can be quite variable. Size of YOY goosefish by their first fall has been variously reported as 64–76 mm TL (Steimle et al., 1999) and as 59 mm TL (Scott and Scott, 1988). However, larger sizes have been reported by Armstrong et al. (1992) for goosefish from southern New England–Mid-Atlantic Bight (average of 123–126 mm TL at age 1 for females and males) and by Hartley (1995) for goosefish from the Gulf of Maine (120–139 mm TL). Scott and Scott (1988) reported fish of 100–114 mm TL to be 2 years of age.

A portion of the National Marine Fisheries Service (NMFS) groundfish survey data and associated collections along the northeast coast of North America have been examined to determine some aspects of the life history and food habits for large juveniles and adult goosefish (Armstrong et al., 1992, 1996; Almeida et al., 1995; Hartley, 1995; Martinez, 1999). These studies focused on reproduction, age, and growth over short time periods and relied on data collected from geographically disparate sources. Recently, goosefish distribution and abundance in relation to depth and temperature were summarized from a large portion of the NMFS database for groundfish surveys in the Gulf of Maine and the Middle Atlantic Bight (Steimle et al. 1999). Steimle et al. (1999) grouped all fish <43 cm TL into the juvenile category. As a result, several age classes were combined and there was no resolution for habitat of YOY goosefish. Prior descriptions of other aspects of the life history and ecology of YOY goosefish include associations of fish with depth and substrate type for Canadian waters (Jean, 1965; Scott, 1982), and with food habits for juveniles and adults (Sedberry, 1983; Armstrong et al., 1996).

The gaps in our knowledge about YOY goosefish, as articulated by Steimle et al. (1999), motivated the efforts reported here. Our objectives were 1) to describe more fully the morphological development of goosefish during the transition from pelagic larvae to benthic juveniles, 2) to estimate the timing, sizes, and ages of early life history events, and the growth rates of YOY goosefish, 3) to determine the distribution of pelagic and benthic juveniles in time and space, and 4) to identify the food habits and habitats of settled YOY goosefish.

Materials and methods

Two species of *Lophius* are found in the waters of the northwestern Atlantic, goosefish (*L. americanus* Valenciennes) and blackfin goosefish (*L. gastrophysus* Miranda-Ribeiro) (Caruso, 2002), and thus correct taxonomic identification is essential. Previously, *L. gastrophysus* was considered to be distributed from Brazil to Florida, and *L. americanus* was considered to range from Nova Scotia to Cape Hatteras (Bigelow and Schroeder, 1953; Scott and Scott, 1988) and to overlap occasionally between Florida and Cape Hatteras (Caruso, 1983). Preliminary data from the NMFS Commercial Cooperative Research goosefish survey indicate that *L. gastrophysus* has a much broader range, which is believed to extend into the Gulf of Maine (Richards[1]). To ensure proper identification of our specimens, we used the diagnostic characters reported for these congeners (Caruso, 1983).

Morphological development

For some species of fish, ontogenetic state of an individual has proven to be a better metric of early life history events than has age (Policansky, 1983; Fuiman et al., 1998). For this reason, we used morphological and meristic data from pelagic and benthic individuals of *L. americanus* as a basis for describing early life history stages and for estimating size and age at settlement. We define planktonic juveniles as those individuals that have completed fin ray formation (>12 mm TL; Everly, 2002), but have not yet settled. Benthic juveniles include all postsettlement YOY and juveniles of older age classes. A total of 88 fish (9.8–188 mm TL) were collected and examined (three fish per 5-mm size class) from a variety of sources (Table 1). These specimens were either collected and frozen, preserved in a solution of 70–95% ethanol or 5% formalin onboard the sampling vessel, or were obtained from museum collections. Shrinkage was determined by measuring fish upon capture and after preservation in ethanol or formalin. In total, 28 morphometric and meristic characters were examined (Table 2). These characters were based largely on those general character definitions provided by Hubbs and Lagler (1958). Modifications to these definitions in our study were due to the unique features possessed by *L. americanus*. Head length was measured from the anterior tip of the premaxillary bone to the gill opening. The length of the first dorsal spine, or illicium, was measured from its base to the base of the esca, the fleshy distal pendant of the illicium. The length of the esca was measured from its base to its distal end. An ocular micrometer was used for lengths ≤10 mm and a dial caliper was used for lengths >10 mm; all measurements were taken to 0.1-mm resolution.

Changes in body proportions that occurred during the pelagic-benthic transition were determined by examining the relation between each morphological character and total length. Such changes in allometry were detected by alteration in the slope of the line relating a focal character and total length (or any other reference character) on a log-log scale. When a fish is growing but not changing shape (i.e., exhibits isometric growth), the slope of this relationship is unity. When an individual or, as used here, an ontogenetic series of individuals, exhibits changes in shape with increasing total length, this means that the character(s) defining shape have changed in relation to total length. This transition in the degree of allometry will be reflected by a systematic deviation of the slope in the bivariate character plot. The magnitude of the slope before and after the transition, as well as the total length at which the transition occurred, were estimated by using piecewise regression (Toms and Lesperance, 2003).

Unlike measures of body proportions, other characters that change during the larval- juvenile-adult states are difficult to quantify. For example, the degree of pigmentation and the development of tubercles (Wiley and Collette, 1970) and cirri (fleshy flaps or tags, see Caruso, 2002) change gradually and in multiple dimensions during the progression from larval to juvenile phenotypes. These types of characters were scored as 0 or 1 for the larval state and juvenile-adult state, respectively. The juvenile-adult state was assumed to be represented by the largest size class that we examined (185–190 mm TL). For each of these characters, the median and standard error (SE) of size at transition to the juvenile/adult state were identified by fitting a cumulative normal distribution to the 0–1 scores by using a probit regression model. Because these estimates are based on data at the population level, our estimate of the mean size at transition was actually the size at which 50% of individuals expressed the juvenile-adult state of the character. The standard error of the median was converted to a 95% confidence interval, which indicates the sizes at which 5% to 95% of individuals express the adult state of the character.

---

[1] Richards, A. 2004. Personal commun. National Oceanic and Atmospheric Administration, National Marine Fisheries Service, Northeast Fisheries Science Center, 166 Water Street, Woods Hole, MA 02543-1026.

Size and age at early life history events

Events during the early life history of goosefish were assessed by examination of sizes of fish at capture and by determination of ages and past events in the life of the fish as reflected in its otolith microstructure. Pelagic and benthic specimens (51–128 mm TL) used for daily otolith increment analysis were collected from a variety of sources (Table 1). An additional set of larvae hatched in the laboratory from egg veils collected in coastal waters off Long Beach Island, New Jersey, were examined for evidence of otolith microstructure that reflected hatching and the absorption of yolk. Preliminary examination of all three otoliths indicated that the lapilli were the easiest to interpret because of the clarity of increments and the lack of secondary growth structures. Hislop et al. (2001) came to a similar conclusion for *L. piscatorius*. Before otolith removal, individual fish were measured to the nearest 1 mm TL. Lapilli were removed, cleaned in bleach, and dried in 95% ethanol before they were mounted on glass slides by using a thermoplastic adhesive (Crystal Bond, Electron Microscopy Sciences, Hatfield, PA). Lapilli from fish >70 mm TL were ground and polished to the primordia on both surfaces with 1500 grit wet-dry sand paper with water as a lubricant, then finely polished with a 0.3-micron micropolish on a Buehler micropolishing cloth. Lapilli from fish <70 mm TL were polished to the primordia with the same materials but on the surface of the sulcus. Lapilli were cleaned with distilled water before they were immersed in oil for viewing. An analysis of

Table 1

Sources of data and specimens from field surveys used to determine aspects of the life history transitions, distribution, and diet of young-of-the-year goosefish (*Lophius americanus*). MAB = Middle Atlantic Bight (Cape Hatteras to Cape Cod); GB = Georges Bank; GOM = Gulf of Maine. NMFS = National Marine Fisheries Service; Mass DEP = Massachusetts Department of Environmental Protection; NJDEP = New Jersey Department of Environmental Protection; ACE = Army Corps of Engineers; VIMS = Virginia Institute of Marine Science.

Source	MAB	GB	GOM	Sampling gear	Sampling period	Sampling frequency	Range of sample depths (m)	Number of specimens (*n*)	Size range of specimens (mm total length)
NMFS	X	X	X	Bongo plankton net (1 m)	1977–87	6–8 cruises per year	11–1400	827	2.9–54.6
NMFS	X	X	X	Otter trawl (24 m)	1982–present	One cruise during fall, winter, and spring	9–365	3551	50–300
Michaels (2001)			X	Frame net	2000–2001	One cruise/year, generally in fall	35.5–818	66	20–210
NMFS	X	X	X	Commercial otter trawl	2001	Two simultaneous cruises	20–600	1093	25–300
NMFS	X	X	X	Scallop dredge	1982–2001	One cruise per year	21–144	9541	20–300
Mass DEP	X		X	Otter trawl (15 m)	1978–2001	Semi-annual sampling; spring and fall	6–82	490	40–300
NJDEP	X			Otter trawl (30 m)	1989–2000	Winter, spring, summer, fall	5–30	118	30–290
ACE	X			Bongo plankton net (1m)	1995–99	Bimonthly during summer	0–7	787	3.6–15.61
VIMS	X			Otter trawl (13.5 m)	1973–76	One cruise per year	35–818	587	53.37–299.37
NMFS	X			Otter trawl	2000	One cruise	20–330	98	180–300
Steves et al. (1999)	X			Beam trawl (2 m)	1996–97	Monthly cruises summer and fall; bimonthly winter and spring	20–90	19	72–233

Table 2

Summary of changes for 18 morphological characters in relation to total length of young-of-the-year goosefish (*Lophius americanus*). All estimates are derived from a linear piecewise regression. "Slope" refers to the estimate of the slope in the allometric equations applied to characters before and after the shift from juvenile to adult state. "Size" refers to the estimated size at which the shift occurs. Back-calculated lower and upper 95% confidence limits (L95 and U95, respectively) pertain to the estimated size at shift. R^2 (coefficient of what?) values and significance levels are for the entire piecewise regression model. ($^{*}P<0.05$, $^{**}P<0.001$, $^{***}P<0.0001$, ^{ns} not significant.)

	Slope						
Character	Pre-shift	Post-shift	Size (mm)	L95	U95	R^2	
Second dorsal ray (Illicium)	2.98	1.06	27.39	24.51	30.75	0.97	***
Esca length	1.61	0.8	84.10	50.91	138.38	0.80	*
Dorsal base length	1.41	0.95	20.11	14.44	28.50	0.98	**
Pectoral fin length	1.24	0.82	46.99	36.23	60.34	0.97	***
Snout length	1.2	0.95	42.56	24.05	75.19	0.97	**
Caudal peduncle depth	1.06	0.59	39.41	26.31	58.56	0.91	***
Head width	1	1.39	39.25	26.58	58.56	0.98	***
Pelvic fin length	0.93	0.24	48.42	41.26	57.40	0.92	***
Standard length	0.84	1.05	26.05	20.49	33.12	0.99	***
Orbit diameter	0.72	0.96	61.19	38.09	98.49	0.95	**
Head depth	0.49	1.1	60.95	34.81	107.77	0.79	***
Second dorsal ray length	0.45	1.06	84.10	67.36	104.58	0.86	***
Predorsal length	0.12	0.79	53.52	40.85	70.11	0.73	***
Caudal peduncle length	0.10	0.90	27.66	20.70	37.34	0.88	***
Head length	1.44	0.45	12.94	2.94	56.26	0.99	ns
Upper jaw length	1.23	1.33	39.25	7.88	197.16	0.98	ns
Third dorsal ray length	0.53	0.36	38.09	3.22	454.86	0.56	ns
Otolith size	0.33	0.71	17.97	10.5	30.91	0.97	**

evidence of allometric shifts in otolith dimensions for pelagic and settled YOY goosefish (8.6–285 mm TL, n=60) was conducted in the same manner as described above for body proportions.

Lapilli were viewed by transmitted light with an Olympus BH-2 compound microscope and Optimus 6.2 video imaging software (OPTIMUS Corp., Fort Collins, CO) at a magnification of 1250×. Distances from the primordium to each of multiple distinct marks (checks) on the otolith (e.g., at hatching, yolksac absorption, settlement, annulus formation) were taken along an axis to the dorsal edge. Increments (which are believed to be formed daily) were counted along the axis that exhibited the least ambiguous sequence of increments and greatest distance from the primordium to the outer edge. Increment counts and location of checks were determined twice on each otolith by a single observer.

Although we were reasonably confident of the age estimates derived with the above approach, we attempted to evaluate the precision and accuracy of our daily increment counts. A subset of otoliths (n=20) from fish (11–251 mm TL) were compared between the primary reader (PJC) and a second reader (K. Lang, NMFS, Woods Hole). The differences between readers in increment counts were small but increased with the size of the otolith from 6.5% (the interval from the hatching check) to 8.8% (focus to yolk absorption), to 10.6% (focus to otolith edge).

Distribution and abundance

Pelagic and benthic goosefish were collected on the continental shelf in waters from the Gulf of Maine, Georges Bank, and the Middle Atlantic Bight (Table 1, Fig. 1A). Major sources of data for pelagic juveniles were the NMFS Hydroacoustic Survey 2000 to 2001, collections from the Harvard Museum of Comparative Zoology (MCZ), and the NMFS Marine Resources Monitoring, Assessment and Prediction Program (MARMAP) Survey spanning from 1977 to 1987 (Morse et al., 1987), as well as miscellaneous collections from throughout the study area. The primary source for recently settled benthic individuals (n=6731; 20–200 mm TL) was the historical scallop survey conducted by NMFS (Serchuk and Wigley, 1986).

Food habits and habitat

Fish used for analysis of food habitats in relation to settlement were collected from a variety of sources (Table 1). Immediately after capture, whole fish were either flash

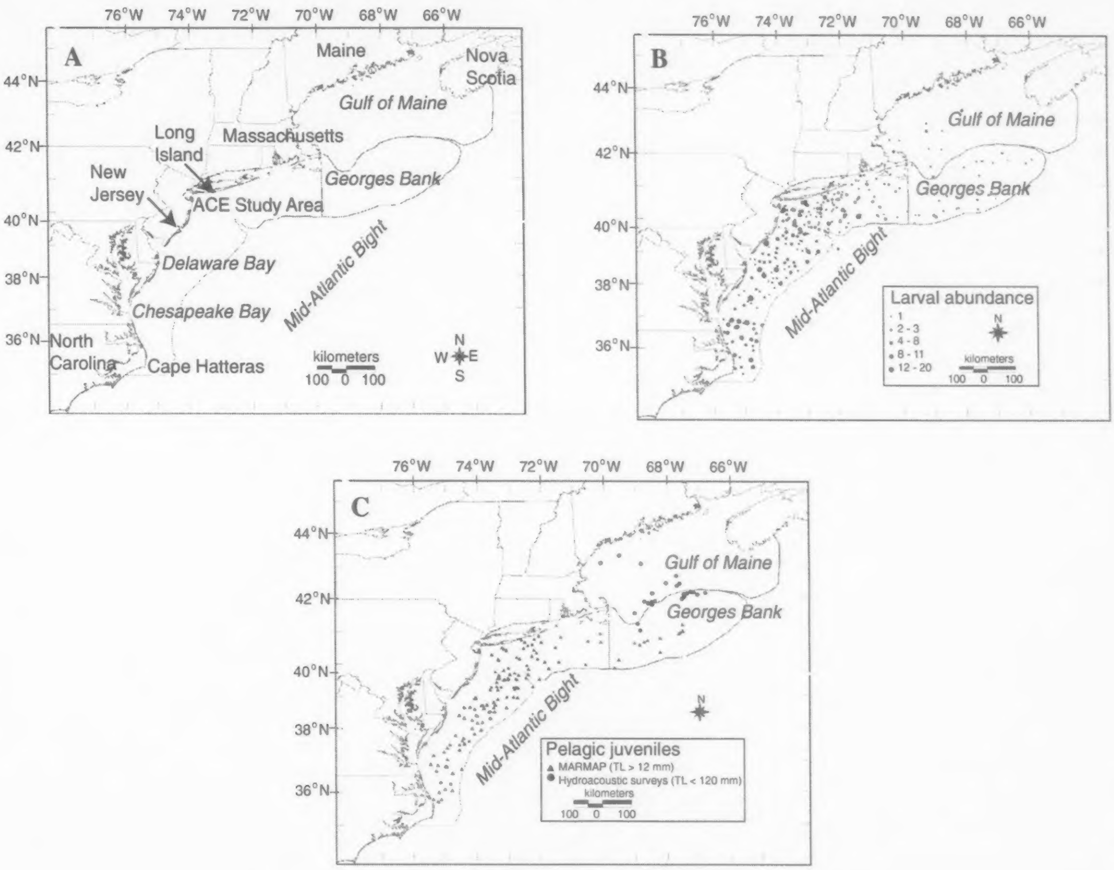
A
76°W
74°W
72°W
70°W
68°W
66°W
44°N
42°N
40°N
38°N
36°N
Maine
Nova Scotia
Gulf of Maine
Long Island
Massachusetts
New Jersey
Georges Bank
ACE Study Area
Delaware Bay
Chesapeake Bay
Mid-Atlantic Bight
North Carolina
Cape Hatteras
kilometers
100 0 100
N
W
E
S
B
Gulf of Maine
Georges Bank
Mid-Atlantic Bight
Larval abundance
1
2-3
4-8
8-11
12-20
C
Gulf of Maine
Georges Bank
Mid-Atlantic Bight
Pelagic juveniles
MARMAP (TL > 12 mm)
Hydroacoustic surveys (TL < 120 mm)

Figure 1

(**A**) Study area, including the Middle Atlantic Bight, Georges Bank, and Gulf of Maine. Study area boundaries are indicated by the light gray lines, which in most instances approximate the 200-m isobath. ACE = Army Corps of Engineers. (**B**) Distribution of larval (≤12 mm total length [TL]) goosefish *(Lophius americanus)* in the study area based on National Marine Fisheries Service and Marine Resources Monitoring, Assessment and Prediction sampling programs during the period from 1977 to 1987. Size of the symbol at each location is in proportion to the composite abundance (number of fish per location). (**C**) The distribution and abundance of pelagic juvenile (>12 to 130 mm TL) goosefish in the study area based on composite collections (Table 1).

frozen or preserved in ethanol to preserve stomach contents. In the laboratory, frozen fish were thawed, fish lengths (TL mm) were recorded, and stomachs were extracted and placed in 95% ethanol. A solution of rose bengal was later added to the stomach contents to aid in the identification of the contents. Upon examination, the proportion (by weight) of each prey category was determined according to the sieve-fractionation method of Carr and Adams (1972), by using sieves of three sizes (2000, 850, and 75 μ). All prey were identified to the lowest taxonomic level practical.

General inferences about the habitats of YOY goosefish were based on the location and depth of collection and the known habitat of items found in the stomach contents of goosefish specimens. Special attention was given to whether the prey was of pelagic or benthic origin, if known, to help us identify presettlement (pelagic) and postsettlement (benthic) goosefish. This method was effective in identifying size at settlement in haddock (*Melanogrammus aeglefinus*) for Mahon and Neilson (1987).

Results and discussion

Morphological development

Goosefish undergo changes in morphological features and pigmentation during the transition from pelagic

Table 3

Summary of changes in seven qualitative characters of goosefish (*Lophius americanus*). Size at shift represents the total length (TL) at which 50% of the individuals in the sample achieved an adult state in the character. SE = standard error. Back-calculated lower (CL [lower]) and upper (CL [upper]) 95% confidence limits are shown.

Character	Size at shift (TL, mm, mean ±SE)	CL (lower)	CL (upper)
Body pigmentation	68.64 ±11.46	46.18	91.10
Fin pigmentation	129.97 ±57.95	16.38	243.56
Tubercle development	78.77 ±20.11	39.35	118.20
Esca pigmentation	64.74 ±18.97	27.55	101.92
Illicium pigmentation	64.74 ±9.76	45.60	83.87
Lateral line pigmentation	71.67 ±16.13	40.06	103.28
Cirri	70.55 ±17.27	36.72	104.39

larvae to settled juveniles. The size range examined here (10–188 mm TL) brackets the interval from late larvae to juveniles. All but four of the 18 morphological characters displayed significant shifts in their relations to total length during the transition from pelagic juveniles (Table 2). These shifts occurred between 20.1 mm TL (dorsal base length) and 84.1 mm TL (esca length) resulting in a transformation from a laterally compressed, pelagic shape to a dorso-ventrally compressed, benthic shape. Eleven of the 14 morphological characters shifted from an allometric (body proportions changing) to isometric (body proportions not changing) growth pattern. Many of the allometric changes in characters that occurred during the pelagic phase were related to the flattening of the head and the reorganization of the dorsal fin, particularly the illicium. Five characters exhibited rapid growth (in relation to total length) during the pelagic phase. These characters were lengths of the dorsal fin base, the second dorsal ray (resulting in the development of the illicium and the esca), the snout (to accommodate the illicium), the esca, and the pectoral fin. Six characters exhibited slow growth (in relation to total length) during the pelagic phase to near isometric growth. These included a decrease in head depth, in orbit diameter, in caudal peduncle length, and in the length of the second dorsal ray. A dramatic reduction also occurred in the predorsal length as the anterior dorsal rays migrate towards the snout.

For the characters changes, better described as qualitative transitions (i.e., for changes in pigment, in the development of tubercle and cirri) and scored either as representing a larval (0) or juvenile-adult (1) state (Table 3), the start of such changes began at about 30 mm TL and ended at about 120 mm TL. The most dramatic changes occurred between 60 and 80 mm TL. The size range over which changes in fin pigmentation occurred was broader (16–243 mm TL). Although the timing of fin pigmentation may be intrinsically more variable than the other qualitative characters that were scored, the variability in fin pigmentation can also be an artifact of preservation technique.

As a result of these procedures, the changes in morphometric and character state traits (i.e., the changes in the shape from a lateral compressed pelagic larvae with long trailing pelvic fins to a dorsoventrally compressed head and body with much shorter pelvic fins as represented in some published illustrations) were quantified (Fahay, 1983; Caruso, 2002). These general changes in body proportions were found to be similar to those of *L. piscatorius* (Tåning, 1923; Dahlgreen, 1928) and *L. budegassa* (Stiasny, 1911; Bowman, 1919).

Several of the specimens evaluated for size-specific character transitions appeared to be at the pelagic juvenile stage (i.e., they were 21.6, 30.7, and 32.3 mm TL), although they were reportedly collected with benthic sampling gear. We suspect that these individuals were inadvertently collected in the water column because 1) they shared the same morphological and pigmentation characters as other pelagic individuals, 2) they were collected with gear that lacked opening and closing capability and thus the specimens could have been collected anywhere in the water column, and 3) the collection data indicated that in each instance the sampling gear spent more time in the water column than it did on the bottom. We therefore treated these individuals, in subsequent analyses, as pelagic juveniles.

Size and age at early life history events

The distribution of YOY goosefish was affected to a large degree by the timing and location of reproduction. Along much of the northeast coast of the United States, spawning occurs from spring through early fall (Wood, 1982; Hartley, 1995; Caruso, 2002), although exact details of spawning locations are lacking (Steimle et al., 1999). Collections during May through July 1996–99 in the surf zone (0–2 m, mean=0.66 individuals/100 m^3) and nearshore (6–7 m, mean=0.68 individuals/100 m^3) off northern New Jersey between Long Branch and Manasquan Inlet (Army Corps of Engineers [ACE] study area, Fig. 1A) showed densities of larval (3.6–15.6 mm TL, mean 7.6 mm) goosefish to be large in June (peak)

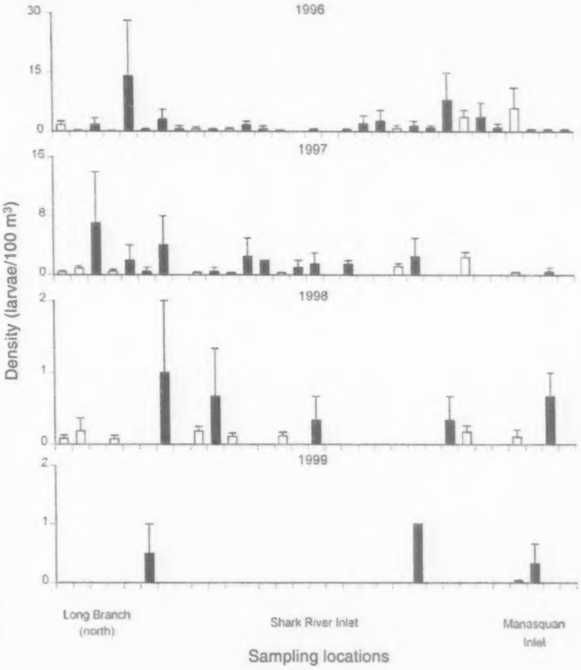

Figure 2

Composite spatial distribution and density (vertical lines above bars=mean standard error) of larval goosefish (*Lophius americanus*) sampled along the northern New Jersey coast (Fig. 1, Army Corps of Engineers) based on nearly equally spaced sampling locations between Long Branch and Manasquan Inlet, NJ, from 1996 through 1999. Samples were collected in the surf zone (0 to 2 m, closed bars, n=22 sampling stations) and in nearshore waters (6 to 7 m, open bars, n=9 sampling stations).

and July (Fig. 2). These collections of goosefish larvae were consistent with a May–June reproductive period estimated from gonadal condition of specimens collected in the area from Cape Hatteras to southern New England (Armstrong et al., 1992).

Our examination of lapillar otoliths provided estimates of the timing of several early life history events. There was good correspondence between the release of just-hatched larvae from the veil and the formation of a hatching check on the lapilli of laboratory-reared individuals. There were multiple microincrements before hatching (mean=5, range: 0–8). The variable number of microincrements prior to a "hatching check" on the lapillar otoliths may reflect the completion of hatching from the chorion and subsequent release of larvae from the egg veil. The completion of the yolk absorption appeared to correspond with a second check. The hatching and yolk absorption checks corresponded to similar checks in the otoliths of *L. piscatorius* (Hislop et al., 2001). Further, examination of otoliths from juvenile goosefish caught in the Middle Atlantic Bight indicated good correspondence between the hatching check and back-calculated mean size at hatching (4.5 mm TL, Fig. 3) and hatching sizes (2.5–4.5 mm TL) (Caruso, 2002). Back-calculations to a hatching check in lapilli (see below) indicated that hatching in specimens collected in the Middle Atlantic Bight occurred from June to October and peaked around July. This prolonged period of spawning and hatching was in agreement with several other spawning and hatching estimates for goosefish in the area (Caruso, 2002). The check on lapillar otoliths corresponding to yolk absorption occurred after 9–26 (mean=18) increments (days) at reported sizes of 6–8 mm TL (Caruso, 2002; Everly, 2002).

A third check (Fig. 3), which we believe corresponded with settlement, occurred in 57% of the lapilli examined. Back-calculated lengths at this check resulted in estimates of sizes at settlement from 52–83 (mean=68) mm TL and at ages 34–71 days after hatching. Individuals at these sizes were undergoing rapid changes in

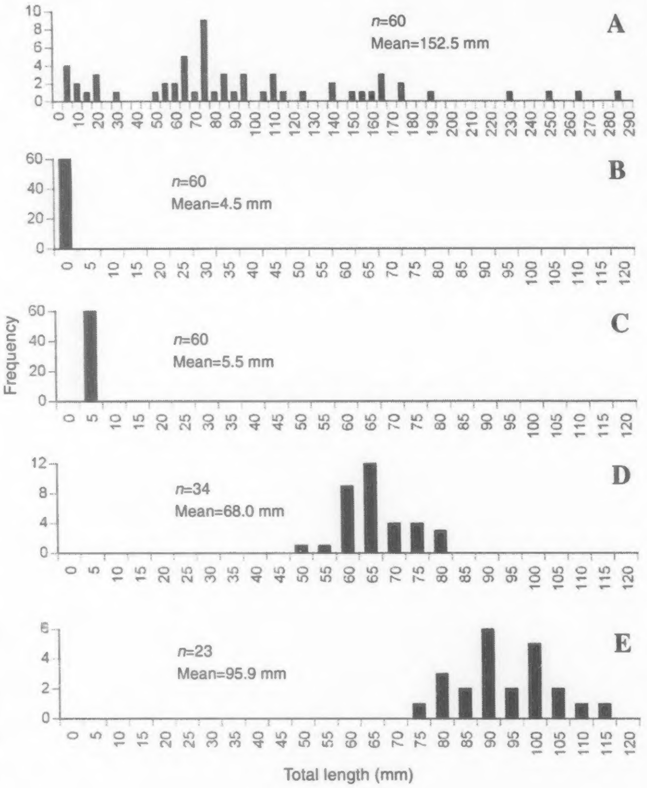

Figure 3

Sizes (total length mm) of goosefish (*Lophius americanus*) during the first year of life. (**A**) Size of goosefish at collection. All other sizes are based on back-calculated sizes from lapillar otoliths. (**B**) Size at formation of hatching check. (**C**) Size at absorption of yolk. (**D**) Size at settlement check. (**E**) Size at formation of first annulus.

relative body proportions as they approached or equaled the juvenile-adult condition (Table 2). Most of these changes occurred between 30 and 120 mm TL and were especially prominent in individuals of 60–80 mm TL. Settlement, as indicated by the length frequency of pelagic and benthic individuals, occurred over a relatively large range of sizes (Figs. 3 and 4). This interpretation may have been influenced by gear biases, the seasonal nature of the collections, and the ability of *Lophius* spp. to re-enter the water column, as occurs for *L. americanus* (Bigelow and Schroeder, 1953) and *L. piscatorius* (Hislop et al., 2000). The overlap in the magnitude of the size range of pelagic and benthic specimens was approximately 30–120 mm depending on the sampling technique (Figs. 3 and 4). Most of the individuals larger than 60 mm TL collected from May to November in the pelagic zone were collected with a mid-water trawl. The smallest benthic individuals (<60 mm TL) were collected in June, July, and August as incidental captures in scallop dredges. Benthic individuals were also collected, at low levels, from September to November. Together, these observations suggest that settlement occurs at sizes of 30–83 mm TL and extends from June into November. The two smallest settled individuals previously reported were 64 and 76 mm (Connolly, 1921). Similarly small-size settled individuals were reported for individuals of *L. piscatorius* (Bowman, 1919).

The growth of YOY goosefish appears to be fast compared to that of other north temperate marine fishes. Using size at capture, as well as estimates of age, size, and life history event checks deduced from otoliths, we estimated growth rates of 1.4 and 1.3 mm/day for the pelagic and benthic YOY life stages, respectively. A marginal increment analysis of lapilli indicated that the first annulus forms at sizes of 70–119 (mean=95.8) mm TL (Fig. 2). This estimate of size at first annulus forma-

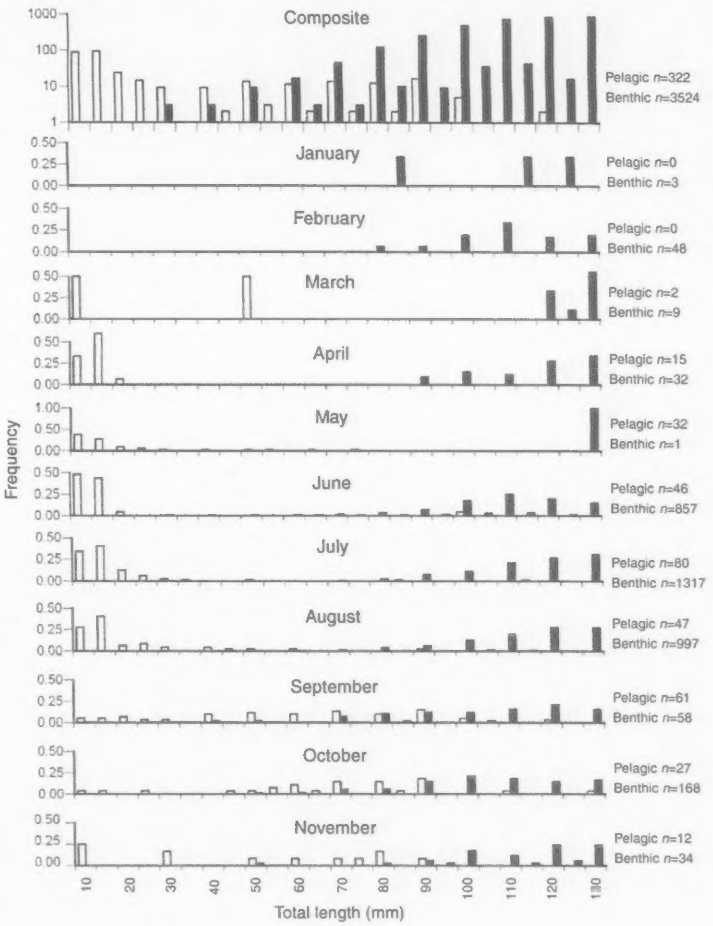

Figure 4

Composite and monthly length-frequency distributions of pelagic (open bars) and benthic (closed bars) goosefish (*Lophius americanus*) based on collections from the Middle Atlantic Bight, Georges Bank, and Gulf of Maine (Table 1; Fig. 1).

tion was consistent with estimates from whole goosefish otoliths made by resource scientists (Lang[2]).

Distribution and abundance

Spawning of goosefish, as inferred from the distribution of larvae ($\leq$12 mm TL) is centered in the Middle Atlantic Bight (Fig. 1B). Far fewer larvae have been collected on Georges Bank and in the Gulf of Maine relative to the Middle Atlantic Bight, although sampling effort was comparable between regions (Steimle et al., 1999). Local collections of goosefish larvae (range: 1.7–10.8 mm notochord length [NL]) along the northern New Jersey coast from 1996 to 1999 reveal their densities to be similar between the surf (mean=0.68 [±0.19] individuals/100 m^3) and nearshore (mean=0.66 [±0.11] individuals/100 m^3) habitats (Fig. 2). The abundance of larvae along the northern New Jersey coast was variable and there were no consistent patterns between years (Fig. 2). These local, inshore data show that the larvae inhabit waters shallower than those surveyed in the NMFS MARMAP program.

---

[2] Lang, K. 2004. Personal commun. National Oceanic and Atmospheric Administration, National Marine Fisheries Service, Northeast Fisheries Science Center, 166 Water Street, Woods Hole, MA 02543-1026.

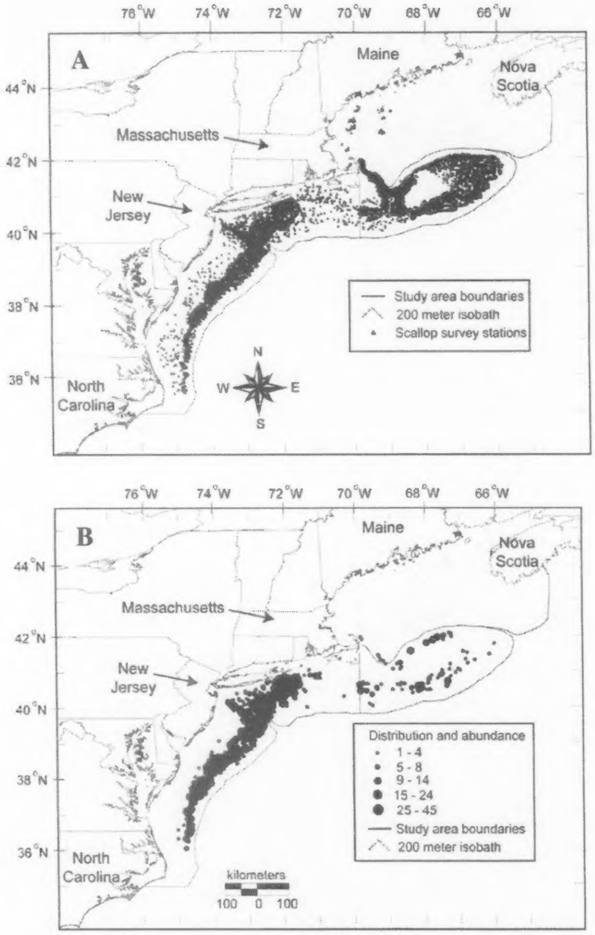
A
76°W
74°W
72°W
70°W
68°W
66°W
44°N
42°N
40°N
38°N
36°N
Maine
Nova Scotia
Massachusetts
New Jersey
North Carolina
N
S
E
W
Study area boundaries
200 meter isobath
Scallop survey stations
B
Distribution and abundance
1-4
5-8
9-14
15-24
25-45
kilometers
100 0 100

Figure 5

Distribution of (**A**) scallop dredge survey stations in the study area during 1982–2001 and (**B**) collections of benthic young-of-the-year (20–130 mm total length) goosefish *(Lophius americanus)* from these same surveys during the same period.

In the Middle Atlantic Bight, settlement may occur in a smaller area than that over which larvae are distributed. Even though the larvae (≤12 mm TL) were generally evenly distributed over the continental shelf up to and including the surf zone (Fig. 1B), pelagic juveniles (>12–120 mm TL) were concentrated in the middle and outer portion of the shelf (Fig. 1C). An exception to this pattern was the collection of some pelagic juveniles in waters close to the coast of Long Island, NY. Although goosefish larvae were not abundant on Georges Bank and in the Gulf of Maine (Fig. 1B), pelagic juveniles were captured there in relatively large numbers along the northern edge of Georges Bank and the adjacent portion of the Gulf of Maine (Fig. 1C). In these latter collections during NMFS hydroacoustic cruises from September through October 2000 and 2001, frame trawls were used to verify fish species. This sampling gear captured pelagic juveniles (50–130 mm TL) at depths ranging from the surface to 95 m within water depths of 65–191 m.

Most of the data and the majority (76%) of the benthic YOY (20–120 mm TL) goosefish specimens were collected from the NMFS scallop assessment surveys in the Middle Atlantic Bight and on Georges Bank during 1982 to 2001 (Fig. 5). The distribution of YOY goosefish reflects the boundaries of this survey. In the Middle Atlantic Bight, benthic YOY goosefish were collected on the central portion of the continental shelf from approximately the Virginia–North Carolina state line north to eastern Long Island, NY, where they were found in shallow nearshore waters. The benthic YOY goosefish also were present up the Hudson Canyon shelf valley. Few benthic YOY goosefish were collected in waters off Rhode Island and southern Massachusetts—likely the result of lower sampling effort (Fig. 5). On Georges Bank, the benthic YOY goosefish were distributed around the perimeter of the bank but were not collected as frequently on the eastern end of the bank, even though these areas were well sampled. YOY goosefish were occasionally collected off the "elbow" of Cape Cod, but were found infrequently in the Gulf of Maine.

Benthic juveniles are probably more widely distributed over the continental shelf and on the upper slope than indicated by the sea scallop survey. The best evidence for their distribution in deeper waters has been from four seasonal cruises centered on the continental shelf and slope off Virginia covering depths to 3080 m (Wenner, 1978; Wenner[3]). Many juveniles were collected at depths from 75–900 m and the greatest density was found at 200–399 m depths. A large number of these individuals (30%) were <120 mm TL and the smallest specimen was 53.4 mm TL.

Food habits and habitats

The stomach contents of YOY goosefish in the Middle Atlantic Bight were diverse (Table 4). The dominant prey group in the stomach contents comprised fish (45.1% frequency of occurrence [FO]) and crustaceans (17.6% FO). The most numerous prey fish were gadids, *Ammodytes*, and bothid and pleuronectid flatfishes. Invertebrates were also consumed, including mollusks, chaetognaths, nematodes, nemerteans, trematodes, polychaetes, and crustaceans. This diversity of prey has been frequently reported for juveniles and adults of *L. americanus* (Sedberry, 1983; Armstrong et al., 1996; Bowman et al., 2000; Caruso, 2002) and other congeners, including *L. piscatorius* (Tsimenidis, 1980; Crozier, 1985, Laurenson and Priede, 2005) and *L. budegassa* (Tsimenidis, 1980). The greater occurrence of invertebrates in the stomachs of *L. americanus* in our study (67.2% FO, Table 4) than in prior studies (Sedberry, 1983; Armstrong et al., 1996) was probably due to our emphasis on examining smaller YOY fish.

Table 4

Prey items of young-of-the-year and small juvenile (age 1+) goosefish (*Lophius americanus*). Gut contents were expressed by percentage frequency of occurrence (% FO) across all specimens examined and average percent total weight in individual stomachs. Determination of prey habitat (P=pelagic, B=benthic, I=indeterminate, potentially both benthic and pelagic habitat) was based on knowledge of the life history of prey.

Prey	Habitat	% FO	% Total weight
Osteichthyes	B, I	79.4	86
Invertebrates		67.2	8.8
Molluska	I, B	1.6	7.2
Chaetognatha	P	3.1	<0.1
Nematoda			
(free-living)	B	3.1	<0.1
(unspecified)	I	1.5	<0.1
Nemertea	B	4.6	<0.1
Trematoda	I	7.6	<0.1
Polychaeta	B	3.8	<0.1
Hirudinea	I	0.8	<0.1
Crustacea	B, P	17.6	0.3
Other	I	58	5.2

The food habits of YOY goosefish varied with fish size; a shift to a larger proportion of fish in the diet occurred at larger sizes (Fig. 6, A and B). Although invertebrates were common in the diet of all YOY examined, they occurred in 100% of the stomach contents at sizes smaller than approximately 50 mm TL and to a variable extent in most larger YOY fish. The vast majority of stomach contents, on the basis of weight (Table 4), were composed of fish in larger goosefish. Prior studies are equivocal on ontogenetic change in diet. Armstrong et al. (1996) reported smaller (<200 mm TL) individuals to have a higher proportion of invertebrates in their diet than we observed. Sedberry (1983) found the diets of all size classes of goosefish, including the two smallest (<100 and 101–200 mm), were dominated by fishes. Our results clarify the sizes at which this change to piscivory occurs (i.e., >50 mm TL).

The food habits also changed as a result of the transition from presettlement (pelagic) to postsettlement (benthic) habitats (Fig. 6, C and D). Individuals that were captured in the water column (<50 mm TL) had pelagic taxa such as chaetognaths, hyperiid amphipods, calanoid copepods, and ostracods in their stomachs. The dominance of pelagic prey was apparent whether prey were quantified as percent weight or percent frequency of occurrence. The stomach contents of larger individuals (60–280 mm TL, YOY, and small juveniles) were dominated by benthic prey when expressed as percent frequency of occurrence. The shift to benthic prey was not as obvious, however, when prey were expressed as percent weight. This was due to a large percentage of prey items that could not be assigned unequivocally to either benthic or pelagic habitats. The benthic prey comprised a variety of fishes and crustaceans including amphipods, cumaceans, mysids, shrimps, nematodes, nemerteans, and polychaetes (Table 4). The location of capture of some prey, such as that of small gadids and squid, was considered indeterminate because these prey could have been consumed by goosefish in either pelagic or benthic habitats.

---

[3] Wenner, C. 2004. Personal commun. Marine Resources Research Institute South Carolina Department of Natural Resources, P.O. Box 12559, Charleston, SC 29422.

Conclusions

It appears that goosefish in the Middle Atlantic Bight spend ~5–10 weeks in the plankton as larvae and pelagic juveniles. As they change from pelagic larvae and juveniles to benthic juveniles (ca. 30–85 mm TL from June to November), they undergo major changes in body shape, pigmentation, and diet. Some of these life history changes are reflected in the microstructure of lapillar otoliths. Overall, changes in these suites of characteristics are most evident before and during settlement. Most of the events in the early life history of goosefish appear to occur without dependency on water depth or location across the continental shelf. Larvae, pelagic juveniles, and benthic juveniles tend to be most abundant on the mid to outer continental shelf, but they are also widely distributed inshore, indicating that they are habitat generalists.

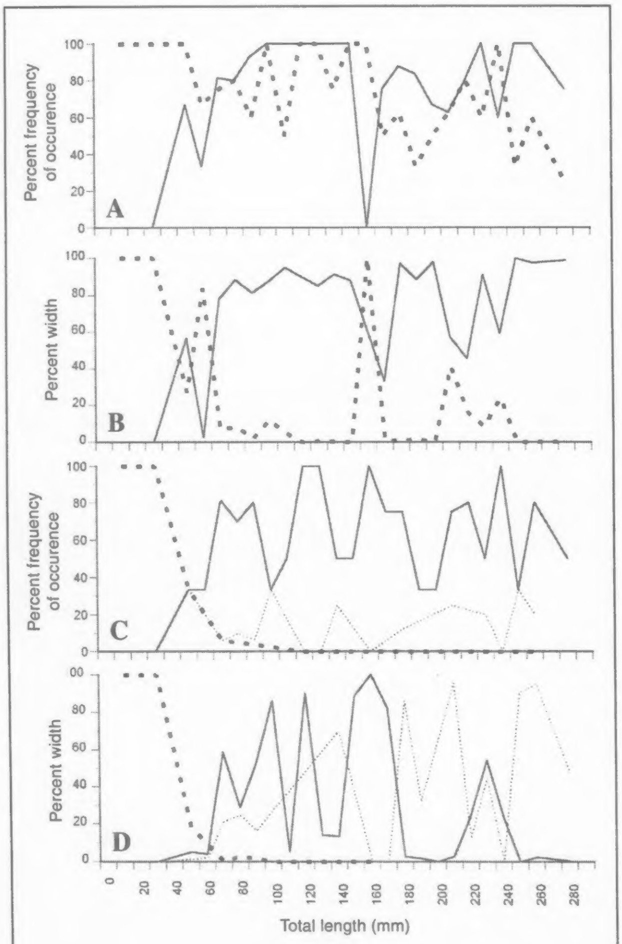

Figure 6

Change in diet (**A, B**) and habitat (**C, D**) of young-of-the-year goosefish *(Lophius americanus)* with increasing total length (TL). Diet changed from mostly invertebrates (dotted line) to mostly fish (solid line), whether expressed as percent frequency of occurrence (A) or percent weight in stomach contents (B). Habitat, determined from stomach contents, changed as a function of goosefish sizes (TL). Prey in stomach was expressed as frequency of occurrence (C) and percent weight (D). Prey habitats, based on knowledge of prey life history, were classified as either benthic (solid line), pelagic (large dotted line), or indeterminate (small dotted line).

Acknowledgments

L. Despres, A. Richards, M. Jech, V. Nordhal, P. Berrien, and V. Guida provided access to distribution and abundance data. K. Lang assisted with otolith interpretation. Others who provided access to data include J. Musick, B. Cowen, M. Sullivan, B. Steves, L. Van Guelpen, C. Wenner, K. Hartel, D. Clarke, and M. Burlas. This research was supported in part by the National Marine Fisheries Service (NMFS)—Rutgers University Cooperative Marine Education and Research (CMER) program, by NMFS Northeast Fisheries Science Center, and by the Institute for Marine and Coastal Sciences (IMCS), Rutgers University. This is Institute of Marine and Coastal Sciences contribution number 2007-2.

Literature cited

Almeida, F. P., D. L. Hartley, and J. Burnett.
1995. Length-weight relationships and sexual maturity of goosefish off the northeast coast of the United States. N. Am. J. Fish. Manag. 15:14–25.

Armstrong, M. P., J. A. Musick, and J. A. Colvocoresses.
1992. Age, growth, and reproduction of the goosefish *Lophius americanus* (Pisces: Lophiiformes). Fish. Bull. 90:217–230.
1996. Food and ontogenetic shifts in feeding of the goosefish, *Lophius americanus*. J. Northwest Atl. Fish. Sci. 18:99–103.

Bigelow, H. B., and W. C. Schroeder.
1953. Fishes of the Gulf of Maine. U.S. Fish Wildl. Serv., Fish. Bull 53, 577 p.

Bowman, A.
1919. The eggs and larvae of the angler (*Lophius piscatorius*) in Scottish waters. Fish Board Scotland Rep. Sci. Invest. 1919:(2):21–23.

Bowman, R. E., C. E. Stillwell, W. L. Michaels, and M. D. Grosslein.
2000. Food of Northwest Atlantic fishes and two common species of squid. U.S. Dep. Commer., NOAA Tech. Memo. NMFS-F/NE-155, 138 p.

Carr, W. E., and C. A. Adams.
1972. Food habits of juvenile marine fishes: evidence of the cleaning habit in the leath-

erjacket, *Oligoplites saurus*, and the spottail pinfish, *Diplodus holbrooki*. Fish. Bull. 70:1111–1120.

Caruso, J. H.

1983. The systematics and distribution of the lophiid anglerfishes: II. Revisions of the genera *Lophiomus* and *Lophius*. Copeia 1983:11–30.

2002. The goosefishes or monkfishes. Family Lophidae. *In* Bigelow and Schroeder's Fishes of the Gulf of Maine (B. B. Collette, and G. Klein-MacPhee, eds.), 561 p. Smithsonian Institution Press, Washington, D.C.

Connolly, C. J.

1921. On the development of the angler (*Lophius piscatorius L.*). Contrib. Can. Biol. 7:115–124.

Crozier, W. W.

1985. Observations on the food and feeding of the angler-fish, *Lophius piscatorius L.*, in the northern Irish Sea. J. Fish Biol. 27:655–665.

Dahlgreen, U.

1928. The habits and life history of *Lophius*, the angler fish. Nat. Hist. 28:18–32.

Everly, A. W.

2002. Stages of development of the goosefish, *Lophius americanus*, and comments on the phylogenetic significance of the development of the luring apparatus in Lophiiformes. Environ. Biol. Fishes 64:393–417.

Fahay, M. P.

1983. Guide to the early stages of marine fishes occurring in the western North Atlantic Ocean, Cape Hatteras to the southern Scotian Shelf. J. Northwest Atl. Fish. Sci. 4:1–423.

Fuiman L., K. R. Poling, and D. M. Higgs.

1998. Quantifying developmental progress for comparative studies of larval fishes. Copeia 3:602–611.

Hartley, D. L.

1995. The population biology of the goosefish, *Lophius americanus*, in the Gulf of Maine. M.S. thesis, 142 p. Univ. of Mass., Amherst, MA.

Hislop, J. R., A. Gallego, M. R. Heath, F. M. Kennedy, S. A. Reeves, and P. J. Wright.

2001. A synthesis of the early life history of the anglerfish, *Lophius piscatorius* (Linnaeus, 1758) in northern British waters. ICES J. Mar. Sci. 58:70–86.

Hislop, J. R. G., J. C. Holst, and D. Skagen.

2000. Near-surface captures of post-juvenile anglerfish in the North-east Atlantic–an unsolved mystery. J. Fish Biol. 57:1083–1087.

Hubbs, C. L., and K. F. Lagler.

1958. Fishes of the Great Lakes region, 332 p. Univ. Michigan Press, Ann Arbor, MI.

Jean, Y.

1965. Seasonal distribution of monkfish along the Canadian Atlantic mainland. J. Fish. Res. Board Can. 22:621–624.

Laurenson, C. H., and I. G. Priede.

2005. The diet and trophic ecology of anglerfish *Lophius piscatorius* at the Shetland Islands, U.K. J. Mar. Biol. Assn. U.K. 85:419–424.

Mahon, R., and J. D. Neilson.

1987. Diet changes in Scotian Shelf haddock during the pelagic and demersal phases of the first year of life. Mar. Ecol. Prog. Ser. 37:123–130.

Martinez, C. M.

1999. The reproductive biology of goosefish, *Lophius americanus*. M.S. thesis, 78 p. Univ. Rhode Island, Naragansett, RI.

Michaels, W. L. (ed.)

2001. Report on the third Northwest Atlantic herring acoustic workshop, Univ. Maine, Darling Marine Center, Walpole, ME, March 13–14, 2001. U.S. Dep. Commer., NOAA Tech. Memo.NMFS-NE-166, 18 p.

Morse, W. W., M. P. Fahay, and W. G. Smith.

1987. MARMAP surveys of the continental shelf from Cape Hatteras, North Carolina to Cape Sable, Nova Scotia (1977–1984). Atlas no. 2: Annual distribution patterns of fish larvae. U.S. Dep. Commer., NOAA Tech. Memo. NMFS-NEFSC, 215 p.

Policansky, D.

1983. Size, age and demography of metamorphosis and sexual maturation in fishes. Amer. Zool. 23:57.63.

Scott, J. S.

1982. Selection of bottom type by groundfishes of the Scotian Shelf. Can. J. Fish. Aquat. Sci. 39:943–947.

Scott, W. B., and M. G. Scott.

1988. Atlantic fishes of Canada. Can. Bull. Fish. Aquat. Sci. 219, 731 p.

Sedberry, G. R.

1983. Food habits and trophic relationships of a community of fishes on the outer continental shelf. NOAA Tech. Rep. NMFS-SSRF-773, 56 p.

Serchuk, F. M., and S. E. Wigley.

1986. Evaluation of USA and Canadian research vessel surveys for sea scallops (*Placopecten magellanicus*) on Georges Bank. J. Northwest Atl. Fish. Sci. 7:1–13.

Steimle, F. W., W. W. Morse, and D. L. Johnson.

1999. Essential fish habitat source document: Goosefish, *Lophius americanus*, life history and habitat characteristics. NOAA Tech. Memo. NMFS-NE-127, 31 p.

Steves, B. P., R. K. Cowen, and M. H. Malchoff.

1999. Settlement and nursery habits for demersal fishes on the continental shelf of the New York Bight. Fish. Bull. 98: 167–188.

Stiasny, G.

1911. Regarding certain postlarval development stages of *Lophius piscatorius* L. Arbeit. Zool. Inst. Vienna 19:54–74. [In German.]

Tåning, Å. V.

1923. *Lophius*. Danish Oceanogr. Exped., 1908–10, Rep. no. 7, vol. 2 (Biol.), A 10, 30 p.

Toms, J. D., and M. L. Lesperance

2003. Piecewise regression: a tool for identifying ecological thresholds. Ecology 84:2034–2041.

Tsimenidis, N. H.

1980. Contribution to the study of the angler-fishes *Lophius budegassa* Spinola, 1807 and *L. piscatorius* L. 1758 in Greek seas. Spec. Publ. Inst. Oceanogr. Fish. Res. Athens 4, 190 p. [In Greek.]

Wenner, C. A.

1978. Making a living on the continental slope and in the deep-sea: life history of some dominant fishes of the Norfolk Canyon area. Ph.D. diss., 294 p. College of William and Mary, Williamsburg, VA.

Wiley, M. L., and B. B. Collette.

1970. Breeding tubercles and contact organs in fishes: their occurrence, structure, and significance. Bull. Am. Mus. Nat. Hist. 143(3):145–216.

Wood, P. W., Jr.

1982. Goosefish, *Lophius americanus*. *In* Fish distribution (M. D. Grosslein, and T. R. Azarovitz, eds.), p. 67–70. MESA New York Bight Atlas Monograph 15. N.Y. Sea Grant Institute, Albany, NY.

Abstract—A generalized Bayesian population dynamics model was developed for analysis of historical mark-recapture studies. The Bayesian approach builds upon existing maximum likelihood methods and is useful when substantial uncertainties exist in the data or little information is available about auxiliary parameters such as tag loss and reporting rates. Movement rates are obtained through Markov-chain Monte-Carlo (MCMC) simulation, which are suitable for use as input in subsequent stock assessment analysis. The mark-recapture model was applied to English sole (*Parophrys vetulus*) off the west coast of the United States and Canada and migration rates were estimated to be 2% per month to the north and 4% per month to the south. These posterior parameter distributions and the Bayesian framework for comparing hypotheses can guide fishery scientists in structuring the spatial and temporal complexity of future analyses of this kind. This approach could be easily generalized for application to other species and more data-rich fishery analyses.

Defining plausible migration rates based on historical tagging data: a Bayesian mark-recapture model applied to English sole (*Parophrys vetulus*)

Ian J. Stewart
Email address: Ian.Stewart@noaa.gov
National Oceanic & Atmospheric Administration
National Marine Fisheries Service
Northwest Fisheries Science Center
2725 Montlake Boulevard East (F/NWC4)
Seattle, Washington 98112-2097

Mark-recapture data are used to estimate growth parameters, mortality rates, and population size (Hilborn and Walters, 1992; Quinn and Deriso, 1999). However, researchers are often interested in home range, site-fidelity, or migration rates which are important quantities for management and the design or evaluation of marine protected areas. The standard approach with mark-recapture data is to use an integrated model linking the underlying dynamics of the tagged population with an observation model describing the predicted recoveries and a likelihood function relating observations with model predictions (Hilborn, 1990). This integrated method has been applied to many fisheries, ranging from those for sablefish (*Anoplopoma fimbria*; Heifetz and Fujioka, 1991) to those for yellowfin tuna (*Thunnus albacares*; Hampton and Fournier, 2001).

Requirements of the integrated method include extensive tag recovery, data on fishing effort, auxiliary information on tag loss, as well as reporting rates in order to adequately estimate movement rates and other parameters (Punt et al., 2000). Analysis often benefits from fixing some model parameters at reasonable values based on external analysis or expert opinion. However, the values selected for these parameters can represent a substantial source of uncertainty in the estimates of movement rates because these parameters are poorly known for many historical tagging projects. Bayesian methods start with prior distributions for the parameters of interest (information available before the analysis), and integrate over the joint posterior distribution of all model parameters, capturing parameter uncertainty as well as the correlation structure among these parameters. The Bayesian approach provides a logical alternative to likelihood methods when the researcher is faced with substantial uncertainty in the data and input parameters and has a desire for a probabilistic interpretation of the results (Punt and Hilborn, 1997).

One way in which uncertainty and auxiliary information about migration rates could be included in stock assessments is through the use of informative priors based on Bayesian analysis of mark-recapture data. Priors specifically applicable to west coast groundfish stock assessments have been derived for survey catchability (Millar and Methot, 2002), the steepness of the stock-recruit function (Dorn, 2002), the relationship between catch per unit of effort (CPUE) and abundance (Harley et al., 2001), and for other studies currently underway. Researchers in other regions have aggregated historical tagging information for commercially important species, such as north Atlantic cod (*Gadus morhua*; Robichaud and Rose, 2004). However, in the northeast Pacific there are many groundfish tagging studies that have never been analyzed simultaneously or used in stock assessments.

Manuscript submitted 6 Novembber 2006 to the Scientific Editor.

Manuscript approved for publication 22 May 2007 by the Scientific Editor.

Fish. Bull. 105:470–484 (2007).

Stock assessments of west coast flatfish (and other groundfish species) have been based on one of two assumptions about latitudinal movement: no movement at all (multiple isolated stocks) or complete mixing (single stock models). In a Bayesian context, these two opposite assumptions fix the magnitude of movement rates before analysis and therefore can be considered highly informative priors. The goal of this study was to provide a generalized method with which to develop informative priors on movement rates based on quantitative analysis of historical tagging data, thereby adding a third choice of prior for use in stock assessments.

Materials and methods

Model development

A model very similar to those used in other mark-recapture studies (e.g., Hilborn, 1990; Hampton and Fournier, 2001) was developed to predict the number of tags returned from multiple tag-release events (tags released in one spatial area over a short period of time; hereafter referred to as a data set) by projecting each population forward in time. Predicted returns are tracked by month and for each spatial area. The predicted number of tags present ($\hat{N}$) in each data set (d), month (t), and area (i) are given by

$$\hat{N}_{d,t,i} = \sum_{j} \left(\hat{N}_{d,t-1,j} P_{t,j\rightarrow i} \right) e^{-\frac{(F_d+M+\Omega)}{12}}, \tag{1}$$

where F_d = the average fishing mortality rate for each data set;
M = the average natural mortality rate; and
Ω = the instantaneous rate of tag loss (ongoing "attrition" due to fouling or mechanical failure; often referred to as "type-2 tag loss" in traditional terms; Beverton and Holt, 1957).

The subscript j denotes all possible source areas, and the proportion of individuals moving from each area to another in any month is given by the matrix P_t. The P_t matrix (area × area for month t) includes nonzero values in only the first off-diagonals, and a variable number of parameters within each diagonal depending on the movement hypothesis to be explored. Instantaneous rates are divided by 12 because they are applied on a monthly basis. Predicted numbers in the first month are the reported tag releases (alternately, type-1 tag loss, those tags that are shed immediately after tagging, could be included by multiplying the initial releases by 1 – type-1 tag-loss rate). The predicted recoveries ($\hat{R}$) by data set, month, and area are then

$$\hat{R}_{d,t,i} = \phi \hat{N}_{d,t,i} \left(\frac{F_d}{F_d + M + \Omega} \right) \left(1 - e^{-\frac{(F_d+M+\Omega)}{12}} \right), \tag{2}$$

where ϕ = the reporting rate of captured tags during the time period over which tag recoveries occurred. Given these dynamics, the tagged population and predicted recoveries for all data sets available may be projected forward simultaneously.

The major departure from previous models is the use of a single average fishing mortality rate for each data set (an approach that reflects a lack of direct effort or of fishing mortality information). If only a single data set is analyzed in this manner, it is clear that any heterogeneity in fishing mortality over time or space could result in substantially biased estimates of movement rates. However, if multiple tagging events are analyzed simultaneously, and there is no consistent relationship between location of tag releases and areas of increased fishing mortality, this potential source of bias may be reduced. Were information on the spatial and temporal variability in fishing mortality available, it would be simple (and recommended) to extend the notation further to either input mortality rates directly into the analysis or to estimate them from relative effort.

Variability in observed recoveries is caused by many factors, including schooling behavior, heterogeneous distribution of fishing effort, tag loss or tag reporting over time and space, and by the stochastic nature of very low recovery rates. Because of the many potential sources of extra-model error, a likelihood function that allows for substantial variation among observations is desired. The negative binomial likelihood is the logical choice for this type of tagging data (e.g., Cormack and Skalski, 1992; Hampton and Fournier, 2001). If each tag-release group is assumed to be independent, the full likelihood (L) of the observed recoveries (R) is given by

$$L\left(R_{d,t,i} \middle| \hat{R}_{d,t,i} k\right) = \prod_{d}\prod_{t}\prod_{i} \frac{(k + R_{d,t,i} - 1)!}{(R_{d,t,i})!(k-1)!} \left(1 + \frac{k}{\hat{R}_{d,t,i}} \right)^{-R_{d,t,i}} \left(\frac{\hat{R}_{d,t,i}}{k} + 1 \right)^{-k}, \tag{3}$$

where $\hat{R}$ = the predicted recoveries in a data set, month, and area; and
k = the overdispersion (variance) parameter.

The negative binomial asymptotically approaches the Poisson distribution as the value of the overdispersion parameter moves to infinity (Bishop et al., 1988).

A common problem with historical data is that only summarized reports are available for analysis. Where tag recoveries have been aggregated across time or space, the model predictions and the original observations are no longer on an equivalent scale. This problem is easily dealt with by aggregating the predicted recoveries to match the observed recoveries, while still maintaining the same predictive model structure. However, this method creates different types of comparisons within the likelihood (monthly recoveries compared to monthly recoveries vs. annual recoveries compared to annual recoveries). The method and notation above is therefore extended to estimate a separate overdispersion parameter (k) for each type of data aggregation included in the analysis. The likelihood equation (Eq. 3) becomes

$$L\left(R_{c,d,l}\middle|\hat{R}_{c,d,l},k_c\right)=$$

$$\prod_c\prod_d\prod_l\frac{\left(k_c+R_{c,d,l}-1\right)!}{\left(R_{c,d,l}\right)!\left(k_c-1\right)!}\left(1+\frac{k_c}{\hat{R}_{c,d,l}}\right)^{-R_{c,d,l}}\left(\frac{\hat{R}_{c,d,l}}{k_c}+1\right)^{-k_c}, \qquad (4)$$

where the likelihood component notation remains the same, but the subscripts are revised to include the following: data aggregation type (c), data set (d), and time-space combination (l, identical within each c; e.g., month-area or year-area depending on the level of data aggregation).

Data sources

English sole (*Parophrys vetulus*) was selected for analysis because of the large amount of tagging data available and the commercial importance of the species. English sole are widely distributed from southern California to Alaska (Hart, 1973) and are frequently captured by the bottom-trawl fisheries of both the United States and Canada. Many English sole tagging programs have been conducted by both U.S. and Canadian scientists since the 1930s. These have included releases off the coast of British Columbia (Ketchen, 1956; Forrester, 1969), Washington (Pattie, 1969), Oregon (Harry, 1956), and California (Jow, 1969). Additional tagging within Puget Sound (Menasveta, 1958; Day, 1976) and the Strait of Georgia have focused specifically on population dynamics within these waters. Most tagging data reported between 1946 and 1979 were available only through unpublished reports from the Research Board of Canada, Oregon Department of Fish and Wildlife, and the Washington Department of Fisheries. In total, 44 tagging events (defined as tags released in one area during a one-month period) resulted in the release of 57,839 tags of which 9988 (17.3 %) were recovered. The primary objective of most of these studies was to determine the amount of migration (as a percentage of the total population) that occurred among areas with the highest abundance of English sole (e.g., Harry, 1956).

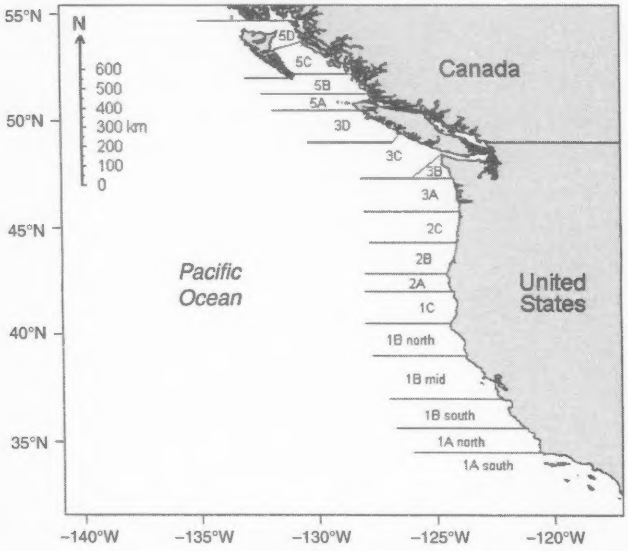

Figure 1

Map of areas based on historical Pacific Marine Fisheries Commission (PFMC) boundaries used in this analysis. The largest PMFC areas, 1A and 2B, were subdivided to make the latitudinal ranges more consistent across all areas.

Tag recoveries have been most frequently reported for the historical Pacific Marine Fisheries Commission (PMFC) areas; these areas were therefore the logical (and only) spatial context in which to analyze the results. To reduce the latitudinal range of the largest PMFC areas, PMFC area 1A was divided into two subareas (north and south of Point Conception) and PMFC area 1B was divided into three subareas (north of Point Arena, between Point Arena and Pigeon Point, and south of Pigeon Point). This division of areas resulted in 17 PMFC-like areas (area 5E is shown for reference only; for simplicity, all data from 5E were treated as if they were collected from 5C or 5D (i.e., 5E data were integrated into similar 5C and 5D areas to make the areas linear) with an average latitudinal span of 138 km (range=83–204 km, Fig. 1). Reporting of tag releases and recoveries was sufficiently detailed to allow an analysis that included these additional boundaries and that did not exclude any studies.

Only studies reporting the area, month, and year for each tagging event were included in this analysis. Additionally, tag recoveries must have been reported at one of four levels of resolution: type-1 resolution, where data were available for year, month, and area for each individual tag recovery; type-2 resolution, where data were available for month and area only; type-3 resolution, where data were available for area only; and type-4 resolution, where data were only available to indicate recovery inside or outside the area of tagging. After this screening (removing 16,375 releases), there were 25 English sole tagging events from the open coast remaining in the analysis, including 17,056 releases and 3464 recoveries; these projects, summarized in Jow (1969), Forrester (1969), and Pattie (1969) ranged from southern California to northern British Columbia and from 1936 to 1965 (Table 1).

There were many differences among individual studies that had to be reconciled or ac-

Table 1

Summary of English sole (*Parophrys vetulus*) tagging events off the coast of the United States and Canada modeled in this article. Years listed include the year of initial tagging through the final tag return. "Number released" represent total numbers tagged in a one Pacific Marine Fisheries Commission (PMFC) area (Fig. 1) in a single month. "Number recovered" and "Percent recovered" represent only those tags with complete recovery information; tags recovered within one month of tagging were excluded. Data quality categories were the following: 1, where data were available for year, month, and PFMC area for each individual tag recovery, 2, where data were available for only month and area, 3, where data were available for area only, and 4, where data were only available to indicate recovery inside or outside the area of tagging. NA = not available.

Years	PMFC area	Number released	Number recovered	Percent recovered	Number excluded	Data quality	Reference
1936–37	1B-south	16	1	6.25	0	1	Jow (1969)
1936–37	1B-south	45	9	20.00	NA	3	Jow (1969)
1938–40	1C	400	25	6.33	5	1	Jow (1969)
1939	1B-south	38	1	2.63	0	1	Jow (1969)
1939–41	1B-mid.	30	4	13.33	0	1	Jow (1969)
1940–42	1B-mid.	746	21	2.82	2	1	Jow (1969)
1940–43	1C	852	61	7.21	6	2	Jow (1969)
1940–46	1B-north	1103	27	3.35	0	1	Jow (1969)
1945–47	3C	24	1	4.35	1	1	Forrester (1969)
1945–51	5D/5E	1505	316	21.21	15	4	Forrester (1969)
1945–51	3C	132	29	21.97	NA	3	Forrester (1969)
1949–51	1B-mid.	926	32	3.47	3	1	Jow (1969)
1949–51	1C	415	69	17.16	13	2	Jow (1969)
1950–51	1C	9	1	11.11	0	1	Jow (1969)
1950–52	1B-south	19	1	5.26	0	1	Jow (1969)
1950–53	1B-mid.	200	5	2.50	0	1	Jow (1969)
1950–56	5D/5E	3039	1405	46.55	21	4	Forrester (1969)
1952–58	5D/5E	2235	737	33.21	16	4	Forrester (1969)
1956–61	3B	871	76	8.82	9	2	Pattie (1969)
1958–59	1C	6	3	50.00	0	3	Jow (1969)
1958–61	1B-mid.	97	6	6.19	0	1	Jow (1969)
1958–63	1C	4130	623	15.84	196	2	Jow (1969)
1959	1B-mid.	103	2	1.94	0	1	Jow (1969)
1963–64	1A-north	2	1	50.00	0	1	Jow (1969)
1963–65	1A-nouth	113	8	7.08	0	3	Jow (1969)
	Total	17,056	3464	20.37	287		

counted for to perform a simultaneous analysis. Where possible, recoveries in the same month as the tagging program were excluded (and subtracted from tag releases, n=287) to avoid potentially skewed estimates of movement and fishing mortality rates before any movement could reasonably have occurred. Exclusion of immediate recoveries is common practice when analyzing tag-recovery data (McGarvey and Feenstra, 2002; Robichaud and Rose, 2004). This decision also obviated having to scale the fishing mortality rate during the first month by the number of days after tagging, which is problematic when tagging has occurred over a number of days or is reported only by the month in which it took place. Many different methods of tagging were used in these studies, but all tags were assumed to have the same rate of tag loss. Comparison of tag loss rates for disk and spaghetti tags, although limited, has not identified substantial differences (Meehan and Milburn[1]), although variation certainly exists given the advances in tagging methods over the four decades spanned by these studies. The reporting rates for tags captured by different fisherman were another source of variability; all recoveries were assumed to have been reported at the same rate in all time periods because there was no information with which to address this issue. Researchers conducting all studies primarily tagged adult fish of both sexes, and recoveries were obtained with commercial or similar fishing gear; however little detail regarding the age or length structure of the fish tagged was available. No accounting was made for

---

[1] Meehan, J. M., and G. S. Milburn. 1965. Comparison of returns from dart and Peterson disc tags on Dover sole. Fish Commission of Oregon Research Briefs. 13:127. Oregon Department of Fish and Wildlife, 3406 Cherry Avenue NE, Salem, OR 97303.

Table 2

General structure of the monthly movement parameter matrices (P) for all models explored in this analysis; p_n = proportion of population moving north, p_s = proportion of population moving south. Movement rates assumed to be zero in all models are indicated in the off-diagonals. The table is compressed over the central 11 areas (denoted by "..."), where the structure of the matrix did not vary from those cells shown.

	To						
From	1A south	1A north	1B south	...	5B	5C	5D
1A south	$1-p_n$	p_n	0	...	0	0	0
1A north	p_s	$1-p_n-p_s$	p_n	...	0	0	0
1B south	0	p_s	$1-p_n-p_s$	...	0	0	0
...	...	...	...	...	...	...	...
5B	0	0	0	...	$1-p_n-p_s$	p_n	0
5C	0	0	0	...	p_s	$1-p_n-p_s$	p_n
5D	0	0	0	...	0	p_s	$1-p_s$

fish size or age in this analysis. Relative fishing effort at the spatial scale of PMFC areas was not available for these years.

Initial examination of the data (for a qualitative assessment) was performed for tagging projects conducted in Puget Sound and the Strait of Georgia (24,408 tags released and 5756 recovered). Many of these experiments were conducted with varied goals (other than that of estimating movement rates) and an attempt to recover tags from distant areas was not undertaken. Therefore, these data were excluded from the mark-recapture model but were used to structure the spatial extent of the analysis.

Movement hypotheses

Many researchers have noted seasonal changes in catch rates in specific areas, and the temporally transient appearance of aggregations of flatfish. For English sole, these aggregations seem to be associated with the winter spawning season (Alverson, 1960). Spawning of English sole occurs from early fall through late spring, and most growth occurs during the rest of the year. December and April appear to be the first and last months of strong spawning activity across all latitudes for English sole (Castillo, 1995); migration associated with movement to and from the spawning grounds could therefore reasonably be expected to take place in the fall and spring just before and following this spawning activity.

For all modeled tag recoveries, movement was restricted to adjacent areas (north or south), and the same rates of movement were applied to all areas along the coast (Puget Sound and the Strait of Georgia were excluded). This simplification restricted the P matrices (area×area for each month) to nonzero values in only the first off-diagonals, and repeated the same parameters within each diagonal (Table 2). The time-increments considered reflect the trade-off between biologically realistic hypotheses and the likely constraints on complexity in future stock assessments. English sole movement over large distances has been observed to occur at a rate of three to eight kilometers per day (Forrester, 1969). With an average latitudinal span of 138 kilometers per area, it could therefore take 17 to 46 days for at least some English sole to cross a single area; this rate of movement indicated that a one-month time-step would be appropriate to accommodate interarea migration. In the simplest hypotheses, movement was considered to take place only at one time per year, and all P matrices contained only zeros except for the month in which movement occurred but allowed northerly and southerly movement to differ. These models included movement occurring in January (the standard break for assessment years), October, November, May, and June. An additional four hypotheses were considered that included movement in the fall and spring and that resulted in two different P matrices—one movement applied in a spring month and one in the fall with two unique parameters (a north and south movement) in each. Five hypotheses included movement during more than two months of the calendar year (Table 3).

Bayesian implementation

Prior distributions are required for each of the model parameters (Table 4). Priors were selected to be noninformative, allowing the likelihood function to dominate the posterior probability distribution. However, the choice of appropriate noninformative priors is difficult and case specific, requiring estimation on the appropriate scale for each parameter, often either diffuse (near uniform) or uniform over log-space (Gelman et al., 1995). In some cases, additional information was available with which to constrain the priors. All movement parameters were bounded between zero and one, and had uniform prior density. The maximum possible reporting rate was estimated by calculating one minus the proportion of recovered tags with incomplete information (no area, date, or both, and were not included in the analysis); this value was 0.92 per tag lifetime. If tag loss rate was

Table 3

Specific structure of the movement parameter matrices (P) for the 14 models explored in this analysis. One-season models (1–5) allowed movement to occur only once per year in the month shown, two-season models (6–9) allowed movement in two months per year, and monthly movement models (10–14) allowed movement in >2 months per year, as specified.

Model	Movement parameter matrices
One-season: two movement parameters (north and south in the month indicated)	
1	October
2	November
3	January
4	May
5	June
Two-seasons: four movement parameters (north and south in the months indicated)	
6	October, May
7	October, June
8	November, May
9	November, June
Monthly movement	
10	One parameter, all months, north=south
11	Two parameters, all months, north and south
12	One parameter, movement from May through November only
13	Two parameters, movement from May through November only, north and south
14	Four parameters, movement from May through October, north and south, and movement in November, north and south

Table 4

Prior distributions applied to parameters in all models. NA = not applicable.

Parameter	Name (number)	Distribution (parameters describing the prior distribution)	Prior distribution parameter values	Parameter bounds: low, high
F_d	Fishing mortality rate/year for each data set (n=25)	Lognormal (median, coefficient of variation)	F_{med}, 0.25	–5, 5
F_{med}	Median fishing mortality rate/year	Scaled beta (*shape1*, *shape2*)	1.02, 1.02	0.01, 0.80
M	Natural mortality rate/year	Fixed	0.26	NA
Ω	Tag loss rate/year	Scaled beta (*shape1*, *shape2*)	1.02, 1.02	0.01, 1.52
ϕ	Reporting rate	Scaled beta (*shape1*, *shape2*)	1.02, 1.02	0.21, 0.92
p_n, p_s	Proportion moving ($\boldsymbol{n}$=1–4, depending on the hypothesis)	Uniform (bounds)	NA	0.00, 1.00
K_c	Overdispersion ($\boldsymbol{n}$=4)	Gamma (shape, rate)	1.001, 0.01	0.001, 1000

zero and all tags were recaptured immediately, then the minimum possible reporting rate would be the ratio of tags returned to total releases; this value, 0.21, is therefore a logical lower bound on reporting rate. These bounds are comparable to the range of reporting rates observed for other species (Gaertner and Hallier, 2004). Long-term tag-induced mortality (included in tag loss in this model) may be twice that of natural mortality (Manzer, 1952). Tag loss was also reported to be high because of corrosion of the tag pins for English sole tagged in a similar fashion over roughly the same period (Forrester and Ketchen, 1955). The proportion of tags lost could not have been greater than 0.78 because 0.22 of the tags were recovered; this value (0.22) is greater than that used to calculate the minimum bound for reporting rate because it includes those tags recovered without full reporting of location information. The value of 0.78 for the proportion of tags lost corresponds to a maximum instantaneous rate of tag loss of 1.52, which was used as the upper bound for this parameter. The tag loss rate was given a lower bound of 0.01 in the absence of other information. The median rate of fishing mortality across data sets (F_{med}) was bounded to lie between 0.01 and 0.8. Reporting rate, tag loss rate, and median fishing mortality rate were all assigned a scaled-beta distributed prior with both shape parameters equal to 1.02. This prior has the desirable properties of a nearly uniform density over most of the parameter space, except immediately adjacent to the bounds, which have zero density. Data set-specific fishing rates (F_d) were assumed to be related in a common hierarchy; the values of these parameters were constrained with a lognormal prior (F_{med}, 0.25). The overdispersion parameters (one for each category of data) were given a gamma-distributed prior (shape=1.001, rate=0.01) and bounded to lie between 0.001 and 1000. This choice reflected the desire for a generally uninformative prior, but one that favored a substantially larger variance than that in a simple Poisson likelihood. Exploration of the sensitivity of the model inference to the choice of priors was conducted by changing the values, rerunning the analysis, and comparing the results. The effect of six key prior distributions were explored through sensitivity analysis by modifying the shape of these distributions: doubling the coefficient of variation of the prior on deviations from F_{med}, using a uniform prior on the log scale for the overdispersion parameter (k), reducing the upper bound on movement parameters to 0.25, extending the prior bounds on reporting rate (0.01 to 1.0), and sequentially setting the priors on tag loss and F_{med} to be uniform.

This model was programmed in AD Model Builder© (Otter Research Ltd., Sidney, B.C., Canada), which uses a Metropolis-Hastings algorithm to sample from the joint posterior distribution of all model quantities. Markov-chain Monte-Carlo (MCMC) sampling was performed for five to fifteen million iterations for each hypothesis. Each chain was thinned by taking every 1000th (or fewer) draws to achieve low autocorrelations (<0.3) within chains and by taking nearly equal actual and effective (modified to account for autocorrelation) sample sizes. Convergence was assumed to have occurred for each chain when the criteria above were met, visual inspection of trace plots and cumulative quantiles (0.05, 0.5, 0.95) indicated stationarity in all model parameters, and most parameters had a Geweke statistic (Geweke, 1992) less than 1.96 (this statistic can be interpreted as a z-score and will produce some significant values due to random chance).

Bayes factors are frequently used in Bayesian analyses to compare the weight of evidence among various model hypotheses, accounting for differences in the number of estimated parameters (Gelman et al., 1995; Burnham and Anderson, 2002). In the present analysis, harmonic mean posterior likelihood for each model was used to calculate approximate Bayes factors (Kass and Raftery, 1995). Model support (amonth those compared) is based on twice the log of the ratio of mean likelihoods (hereafter referred to as the Transformed Bayes Factor, TBF), judged on the following scale: 0–2, not worth more than a bare mention; 2–6, positive; 6–10, strong; and >10, very strong support for one model over another (Kass and Raftery, 1995). For this application, the TBF metric appeared quite stable and robust to sampling effects arising from the posterior distributions in preliminary testing.

Results

Most of the recoveries of tagged fish across all data sets occurred in the area that initial tagging took place, indicating relatively low rates of movement over all areas and time periods. Of the 3464 tagged English sole recovered off the open coast, only 130 (3.8%) of these had moved from the area of tagging and only 55 (1.6%) had moved more than one area. Low levels of exchange were particularly pronounced for those fish released in Puget Sound and the Strait of Georgia. Of 24,408 tagged English sole released in Puget Sound and the Strait of Georgia, only 12 (0.002%) of the 5756 recoveries were captured off the open coast. Conversely, only 3 (0.001%) of 4232 tagged fish recovered from 32,431 released fish (including some that could not be included in the quantitative analysis) on the open coast were recaptured within Puget Sound or the Strait of Georgia. A single release of 282 English sole in the Strait of Juan de Fuca (Forrester, 1969) resulted in 59 recoveries, 34 of which were from the open coast, mostly off Washington, but recoveries ranged as far south as Oregon. In aggregate, these results indicate that Puget Sound and the Strait of Georgia are substantially isolated from the open coast, but that mixing of adults does occur in the Strait of Juan de Fuca (and possibly at the north end of the Strait of Georgia). Therefore, in all model hypotheses considered in this analysis, Puget Sound and the Strait of Georgia were not included as part of the coastal population.

All five single time-step models resulted in English sole movement estimates that were three to four times more southerly than northerly, although the posterior distributions for the movement parameters were not identical (Fig. 2). TBFs of 49–152 indicated strong support for the model, allowing movement only in November over all other single time-step models (Table 5) . In this model, the posterior median proportion of English sole expected to move to the north each year was 0.08, and the 90% posterior interval ranged from 0.05 to 0.12, and 0.31 (0.25–0.39) to the south. The model including movement in January was second best (TBF=49) and qualitatively similar with 0.06 (0.04–0.09) moving to the north, and 0.26 (0.19–0.34) moving to the south each year.

The two-season models also showed some consistency in parameter estimates regardless of the months in which movement was allowed to occur (Fig. 3). TBFs of 16–26 indicated strong support for the model allowing movement in November and May (Table 5). Results from this two-season model showed that the proportion of English sole moving in the spring and to the

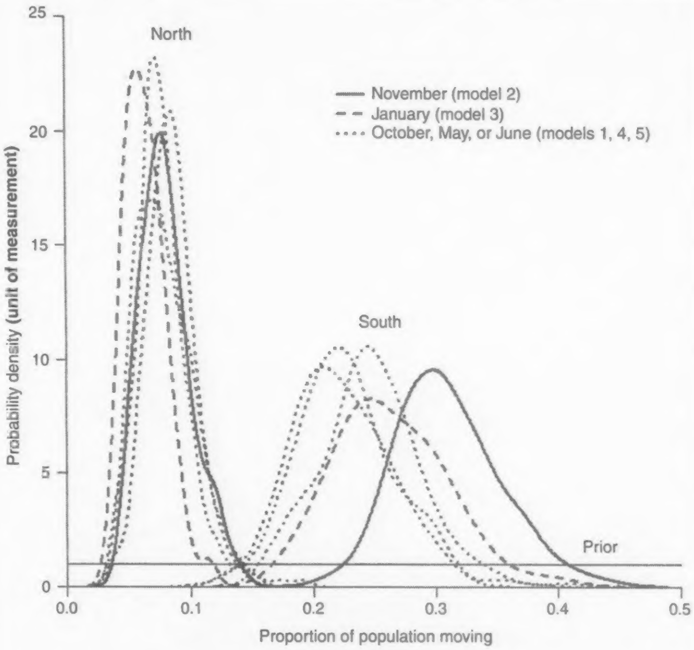

Figure 2

Prior (horizontal line) and posterior distributions for movement parameters (proportion of the population moving) in the single-season models (1–5). Solid lines indicate movement to the north and south in November (model 2), dashed lines show movement only in January (model 3), and dotted lines show movement in October, May, or June (nodels 1, 4, 5; not separated in the legend).

north to be 0.10 (0.04–0.18) and to be 0.09 (0.04–0. 17) to the south. In the fall, parameter medians were 0.05 (0.02–0.09) to the north and 0.27 (0.17–0.38) to the south. This model was strongly supported over the best single-season model (TBF=49). The next best two-season model (TBF=16) allowed movement in October and May. Movement rates estimated from two-season models showed a similar pattern to those estimated from the single time-step models. Net movement to the south was identified in both cases, primarily in the fall, and although movement rates from two-season models were somewhat reduced, they were applied twice per year. The cumulative expected value for movement in the best two-season model was 0.11 to the north and 0.30 to the south, very close to the values from the best single-season model.

When movement was allowed in each month of the year, parameter estimates were much smaller per month (implying a similar magnitude of annual movement), but greater movement was still predicted to the south than to the north (Fig. 4). The best monthly model (no. 11) included separate proportions moving north (0.02 [0.02–0.03]), and south (0.04 [0.03–0.04]). This model received strong support over the best two-season model (TBF=101), but only slightly more support from the data (TBF=3) than constant and equal movement all year (model10). The cumulative expected value of this movement was 0.21 to the north and 0.29 to the south, similar to the best two-season model, but with more net movement to the north. With only a single movement parameter, the median proportion moving in model 10 was 0.03 (0.02–0.04). Although more complex models including movement in only some months were explored, none were supported by the data (TBFs 16–34) over models 10 or 11 (Table 5).

Model parameters other than movement rates showed no obvious restriction by their priors, although posterior distributions included much of the marginal parameter space within the prior bounds. For all models, the overdispersion parameters (k_c) for each data type had substantial density below 1.0, indicating variability far in excess of that expected from a Poisson distribution (Fig. 4). Reporting rate was generally less than 0.75 and was highly correlated with the median fishing mortality rates. Tag loss rates were predicted to be high (often greater than 0.5), but quite uncertain. Sensitivity analysis to the shape of key prior distributions did not result in any substantial changes for the posterior

Table 5

Transformed Bayes Factors (TBFs) used for comparison of models allowing movement in only one month (one-season), in two months (two-seasons), or in >2 months of each year (monthly). Support for one model over another was based on the following TBF scale: 0–2, not worth more than a bare mention; 2–6, positive; 6–10, strong; and >10, very strong (Kass and Raftery, 1995).

Comparison	Model	Number of estimated parameters	TBFs: 2×log (*likelihood of the best model / likelihood of model on row)*
Among one-season models:	1	34	97
	2	34	Best one-season model
	3	34	49
	4	34	134
	5	34	152
Among two-season models:	6	36	16
	7	36	26
	8	36	Best two-season model
	9	36	20
Among monthly models:	10	33	3
	11	34	Best monthly model
	12	33	16
	13	34	14
	14	36	34
Among time-steps:			
Best one-season model	2	34	151
Best two-season model	8	36	101
Best monthly model	11	34	Best model

distributions of the movement parameters for any of the six alternate sets of parameter values considered (Fig. 5). A further check was made by rerunning the model assuming high (75%) initial tag loss; again no appreciable change in posterior distributions was observed, and median parameter values changed by less than 0.001.

The ability to quantify the plausibility of the observed data given the fitted model, Bayesian goodness-of-fit, was examined by checking the posterior predictive distribution (the probability distribution for an unobserved data point), which can indicate the degree to which the model structure, priors, and likelihoods assumed in the model are appropriate (Gelman et al., 1995). The posterior predictive distribution for expected recoveries corresponding to each of the observed recoveries was generated during MCMC sampling. The posterior predictive check compares the observed data to a distribution of predictions and summarizes the information across data types. The mean standardized residuals were calculated by dividing the raw residual (between the observed value and the x^{th} percentile of the posterior predictive distribution) by the expected standard deviation (based on the negative binomial likelihood), and by taking the mean of these values for each number of observed recoveries. Figure 6 shows the mean standardized residual for the 95th, 50th, and 25th percentiles of the posterior distribution of expected recoveries for each of the four types of data. There are a few observations well in excess of the range expected for standardized residuals, primarily for the type-1 data sets. In addition, some trend was observed in the residuals for the type-4 data sets with larger residuals occurring at the largest observed values. Further, although the zero-line for the 5th percentile of the predictions does lie below more than 95% of the residuals, there appears to be an excess of residuals above the zero-line for the 95th percentile of the posterior predictions. This excess of residuals indicates that model predictions generally resulted in fewer recoveries (for some time and space combinations) than were observed.

Discussion

Bayesian analyses are ideal for fisheries applications because uncertainty is explicitly and transparently incorporated into them, they allow for the use of several data sources (Hilborn and Mangel, 1997), provide easily interpretable probability inference (Wade, 2000), and yield results suitable for formal decision analysis (McAllister et al., 1994). The Bayesian framework developed here allows calculation of probability distributions for key parameters governing English sole movement rates. The results from this analysis qualitatively support what can be directly inferred from the original

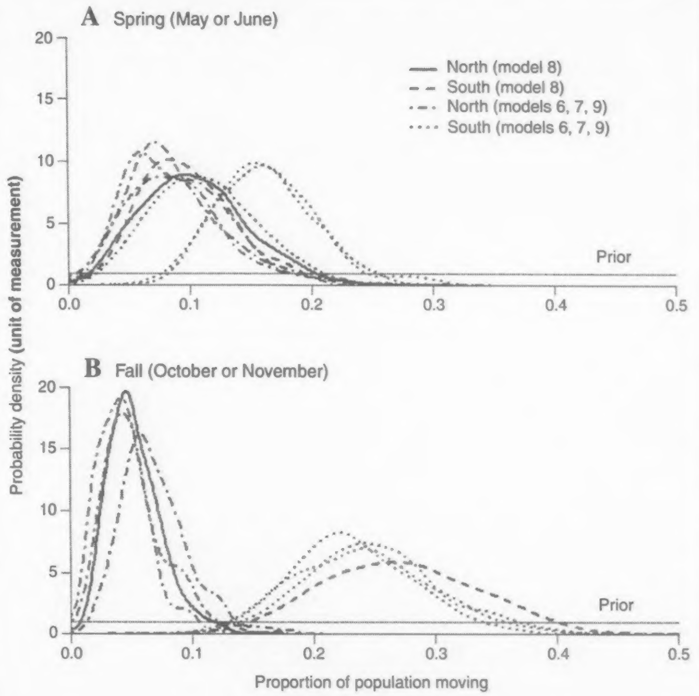

Figure 3

Prior (horizontal lines) and posterior distributions for the movement parameters (proportion of the population moving) in the two-season models (6–9) allowing movement in either the spring (May or June) or fall (October or November). Solid lines indicate movement to the north and dashed lines indicated movement to the south for model 8. Movement to the north is indicated by the dashed and dotted lines, movement to the south indicated by the dotted lines for models 6–9 (not separated in the legend).

published analyses of these data sets: English sole are not highly mixed across the entire coast but are also not sedentary at the scale of hundreds of kilometers. The approach of modeling the open coast separately is supported by the observation that only rarely are tagged English sole observed to move between the open coast and Puget Sound or the Strait of Georgia. This result may be specific to the biological and ecological habits of the species but it is commonly assumed to be the result for other species as well.

Also in concordance with historical observations about the seasonal and latitudinal movements of flatfish, the current analysis supports models that include more than just one movement per year. Movement appears to be of greater magnitude in the fall, just before the spawning season, but this pattern is not supported when monthly hypotheses are explored. This lack of a consistent pattern could be due to interannual variability in spawning activity. Research shows that spawning, in the case of English sole, is related to temperature (Kruse and Tyler, 1983; Peterman et al., 1987), as well as latitude (Castillo, 1995). Because this analysis lacked temperature as a covariate, there may not be adequate data support for specific spring and fall movement rates with the potential variation in timing of spawning activity (when compared to uniform monthly movement). If specific environmental information were available for each year of the analysis, covariates could be developed to improve assignment of the correct month for prespawning migration to the south and post-spawning migration to the north.

Of potential importance to stock assessment is the net movement to the south predicted by nearly all of the models. Although this pattern does not fit the data substantially better than simple diffusion (equal movement north and south) throughout the year, increased movement to the south estimated in simpler models may be worth further investigation. The effect of net

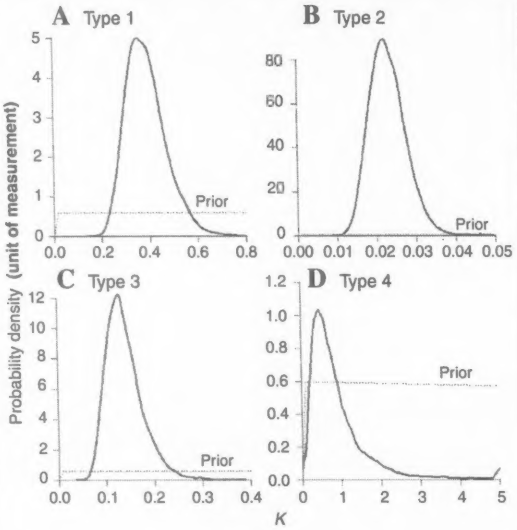

Figure 4

Prior (dotted lines) and posterior distributions for overdispersion parameters (K) by data type (type 1, where data were available for year, month, and PFMC area for each individual tag recovery; type 2, where data were available for only month and area; type 3, where data were available for area only; and type 4, where data were only available to indicate recovery inside or outside the area of tagging for model 11. Priors are scaled to be more visible on the plot.

southerly movement on equilibrium harvests of adult English sole should be explored because this movement would have implications for current and future management strategies.

Given the presence of significant outliers, the degree of support among models based on the posterior probability should be interpreted with caution. There are many potential reasons for the outliers in observed recoveries present in the data. Although an attempt was made to retain a structure commensurate with what might be possible to replicate in a stock assessment, the analysis may simply not be complex enough. Many parameters, such as fishing mortality, reporting rate, and tag loss rate, are assumed to be temporally and spatially invariant because of a lack of available data. Spatial differences in the location of the initial tagging within the larger PMFC area were not accounted for and reporting rates could be variable due to a mixture of Canadian and U.S. fishing vessels with varied incentives for returning tags. During much of the time period over which tags were recovered, there was a substantial fishery for mink food; this fishery may have had very different handling and tag-recovery practices than those of the concurrent fishery targeting fish for human consumption. The relative effects of violating these various assumptions could be addressed in the future through simulation testing.

Spatially and temporally local increases in fishing-induced mortality rates, resulting in additional recaptured tags, could have generated many of the positive residuals from a model that does not allow fishing mortality to vary within a single data set. Exploration of how model parameters are influenced by localized increases in fishing mortality should be explored through future simulation analysis. Another potential use of this method is to extend the hierarchal model of fishing mortality rates, allowing them to vary over space, time (or both) within a data set. Estimation of the coefficient of variation of this distribution could also be explored. The coefficient of variation of total U.S. catch over the years in which tagging projects were conducted for English sole is on the order of 0.5, indicating that interannual variation in fishing mortality rate may be an important factor absent from the analysis. Similarly, a hierarchical approach could be taken with regard to movement parameters between specific areas. Geographic regions could be defined on the basis of likely bathymetric features such as submarine canyons or rocky headlands

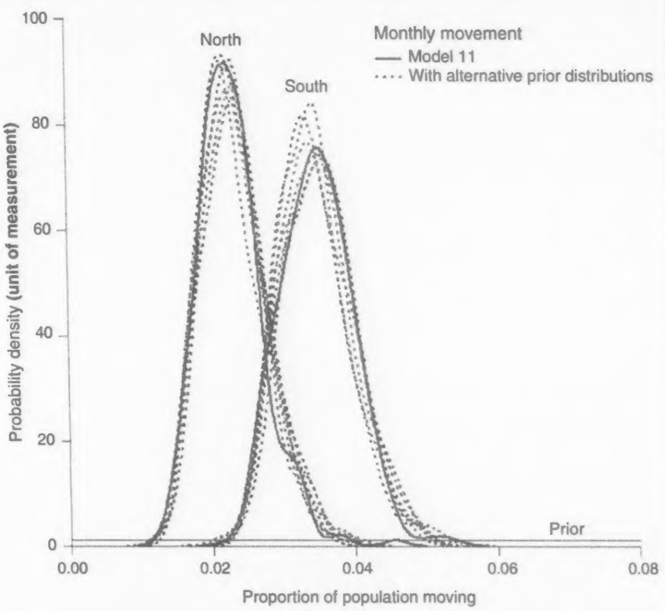

Figure 5

Prior (horizontal line) and posterior distributions for monthly movement parameters (proportion of the population moving) in the model allowing separate movement north and south (model 11, solid line) and distributions resulting from alternate prior distributions on model parameters (dotted lines, see text for list of alternate priors explored).

that might serve to disrupt movement along the coast. Although conceptually appealing, these extensions may cause technical problems for MCMC because of the low information content of the aggregated historical tagging data.

Movement rates are notoriously difficult to estimate (Xiao, 1996). However, the general approach to integrated tag analysis based on maximum likelihood has been found to be reliable through simulation testing (Maunder, 2001). In this application, the error structure, although intended to accommodate clustered recoveries and the inclusion of zero recoveries in many space-time combinations, may be inadequate for the observed level of variability in recoveries. Specifically, there were many cases of observed recoveries in areas where no recoveries could have been predicted under simple models, given the structure imposed by the population dynamics that were assumed. Future extension and simulation testing to evaluate other error structures, such as zero-inflated Poisson or negative binomial models, should be undertaken. Further, there may be interactive effects of the prior distributions used, despite lack of observed response to one-dimensional sensitivity testing. Some important elements of uncertainty may not have been included in the present analysis; however, uncertainty is a problem faced by most modeling applications in fisheries.

It is unlikely that future stock assessments will be structured around areas as small as PMFC areas. Conversion of the movement rates reported here for use as priors in stock assessments will require assumptions regarding the distribution of biomass within areas modeled and the correspondence of the areas modeled to PMFC areas. Research survey data may provide a fishery-independent source on which to base these assumptions. The estimation of fishing mortality in this analysis should also be considered if it is to be applied within a stock assessment framework. These issues would appear to be no more daunting than currently accepted assumptions of thorough mixing across the coast or of completely isolated stock groups.

Tagging programs for groundfish species off the U.S. west coast have generally decreased over the last 75 years, and there are no plans for large-scale tagging programs in the future. An analysis of all available tagging data may therefore provide the only quantitative source of guidance and an important avenue to allow for uncertainty in movement rates without new data with which to estimate these rates. This type of method

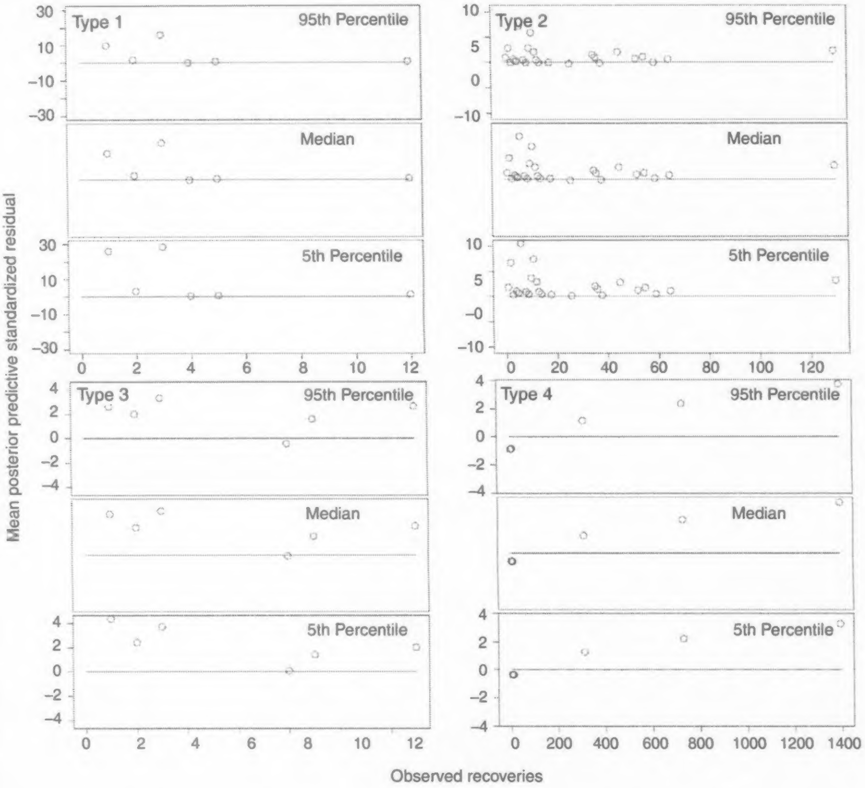

Figure 6

Distribution of mean posterior predictive standardized residuals showing plausibility of observed data, given the model and error structure. Residuals were calculated by dividing the raw residual between the observed value and the X^{th} percentile of the posterior predictive distribution by the expected standard deviation and by taking the mean of these values for each data type (type 1, where data were available for year, month, and PFMC area for each individual tag recovery; type 2, where data were only available for only month and area; type 3, where data were available for area only; and type 4, where data were only available to indicate recovery inside or outside the area of tagging) and percentile of the posterior predictive distribution.

has been demonstrated for English sole but could be extended to other species that have also been the subject of multiple tagging projects. When compared with the status quo assumptions invoked with single (unit) or multiple independent stocks, these results may provide a more realistic integration of spatial movement off the west coast of North America into assessment models. Use of these results could lead to a better representation of the uncertainty associated with estimates of biomass and in the case of stock assessments, they could lead to predictions of exploitation rates that allow a sustainable resource.

Acknowledgments

T. Branch, D. Gunderson, A. Magnusson, C. Minte-Vera, and A. Silva all generously assisted with data sources or analysis. This article was significantly improved by comments on preliminary drafts from T. Branch, R. Hilborn, R. Methot, A. Punt, and I. Taylor. Three anonymous reviewers and A. Moles made many suggestions improving the clarity and content of the manuscript. The author was supported by a National Marine Fisheries Service/National Sea Grant fellowship in population dynamics.

Literature cited

Alverson, D. L.
1960. A study of annual and seasonal bathymetric catch patterns for commercially important groundfishes of the Pacific Northwest coast of North America. Pac. Mar. Fish. Comm. Bull. 4:1–99.

Beverton, R. J. H., and S. J. Holt.
1957. On the dynamics of exploited fish populations, 533 p. Chapman and Hall, London.

Bishop, Y. M. M., S. E. Feinberg, and P. W. Holland.
1988. Discrete multivariate analysis: theory and practice, 9th ed., 557 p. Massachusetts Inst. Technology Press, Cambridge, MA.

Burnham, K. P., and D. R. Anderson.
2002. Model selection and multimodel inference: a practical information-theoretic approach, 2nd ed., 488 p. Springer-Verlag, New York, NY.

Castillo, G. C.
1995. Latitudinal patterns in reproductive life history traits of northeast Pacific flatfish. *In* Proceedings of the international symposium on north Pacific flatfish, p. 51–72. Alaska Sea Grant College Program, Univ. Alaska, Fairbanks, AK.

Cormack, R. M., and J. R. Skalski.
1992. Analysis of coded wire tag returns from commercial catches. Can. J. Fish. Aquat. Sci. 49:1816–1825.

Day, D. E.
1976. Homing behavior and population stratification in central Puget Sound English sole (*Parophrys vetulus*). J. Fish. Res. Board Can. 33:278–282.

Dorn, M. W.
2002. Advice on West Coast rockfish harvest rates from Bayesian meta-analysis of stock-recruit relationships. N. Am. J. Fish. Manage. 22:280–300.

Forrester, C. R.
1969. Results of English sole tagging in British Columbia waters. Pac. Mar. Fish. Comm. Bull. 7:1–10.

Forrester, C. R., and K. S. Ketchen.
1955. The resistance to salt water corrosion of various types of metal wire used in the tagging of flatfish. J. Fish. Res. Board Can. 12:134–142.

Gaertner, D., and J.-P. Hallier.
2004. Combining Bayesian and simulation approaches to compare the efficiency of two types of tags used in tropical tuna fisheries. Aquat. Living Res. 17:175–183.

Gelman, A., J. B. Carlin, and D. B. Stern.
1995. Bayesian data analysis, 526 p. Chapman and Hall/CRC, Boca Raton, FL.

Geweke, J.
1992. Evaluating the accuracy of sampling-based approaches to the calculation of posterior moments. *In* Bayesian statistics 4 (J. M. Bernardo, J. Berger, A. P. Dawid, and A. F. M. Smith, eds.), p. 169–193. Oxford Univ. Press, Oxford.

Hampton, J., and D. A. Fournier.
2001. A spatially disaggregated, length-based, age-structured population model of yellowfin tuna (*Thunnus albacares*) in the western and central Pacific Ocean. Mar. Freshw. Res. 52:937–963.

Harley, S. J., R. A. Myers, and A. Dunn.
2001. Is catch-per-unit-effort proportional to abundance? Can. J. Fish. Aquat. Sci. 58:1760–1772.

Harry, G. Y., Jr.
1956. Analysis and history of the Oregon otter-trawl fishery. Ph. D. diss., 329 p. Univ. Washington, Seattle, WA.

Hart, J. L.
1973. Pacific fishes of Canada, 740 p. Fish. Res. Board Canada, St. Andrews, New Brunswick, Canada.

Heifetz, J., and J. T. Fujioka.
1991. Movement dynamics of tagged sablefish in the northeastern Pacific. Fish. Res. 11:355–374.

Hilborn, R.
1990. Determination of fish movement patterns from tag recoveries using maximum likelihood estimators. Can. J. Fish. Aquat. Sci. 47:635–643.

Hilborn, R., and M. Mangel.
1997. The ecological detective: confronting models with data, 315 p. Princeton Univ. Press, Princeton, N.J.

Hilborn, R., and C. J. Walters.
1992. Quantitative fisheries stock assessment: choice, dynamics and uncertainty, 570 p. Chapman and Hall, London.

Jow, T.
1969. Results of English sole tagging off California. Pac. Mar. Fish. Comm. Bull. 7:15–33.

Kass, R. E., and A. E. Raftery.
1995. Bayes factors. J. Am. Stat. Assoc. 90:773–795.

Ketchen, K. S.
1956. Factors influencing the survival of the lemon sole (*Parophrys vetulus*) in Hecate Strait, British Columbia. J. Fish. Res. Board Can. 13:647–694.

Kruse, G. H., and A. V. Tyler.
1983. Simulation of temperature and upwelling effects on the English sole (*Parophrys vetulus*) spawning season. Can. J. Fish. Aquat. Sci. 40:230–237.

Manzer, J. I.
1952. The effects of tagging upon a Pacific coast flounder, *Parophrys vetulus*. J. Fish. Res. Board Can. 8:479–485.

Maunder, M. N.
2001. Integrated tagging and catch-at-age analysis (ITCAAN): model development and simulation testing. *In* Spatial processes and management of marine populations (G. H. Kruse, N. Bez, A. Booth, M. W. Dorn, S. Hills, R. N. Lipcius, D. Pelletier, C. Roy, S. J. Smith, and D. Witherell, eds.), p. 123–146. Alaska Sea Grant College Program, Univ. Alaska, Fairbanks, AK.

McAllister, M. K., E. K. Pikitch, A. E. Punt, and R. Hilborn.
1994. A Bayesian approach to stock assessment and harvest decisions using the sampling/importance resampling algorithm. Can. J. Fish. Aquat. Sci. 51:2673–2687.

McGarvey, R., and J. E. Feenstra.
2002. Estimating rates of fish movement from tag recoveries: conditioning by recapture. Can. J. Fish. Aquat. Sci. 59:1054–1064.

Menasveta, D.
1958. Migration and fishing mortality of English sole (*Parophrys vetulus*) in Saratoga Passage, and adjacent waters. M.S. thesis, 84 p. Univ. Washington, Seattle, WA.

Millar, R. B., and R. D. Methot.
2002. Age-structured meta-analysis of the U.S. West Coast rockfish (Scorpaenidae) populations and hierarchical modeling of trawl survey catchabilities. Can. J. Fish. Aquat. Sci. 59:383–392.

Pattie, B. H.
1969. Dispersal of English sole, *Parophrys vetulus* tagged off the Washington coast in 1956. Pac. Mar. Fish. Comm. Bull. 7:11–14.

Peterman, R. M., M. J. Bradford, and G. H. Kruse.
1987. Simulation model of English sole (*Parophrys vetulus*) population dynamics in Washington and Oregon coastal waters. Can. J. Fish. Aquat. Sci. 44:1870–1878.

Punt, A. E. and R. Hilborn.
1997. Fisheries stock assessment and decision analysis: the Bayesian approach. Rev. Fish Biol. Fish. 7:35–63.

Punt, A. E., F. Pribac, T. I. Walker, B. L. Taylor and J. D. Prince.
2000. Stock assessment of school shark, *Galeorhinus galeus*, based on a spatially explicit population dynamics model. Mar. Freshw. Res. 51:205–220.

Quinn, T. J. II., and R. B. Deriso.
1999. Quantitative fish dynamics, 542 p. Oxford Univ. Press, New York., NY.

Robichaud, D., and G. A. Rose.
2004. Migratory behaviour and range in Atlantic cod: inference from a century of tagging. Fish Fish. 5:185–214.

Wade, P. R.
2000. Bayesian methods in conservation biology. Cons. Biol. 14:1308–1316.

Xiao, Y.
1996. A framework for evaluating experimental designs for estimating rates of fish movement from tag recoveries. Can. J. Fish. Aquat. Sci. 53:1272–1280.

Abstract—Adult horseshoe crabs (*Limulus polyphemus*) are the preferred bait in the U.S. east coast whelk pot fishery, but their harvest is being restricted because of severe population declines in the Chesapeake and Delaware bays. To identify other baits, the activity in the pallial nerve of whelks was determined during exposure of the osphradium to odorant solutions prepared from horseshoe crab eggs, horseshoe crab hemolymph, and hard clam (*Mercenaria mercenaria*) tissue. All three elicited significant responses; bait based on them may provide an alternative to the use of adult horseshoe crabs, although extensive behavioral testing remains to be done. Channeled whelk did not respond to molecular weight fractions (>3 kDa and <3 kDa) prepared from horseshoe crab egg odorant solutions but did respond when the molecular weight fractions were recombined. Whelks appear to have broadly tuned chemoreceptors and manufactured baits may need to mimic the complex mixture of odorants derived from natural sources.

Activity in the pallial nerve of knobbed (*Busycon carica*) and channeled (*Busycotypus canaliculatum*) whelks recorded during exposure of the osphradium to odorant solutions

Christopher Magel
Virginia Institute of Marine Science
P.O. Box 1346
Gloucester Point, Virginia 23062

Kirstin Wakefield
Nancy Targett
College of Marine and Earth Studies
University of Delaware
Lewes, Delaware 19958

Richard Brill (contact author)
Email address for R. Brill: rbrill@vims.edu
National Marine Fisheries Service
National Oceanic and Atmospheric Administration
Northeast Fisheries Science Center
Present address: Virginia Institute of Marine Science
P.O. Box 1346
Gloucester Point, Virginia 23062

Manuscript submitted 13 February 2007 to the Scientific Editor's Office.
Manuscript approved for publication 23 May 2007 by the Scientific Editor.
Fish. Bull. 105:485–492 (2007).

Knobbed and channeled whelks (*Busycon carica* and *Busycotypus canaliculatum*, respectively) are common in inshore areas of the east coast of the United States from Georgia to Massachusetts (Walker, 1988) and form the basis of a substantial commercial fishery. The currently preferred bait in the pot fishery is adult horseshoe crabs (*Limulus polyphemus*) (Ferrari and Targett, 2003). The directed harvesting for bait has contributed to severe population declines of horseshoe crabs in the Chesapeake and Delaware bays (Berkson and Shuster, 1999) and increasingly stringent catch restrictions are being implemented. These restrictions include a moratorium on horseshoe crab harvest from Delaware Bay (issued by the Delaware Department of Natural Resources and Environmental Control and the New Jersey Department of Environmental Protection in 2006). These restrictions are being promulgated in large measure because horseshoe crab eggs are a primary food source for migratory shorebirds, such as the red knot (*Calidris canutus*), during their northward spring migrations (Tsipoura and Burger, 1999; Weidensaul, 2006). Because of a continuing decline in the breeding population of the red knot (Morrison et al., 2004), the species has been proposed for inclusion on the Endangered Species List (Weidensaul, 2006).

Work is underway to create alternative bait for the whelk pot fishery (Ferrari and Targett, 2003). As part of these efforts, the sensitivities of knobbed and channeled whelks to odorant solutions prepared from horseshoe crab eggs, horseshoe crab hemolymph, and hard clam (*Mercenaria mercenaria*) tissue were examined. Odorant solutions prepared from horseshoe crab eggs, and molecular weight fractions of these, were tested because they have been reported to be attractive to mud snails (*Ilyanassa obsoleta*), and because horseshoe crab eggs have been proposed as a source of compounds for inclusion in manufactured bait (Ferrari and Targett, 2003). Horseshoe crab hemolymph was tested as a potential source of attractant for inclusion in replacement bait because it is a readily available natural product. It is a waste product produced during the preparation of *Limulus* amoebocyte lysate (LAL), a clotting agent used worldwide to test for bacterial contamination of pharmaceuticals and implantable medical devices. More importantly, when handled properly, horseshoe crabs used for hemolymph collection show low rates of postrelease mortality (Walls and Berkson, 2000). A patent has been issued for hemolymph-based bait for whelks (U.S. Patent 6391295), but we are unaware of any published studies documenting its efficacy in the whelk pot fishery. Odorant solutions prepared from hard clam tissue were tested because bivalve mollusks are a common prey item for whelks (Walker, 1988).

Electrophysiological techniques were used to test each proposed bait, rather than behavioral methods, because the former allows precise control of stimulus parameters and the rapid assay of various compounds and concentrations on individual animals. Electrophysiological techniques, moreover, have been used for many years to investigate successfully chemosensory questions in both aquatic invertebrates (e.g., Borroni et al., 1986; Kamio et al., 2005) and vertebrates (e.g., Hara, 1975; Wilson, 2004). Behavioral methods, such as flume choice (Y-maze) experiments, can also be difficult with whelks. A large cross-sectional area within a flume is necessary to accommodate adult whelks. This large cross-sectional area requires a high-volume flow rate and concomitantly large volumes of odorant solution to achieve a detectable concentration over the long time periods necessary for whelk to respond behaviorally (Ferner and Weissburg, 2005); large volumes of odorant solutions can be difficult and costly to produce (Ferrari and Target, 2003; Ferner and Weissburg, 2005). Electrophysiological techniques, however, cannot differentiate between attractive and repulsive odors and must subsequently be paired with behavioral studies.

Activity in the pallial nerve was recorded while odorant solutions were applied directly to the osphradium. The pallial nerve connects the osphradium to the supraesophageal ganglia, which is part of the central nervous system (Alexander, 1970). The osphradium is considered to be the primary chemosensory organ of prosobranch mollusks because its leaf-like structure bears a strong resemblance to the nasal rosettes of aquatic vertebrates (Hansen and Reutter, 2004), and because its location at the base of the incurrent siphon maximizes exposure to odorants (Bailey and Laverack, 1966; Emory, 1992). It should be noted, however, that the osphradium is not the only chemosensory organ in gastropod mollusks. The rhinophores may also provide sensory information allowing gastropod mollusks to track odor plumes (Levy et al., 1997, Rahman et al., 2000; Ferner and Weissburg, 2005). Indeed, the rhinophores are considered a primary chemosensory organ in nudibranch mollusks (Alexander, 1970; Wedemeyer and Schild, 1995). A record of activity in the pallial nerve during exposure of the osphradium to odorant solutions derived from various sources therefore provides a robust method to determine whether a specific odorant solution is detectable by whelks and is a candidate for subsequent behavioral testing.

Materials and methods

Knobbed and channeled whelks were obtained from local processing plants or collected from estuaries behind the barrier islands on the eastern shore of Virginia. They were maintained at the Virginia Institute of Marine Science (VIMS) (Gloucester Point, VA) and also at the VIMS Eastern Shore Laboratory (Wachapreague, VA) in tanks supplied with running water drawn directly from the mouth of the York River or the Virginia eastern shore estuaries, respectively.

Horseshoe crab eggs were obtained from beaches bordering the Chesapeake and Delaware Bays, sealed in sterile 50-mL plastic tubes, and stored frozen. Hard clams were obtained from stocks maintained by the VIMS Eastern Shore Laboratory and only fresh tissue was used. Stock odorant solutions were prepared according to methods described by Ferrari and Targett (2003). In brief, horseshoe crab eggs were mixed (1:2 egg to liquid volume) with aerated, filtered, and ultraviolet sterilized water (FSW) drawn from the same sources supplying the holding tanks. The tissue was then crushed with a clean mortar and pestle and the mixture was allowed to sit overnight at 4°C. It was then centrifuged to remove cellular debris and sand. Clam tissue was treated likewise. In addition, horseshoe crab extract solution was prepared as described above, with the exception that 50 mM Tris buffer solution (pH 7.5, a mixture of Trizma HCl and Trizma Base, Sigma Chemical Co, St. Louis, MO) was used instead of FSW. Two molecular weight fractions (>3 kDa and <3 kDa) were then generated by using stirred cell ultra-filtration with YM-3 membranes (Millipore Inc., Billerica, MA). The molecular weight fractions were tested individually on channeled whelk, and after they were recombined. The stock odorant solutions were diluted with FSW $1:10^3$, $1:10^4$, $1:10^5$, and $1:10^6$ (volume to volume) immediately before experiments. Horseshoe crab hemolymph (free of any anticoagulants or preservatives) was obtained from Wako Chemicals (Cape Charles, VA) and stored at 4°C. It was likewise diluted (1:100, 1:133, 1:200, and 1:400) with FSW immediately before use.

During experiments, an individual whelk was presented with at least four concentrations of an individual odorant solution, plus controls consisting of FSW or a 50 mM Tris buffer solution in random order. The limited funding available for this project precluded the testing of all odorants on both species of whelks. The specific odorants presented to each whelk species are summarized in Table 1.

Table 1

Summary of odorant solutions derived from various sources tested on knobbed (*Busycon carica*) and channeled (*Busycotypus canaliculatum*) whelks. The odorant solutions that were tested on a species are indicated by an "X". FSW = aerated, filtered, and ultraviolet sterilized water.

	Knobbed whelk	Channeled whelk
Horseshoe crab (*Limulus polyphemus*) eggs extracted with FSW	X	X
Hard clam (*Mercenaria mercenaria*) tissue	X	
Horseshoe crab hemolymph	X	X
Horseshoe crab eggs extracted with 50 mM Tris buffer solution, <30 kDa and >30 kDa molecular weight fractions of horseshoe crab eggs produced by ultrafiltration, and the molecular weight fractions recombined		X

Quantifying activity in the pallial nerve in response to odorant solutions required that the whelk be removed from its shell, the pallial nerves exposed, and the osphradium isolated. To remove the animal from its shell, the apex of the shell was cut away at the spire, the columella muscle detached from the central column, and the animal gently pulled through the opercular opening. The individual was then immediately submerged in a large dish of aerated FSW. The viscera and the majority of the foot were removed and the mantle cavity opened with a dorsal incision starting medially between the cephalic eye stalks. The preparation was pinned to a Sylgard® (Dow Corning Corp., Midland, MI) lined Petri dish such that the body cavity was open and the buccal mass held out of the way. The overlying connective tissue was carefully dissected to expose the circumesophageal ganglia, specifically the supraesophageal ganglion, and the Petri dish holding the preparation was moved to a second plastic chamber (filled with FSW) mounted under a dissecting microscope. A modified 10-mL plastic syringe barrel with a small amount of quick-setting silicon elastomer (Kwik-Cast®, World Precision Instruments, Sarasota, FL) around the base was placed over the osphradium to isolate it from the fluid in the chamber containing the animal (Fig. 1A) .

The odorant delivery system consisted of a glass reservoir (filled with FSW) and polyethylene and stainless steel tubing (Fig. 1A). FSW was continuously delivered to the osphradium chamber by gravity at approximately 6 ml/min. Odorant solutions were switched into the delivery system without a change in flow rate by using a three-way stopcock. The 10-mL volume odorant solution was therefore delivered to the osphradium chamber within approximately 90 seconds, and then flushed out of the osphradium chamber by switching the flow back to FSW. Because the volume of liquid in the osphradium chamber was maintained as close to 2 mL as possible, peak stimulus concentration in the osphradium chamber reached approximately 60% of the original stimulus concentration (Fig. 1B) (Steffensen, 1989).

To record activity in the pallial nerve associated with the exposure of the osphradium to odorant solutions, the nerve was cut and the afferent end was drawn into a suction electrode (Fig. 1B). The resulting signal was amplified (80 dB gain) and filtered (10 Hz high pass and 1 k Hz low pass) by using a DAM-50 amplifier (World Precision Instruments, Sarasota, FL). The signal was further conditioned to remove 60 Hz noise with the use of a Humbug® active electronic filter (Quest Scientific, North Vancouver, B.C., Canada), and then displayed on a digital storage oscilloscope. The signal was digitized (at 1 kHz sampling rate) with a USB analog to digital I/O interface (model 1208LS, Measurement Computing, Middleboro, MA). The digital data were filtered (5 Hz high pass and 75 Hz low pass filters), processed, recorded, and displayed on a computer screen by using a custom designed computer program developed within Dasylab (version 7.0, National Instruments Corp., Austin, TX).

It was not practical to quantify responses by discrimination and by counting single nerve spikes because the recordings contained a broad amplitude signal due to activity in multiple nerve fibers, and because of the long intervals of activity in response to odorant solutions (Fig. 2) . Instead, the differentiation and integration module within Dasylab was used to generate an output value proportional to the integral of the filtered nerve signal (Fig. 2B). The module was programmed to integrate over 10.2-second intervals (i.e., 20 data blocks, as defined within the Dasylab program) to reset the output to zero, and then resume integrating. The digital system was thus functionally equivalent to an analog electronic "leaky RC integrator" circuit commonly used to measure the magnitude of nerve activity (e.g., Hara, 1975; Kamio et al., 2005).

For each trial, data were recorded for 12 minutes: 6 minutes before the introduction of an odorant solution into the osphradium chamber, and 6 minutes after. This recording interval was chosen on the basis of long integration times reported for the chemosensory abilities of whelks (Ferner and Weissburg, 2005) and other mollusks (Murphy and Hadfield, 1997). An additional 3 minutes were allowed between odor trials to ensure that the odorant solution was flushed from the osphradium chamber and that the activity in the pallial nerve had returned to prestimulus levels (Fig. 2). Only data

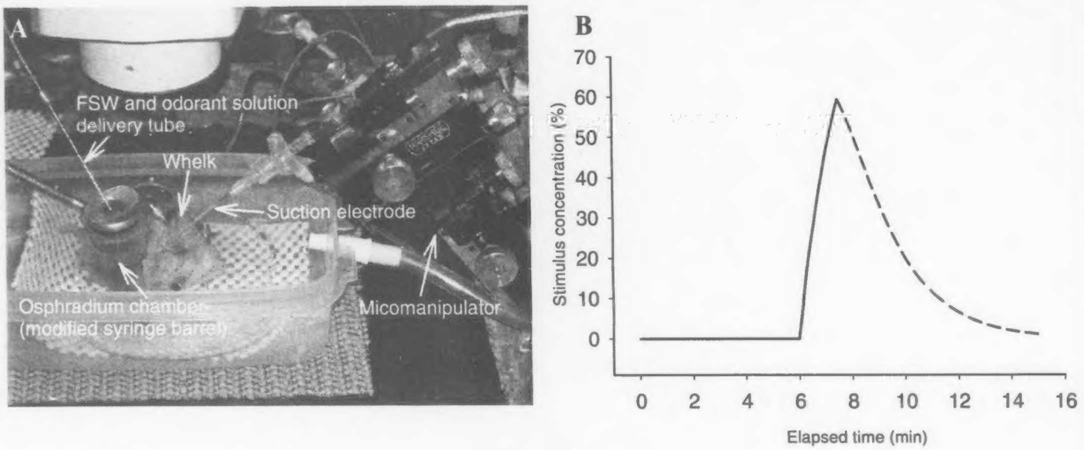

Figure 1

(**A**) Experimental setup showing a whelk, the osphradium chamber (modified syringe barrel), the aerated, filtered, and ultraviolet sterilized water (FSW) and odorant solution delivery tube, and the micromanipulator holding the suction electrode. (**B**) The predicted growth (solid line) and decay (dashed line) of the concentration of stimulus within the osphradium chamber over the course of a 15-minute trial, expressed as a percentage of the original odorant solution concentration.

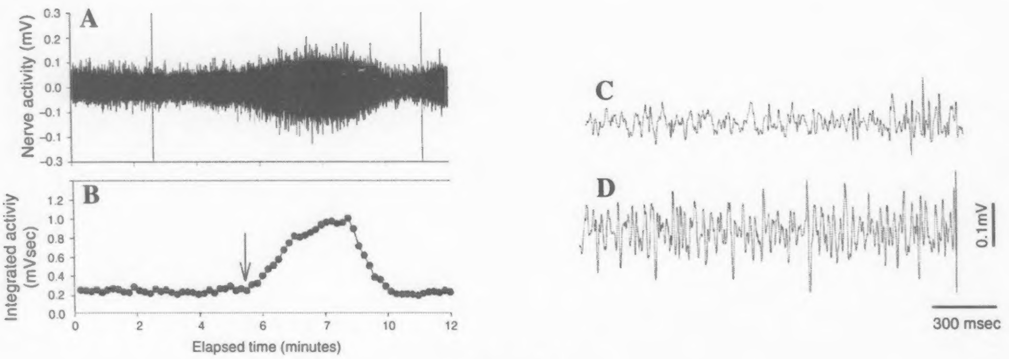

Figure 2

(**A**) Activity in the pallial nerve in a channeled whelk (*Busycotypus canaliculatum*) before and during exposure of the osphradium to an odorant solution prepared from horseshoe crab (*Limulus polyphemus*) eggs. The arrow in panel B indicates the approximate initial entry of the odorant solution into the osphradium chamber. The two brief large increases in activity (occurring at approximately 2 and 11 minutes after the start of the record) were associated with slight movements of the animal. (**B**) Nerve activity integrated over 10.2-second intervals was documented with Dasylab 7.0 software (National Instruments Corp., Austin, TX). (**C**) Nerve activity recorded before initial entry of the odorant solution into the osphradium chamber (3 minutes after the beginning of the record shown in Panel A). (**D**) Nerve activity at the apex of the response to the odorant solution (8 minutes after the beginning of the record shown in Panel A).

recorded 5 minutes immediately before and 5 minutes immediately after the initial introduction of an odorant solution were analyzed. This procedure resulted in approximately thirty equally spaced data points (i.e., one data point recorded every 10.2 seconds for five minutes), representing integrated nerve activity in each time period (Fig. 2B). The area under the curves representing integrated nerve activity (Fig. 2) was calculated by summing the points from each 5- minute period (i.e., the data recorded before and during presentation of an

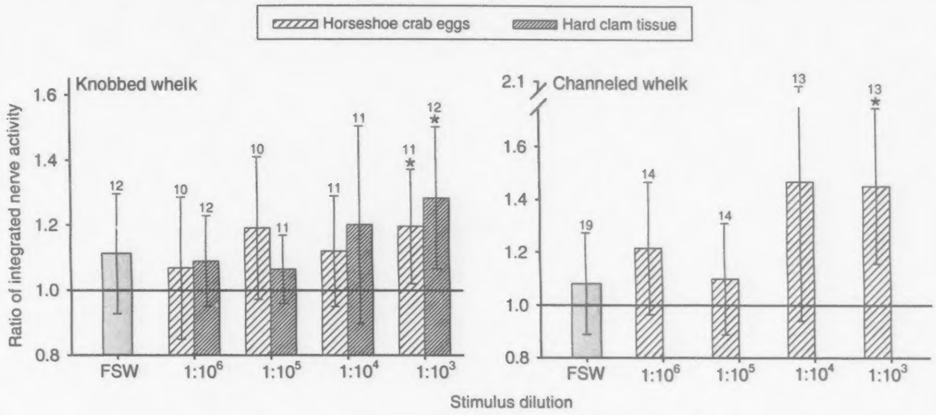

Figure 3

Mean responses (±95% CI) of knobbed (*Busycon carica*) and channeled (*Busycotypus canaliculatum*) whelks to odorant solutions prepared from horseshoe crab (*Limulus polyphemus*) eggs and hard clam (*Mercenaria mercenaria*) tissue. FSW refers the use of filtered sterilized water in place of an odorant solution. The data are the ratio of integrated activity in the pallial nerve recorded *during* exposure of the osphradium to integrated activity in the pallial nerve recorded *before* exposure to the odorant solutions. The numbers of individuals used in each trial (*n*) are shown above each bar. A significant response (indicated by "*") was determined to have occurred when the mean ratio of integrated nerve activity was significantly different from 1.0 (based on the 95% confidence interval). The solid line indicates a ratio of integrated activity value = 1.0.

odorant solution). The ratios of nerve activities during application of the odorant solutions to that recorded immediately before application were calculated to test for the presence of responses. This technique reduces the influence of interanimal variability, as well as the inherent variability associated with the use of suction electrodes (Stys et al., 1991).

Data sets were screened for normal distributions with the Anderson-Darling test (Minitab version 14.20.2, Minitab Inc., State College, PA) and all passed. Data were averaged across individuals for each species of whelk, and the standard errors (SE) and 95% confidence intervals (CIs) were calculated. A significant response to an odorant solution was deemed to have occurred if the 95% CI of the mean ratio of integrated nerve activity did not overlap 1.0. This was equivalent to using a two-tailed *t*-test with $P < 0.05$ taken as the level of significance.

Results

The pallial nerve typically showed spontaneous activity, although nerve activity clearly increased as the concentration of a detectable odorant solution in the osphradium chamber reached maximal concentration (Fig. 2). Once the flow of FSW was resumed (90 seconds after stimulus onset), the concentration of odorant solution in the osphradium chamber decreased (Fig. 1B) and nerve activity diminished (Fig. 2). Nerve activity generally returned to near prestimulus levels within the recording period (Fig. 2).

Neither species responded to FSW alone (Fig. 3). Odorant solutions extracted from horseshoe crab eggs with FSW elicited a significant increase in pallial nerve activity in both knobbed and channeled whelks at a dilution of 10^3:1, but not at any of the higher dilution ratios (i.e., lower concentrations) (Fig. 3). Odorant solutions extracted from hard clam tissue also elicited a significant increase in pallial nerve activity of knobbed whelk at the 10^3:1 dilution ratio, but not at higher dilutions (Fig. 3). This solution was not tested on channeled whelk. In contrast to odorant solutions prepared from horseshoe crab eggs by using FSW, odorant solutions containing horseshoe crab hemolymph generated a species-specific pattern of responses. These elicited significant increases in pallial nerve activity in knobbed whelk at both 100:1 and 133:1 dilutions, whereas channeled whelk did not respond to any of the four concentrations tested (Fig. 4).

Odorant solutions prepared from horseshoe crab eggs by using 50 mM Tris buffer solution were tested only on channeled whelk (Table 1). This stimulus elicited a significant increase in pallial nerve activity at a dilution of 10^3:1, but not at higher dilutions (Fig. 5)—a result identical to that recorded in channeled whelk with the use of horseshoe crab eggs odorant solutions prepared with FSW (Fig. 3). Channeled whelk did not respond to the Tris buffer solution alone (Fig. 5). Nor did they respond to either of the molecular weight fractions (>3 kDa nor <3 kDa) prepared from the horseshoe crab egg odorant solutions by ultrafiltration at any concentration tested (Fig. 5). When recombined, the molecular weight fractions again induced a response at 10^3:1 dilution (Fig 5).

Discussion

Electrophysiological techniques appear suitable for determining odorant solutions that stimulate the pallial nerve in both knobbed and channeled whelks. The sustained increases in nerve activity of the pallial nerves of these two species (exemplified by the results shown in Fig. 2) are similar to those recorded by Bailey and Laverack (1963, 1966) upon exposure of the osphradium of the common whelk (*Buccinum undatum*) to extracts prepared from the blue mussel (*Mytilus edulis*). Bailey and Laverack (1966) also observed extended periods of increased nerve activity, which they termed "the *Mytilus* response." Wedemeyer and Schild (1995) demonstrated similar increases in activity of the pallial nerves of the pond snail (*Lymnaea stagnalis*) in response to exposure of the osphradium to mixtures of amino acids, to hypercapnia, and to hypoxia. The sustained activity in the pallial nerve during odor stimulation observed in knobbed and channeled whelks (exemplified in Fig. 2) is also consistent with Ferner and Weissburg's (2005) findings that slow moving gastropod mollusks locate odor sources in turbulent flow conditions by temporally averaging odor concentrations across a plume. In contrast, the more rapid onset and offset of olfactory responses (i.e., shorter temporal resolution) of the crustacean olfactory system (Gomez and Atema, 1996) appears to hinder their olfactory navigation in turbulent environments (Weissburg and Zimmer-Faust, 1993, 1994).

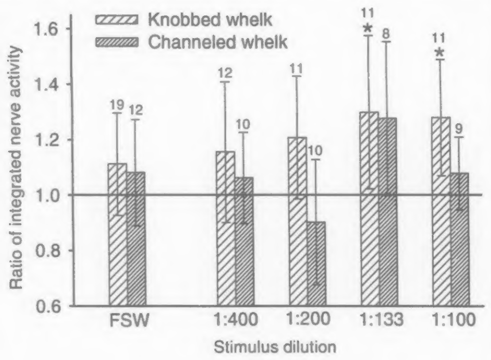

Figure 4

Mean responses (±95% confidence interval) of knobbed (*Busycon carica*) and channeled (*Busycotypus canaliculatum*) whelks to horseshoe crab (*Limulus polyphemus*) hemolymph diluted with filtered sterilized water. The data are the ratio of integrated activity in the pallial nerve recorded *during* exposure of the osphradium to odorant solutions to intergrataed activity recorded *before* exposure to odorant solution. The numbers of individuals used in each trial are shown above each bar (*n*). A significant response (indicated by "*") was determined to have occurred when the mean ratio of integrated nerve activity was significantly different from 1.0 (based on the 95% CI). The solid line indicates a ratio of integrated activity value = 1.0.

It is possible that increases in nerve activity in response to odorant solutions also include increases in proprioceptor activity resulting from odor-induced muscular contractions. The pallial nerve appears to be a sensory nerve that conveys a suite of information to the circumesophogeal ganglion (Laverack and Bailey, 1963). The pallial nerves of whelks show a low level of almost constant spontaneous activity (Fig. 2C), and rapid onset and offset increases in activity associated with slight spontaneous movements of the head, proboscis, or siphon (Fig. 2A). The origin of the spontaneous activity is unknown, but the latter (the rapid onset and offset increases in activity) are most likely due to activity of axons within the pallial nerve originating from proprioceptors (Laverack and Bailey, 1963). It is possible, therefore, that the ultimate origin for nerve activity seen during application of odorant solutions to the osphradium are proprioceptors, and that these are being stimulated by increased movements in response to application of odorant solutions to the osphradium. This does not, however, invalidate the results. Responses to odorant solutions are still being recorded, albeit not directly in the manner assumed.

One of the objectives of the present project was to determine whether odorant solutions prepared from horseshoe crab eggs stimulated chemosensory receptors in the whelk species targeted by the pot fishery. Ferrari and Targett (2003) suggested the potential use of olfactory attractants from horseshoe crab egg extracts as an alternative to horseshoe crab bait. Their conclusion was based on the behavioral responses of the common mud snail to heat-stable proteinaceous compounds extracted from horseshoe crab eggs. Because both knobbed and channeled whelks respond to horseshoe crab egg odorant solutions prepared with FSW at a 10^3:1 dilution (Fig. 3), our results support their findings. Horseshoe crab eggs clearly contain a compound (or compounds) detectable by whelks even at low concentrations; therefore odorant solutions prepared from horseshoe crab eggs need to be examined further.

Defining chemical cues from a specific molecular weight class that elicit a response in whelks may prove to be difficult. Channeled whelk responded to odorant solutions prepared from horseshoe crab eggs with Tris buffer solution, as well as the recombined molecular weight fractions (i.e., >3 kDa and <3 kDa). They did not respond to either molecular weight fraction independently (Fig. 5). These results imply that neither the initial extraction (FSW vs. Tris buffer solution) nor ultrafiltration procedures destroy the stimulatory components present within the horseshoe crab egg extract. These results also imply that channeled whelk have broadly tuned chemoreceptors requiring a range of low and high molecular weight constituents to elicit a response. Channeled whelk thus appear to differ from other aquatic animals that generally respond to a narrow spectrum of chemical stimulants (e.g., fishes, Carr et al., 1996; Zielinski and Hara, 2007, and crustaceans, Borroni et al., 1986; Kozlowksi et al., 2001). Our results from whelk also differ from behavioral experiments on mud snails, in that mud snails are apparently capable of detecting the low molecular weight fractions (<10 kDa) of horseshoe crab egg extracts prepared by ultrafiltration (Ferrari and Targett, 2003).

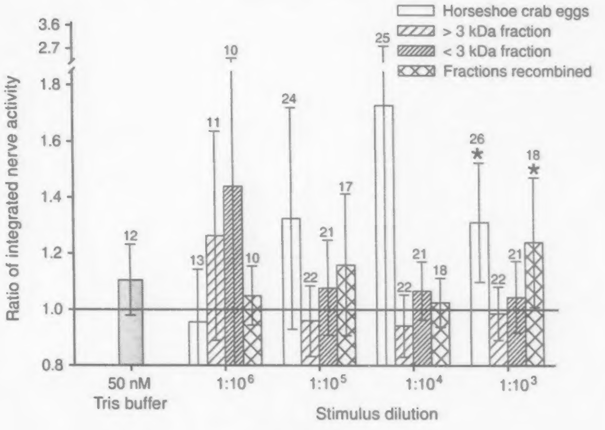

Figure 5

Mean responses (±95% confidence interval) of channeled whelk (*Busycotypus canaliculatum*) expressed as the ratio of integrated activity in the pallial nerve before the introduction odorant solutions or 50 mM Tris buffer solution. The odorant solutions were prepared from horseshoe crab (*Limulus polyphemus*) eggs extracted with 50 mM Tris buffer solution, two molecular fractions (>3 kDa and <3 kDa) of this odorant solution prepared by ultrafiltration, and the two molecular weight fractions recombined. The numbers of individuals exposed to various odorant solutions are shown above each bar (*n*). A significant response (indicated by "*") was determined to have occurred when the mean ratio of integrated nerve activity was significantly different from 1.0 (based on the 95% CI). The solid line indicates a ratio of integrated activity value = 1.0.

Knobbed whelk responded to an odorant solution prepared from hard clam tissue (Fig. 3). Because hard clams are a common prey item of whelks (Magalhaes, 1948; Walker, 1988), we surmise that channeled whelk would respond similarly. Bait based on hard clam tissue, or some extract thereof, could potentially serve as replacement for horseshoe crabs in the whelk pot fishery. The cost of raw material may be prohibitive, however, because hard clams are also harvested for human consumption. Likewise, knobbed whelk responded to horseshoe crab hemolymph even when diluted 133:1 (Fig. 4). Surprisingly, hemolymph did not induce a response in channeled whelk at even the highest concentration tested. There is no apparent explanation for this difference in response by the two species. Horseshoe crab hemolymph may offer some promise as the basis for manufactured bait for the whelk pot fishery primarily because it can be obtained in large quantities from an ecofriendly source (i.e., from the pharmaceutical companies producing LAL), and probably at a reasonable cost. It should be noted that horseshoe crab blood is generally treated with proprietary chemical mixtures during LAL production to prevent clotting and to prepare the amoebocyte cells for further processing. If the chemicals are toxic, this could prevent the use of waste hemolymph directly in manufactured baits and preclude their eventual release into the environment.

In summary, electrophysiological techniques recording afferent activity in the pallial nerves of whelks can be used to identify effective odorant solutions, as well as approximate detectable odor concentration limits. Knobbed and channeled whelks responded to extracts prepared from horseshoe crab eggs, and the former responded to horseshoe crab hemolymph diluted up to 133 times, as well as to extracts prepared from hard clam tissue. Channeled whelk do not respond to individual molecular weight fractions of horseshoe crab egg extracts, and this result implies that whelks have broadly tuned chemoreceptors and that manufactured baits may need to mimic the complex mixture of odors derived from natural sources.

Acknowledgments

This project was supported by grants from the National Oceanic and Atmospheric Administration Chesapeake Bay Office (PO no. DG133F04SE1208), the National Marine Fisheries Service (Northeast Fisheries Science Center), Delaware Sea Grant (RF-9 05/07), Delaware Department of Natural Resources and Environmental Control, and the National Fish and Wildlife Foundation. We acknowledge R. Fisher (Virginia Institute of Marine Science Sea Grant Program) for his support throughout the project; R. Robins Jr. and M. Pegg for donations of live whelk and horseshoe crab hemolymph; J. Harding, R. Mann, and J. Shields (VIMS) for their help in getting us started; the VIMS Eastern Shore Laboratory for providing live whelk, hard clams, animal holding space, and laboratory facilities. This is contribution no. 2828 from the Virginia Institute of Marine Science.

Literature cited

Alexander, C. G.
1970. The osphradium of *Conus flavidus*. Mar. Biol. 6:236–240.

Bailey, D. F., and M. S. Laverack.
1963. Central nervous responses to chemical stimulation of a gastropod osphradium. Nature 200:1122–23.
1966. Aspects of the neurophysiology of *Buccinum undatum L.*—central responses to stimulation of the osphradium. J. Exp. Biol. 44:131–148.

Berkson, J., and C. N. Shuster.
1999. The horseshoe crab: the battle for a true multiple-use resource. Fisheries 24:6–11.

Borroni, P. F., L. S. Handrich, and J. Atema.
1986. The role of narrowly tuned taste cell populations in lobster (*Homarus americanus*) feeding behavior. Behav. Neurosci. 100:206–212.

Carr, W. E. S., J. C. Netherton, R. A. Gleeson, and C. D. Derby.
1996. Stimulants of feeding behavior in fish: analyses of tissues of diverse marine organisms. Biol. Bull. 190:149–160.

Emory, D. G.
1992. Fine structure of olfactory epithelia of gastropod mollusks. Microsc. Res. Techniq. 22:307–324.

Ferner, M. C., and M. J. Weissburg.
2005. Slow-moving predatory gastropods track prey odors in fast and turbulent flow. J. Exp. Biol. 208:809–819.

Ferrari, K., and N. M. Targett.
2003. Chemical attractants in horseshoe crab, *Limulus polyphemus*, eggs: the potential for an artificial bait. J. Chem. Ecol. 29:477–496.

Gomez, G., and J. Atema.
1996. Temporal resolution in olfaction: Stimulus integration time of lobster chemoreceptor cells. J. Exp. Biol. 199:1771–1770.

Hansen, A., and K. Ruetter.
2004. Chemosensory systems in fish: structural, functional and ecological aspects. *In* The senses of fish (G. von der Emde, J. Mogdans, and B. G. Kapoor, eds.), p. 55–89. Kluwer Academic Publs., Boston, MA.

Hara, T. J.
1975. Olfaction in fish. Prog. Neuro. Biol. 5:271–335.

Kamio, M., A. Makota, T. Nagayama, S. Matsunaga, and N. Fusetani.
2005. Behavioral and electrophysiological experiments suggest that the antennular outer flagellum is the site of pheromone reception in the male helmet crab *Telmessus cheiragonus*. Biol. Bull. 208:12–19.

Kozlowski, C., K. Yopak, R. Voigt, and J. Atema
2001. An initial study on the effects of signal intermittency on the odor plume tracking behavior of the American lobster, *Homarus americanus*. Biol. Bull. 201: 274–276.

Laverack, M. S., and D. F. Bailey.
1963. Movement receptors in *Buccinum undatum*. Comp. Biochem. Physiol. 8:289–98.

Levy, M., S. Blumberg, and A. J. Susswein.
1997. The rhinophores sense pheromones regulating multiple behaviors in *Aplysia fasciata*. Neurosci. Lett. 225:133–16.

Magalhaes, H.
1948. An ecological study of snails of the genus *Busycon* at Beaufort, North Carolina. Ecol. Monogr. 18:377–409.

Morrison, R. I. G., R. K. Ross, and L. J. Niles.
2004. Declines in wintering populations of red knots in southern South America. Condor 106:60–70.

Murphy, B. F., and M. G. Hadfield.
1997. Chemoreception in the nudibranch gastropod *Phestilla sibogae*. Comp. Biochem. Physiol. A. 118:727–35.

Rahman, Y. J., R. B. Forward, and D. Rittschof.
2000. Responses of mud snails and periwinkles to environmental odors and disaccharide mimics of fish odor. J. Chem. Ecol. 26:679–696.

Steffensen, J. F.
1989. Some errors in respirometry of aquatic breathers: how to avoid and correct them. Fish. Physiol. Biochem. 6:49–59.

Stys, P. K., B. R. Ransom, and S. G. Waxman.
1991. Compound action potential of nerve recorded by suction electrode: a theoretical and experimental analysis. Brain Res. 546:18–32.

Tsipoura, N., and J. Burger.
1999. Shorebird diet during spring migration stopover on Delaware Bay. Condor 101:635–644.

Walker, R. L.
1988. Observations of intertidal whelk (*Busycon* and *Busycotypus*) populations in Wassaw Sound, Georgia. J. Shellfish Res. 7:473–478.

Walls, E. A., and J. Berkson.
2000. Effects of blood extraction on the mortality of the horseshoe crab, *Limulus polyphemus*. Va. J. Sci. 51: 195–198.

Wedemeyer, H., and D. Schild.
1995. Chemosensitivity of the osphradium of the pond snail *Lymnaea stagnalis*. J. Exp. Biol. 198:1743–1754.

Weidensaul, S.
2006. Red knots in a bind: conservationists race to save these wandering shorebirds from extinction. Defenders 81:13–19.

Weissburg, M. J., and R. K. Zimmer-Faust.
1993. Life and death in moving fluids: hydrodynamic effects on chemosensory mediated predation. Ecology 74:1428–1443.
1994. Odor plumes and how blue crabs use them to find prey. J. Exp. Biol. 197:349–375

Wilson, D. A.
2004. Fish smell. Focus on "odorant specificity of single olfactory bulb neurons to amino acids in the channel catfish". J. Neurophysiol. 92:38–39.

Zielinski, B. S., and T. J. Hara.
2007. Olfaction. *In* Sensory systems neuroscience (T. J. Hara, and B. S. Zielinski, eds.), p. 1–44. Fish physiology, vol. 25. Academic Press, San Diego, CA.

Incorporating fishery observer data into an integrated catch-at-age and multiyear tagging model for estimating mortality rates and abundance

J. Paige Eveson (contact author)[1]

Tom Polacheck[1]

Geoff M. Laslett[2]

Email for J. Paige Eveson: paige.eveson@csiro.au

[1] Commonwealth Scientific and Industrial Research Organization (CSIRO)
Marine and Atmospheric Research
Castray Esplanade
Hobart, Tasmania 7000, Australia
Postal address: GPO Box 1538
Hobart, Tasmania 7001, Australia

[2] CSIRO Mathematical and Information Sciences
Private Bag 33
Clayton South, Victoria 3169, Australia

Abstract—Tagging experiments are a useful tool in fisheries for estimating mortality rates and abundance of fish. Unfortunately, nonreporting of recovered tags is a common problem in commercial fisheries which, if unaccounted for, can render these estimates meaningless. Observers are often employed to monitor a portion of the catches as a means of estimating reporting rates. In our study, observer data were incorporated into an integrated model for multiyear tagging and catch data to provide joint estimates of mortality rates (natural and fishing), abundance, and reporting rates. Simulations were used to explore model performance under a range of scenarios (e.g., different parameter values, parameter constraints, and numbers of release and recapture years). Overall, results indicated that all parameters can be estimated with reasonable accuracy, but that fishing mortality, reporting rates, and abundance can be estimated with much higher precision than natural mortality. An example of how the model can be applied to provide guidance on experimental design for a large-scale tagging study is presented. Such guidance can contribute to the successful and cost-effective management of tagging programs for commercial fisheries.

Manuscript submitted 10 December 2006 to the Scientific Editor's Office.

Manuscript approved for publication 24 May 2007 by the Scientific Editor.

Fish. Bull. 105:493–508 (2007).

Tagging experiments are becoming increasingly important in large pelagic fisheries as a means of providing estimates of stock abundance and fishing mortality rates that are independent of catch-rate data (Polacheck and Hearn, 2003). In Polacheck et al. (2006), we developed a maximum likelihood model that combines two traditional, but fundamentally different, approaches for analyzing tagging data with a single, terminal recapture (note that we refer to this as "tag-recapture" data, but the term "tag-recovery" data is often used in the literature). The first approach, generally referred to as a Brownie model (Brownie et al., 1985), uses tag-recapture data from multiple years of tagging to provide annual estimates of mortality rates by comparing return rates over time from the releases in consecutive years. Only the numbers of tag releases and returns by year are required, not the number of animals examined for tags. The standard Brownie model is formulated in terms of rates of survival and tag recovery, but can also be expressed in terms of instantaneous rates of natural mortality and exploitation (Pollock et al., 1991; Hoenig et al., 1998a). This latter formulation is particularly useful in fishery applications (e.g., Hampton, 2000; Frusher and Hoenig, 2001; Polacheck et al., 2006). The second approach, known as a Petersen model (e.g., Seber, 1982), uses data from a single release event to provide an estimate of population size at the time of tagging based on the ratio of the number of tags returned from a sample of the population to the total number of tags in the population. In fishery applications, commercial catch data usually constitute the sample from which tags are returned.

The model developed by Polacheck et al. (2006) integrates catch data with data from a multiyear tagging experiment and, in essence, incorporates a Petersen estimator into a Brownie model; we will refer to it as the Brownie-Petersen (BP) model. The BP model involves a likelihood for the tag-recapture data and a likelihood for the catch data, which can be jointly maximized to provide estimates of natural mortality rates, fishing mortality rates, and abundance. The addition of catch data to the traditional Brownie model not only allows for the population size at the time of first tagging to be estimated but also improves the precision of the mortality-rate estimates (Polacheck et al., 2006). For readers familiar with multiple-recapture tagging models, the BP model has similarities with an age-structured Jolly-Seber (JS) model (Jolly, 1965; Seber, 1965; Pollock, 1981). Both the BP and JS models have a likelihood component for the recapture data, from which survival rates can be estimated. For the BP model, this component equates to a Brownie model, and for the JS model, it equates to a Cormack-Jolly-Seber (CJS) model (Cormack, 1964). Additionally, they both have a likelihood component involving the total number of animals sampled, from which abundance can be estimated (i.e., the Petersen component). However, for the JS model there is an unresolved problem with the Petersen component regarding how the information from unmarked animals should be integrated into the likelihood, and a variety of approaches have been developed to address this problem (see section 4.3 of Schwarz and Seber, 1999, and references therein). The Petersen component of the BP model (i.e., the catch component) is more general and integration into the likelihood is more straightforward.

A recognized problem with applying tagging experiments in fishery situations is that of nonreporting. When recapture information comes from commercial fisheries, it is unlikely that all recaptured tags will be reported, or that the rate of reporting will be known. Although Brownie models can provide estimates of total mortality rates when reporting rates are unknown (Brownie et al., 1985), the separation of natural mortality from fishing mortality generally requires that reporting rates are either known or estimable (Pollock et al., 1991; Hoenig et al., 1998a). Petersen models also require reporting rates to determine abundance estimates.

A number of methods exist for estimating reporting rates (see Pollock et al., 2001). For some methods, such as planted (also called "seeded") tag experiments, the data are independent of the tag-recapture and related catch data from the primary tagging study. In developing the BP model, we assumed that independent reporting rate data were available; therefore a likelihood could be constructed for these data and simply multiplied to the likelihoods for the tag-recapture and catch data. Another common method for estimating reporting rates is to have observers monitor a portion of the catches. Under the assumption that 100% of tags will be returned (i.e., reported) from the observed catches, the reporting rate for the unobserved catches can be estimated by using the relative return rate of tags from the unobserved versus observed catches (Hearn et al., 1999). In the case of longline fisheries, where fish are not brought into port for processing, the use of observers to estimate reporting rates is probably the most viable approach. Unlike data from a planted tag experiment, observer data cannot be considered independent of the tagging or related catch data and therefore incorporating the estimation of reporting rates into the BP model is more complicated.

Pollock et al. (2002) showed how a standard Brownie model can be modified to include the estimation of reporting rates when one component of a multicomponent fishery has 100% reporting rates (e.g., one component has observers). This modification required that supplementary catch data be brought into the model to assist in the estimation of reporting rates. Pollock et al. (2002) acknowledged that uncertainty in the catch data was not accounted for in their model, and also that it would be resourceful to take advantage of the extra information provided by the catch data to estimate population size. As a topic of future research, they advocated the development of an integrated analysis that estimates all parameters (fishing mortality, natural mortality, population size, and reporting rates) within a single likelihood.

In this article, the BP model is extended to include the estimation of reporting rates by using observer data. We will refer to this extended model as the BPO model, short for the Brownie-Petersen model with observers. The BPO model fulfills the goal of Pollock et al. (2002) for an integrated likelihood that can provide joint estimates of mortality rates, abundance, and reporting rates, and it also directly incorporates uncertainty in the catch data. Results from applying the model to simulated data are presented which demonstrate the accuracy and precision that can be achieved in the parameter estimates under various scenarios (e.g., different parameter values, different numbers of release and recapture years, different parameter constraints). Tag-recapture data and catch data from most field studies will exhibit more variability than the model predicts (i.e., will be overdispersed). Thus, extra variability was included in the simulated data sets to investigate the consequences of applying the model to overdispersed data. Finally, a practical illustration is given of how the model can be used to evaluate the trade-off between releasing more tags and increasing the level of observer coverage in terms of the accuracy and precision of the parameter estimates. Polacheck and Hearn (2003) investigated this issue using a much simpler model (e.g., only one release event; only fishing mortality rates estimated) and making many simplifying assumptions (e.g., natural mortality known; no uncertainty in the catch data; no overdispersion in the data). The BPO model provides a much more comprehensive framework for evaluating such trade-offs and can thereby make an important contribution to the successful and cost-effective management of tagging programs for commercial fisheries.

Materials and methods

Model description

Consider a multiyear tagging study in which a single cohort of fish is tagged in A consecutive years starting at age 1 (i.e., at age 1 in year 1, age 2 in year 2, up to age A in year A). Fish from this cohort are subsequently caught in a fishery over years, or ages, 1 to I ($I \geq A$), and a percentage of the tags that are recaptured each year are reported. Observers monitor a portion of the catches, and 100% of recaptured tags are reported from the observed component of the fishery. Furthermore, all fish caught in the observed component of the fishery are sampled for length or age, but no fish from the unobserved component are sampled. The catch monitored by observers is assumed to be representative of the total catch (i.e., catches from the observed and unobserved components have the same expected age distribution). If the expected catch-at-age distribution differed between the two components, then separate age information would need to be available for each component and the catch likelihood presented below would need to be modified.

The basic assumptions common to all multiyear tagging models, as summarized in Pollock et al. (1991), are also required for the BPO model. The most important of these are: 1) tagged and untagged fish are thoroughly mixed throughout the population of interest, 2) the fate of each fish is independent of the fate of other fish, 3) all fish of a given age class have the same survival and capture probabilities, and 4) there is no tag shedding or tag-induced mortality. If tag shedding or tag-induced mortality, or both, exist at non-trivial levels (i.e., assumption 4 is not met), then additional parameters and potentially additional data need to be introduced to account for them. Failing to do so will lead to biased parameter estimates and overly optimistic estimates of their precision. If any of assumptions 1 to 3 is violated, then the variance of the tag return counts will be underestimated by the model. Similarly, if assumption 2 or 3 is violated, the variance of the catch numbers will be underestimated. Extra variability, or overdispersion, in the tag return and catch data is discussed in the next section.

Assumption 1 implies that newly tagged fish are mixed throughout the population immediately after tagging. This mixing can be difficult to achieve in practice, especially when the population has a widespread geographical distribution or tagging occurs in a limited area of its distribution. Hoenig et al. (1998b) showed how delayed mixing of newly tagged fish can be incorporated into a Brownie model by allowing these fish to have a different fishing mortality rate in the year of tagging than that of previously tagged fish. In our application of the BP model to southern bluefin tuna (SBT, *Thunnus maccoyii*) data in Polacheck et al. (2006), we allowed for initial nonmixing with this approach. Only the tag-recapture component of the model needed to be modified. It would be straightforward to modify the tag-recapture component of the BPO model in an analogous manner in situations where modification was considered necessary.

Before proceeding, we introduce the notation that will be used throughout this study. The data required by the model are

N_a = the number of tag releases of age a fish from a particular cohort;

$R^o_{a,i}$ = the number of tag returns from fish that were tagged at age a and recaptured at age i in the observed (o) component of the fishery;

$R^u_{a,i}$ = the number of tag returns from fish that were tagged at age a and recaptured at age i in the unobserved (u) component of the fishery; and

C^o_i = the estimated number of age i fish from the cohort of interest caught in the observed (o) component of the fishery.

The model parameters assumed to be known are

δ_i = the proportion of fish from the cohort of interest caught in the observed component of the fishery in year i;

η^2_i = the variance of the aging error for C^o_i.

The model parameters to be estimated from the data are

M_i = the instantaneous natural mortality rate for age i fish;

F_i = the instantaneous fishing mortality rate for age i fish;

P_1 = the population size of the tagged cohort at the age of first tagging (assumed to be age 1 for convenience); and

λ_i = the tag reporting rate for fish captured at age i in the unobserved component of the fishery.

In addition, the annual survival rate (S_i) and exploitation rate (u_i), respectively, of an age i fish, are defined to be

$$S_i = \exp\left(-\left(F_i + M_i\right)\right);$$

$$u_i = \frac{F_i}{F_i + M_i}\left(1 - S_i\right).$$

Note that because only a single cohort of fish is being considered, age and year can be used interchangeably in the above definitions. If more cohorts were added to the model, it would then be important to distinguish whether the parameters vary by year, by age, or both. For example, λ may vary by year, M by age, and F by both. Because the age distribution of the catch is assumed to be the same for the observed and unobserved components, δ would vary with year, not age, when there is more than one cohort (i.e., the probability of a fish being caught in the observed component of the fishery in year i would be the same for all ages within the year). If the age distribution of the catch was allowed to differ between the observed and unobserved components, then δ would need to vary with both year and age, but it would not be estimable unless information was available about the age distribution of the unobserved catches.

First consider the tag-recapture component of the model. The probability of a fish, tagged at age a, being caught in the observed component of the fishery at age i, and having its tag returned, is

$$p^o_{a,i} = \begin{cases} \delta_i u_i & i = a \\ \delta_i S_a \cdots S_{i-1} u_i & i > a \end{cases}. \tag{1}$$

Similarly, the probability of a fish, tagged at age a, being caught in the unobserved component of the fishery at age i, and having its tag returned, is

$$p_{a,i}^{u} = \begin{cases} (1-\delta_i)u_i\lambda_i & i=a \\ (1-\delta_i)S_a \cdots S_{i-1}u_i\lambda_i & i>a \end{cases}. \tag{2}$$

Thus, the probability of a fish, tagged at age a, not being recaptured by age I from either component is p'_a = $1- p^o_{a,i} - p^u_{a,i}$. Here, and below, a dot in the subscript denotes summation over the index it replaces.

For tags released at age a, the numbers of returns at ages a to I from the observed component ($R^o_{a,i}$, $i=a, \dots, I$) and unobserved component ($R^u_{a,i}$, $i=a, \dots, I$), plus the number not returned by age I from either component ($R'_a=N_a - R^o_{a,i} - R^u_{a,i}$), are multinomial with probabilities given by Equations 1, 2 and p'_a, respectively. Thus, the likelihood equation for the returns from tags released at all ages is the product of multinomials, given by

$$L_R = \gamma \prod_{a=1}^{A} \left\{ (p'_a)^{R'_a} \prod_{i \ge a}^{I} (p^o_{a,i})^{R^o_{a,i}} (p^u_{a,i})^{R^u_{a,i}} \right\}, \tag{3}$$

where

$$\gamma = \prod_{a=1}^{A} \frac{N_a!}{R'_a! \prod_{i \ge a} \left(R^o_{a,i}!\, R^u_{a,i}! \right)}.$$

Note that γ is a constant that can be left out when maximizing the liklehood.

Next, consider the catch component of the model. Recall that no age information is obtained for the unobserved catches; therefore only catch-at-age data from the observed component are available for inclusion in the model. The probability of an age-1 fish from the cohort of interest subsequently being caught at age i in the observed component of the fishery is

$$\pi_i^o = \begin{cases} \delta_i u_i & i=1 \\ \delta_i S_1 \cdots S_{i-1} u_i & i>1 \end{cases}. \tag{4}$$

If the numbers of fish from the cohort of interest that are caught at ages 1 to I in the observed component of the fishery (C^o_i, $i=1, \dots, I$) are known accurately, then these numbers, along with the number of fish from the cohort not caught by age I, are multinomial and have probabilities given by Equation 4. Usually, however, the numbers of fish caught at each age are not known precisely because the ages are estimated either from lengths or from annuli in hard parts (the estimates will be more accurate in the latter case, but will still contain uncertainty). We assume the aging error of the age i catch has a Gaussian distribution with mean 0 (i.e., no bias) and a variance η^2_i.

Rather than modeling the catch data with both multinomial process error and Gaussian aging error, which would require a fairly complex approach, we approximated the distribution of the catch of age i fish in the observed component, C^o_i, as Gaussian with overall variance $\sigma^2_i=\eta^2_i+\tau^2_i$, where $\tau^2_i=P_1\pi^o_i(1-\pi^o_i)$, is the multinomial variance component. The aging error, unless negligible, will tend to dominate the process error when the cohort size is reasonably large (≥100,000 individuals), as would be expected in most commercial fishery situations. For example, if the coefficient of variation (CV) of the aging error is 0.10, the cohort size is 100,000 and the probability of catching an age i fish (in either the observed or unobserved component of the fishery) is 0.10, then the ratio of the aging error variance to the process error variance is ~10 when the proportion of the catch in the observer component is 0.10, and it is ~50 when the proportion of the catch in the observer component is 0.50.

Thus, assuming that the C^o_i's are independent between ages, the likelihood for the observer catch data is

$$L_C = \prod_{i=1}^{I} \frac{1}{\sqrt{2\pi\sigma_i^2}} \exp\left(-\frac{1}{2\sigma_i^2} \left(C_i^o - E(C_i^o) \right)^2 \right), \tag{5}$$

where $E(C^o_i)=P_1\pi^o_i$.

When only a single cohort of fish is being modeled, the assumption that the catch data are independent between ages (i.e., years) should be reasonable in most situations. First, the correlation in the multinomial errors will be close to zero when the size of the cohort is much larger than the size of the catch (as would be expected in most fisheries). Second, the aging errors should be uncorrelated between years provided sampling and aging data are collected each year. However, in some situations, particularly where age is being estimated from a growth curve, covariance in the estimates between years may exist and should be accounted for. Furthermore, if more than one cohort is being modeled, then catch data from multiple ages within the same year will enter the model, and aging errors within a year will be correlated across ages. The level of correlation, and thus the degree to which the independence assumption is violated, will depend on the specifics of the situation, such as how many age classes are present in the year's catch. When the correlation is strong, a more sophisticated approach for modeling the catch data may be required.

The overall likelihood for the combined recapture and catch data can be obtained by multiplying likelihoods (Eqs. 3 and 5) together:

$$L = L_R \times L_C. \tag{6}$$

In a tagging experiment with A consecutive release years, estimates can be obtained, at most, for A–1 natural mortality-rate parameters (regardless of the number of recapture years) because information for estimating M_i comes from the differential between the expected returns at age i+1 of fish released at age i and those released at age i+1. One option is to assume that $M_i=M_{A-1}$ for $i \ge A$, but other options, such as assuming M is constant or linear with age, are also possible. Furthermore, there is not enough information in the current formulation to estimate the proportion of fish caught each year in the observed component of the fishery (i.e., the δ_i's). To estimate this proportion would require knowing the total observer catch in each year, as well as the total overall catch in each year. Rather than bringing these data into the model, we assumed that the total catches are known well enough that the δ_i's can be treated as known without error. Lastly, the aging error variance parameters for the observer catches (i.e., the η_i^2's) cannot be estimated reliably and therefore they are assumed to be known without error. In Polacheck et al. (2006), we gave a detailed explanation of why the catch variance cannot be estimated reliably in the BP model, and the same argument applies here. We found, however, that the model results were fairly insensitive to the value used for the catch variance so long as it was in the right ballpark (e.g., within ~40% of the true value). The parameters that can be estimated by maximizing Equation 6 are F_i and λ_i for $i = 1$ to I, M_i for $i = 1$ to A–1, and P_1.

As is true when combining any sources of information, it is important to check that the tag-recapture data and the catch data are consistent. This can be done by maximizing the tag-recapture likelihood (Eq. 3) alone and comparing the mortality-rate estimates with those obtained from the joint likelihood (Eq. 6) (note that the catch likelihood alone is insufficient to yield parameter estimates). If the estimates are significantly different, this result would indicate that the tag-recapture and catch data are inconsistent and should not be combined; doing so would yield average values with little biological meaning. Instead, the source of the inconsistency should be investigated (i.e., does it stem from problems with the data or with the applicability of the assumptions in the model?).

Overdispersion in the recapture and catch data

In the model a multinomial distribution is assumed for the tag-recapture data. If one (or more) of model assumptions 1 to 3 is violated, then the observed return counts are expected to be more variable than predicted by a multinomial distribution; i.e., to be overdispersed in relation to multinomial data. Polacheck et al. (2006) provided a thorough discussion of possible sources of overdispersion and ways in which it can be accounted for. When overdispersion exists in the return counts, the parameter estimates obtained by using a multinomial likelihood should still be unbiased, but their standard errors, as estimated from traditional likelihood methods (i.e., from the inverse Hessian matrix), would be too small. A number of possible methods for obtaining more realistic standard errors are discussed in Polacheck et al. (2006) and Pollock et al. (2001), one of which is to use bootstrap procedures.

If overdispersion exists in the recapture data as a result of model assumptions 2 or 3 being violated, then it will also exist in the catch data. That is, the component of the variance in the catch-at-age numbers due to process error will be underestimated by a multinomial distribution. As asserted previously, aging error will generally dominate the multinomial process error in the catch data. This will often still be true when the process error is overdispersed. For example, assume that the process error variance is φ times that of multinomial variance; i.e., $\tau^2_i = \varphi P_1 \pi_i^o (1-\pi_i^o)$. Then, in the example that was given above for multinomial process error, if $\varphi=3$, the ratio of the aging error variance to the process error variance would still be 3.3 (=10/3) and 17 (=50/3) when the proportion of catch in the observer component is 0.10 and 0.50, respectively. In situations where the aging error dominates, not accounting for overdispersion in the catch data should have little effect on the standard error estimates of the parameter estimates.

The degree to which the likelihood-based estimates of the standard errors are underestimated by not accounting for overdispersion in the tag-recapture data and catch data was investigated through simulations, as described below.

Simulation methods

Model performance To evaluate how the model performs in terms of the accuracy and precision of the parameter estimates, a series of Monte-Carlo simulations were conducted. The first scenario considered, which we will refer to as scenario 1, involved a single cohort of fish being tagged in five consecutive years starting at age 1 (i.e., at age i in year i for i=1, . . . , 5), and recaptured over the same five years. The number of tag releases was set to be 1000 at each age. Corresponding to the releases at each age, tag returns were generated from the observed and unobserved fishery components by using a Dirichlet-multinomial (D-M) distribution (Mosimann, 1962). The D-M distribution allows for overdispersion in the return counts by modeling the return probabilities as random Dirichlet variables (see Appendix A of Polacheck et al., 2006). It can be parameterized in terms of the return probabilities and an overdispersion factor, φ, that specifies the amount of extra variation in relation to multinomial data. For scenario 1, φ was set to be 3 (i.e., three times greater variance than a multinomial distribution). Other parameters were set as follows: F_i=0.15, M_i=0.2, λ_i=0.75, and δ_i=0.10, for i=1, ... , 5. Catch-at-age numbers (ages 1 to 5) for the observer component of the fishery were generated by using, first, a D-M distribution with P_1 = 100,000 and the same φ, δ_i, M_i, and F_i values as for the tag-recapture data. To these catch-at-age numbers, additional Gaussian aging error was added by using a constant CV of v = 0.10 for all ages (i.e., $\eta_i = v\mathrm{E}(C_i^o)$).

The BPO model was fitted to the simulated tag-recapture and catch data by maximizing Equation 6. For this process, φ and v were assumed to be known without error, and natural mortality was constrained to be the same at ages 4 and above (i.e., M_4=M_5; recall that only four natural mortality parameters can

Table 1

Description of simulation scenarios. In all scenarios, data were generated for a single cohort of fish tagged at ages 1 to A and recaptured at ages 1 to I, by using an age 1 cohort size of P_1, a constant natural mortality rate of M, a constant fishing mortality rate of F, a constant reporting rate in the unobserved fishery component of λ, a constant coefficient of variation for the catch aging error of ν, and an overdispersion factor of φ (values specified in table). Unless otherwise stated, data were generated by using N=1000 releases per year and a constant proportion of observer coverage of δ=0.20. In fitting the model, φ and ν were assumed to be known, and natural mortality was constrained to be the same for ages A–1 to I. Additional parameter constraints for each scenario are specified in the table. Bold text for a given scenario indicates a difference from scenario 1.

	Parameter values used to generate data								Parameter constraints imposed for model fitting
Scenario	A	I	P_1	M	F	λ	υ	φ	
1	5	5	100,000	0.20	0.15	0.75	0.10	3	λ constant
2	5	5	100,000	**0.40**	0.15	0.75	0.10	3	λ constant
3	5	5	100,000	0.20	**0.30**	0.75	0.10	3	λ constant
4	5	5	100,000	0.20	0.15	**0.50**	0.10	3	λ constant
5	5	5	100,000	0.20	0.15	**0.90**	0.10	3	λ constant
6	5	5	100,000	0.20	0.15	0.75	0.10	**1**	λ constant
7	5	5	100,000	0.20	0.15	0.75	0.10	**9**	λ constant
8	5	5	100,000	0.20	0.15	0.75	0.10	3	λ constant; ***M* constant**
9	5	5	100,000	0.20	0.15	0.75	0.10	3	λ constant; ***F* linear**[1]
10	5	5	100,000	0.20	0.15	0.75	0.10	3	**none**
11	**3**	**3**	100,000	0.20	0.15	0.75	0.10	3	λ constant
12	**3**	5	100,000	0.20	0.15	0.75	0.10	3	λ constant

[1] The line is parameterized in terms of F_1 and F_5; i.e., $F_i = F_1 + (i-1)\times(F_5-F_1)/4$ for $i = 1,\ldots,5$.

be estimated with five release years). The unobserved tag reporting rate was also constrained to be constant over all recapture years (i.e., $\lambda_i=\lambda$ for i=1, … , 5). It seems reasonable that the tag reporting rate would be constant, or at least similar, over the course of the experiment. Exceptions would occur if there was a significant change in the fishery or in tag-return promotional activities during this time, or if the fishery involves multiple fleets with different reporting rates so that the overall reporting rate would change if the distribution of catches among fleets changed. To account for such situations, year-specific reporting rates were allowed for in a later scenario (see next paragraph). The only other constraints imposed were simple bound constraints to keep all parameters positive and to keep the reporting rate from exceeding one. Thus, the parameters estimated were F_i (i=1, … , 5), M_i (i=1, … , 4), P_1, and λ.

Model performance will be affected by a large number of factors, including the following: 1) the parameter values used for the mortality rates, cohort size, reporting rates, catch aging error, and overdispersion factor; 2) model parameterization (i.e., whether parameters are assumed to vary with age, year, or both, or to have a particular functional form); and 3) the design of the tagging experiment (e.g., number of release and recapture years; number of releases per year; level of observer coverage). There are endless possibilities with regard to these factors; therefore we have chosen a number of scenarios that we feel are most illustrative for which to present results (Table 1). All of these scenarios use scenario 1 as a base but include a variation on one of the factors.

Scenarios 2 through 7 investigate changes to the parameter values (factor 1). In particular, scenario 2 increases the natural mortality rate, scenario 3 increases the fishing mortality rate, scenarios 4 and 5 decrease and increase the reporting rate, respectively, and scenarios 6 and 7 decrease and increase the overdispersion factor, respectively. Changes to the cohort size and variance of the catch aging error had less impact on the results and are therefore not included here.

Model parameterization (factor 2) can have a large effect on how well parameters can be estimated. For example, if natural mortality can be assumed to be constant across ages (this is a fairly common assumption in fishery models, at least over a limited range of age classes), then the precision and accuracy of the natural mortality-rate estimate should improve, which in turn may lead to improvements in other parameter estimates. Scenario 8 explores the benefits of having a constant natural mortality rate. Another standard way of reducing the number of parameters in fishery models is to model fishing mortality as a function of age by using an appropriate selectivity curve. Scenario 9 considers the situation where fishing mortality is constrained to be a linear function of age. Note that we parameterized the line in terms of F_1 and F_5 (i.e., $F_i=F_1+(i-1)*(F_5-F_1)/4$), because this made it easy to constrain the fishing mortality rates to be positive. Instead of imposing additional constraints, scenario 10 relaxes the assumption of a constant reporting rate and allows reporting rates to differ across years. This scenario has the maximum number of parameters that can be estimated by the model (i.e., the model is saturated).

In terms of experimental design (factor 3), the effect of varying the number of tag releases and the proportion of observer coverage is investigated in detail in the next section; therefore only variations to the numbers of release and recapture years are considered here. In particular, scenario 11 reduces the number of release and recapture years from five to three, whereas scenario 12 still has five recapture years but only three release years. For both scenarios, natural mortality was constrained to be equal at ages 2 and above, because only two natural mortality parameters can be estimated with three release years. For scenario 12, this meant constraining natural mortality to be equal at ages 2 to 5. In such a case, alternative constraints may be preferable, such as assuming natural mortality is a linear function of age. This was the approach taken in our application of the BP model to SBT data in Polacheck et al. (2006).

For each scenario in Table 1, 1000 sets of data were generated, as described above for scenario 1, and fitted by using the BPO model. For each parameter estimated, the percent median bias and the CV of the 1000 estimates were calculated, where percent median bias is defined as (median–true)/true×100% and CV is defined as SD/true (where SD denotes standard deviation). The median was used instead of the mean in calculating the bias because many of the parameter estimates had a skewed distribution, making the median a better measure of centrality (see "Results" section). The SDs of the parameter estimates obtained from the 1000 simulation runs (which approximate the true standard errors of the estimates) were compared with the standard error estimates obtained from the inverse Hessian matrix (these are obtained for every run; therefore we averaged the standard errors over the 1000 runs). The purpose was to see how much the Hessian-based standard errors were underestimated by applying a model that does not account for overdispersion in the data.

Trade-off between number of releases and observer coverage Of the factors that affect model performance, only the experimental design can be directly controlled by the researcher in a real application. Although model parameterization is superficially in the researcher's control, it is the true parameter values that will determine whether any parameter constraints are advantageous (i.e., imposing constraints on parameters that do not represent the true situation will lead to poorer model performance, not improved performance). Thus, in designing a tagging experiment and deciding how best to distribute resources, it would be very useful for the researcher to know the level of performance that can be achieved under different designs, as well as which design elements have the most influence on the results. Here, we illustrate how the BPO model can be used to provide such information. In particular, simulations are used to evaluate how well the parameters are estimated with different numbers of tag releases and different proportions of observer coverage, and to evaluate the trade-off between releasing more tags versus increasing observer coverage (i.e., to evaluate which leads to larger improvements in accuracy and precision of the parameter estimates).

Initially, simulations were carried out under scenario 1. For simplicity, the number of releases was kept the same for all release ages (i.e., $N_a=N$ for all a) and the proportion of observer coverage was the same over all recapture years (i.e., $\delta_i=\delta$ for all i). N was varied from 250 to 2500, and δ from 0.05 to 0.50. For each combination of N and δ, 1000 tag-recapture and corresponding catch data sets were generated, as described in the previous section, and fitted by using the BPO model. The results were used to evaluate how the percent median bias and CV of the parameter estimates changed as the number of releases and level of observer coverage changed.

For a true field study, the researcher would need to carry out such simulations using parameter values and model constraints that roughly represent the population and fishery dynamics for their situation. Our purpose was not to provide guidance on appropriate numbers of releases and observer coverage for any specific situation, but to illustrate how the model could be used to this end. Nevertheless, it is of interest to know whether the general findings using scenario 1 are likely to remain similar under other scenarios. The absolute levels of accuracy and precision that can be achieved will clearly depend on the scenario, but it is less clear whether the relative changes in these measures from increasing tag releases or increasing observer coverage will be highly scenario dependent. To investigate, we repeated the trade-off simulations using a subset of the other scenarios (4, 6, 8, 10, 11, and 12).

Results

Model performance

The biases in the medians of the parameter estimates were small for almost all parameters and scenarios (Table 2). A few of the natural mortality estimates had negative biases of greater than 5%, but this result more likely reflects the large variability and non-normality of these estimates (see next paragraph) than true biases.

Histograms of the parameter estimates revealed features that are important for evaluating biases. In particular, the natural mortality estimates often hit the lower bound of zero, and the proportion that did so was highest when the variability was largest (e.g., scenario 7, which has a high amount of overdispersion; Fig. 1). This feature makes it difficult to assess bias for these parameters and explains why the median biases seen in some of the natural mortality-rate estimates, such as scenario 7, are not likely to be meaningful. In scenarios 5, 7, and 10, the reporting-rate estimates often hit their

Table 2

Percent median bias (i.e., (median−true)/true×100%) of the parameter estimates for each scenario listed in Table 1. Results were based on 1000 simulation runs per scenario. M_i= natural mortality rate for age i fish; F_i= fishing mortality rate for age i fish; P_1= population size of tagged cohort at age 1; λ_i= tag reporting rate for fish captured at age i in the unobserved component of the fishery.

Scenario	M_1	M_2	M_3	M_4	F_1	F_2	F_3	F_4	F_5	P_1	λ_1	λ_2	λ_3	λ_4	λ_5
1	−1.0	−3.0	−1.5	−2.0	−1.3	−1.3	−0.7	−0.7	0.7	1.0	0.5	—	—	—	—
2	0.3	−1.3	−1.8	0.0	−0.7	−1.3	−0.7	0.0	0.7	1.0	0.0	—	—	—	—
3	0.0	−2.0	−1.5	0.5	−0.7	0.0	−0.7	−1.0	0.3	0.0	−0.1	—	—	—	—
4	1.5	−9.5	−4.0	−3.0	0.0	0.0	−0.7	1.3	1.3	0.0	−0.8	—	—	—	—
5	−2.0	−5.5	1.5	−0.5	0.0	−0.7	0.0	0.7	0.0	0.0	0.6	—	—	—	—
6	3.5	−1.5	−2.0	1.5	0.0	0.0	−1.3	−0.7	0.0	−1.0	0.4	—	—	—	—
7	−0.5	−13.0	−5.0	−16.0	−4.0	−2.0	−2.0	0.0	2.7	6.0	1.7	—	—	—	—
8	0.5	—	—	—	−2.0	−0.7	−0.7	−1.3	−0.7	1.0	0.4	—	—	—	—
9	1.5	−0.5	3.5	−0.5	−1.3	—	—	—	−0.7	1.0	0.5	—	—	—	—
10	−2.5	−3.0	−2.5	1.0	0.0	−1.3	−0.7	−0.7	1.3	0.0	−2.3	1.2	0.1	0.3	0.4
11	−5.5	−6.5	—	—	−0.7	−1.3	−3.3	—	—	1.0	1.6	—	—	—	—
12	1.5	−3.0	—	—	−0.7	−1.3	−0.7	−2.0	−2.0	1.0	0.4	—	—	—	—

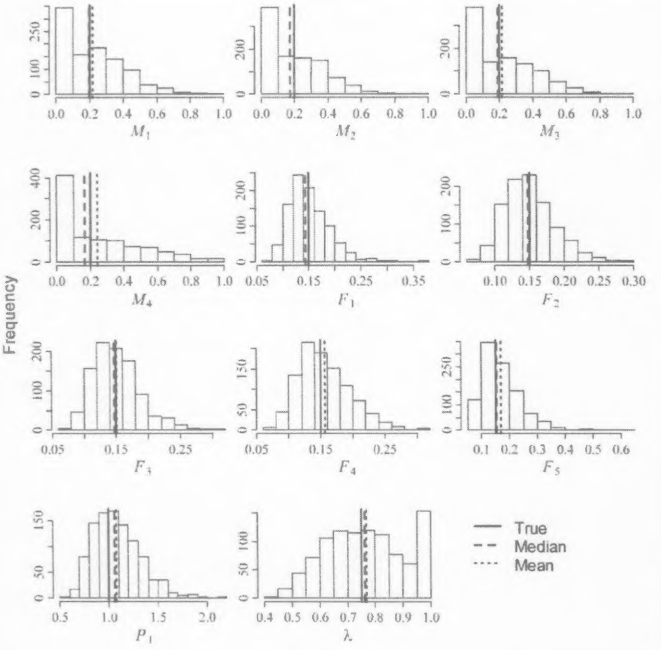

Figure 1

Histograms of the 1000 estimates obtained for each parameter under scenario 7 (see Table 1). The true parameter value, median, and mean of the estimates are indicated by vertical lines. M_i = natural mortality rate for age i fish; F_i= fishing mortality rate for age i fish; P_1 = population size of tagged cohort at age 1 (in 100,000s); λ = tag reporting rate for the unobserved component of the fishery (assumed to be constant for scenario 7).

upper bound of 1.0, and the frequency was greatest in scenario 5 where the true value was 0.90. Nevertheless, the median biases were still small. The fishing mortality estimates generally had distributions that were right skewed, and the degree of skewness became more pronounced at older ages. The skewness was usually small enough that the mean and median were still similar (e.g., scenario 1; Fig. 2). However, this was not always true. For example, in scenario 7 (Fig. 1), the median bias for F_5 was 2.7%, whereas the mean bias was 13.3%.

In Polacheck et al. (2006), we used mean bias to summarize simulation results obtained with the BP model. This meant that positive biases in the fishing mortality estimates that increased with age were reported, as well as positive biases in the natural mortality estimates. Had median bias been used instead, the bias results would have been similar to those presented here (i.e., negative biases in the natural mortality estimates, and only small biases in any of the fishing mortality estimates). In retrospect, we believe that the median provides a more reliable measure of bias. This is especially true in cases where the estimates have a skewed distribution, but should also be true in cases where a large proportion of the estimates fall on a bound.

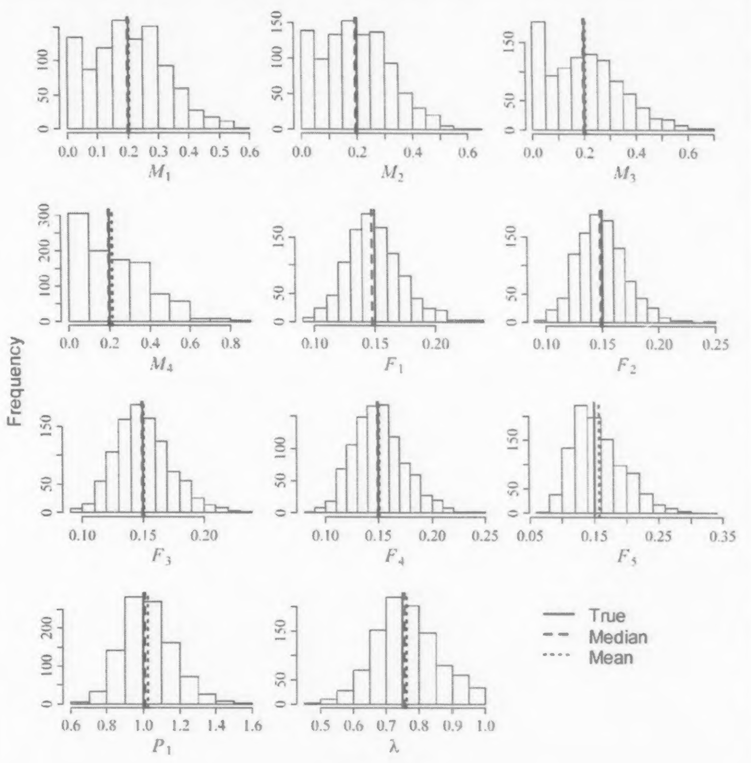

Figure 2

Histograms of the 1000 estimates obtained for each parameter under scenario 1 (see Table 1). The true parameter value, median, and mean of the estimates are indicated by vertical lines. M_i= natural mortality rate for age i fish; F_i = fishing mortality rate for age i fish; P_1 = population size of tagged cohort at age 1 (in 100,000s); λ= tag reporting rate for the unobserved component of the fishery (assumed to be constant for scenario 1).

In regard to precision, we estimated fishing mortality rates, cohort size, and reporting rates with much greater precision (CVs generally in the range of 0.10 to 0.20) than that for the natural mortality estimates (CVs often exceeding 0.50) across all scenarios (Table 3). Only when natural mortality was constrained to be constant across ages (scenario 8) was reasonable precision achieved for this parameter (CV of 0.22). Of the fishing mortality parameters, the estimates for the oldest age of recapture (i.e., F_3 in scenario 11, F_5 in all other scenarios) always had the highest CV, and usually notably so.

Comparing the CVs for a specific scenario with those for scenario 1, we found that the results were generally predictable, at least in terms of direction (Table 3). For example, increasing the value used for the fishing mortality rate (scenario 3) or for the reporting rate (scenario 5) resulted in greater precision (i.e., lower CVs) for all parameters, because these changes lead to more tag returns. The results for scenario 2 were not instantly as intuitive. We would expect increasing natural mortality to give higher CVs because more fish would die naturally, leaving fewer tagged fish to be caught. Although small increases were observed in the CVs for the other parameters, large decreases were observed for the natural mortality estimates. This serves as a reminder that the CV is calculated in relation to the true parameter value, and therefore direct comparisons for parameters whose true values have been changed are more complicated. When the SDs of the natural mortality estimates from scenario 2 were compared with those from scenario 1 instead of the CVs, they did in fact increase (although this may in part be due to the fact that fewer estimates are truncated at their lower bound of zero when the value used for natural mortality is higher).

Table 3

Coefficient of variation (CV) of the parameter estimates for each scenario listed in Table 1. Results were based on 1000 simulation runs per scenario. M_i= natural mortality rate for age i fish; F_i= fishing mortality rate for age i fish; P_1= population size of tagged cohort at age 1; λ_i= tag reporting rate for fish captured at age i in the unobserved component of the fishery.

Scenario	M_1	M_2	M_3	M_4	F_1	F_2	F_3	F_4	F_5	P_1	λ_1	λ_2	λ_3	λ_4	λ_5
1	0.62	0.62	0.72	0.87	0.15	0.14	0.15	0.16	0.27	0.14	0.13	—	—	—	—
2	0.40	0.43	0.47	0.55	0.17	0.17	0.17	0.19	0.30	0.16	0.14	—	—	—	—
3	0.46	0.51	0.55	0.69	0.12	0.11	0.12	0.12	0.21	0.11	0.10	—	—	—	—
4	0.72	0.74	0.79	0.98	0.15	0.15	0.15	0.17	0.32	0.15	0.13	—	—	—	—
5	0.56	0.59	0.66	0.82	0.14	0.13	0.13	0.15	0.25	0.12	0.10	—	—	—	—
6	0.39	0.42	0.46	0.58	0.09	0.09	0.09	0.10	0.15	0.09	0.07	—	—	—	—
7	0.94	0.90	0.99	1.28	0.25	0.24	0.25	0.27	0.47	0.23	0.19	—	—	—	—
8	0.22	—	—	—	0.15	0.14	0.15	0.15	0.17	0.13	0.13	—	—	—	—
9	0.62	0.59	0.64	0.56	0.13	—	—	—	0.19	0.14	0.13	—	—	—	—
10	0.66	0.64	0.73	0.88	0.15	0.15	0.16	0.17	0.29	0.13	0.22	0.20	0.18	0.18	0.18
11	0.72	0.85	—	—	0.18	0.19	0.27	—	—	0.18	0.17	—	—	—	—
12	0.61	0.63	—	—	0.16	0.16	0.21	0.37	0.75	0.15	0.14	—	—	—	—

Several other points are worth noting. Changing the level of overdispersion in the data (scenarios 6 and 7) had the greatest influence on the CVs across all parameters. The only exception was that constraining natural mortality to be constant (scenario 8) had a greater effect on the CV of the natural mortality-rate estimation. Constraining natural mortality to be constant (scenario 8) not only reduced the CV of the M estimate substantially, but also the CV of the F_5 estimate. Similarly, constraining fishing mortality to be linear (scenario 9) substantially reduced the CV of the F_5 estimate, but also the M_4 estimate, and to a lesser degree the M_3 estimate. Interestingly, however, neither of these constraints affected the CVs of the P_1 and λ estimates. Also of interest is that allowing reporting rates to vary across years (scenario 10) had only a small effect on the precision of the mortality rate and abundance estimates. The reporting-rate estimates themselves were less precise and had a high tendency to hit the upper bound of one, but usually these parameters are not the ones of primary interest. Lastly, we note that having five recapture years but only three release years (scenario 12) resulted in much higher CVs for the F_3, F_4, and F_5 estimates, and increasingly so with age (with a CV of 0.75 for F_5). Thus, having more recapture years allows for more years of fishing mortality rates to be estimated, but these estimates quickly become uninformative unless the number of release years is also increased.

High correlations were present between many of the parameter estimates (Table 4; results are shown for scenario 1, but the patterns are very similar for all scenarios). Given the nature of the model, high correlations were expected, and have already been documented and discussed for the BP model in Polacheck et al. (2006). For example, to yield the same number of tag returns in a particular year, a higher estimate of fishing mortality for that year could be compensated by a higher estimate of natural mortality for the previous year, so that estimates of F_i and M_{i-1} tend to be positively correlated. Alternatively, it could be compensated by a higher estimate of the reporting rate; hence estimates of F_i and λ tend to be negatively correlated. When two parameters have highly correlated estimates, a large CV for one of these parameters will tend to mean a large CV for the other parameter. This may explain some of the results observed above. For example, in scenarios 1–7, 9, and 10, estimates of F_5 and M_4 were highly correlated; therefore the high uncertainty in F_5 is likely due to the very high uncertainty in M_4. An analogous statement can be made about F_3 and M_2 in scenario 11. The high correlation between estimates of F_5 and M_4 also explains why, in scenarios 8 and 9, constraints that improved the precision of one of these parameters also improved the precision of the other.

The Hessian-based standard error estimates in relation to the standard errors derived from the simulations are presented in Table 5. In all of the scenarios with φ=3, the Hessian-based standard errors were underestimated by a factor close to $\sqrt{3} = 1.73$, and had a mean across all parameters and scenarios of 1.67 (ranging from 1.45 to 1.91). In the scenario with φ=1 (i.e., multinomial data), the Hessian-based and simulation-based standard errors were very similar, as expected. In the scenario with φ=9, the Hessian-based estimates were underestimated by a factor reasonably close to $\sqrt{9}=3.0$—the largest exception being a factor of 2.49 for P_1. Nevertheless, these results indicate that if φ can be estimated after fitting the model (e.g., from the residuals), then multiplying the Hessian-based standard error estimates by $\sqrt{\varphi}$ can provide improved, and perhaps adequate, estimates of the true standard errors. Further investigation of additional scenarios

Table 4

Correlation matrix for the parameter estimates obtained using scenario 1 (see Table 1). Results were based on 1000 simulation runs. M_i= natural mortality rate for age i fish; F_i= fishing mortality rate for age i fish; P_1= population size of tagged cohort at age 1; λ = tag reporting rate for the unobserved component of the fishery (assumed to be constant for scenario 1).

	M_1	M_2	M_3	M_4	F_1	F_2	F_3	F_4	F_5	P_1	λ
M_1	1.00	–0.40	0.00	0.01	0.01	0.10	–0.07	–0.06	–0.03	0.55	0.14
M_2		1.00	–0.38	–0.06	–0.27	0.03	0.14	–0.06	–0.07	0.12	0.11
M_3			1.00	–0.35	–0.10	–0.25	0.08	0.26	–0.12	0.12	0.06
M_4				1.00	0.00	–0.04	–0.19	0.19	0.77	–0.01	0.06
F_1					1.00	0.47	0.40	0.37	0.27	–0.56	–0.61
F_2						1.00	0.49	0.38	0.27	–0.41	–0.63
F_3							1.00	0.52	0.25	–0.39	–0.63
F_4								1.00	0.59	–0.37	–0.59
F_5									1.00	–0.27	–0.39
P_1										1.00	0.67
λ											1.00

Table 5

Simulation-based standard error divided by Hessian-based standard error of the parameter estimates for each scenario listed in Table 1. Results were based on 1000 simulation runs per scenario. Recall that an overdispersion factor of φ = 3 was used in all scenarios except scenario 6, for which φ = 1, and scenario 7, for which φ = 9. M_i = natural mortality rate for age i fish; F_i= fishing mortality rate for age i fish; P_1= population size of tagged cohort at age 1; λ_i = tag reporting rate for fish captured at age i in the unobserved component of the fishery.

Scenario	M_1	M_2	M_3	M_4	F_1	F_2	F_3	F_4	F_5	P_1	λ_1	λ_2	λ_3	λ_4	λ_5
1	1.71	1.64	1.76	1.75	1.60	1.60	1.69	1.70	1.73	1.54	1.76	—	—	—	—
2	1.65	1.74	1.74	1.70	1.62	1.66	1.67	1.74	1.75	1.54	1.69	—	—	—	—
3	1.68	1.74	1.71	1.78	1.61	1.64	1.73	1.65	1.77	1.47	1.68	—	—	—	—
4	1.73	1.77	1.72	1.74	1.56	1.59	1.62	1.66	1.78	1.55	1.75	—	—	—	—
5	1.65	1.68	1.69	1.70	1.54	1.61	1.64	1.66	1.73	1.48	1.82	—	—	—	—
6	1.01	1.02	0.99	0.99	0.99	0.99	0.97	1.03	0.98	1.00	0.97	—	—	—	—
7	3.07	2.97	3.00	3.20	2.67	2.73	2.86	2.86	3.05	2.49	3.08	—	—	—	—
8	1.72	—	—	—	1.62	1.63	1.73	1.71	1.76	1.53	1.76	—	—	—	—
9	1.70	1.64	1.72	1.58	1.62	—	—	—	1.71	1.53	1.76	—	—	—	—
10	1.74	1.66	1.77	1.76	1.45	1.47	1.57	1.58	1.68	1.50	1.62	1.65	1.59	1.62	1.68
11	1.69	1.70	—	—	1.64	1.64	1.70	—	—	1.56	1.70	—	—	—	—
12	1.69	1.65	—	—	1.61	1.66	1.70	1.73	1.91	1.56	1.73	—	—	—	—

may allow for more accurate correction factors to be developed.

Trade-off between number of tag releases and observer coverage

We first concentrated on the results for scenario 1, and how changes in N and δ affected the accuracy of the parameter estimates. For all parameters, biases in the median of the estimates decreased rapidly as N increased, especially between 250 and 1000 releases (Fig. 3). Biases also tended to decrease as δ increased, especially for P_1, λ, and F_1 to F_3. In any case, only the biases in natural mortality estimates at the lowest release numbers ($N \leq 500$) were large enough to be of concern, and further investigation showed they were the result of a large proportion of the estimates falling on the lower bound of zero.

As seen in the previous section, evaluating biases could be complicated in some scenarios because of natural mortality estimates hitting a lower bound of zero, reporting-rate estimates hitting an upper bound of one, and fishing morality estimates having right-skewed distributions, especially at older ages. These problems became more pronounced as N and δ decreased, such that with N=250 and δ=0.05 the median and mean differed significantly for many parameters (e.g., M_4 had a median bias of –23% but a mean bias of +23%;

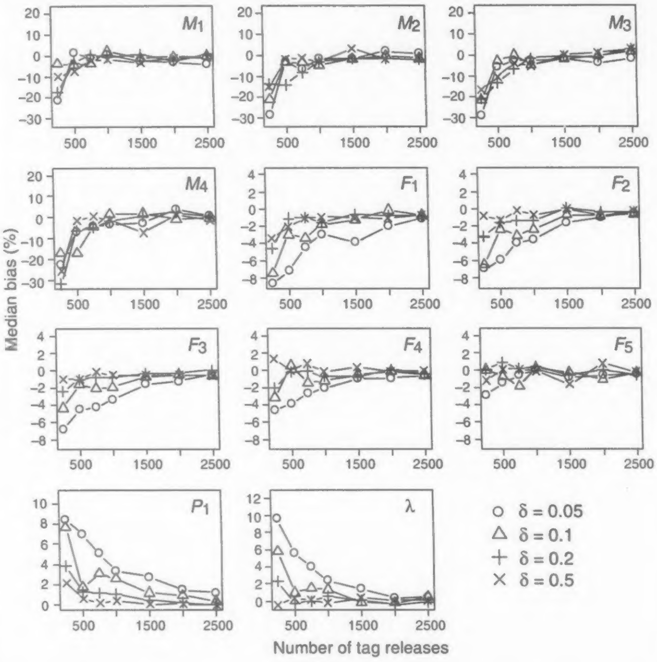

Figure 3

Effect of changing the number of releases at various proportions of observer coverage (δ) on the percent median bias (i.e., (median–true)/true×100%) of the parameter estimates. Results are shown for scenario 1 (see Table 1) and are based on 1000 simulation runs per combination of tag releases and observer coverage. M_i= natural mortality rate for age i fish; F_i= fishing mortality rate for age i fish; P_1= population size of tagged cohort at age 1; λ = tag reporting rate for the unobserved component of the fishery (assumed to be constant for scenario 1).

F_5 had a median bias of only –3% but a mean bias of +16%). Thus, with small N and δ, the real issue was not with biases, but with the non-normality and very high variability (as seen next) of the estimates.

We now consider how changes in N and δ affected the precision of parameter estimates. For a given value of δ, increasing N reduced the CVs of all estimates in an exponential fashion (Fig. 4). For the fishing mortality estimates, the rate of decline became greater with age, and was particularly notable for F_5. The CVs of the fishing mortality, abundance, and reporting rate estimates all decreased as δ increased; however, the natural mortality estimates did not change much. Overall, larger gains were achieved in the precision of the fishing mortality, abundance, and reporting rate estimates by increasing δ from 0.05 to 0.50 than by increasing N from 500 to 2500 (note that going from 250 to 500 releases led to significant decreases in the CVs of most parameter estimates). On the contrary, much larger gains were achieved in the precision of the natural mortality estimates by increasing N than by increasing δ.

As a specific example of using such simulation results to aid in the design of a tagging study, suppose a researcher's goal was to achieve a CV of 0.20 or lower in the estimate of abundance. This could be accomplished under scenario 1 with the following: N=250 and δ= 0.50; N=500 and δ=0.20; N=1000 and δ=0.10; or, N= 2000 and δ=0.05. If, in addition, the researcher's goal was to achieve a CV of 0.30 or lower in all of the fishing mortality estimates, then only the latter two of these options would still be acceptable.

Although the magnitude of the CVs varied significantly between scenarios (as seen in Table 3), the relative changes that resulted from increasing N or δ were very similar to those seen for scenario 1. The most significant difference came from constraining natural mortality to be constant (scenario 8), in which case the precision of the natural mortality parameter became influenced by changes in δ (Fig. 5).

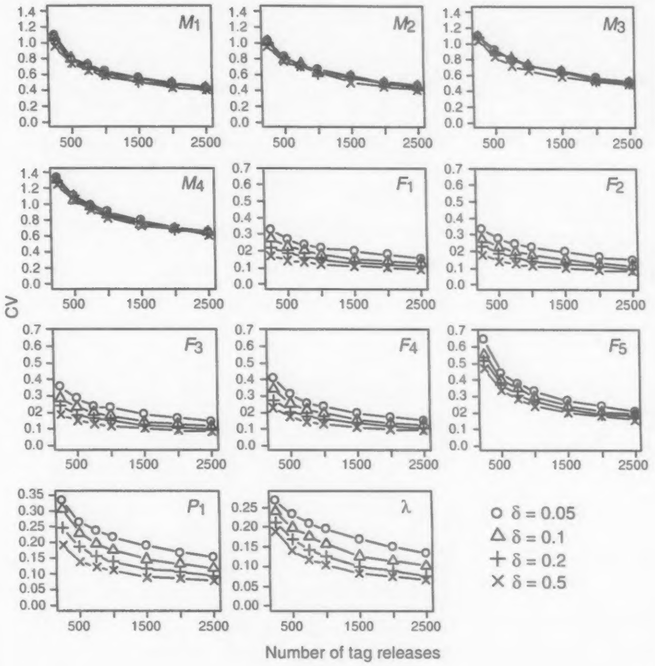

Figure 4

Effect of changing the number of tag releases at various proportions of observer coverage (δ) on the coefficient of variation (CV) of the parameter estimates. Results are shown for scenario 1 (see Table 1) and are based on 1000 simulation runs per combination of tag releases and observer coverage. M_i = natural mortality rate for age i fish; F_i = fishing mortality rate for age i fish; P_1= population size of tagged cohort at age 1; λ = tag reporting rate for the unobserved component of the fishery (assumed to be constant for scenario 1).

Discussion

The current article extends the integrated BP model for tag-recapture and catch data developed in Polacheck et al. (2006) to incorporate the estimation of reporting rates through observer data, which we refer to as the BPO model. This is an important and practical extension because nonreporting of tags is a serious problem in many commercial fisheries that needs to be accounted for in the model to obtain meaningful results, and observer data often provide the most viable means of doing so.

In the way the BPO model was formulated, increasing the level of observer coverage improves the parameter estimates not only by improving the reporting rate estimates, but also by improving the precision of the catch-at-age data. If all fish caught in the observer component were not sampled, then the improvements would not be expected to be as great. As an extreme case, the precision of the catch-at-age data could be assumed to be independent of the level of observer coverage, in which case increasing the level of observer coverage would only improve the parameter estimates through the reporting-rate estimates. However, it is difficult to envisage a situation where observers would not take age or length samples from at least a portion of the catches.

In the study by Pollock et al. (2002), where a standard Brownie model was modified to include the estimation of reporting rates when one component of a multicomponent fishery has observers (i.e., 100% reporting rates), the authors show how the overall likelihood for their model can be partitioned into two conditionally independent components. They argue that the reporting rates can be estimated by maximizing the second likelihood component, and then plugged into the first component to estimate the mortality rates, and that doing so provides the maximum likelihood estimates of the reporting rates and mortality rates for the joint likelihood. Although a similar partitioning could be done for the BPO model, the estimates obtained from

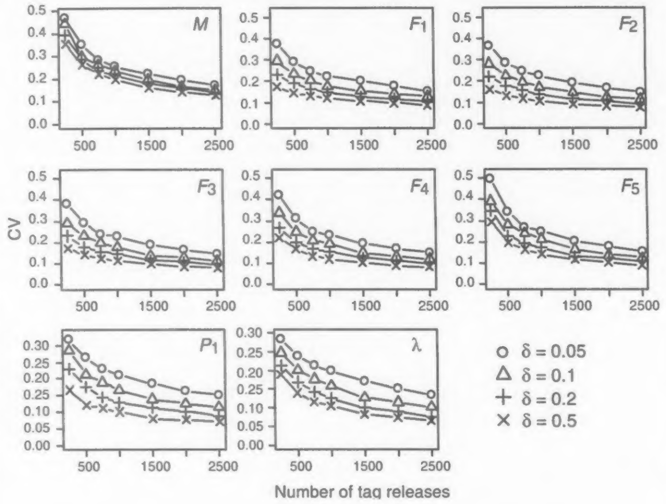

Figure 5

Effect of changing the number of tag releases at various proportions of observer coverage (δ) on the coefficient of variation (CV) of the parameter estimates. Results are shown for scenario 8 (see Table 1) and are based on 1000 simulation runs per combination of tag releases and observer coverage. M = natural mortality rate (assumed to be constant for scenario 8); F_i= fishing mortality rate for age i fish; P_1= population size of tagged cohort at age 1; λ = tag reporting rate for the unobserved component of the fishery (assumed to be constant for scenario 8).

maximizing the separate components would not be the overall maximum likelihood estimates because there is information in the catch data about the mortality rates. Furthermore, we assert that even in the model by Pollock et al. (2002), the estimates obtained from the two-step likelihood procedure are only the maximum likelihood estimates of the overall likelihood when the reporting rates are allowed to vary by year and age, and not, as the study would indicate, when there are any constraints on these parameters.

The BPO model allows for simultaneous estimation of age-specific fishing mortality rates, natural mortality rates, and reporting rates, as well as cohort size at first tagging, for a cohort tagged in consecutive years. All parameters appear to be estimated with reasonable accuracy, but the level of precision that can be achieved varies greatly, depending on the specifics of the population, the fishery, and the experimental design, and also on the parameter. Nevertheless, some general observations can be made based on our simulations. Cohort size appears to be estimated well in all situations (with a CV between 0.10 and 0.20 in the majority of scenarios considered). With the exception of the oldest age of fish at recapture, the fishing mortality rates also tend to be estimated with good precision (CVs of less than 0.20 achievable in many situations). In general, natural mortality is estimated poorly in comparison to the other parameters, with CVs above 0.60 in many cases. If, however, natural mortality can be assumed constant over enough release years (or otherwise constrained), then it too can be estimated with reasonable precision (e.g., CV on the order of 0.20 for our scenario 8 with 1000 releases per year).

Reducing the number of parameters that need to be estimated through imposing parameter constraints can greatly improve the accuracy and precision of the estimates. However, this is only true if the constraints imposed approximate reality; for example, modeling natural mortality as a constant will not lead to better parameter estimates if in fact natural mortality changes significantly with age. In practice, standard model selection techniques, such as Akaike's information criterion (AIC; Akaike, 1974) and its many variations (e.g., AIC_c for small sample sizes, QAIC for overdispersed data; see Burnham and Anderson, 1998, and references therein), can be used to determine which parameter constraints are most supported by the data.

For ease of presentation, the model was developed for, and applied to, one cohort of tagged fish. In practice, it is likely that several cohorts (i.e., age classes) would be tagged in each year of tagging. If all parameters being estimated are both year- and age-dependent, then modeling multiple cohorts simultaneously will give very similar results to modeling each cohort individually. The results would be identical if the catch-at-age data for all cohorts were modeled as independent, but there is likely to be correlation between catch estimates for different cohorts in the same year that should be accounted for. If some constraints can be put on the parameters, such as natural mortality varying only with age or fishing mortality following an age selectivity curve, then precision in the parameter estimates should improve. For example, we re-ran the simulations for scenario 1 as described in the model performance section, but with data generated for three cohorts instead of one. In fitting the model, both natural mortality and fishing mortality were allowed to vary only with age. In comparison to the CVs obtained for scenario 1 with one cohort (Table 3), the CVs obtained with three cohorts were roughly 35–40% less for all parameters. Again, to determine which parameter constraints are most appropriate in a real situation, standard model selection procedures such as AIC can be used.

As was illustrated, the BPO model can be used to evaluate the effect of releasing more tags versus increasing observer coverage on the precision and bias of the parameter estimates. Because these programs can be costly to run and resources are usually limited, it is useful to have a statistical framework for comparing how alternate allocations of resources affect the results that can be achieved. Our results confirm the general conclusion of Polacheck and Hearn (2003) that it is important to ensure both adequate numbers of tag releases and adequate observer coverage (the latter for robust estimation of reporting rates, as well as for improved estimation of catch-at-age numbers in our model). However, while Polacheck and Hearn (2003) found a relatively direct trade-off between the level of observer coverage and number of tag releases with their approximate model, we found with our more comprehensive model that the trade-off depends on the parameters of interest. In particular, greater improvements could generally be achieved in the precision of the fishing mortality and cohort size estimates by increasing the proportion of observer coverage than by increasing the number of releases. On the contrary, much larger gains were achieved in the precision of the natural mortality-rate estimates by increasing the number of tag releases than by increasing the proportion of observer coverage. Although the results will be highly case-specific, these general observations were true in all of the scenarios we considered, and we expect they will hold true in a fairly wide range of scenarios. That being said, the purpose of the simulations was not to draw any specific conclusions, but to illustrate how the model can be used to provide practical guidance about the experimental design of a tagging study.

A version of the BPO model has been used to provide advice to the Commission for the Conservation of Southern Bluefin Tuna (CCSBT) on the levels of observer coverage and tag releases necessary to achieve their objectives for a long-term tagging program conducted on SBT. To make the model more closely resemble the situation for SBT it was necessary to extend the model to a two-fishery situation with a purse-seine fishery and a longline fishery, where tag reporting rates were estimated from planted tags in the purse-seine fishery and from observer data in the longline fishery. Simulations, similar to those presented here, were conducted with input parameter values that best simulate the situation for SBT. The results showed that the numbers of tags that were being released each year were adequate, but that an increase in the CCSBT's target level of observer coverage from 10% to about 30% was required to meet the objectives of the program regarding precision of the mortality-rate estimates.

In summary, the model presented here provides a robust statistical framework for obtaining joint estimates of mortality rates and abundance from tagging data in situations where observers are present in the fishery. The model can be used to provide insight into design issues for those starting up new, or modifying current, tagging and observer programs for the purposes of estimating mortality rates and abundance.

Acknowledgments

We thank K. Pollock, D. Peel, and three anonymous reviewers for constructive comments and suggestions on drafts of this manuscript. The Australian Fisheries Research and Development Corporation (FRDC) provided funding support for this research.

Literature cited

Akaike, H.
1974. A new look at the statistical model identification. IEEE (Inst. Electrical and Electronics Engineers) Transactions on Automatic Control 19:716–723.
Brownie, C., D. R. Anderson, K. P. Burnham, and D. S. Robson.
1985. Statistical inference from band recovery data: a handbook, 2nd ed., 305 p. U.S. Fish Wildl. Serv. Resour. Publ. 156.
Burnham, K. P, and D. R. Anderson.
1998. Model selection and inference: a practical information-theoretic approach, 353 p. Springer-Verlag, New York, NY.
Cormack, R. M.
1964. Estimates of survival from the sighting of marked animals. Biometrika 51:429–438.
Frusher, S. D., and J. M. Hoenig.
2001. Estimating natural and fishing mortality and tag reporting rate of southern rock lobster *Jasus edwardsii* from a multiyear tagging model. Can. J. Fish. Aquat. Sci. 58:2490–2501.
Hampton, J.
2000. Natural mortality rates in tropical tunas: size really does matter. Can. J. Fish. Aquat. Sci. 57:1002–1010.
Hearn, W. S., T. Polacheck, K. H. Pollock, and W. Whitelaw.
1999. Estimation of tag reporting rates in age-struc-

tured multicomponent fisheries where one component has observers. Can. J. Fish. Aquat. Sci.56:1255–1265.

Hoenig, J. M., N. J. Barrowman, W. S. Hearn, and K. H. Pollock.
1998a. Multiyear tagging studies incorporating fishing effort data. Can. J. Fish. Aquat. Sci. 55:1466–1476.

Hoenig, J. M., N. J. Barrowman, K. H. Pollock, E. N. Brooks, W. S. Hearn, and T. Polacheck.
1998b. Models for tagging data that allow for incomplete mixing of newly tagged animals. Can. J. Fish. Aquat. Sci. 55:1477–1483.

Jolly, G. M.
1965. Explicit estimates from capture-recapture data with both death and immigration—stochastic model. Biometrika 52:225–247.

Mosimann, J. E.
1962. On the compound multinomial distribution, the multivariate β-distribution, and correlations among proportions. Biometrika 49:65–82.

Polacheck, T., J. P. Eveson, G. M. Laslett, K. H. Pollock, and W. S. Hearn.
2006. Integrating catch-at-age and multi-year tagging data: a combined Brownie and Petersen estimation approach in a fishery context. Can. J. Fish. Aquat. Sci. 63:534–538.

Polacheck, T., and W. Hearn.
2003. Designing tagging programs for pelagic longline fisheries: trade-offs between the number of releases and observer coverage. N. Am. J. Fish. Manage. 23: 810–821.

Pollock, K. H.
1981. Capture-recapture models allowing for age-dependent survival and capture rates. Biometrics 37: 521–529.

Pollock, K. H., W. S. Hearn, and T. Polacheck.
2002. A general model for tagging on multiple component fisheries: an integration of age-dependent reporting rates and mortality estimation. Environ. Ecol. Stat. 9:57–69.

Pollock, K. H., J. M. Hoenig, W. S. Hearn, and B. Calingaert.
2001. Tag reporting rate estimation: 1. An evaluation of the high-reward tagging method. N. Am. J. Fish. Manage. 21:521–532.

Pollock, K. H., J. M. Hoenig, and C. M. Jones.
1991. Estimation of fishing and natural mortality when a tagging study is combined with a creel survey or port sampling. Am. Fish. Soc. Symp. 12:423–434.

Schwarz, C. J., and G. A. F. Seber.
1999. Estimating animal abundance: review III. Statist. Sci. 14:427–456.

Seber, G. A. F.
1965. A note on the multiple recapture census. Biometrika 52:249–259.
1982. The estimation of animal abundance and related parameters, 2nd ed., 654 p. Macmillan Publ. Co., New York, NY.

Abstract—The abundance and population density of cetaceans along the U.S. west coast were estimated from ship surveys conducted in the summer and fall of 1991, 1993, 1996, 2001, and 2005 by using multiple-covariate, line-transect analyses. Overall, approximately 556,000 cetaceans of 21 species were estimated to be in the 1,141,800-km^2 study area. Delphinoids (Delphinidae and Phocoenidae), the most abundant group, numbered ~540,000 individuals. Abundance in other taxonomic groups included ~5800 baleen whales (Mysticeti), ~7000 beaked whales (Ziphiidae), and ~3200 sperm whales (Physeteridae). This study provides the longest time series of abundance estimates that includes all the cetacean species in any marine ecosystem. These estimates will be used to interpret the impacts of human-caused mortality (such as that documented in fishery bycatch and that caused by ship strikes and other means) and to evaluate the ecological role of cetaceans in the California Current ecosystem.

Manuscript submitted 4 October 2006 to the Scientific Editor's Office.

Manuscript approved for publication 27 June 2007 by the Scientific Editor.

Fish. Bull. 105:509–526 (2007).

Abundance and population density of cetaceans in the California Current ecosystem

Jay Barlow (contact author)[1]

Karin A. Forney[2]

Email address for J. Barlow: Jay.Barlow@noaa.gov

[1] National Ocean and Atmospheric Administration
Southwest Fisheries Science Center
8604 La Jolla Shores Drive
La Jolla, California 92037

[2] NOAA Southwest Fisheries Science Center
110 Shaffer Road
Santa Cruz, California 95060

Estimates of cetacean abundance, biomass, and population density are key to assessing the potential effects of anthropogenic perturbations on cetacean populations (Carretta et al., 2006) and in understanding the ecological role of cetaceans in marine ecosystems (Trites et al., 1997). Along the U.S. west coast, most cetacean species are vulnerable as bycatch in gillnet fisheries (Julian and Beeson, 1998; Carretta et al., 2005), and fisheries catch many of the same species that cetaceans consume (Trites et al., 1997). Large whales also die from ship strikes (Carretta et al., 2006). West coast cetaceans may be affected by anthropogenic sound (e.g., sonar, ship noise, and seismic surveys) and climate change. There is little published information on current abundance to evaluate direct anthropogenic impacts on cetacean species and to estimate their resource needs.

The abundance of cetaceans along the U.S. west coast was previously estimated for some species in some areas, but most available estimates are based on surveys that were conducted 16 to 30 years ago (Dohl et al., 1986; Barlow, 1995). In addition, most estimates are based only on surveys that were conducted within 185 km of the coast. There was only one survey (in 1991) in waters greater than 185 km offshore of California, and there are no published estimates of cetacean abundance for far offshore waters of Oregon or Washington. The lack of recent estimates and the lack of estimates for offshore waters represent clear gaps in our knowledge of west coast cetaceans.

In this study, new estimates of abundance were determined in order to fill our gaps in knowledge about cetaceans in the California Current ecosystem. Line-transect methods were used to analyze data collected from Southwest Fisheries Science Center (SWFSC) ship surveys in 1991, 1993, 1996, 2001, and 2005 off the U.S. west coast. A new multiple-covariate, line-transect approach (Marques and Buckland, 2003) was used to account for multiple factors that affect the distance at which cetaceans can be seen in different conditions. Because cetaceans dive and can be missed by visual observers, the probability of detecting a group of cetaceans directly on the transect line was estimated from observations made by independent observers on those 1991–2005 surveys and from other sources. Observer-specific corrections were applied to remove a bias in estimating group sizes. These results represent one of the most comprehensive analyses of cetacean abundance and density for any large marine ecosystem.

Materials and methods

Survey

Surveys in 1991, 1993, 1996, 2001, and 2005 were conducted in summer and fall with the same line-transect survey methods from two National Oceanographic and Atmospheric Administration (NOAA) research vessels: the 53-m RV *McArthur* and the 52 m RV *David Starr Jordan*. A third ship, the 62-m RV *McArthur II*, was also used for a very short time in 2005. Transect lines followed a grid that was established before each survey to uniformly cover waters between the coast and approximately 556 km (300 nmi) offshore. Surveys were designed with a uniform grid of transect lines anchored by a randomly chosen start point. Ships traveled at 16.7–18.5 km/h (9–10 kt) through the water. The 1991 and 1993 surveys only covered waters off California, but the subsequent surveys also included waters off Oregon and Washington (Fig. 1).

Experienced field biologists (henceforth referred to as "observers") searched for cetaceans from the flying bridge deck of the ships (observation height ~10.5 m for the two primary vessels, 15.2 m for the RV *McArthur II*). Typically, six observers rotated among three observation stations (left station, where 25× binoculars were used; forward station where the data recorder was positioned; and right station, where 25× binoculars were used). Each observer and recorder watched for 2 hours and then rested for 2 hours. The recorder searched with unaided eyes (and occasionally 7× binoculars) and entered effort and sighting data using a data entry program on a laptop computer. The observers were selected on the basis of previous experience searching for and identifying marine mammals at sea; at least four observers on each ship had previous line-transect experience with cetaceans and at least two were experts in marine mammal identification at sea. Before each survey, observers were given a refresher course in marine mammal identification and group size estimation. Group size and the percentage of each species in a group were estimated and recorded independently and confidentially by each on-duty observer. Generally, after a group of cetaceans was seen, observers took as much time as necessary to estimate group size and species composition. Starting in 1996, at least one hour was allocated to group size estimation for sperm whales to provide reasonable confidence that all members of the group surfaced at least once. Species determinations were recorded only if observers were certain of their species identification; otherwise, animals were identified to the lowest taxonomic level or general category (e.g., large whale or baleen whale) that an observer could determine with certainty. Observers were also encouraged to record separately the most probable species if the actual species could not be determined with certainty. In this article, we used probable species identifications if certain identifications were missing, rather than prorating the unidentified sightings into species categories, as done in other studies (Gerrodette and Forcada, 2005). If probable species identifications were not available, species were classified as unidentified delphinoids, small whales, beaked whales, rorqual whales, or large whales. Common and scientific names for all species are given in Table 1.

Most surveys were conducted in closing mode during which the ship diverted from the trackline as necessary to allow closer estimation of group size and species composition. The ship was not diverted if observers felt that group size and species could be determined from the transect line, as was frequently the case of nearby sightings of Dall's porpoise or large baleen whales. To investigate potential biases associated with the use of closing mode surveys, every third day of effort in 1996 was conducted in passing mode during which the ship did not divert from the trackline except for species of particular interest (sperm whales, short-finned pilot whales, and Baird's beaked whales). No consistent biases were found between the two survey modes; however, group size estimation and species determination suffered in passing mode, and therefore the latter (passing mode) was not undertaken during subsequent surveys.

Frequently, a fourth observer searched for cetacean groups that were missed by the primary team of three observers. Sightings made by this fourth observer were recorded after the group had passed abeam and had been clearly missed by the primary team. The data from the fourth observer were considered conditionally independent of the primary team (conditioned on the animals not being seen by the primary team) and were used to estimate the proportion of sightings missed by the primary team.

Calibration of group size

Individual observers may tend to over- or under-estimate group sizes, and their estimates can be improved by calibration based on a subset of groups with known size (Gerrodette and Forcada, 2005) or based on comparison to data from an unbiased observer (Barlow, 1995). Calibration factors were used to correct estimates made by observers who were previously calibrated by using aerial photographic estimates of group size taken from a helicopter on dolphin surveys in the eastern tropical Pacific (Gerrodette and Forcada, 2005). These calibrations were not applied to groups whose size was outside the range of sizes used in the calibration study. A direct helicopter calibration could not be used on these west coast surveys because the weather was too rough and the water is too turbid. Therefore, we used an indirect calibration method (Barlow, 1995) to calibrate these remaining observers in relation to the directly calibrated observers. The indirect calibration coefficient, β_0, for a given observer was estimated by comparison to calibrated estimates of directly calibrated observers by using log-transformed, least-squares regression through the origin:

$$\ln S^{*} = \beta_0 \cdot \ln \overline{S}, \tag{1}$$

where S^{*} = the observer's best estimate of group size; and

$\overline{S}$ = the mean of calibrated, bias-corrected estimates for all other calibrated observers.

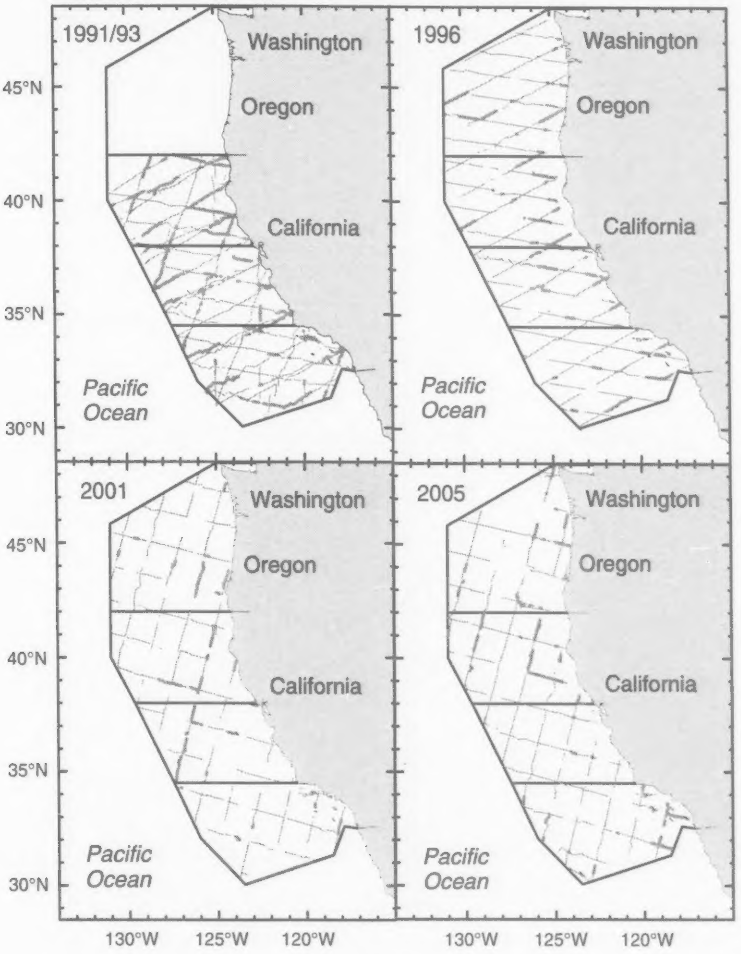

Figure 1

Transect lines (gray) surveyed during 1991 and 1993, 1996, 2001, and 2005 surveys. Thick transect lines were surveyed in Beaufort sea states of 0–2 and thin lines in Beaufort sea states 3–5. Black lines on all maps indicate the boundaries of the four geographic regions.

Logarithms were used in Equation 1 because standard errors were found to be proportional to the mean. Sightings were included in calculating indirect calibration coefficients if group size estimates were made by at least two other directly calibrated observers. We use a weighted geometric mean of the individual, calibrated group-size estimates (weighted by the inverse of the mean squared estimation error) as the best estimate of overall group size in all of the analyses presented here.

Estimation of abundance from line-transect data

Cetacean abundance was estimated by using line-transect methods (Buckland et al., 2001) with multiple covariates (Marques and Buckland, 2003). The entire study area (1,141,800 km^2) was divided into four geographic strata (Fig. 1): 1) waters off Oregon and Washington (322,200 km^2 north of 42°N); 2) northern California (258,100 km^2 south of 42°N and north of Point Reyes at 38°N); 3) central California (243,000 km^2 between Point Conception at 34.5°N and Point Reyes); and 4) southern California (318,500 km^2 south of Point Conception). The OR-WA region was not surveyed in 1991 or 1993 and thus received less survey effort. The density, D_i, for a given species within geographic region i was estimated as

$$D_i = \frac{1}{2L_i} \sum_{j=1}^{n_i} \frac{f(0|z_j)\cdot s_j}{g_j(0)}, \qquad (2)$$

Table 1

Species groups that were pooled and the range of Beaufort sea states used in estimating line-transect detection probabilities as functions of perpendicular sighting distance and other covariates. Within a group, the indicated subgroups were identified and tested as covariates in the line-transect parameter estimation. When sample size and patterns of species co-occurrence permitted, groups and subgroups comprised only one species. Mean effective strip widths (ESWs) are the product of the truncation distance (W) and the mean probability of detection within that distance for each group.

Species group Subgroup Common name	Scientific name(s)	Beaufort sea state	Mean ESW (km)	Truncation distance, W (km)
Delphinids				
Small delphinids				
Short-beaked common dolphin	*Delphinus delphis*	0–5	2.22	4.0
Long-beaked common dolphin	*Delphinus capensis*	0–5	2.85	4.0
Unclassified common dolphin	*Delphinus* spp.	0–5	2.28	4.0
Striped dolphin	*Stenella coeruleoalba*	0–5	2.41	4.0
Pacific white-sided dolphin	*Lagenorhynchus obliquidens*	0–5	2.24	4.0
Northern right whale dolphin	*Lissodelphis borealis*	0–5	2.05	4.0
Unidentified delphinoid		0–5	1.71	4.0
Large delphinids				
Bottlenose dolphin	*Tursiops truncatus*	0–5	2.54	4.0
Risso's dolphin	*Grampus griseus*	0–5	2.37	4.0
Short-finned pilot whale	*Globicephalus macrorhynchus*	0–5	2.70	4.0
Dall's porpoise	*Phocoenoides dalli*	0–2	1.09	2.0
Small whales				
Small beaked whales				
Mesoplodon spp.	*Mesoplodon* spp.	0–2	2.85	4.0
Cuvier's beaked whale	*Ziphius cavirostris*	0–2	2.68	4.0
Unidentified ziphiid whale	*Mesoplodon* spp. or *Z. cavirostris*	0–2	2.95	4.0
Kogia spp.	*Kogia breviceps* or *Kogia sima*	0–2	1.01	4.0
Minke whale	*Balaenoptera acutorostrata*	0–2	2.16	4.0
Unidentified small whale		0–2	2.71	4.0
Medium-size whales				
Baird's beaked whale	*Berardius bairdii*	0–5	1.94	4.0
Bryde's whale	*Balaenoptera edeni*	0–5	3.54	4.0
Sei whale	*Balaenoptera borealis*	0–5	1.59	4.0
Sei or Bryde's whale	*B. edeni* or *B. borealis*	0–5	2.89	4.0
Fin, blue, and killer whales				
Fin whale	*Balaenoptera physalus*	0–5	2.61	4.0
Blue whale	*Balaenoptera musculus*	0–5	2.58	4.0
Killer whale	*Orcinus orca*	0–5	2.65	4.0
Humpback whale	*Megaptera novaeangliae*	0–5	3.20	4.0
Sperm whale	*Physeter macrocephalus*	0–5	2.97	4.0
Unidentified rorqual		0–5	2.70	4.0
Unidentified large whale		0–5	2.78	4.0

where L_i = the length of on-effort transect lines in region i;
$f(0|z_j)$ = the probability density function evaluated at zero perpendicular distance for group j with associated covariates z;
s_j = the number of individuals of that species in group j;
$g_j(0)$ = the trackline detection probability of group j; and
n_i = the number of groups of that species sighted in region i.

Annual abundances for each species in California (1991–2005) and in Oregon–Washington (1996–2005) were estimated from Equation 2 based on the sightings and search effort for the given year. The California total was the sum of the three California region. Because transects covered only 35 km in calm conditions in the central California region in 2005, that region was pooled in 2005 with the northern California region to estimate abundance for Dall's porpoises and small whales (whose abundance was based only on surveys in calm sea states—see below). Only half-normal detection models were considered for estimating $f(0|z_j)$ because hazard-rate models have been shown to give highly variable estimates (Gerrodette and Forcada, 2005) and because hazard-rate models often did not converge on best-fit solutions. In estimating $f(0|z_j)$, data from all years and geographic strata were pooled, and species were pooled into groups with similar sighting characteristics (Barlow et al., 2001): delphinids (excluding killer whales); Dall's porpoise; small whales; medium whales; blue, fin, and killer whales; humpback whales; and sperm whales (Table 1). To improve the ability to fit the probability density function, $f(0|z_j)$, sightings were excluded if they were farther from the trackline than an established truncation distance (Buckland et al., 2001): 2 km for Dall's porpoises and 4 km for all other species. This procedure eliminated approximately 15% of sightings. The covariates for the $f(0)$ function were chosen by forward step-wise model building by using the corrected Akaike information criterion (AIC_c). Potential covariates included the total group size or its natural logarithm (*TotGS* or *LnTotGS*), Beaufort sea state (*Beauf*), survey year (*Year*: 1991, 1993, 1996, 2001, or 2006), survey vessel (*Ship*: *McArthur* or *Jordan*), geographic region (*Region*), the presence of rain or fog within 5 km of the ship (*RainFog*), the presence of glare on the trackline (*Glare*), the estimated visibility in nautical miles (*Vis*), the method used to first detect the group (*Bino*: 25× binoculars or other tool), and the cue that first drew an observer's attention to the presence of a group (*Cue*: splash, blow, or other). As covariates, *TotGS*, *LnTotGS*, *Beauf*, and *Vis* were treated as continuous variables and the others as categorical. Categorical covariates were used only if all factor levels had at least ten observations. See Barlow et al. (2001) for a more complete description of these covariates and their influence on the distance at which various species can be seen. When sample size permitted, another covariate (*SppGroup*, a coded value for the most abundant species within a group) was added to sub-stratify a species group, allowing for differences in detection distances between members of the *a priori* species groupings (Table 1). Because very few cryptic species, such as small whales and Dall's porpoise, are seen in rough conditions and sample sizes were too small to estimate $g(0)$ for those conditions, the abundance of these species was estimated by using search effort conducted only in calm seas (Beaufort sea state 0 to 2); abundance of other species was based on search effort in Beaufort sea states 0 to 5.

Some animals sighted could not be identified to species or probable species, and, for completeness, we also estimated the abundance of the cetaceans represented by these sightings. Sample sizes were small; therefore these unidentified categories were pooled with other similar species for estimating $f(0|\ z_j)$. Unidentified delphinoids were pooled with all delphinids; unidentified small whales were pooled with *Ziphius*, *Mesoplodon* and *Kogia* spp.; unidentified rorquals were pooled with all rorqual species; and unidentified large whales were pooled with rorquals and sperm whales.

In traditional (noncovariate) line-transect analyses, effective strip width (ESW) gives a measure of the distance from the trackline at which species were seen (with an upper limit defined by a chosen truncation distance). For the covariate line-transect method, ESW varies with the covariates for each sighting. The mean ESW was calculated as the truncation distance multiplied by the mean probability of detecting a group within that distance for all sightings of a species.

The total abundance, N, for a species was estimated as the sum over the four geographic regions of the densities, D_i, in each stratum multiplied by the size of the stratum, A_i :

$$N = \sum_{i=1}^{4} D_i \cdot A_i. \tag{3}$$

Abundance and density were not estimated for harbor porpoises (*Phocoena phocoena*), gray whales (*Eschrichtius robustus*), or the coastal stock of bottlenose dolphins (*Tursiops truncatus*) because their inshore habitats were inadequately covered in our study and because good abundance estimates are available for these species from specialized studies (Carretta et al., 1998; Rugh et al., 2005; Carretta et al., 2006).

The areas, A_i , within each stratum were limited to waters deeper than 20 m (the safe operating limit of the vessels). The total areas between the coast and the offshore boundaries were estimated with the program GeoArea (available from Gerrodette[1]). The stratum areas were estimated by subtracting the area between 0 and 20 m depth (and the areas of the Channel Islands in the southern California stratum) from these total areas. The area between the 0- and 20-m depth contours in the southern California stratum (including the Channel Islands) was estimated with the ArcGIS 9.1 software package. The 20-m contour was derived from a bathymetry data set with grids providing 200 m horizontal resolution, 0.1 m vertical resolution) from the California Department of Fish and Game, Marine Region. Coastline data from the NOAA National Ocean Service Medium Resolution Digital Vector Shoreline (1:70,000 scale) was used for the 0-m contour.

The coefficients of variation (CV) for abundance were estimated by using mixed parametric and nonparametric bootstrap methods (Efron and Gong, 1983). Variance attributed to sampling and model fitting were estimated with the nonparametric bootstrap method by using 150-km segments of survey effort as the sampling unit (roughly the distance surveyed in one day). Adjacent survey segments, sometimes from different days, were appended together to make bootstrap segments. A new bootstrap segment was begun for each survey and whenever a ship crossed into a new region. Within each geographic region, effort segments were

---

[1] Gerrodette, T. 2007. National Oceanic and Atmospheric Administration, Southwest Fisheries Science Center, 8604 La Jolla Shores Dr., La Jolla CA 92037. Website: http://swfsc.noaa.gov/prd.aspx (accessed 26 June 2007).

sampled randomly with replacement from all survey years, and the sightings associated with those segments were used with step-wise model building to fit the multiple-covariate model of $f(0|z_j)$. For each of 1000 bootstrap iterations, a parametric bootstrap was used to choose the values of $g(0)$ by drawing randomly from a logit-transformed normal distribution with a mean and variance selected to give the values of $g(0)$ and CV($g(0)$) used for abundance estimation.

Probability of detection of a cetacean group along the trackline

The line-transect parameter $g(0)$ represents the probability of detecting a group that is located directly on the transect line. This value is often assumed to be 1.0 in estimating abundance for dolphins that are found in large groups (Gerrodette and Forcada, 2005); therefore, in these analyses it was implicit that 100% of the groups located on the trackline were detected. In our study, for dolphins, porpoises, and large baleen whales, data from the conditionally independent observer were used to estimate the trackline detection probability for the primary observer team, $g_1(0)$, with the method developed by Barlow (1995):

$$g_1(0) = 1.0 - \frac{n_{w2} \bullet f_2(0)}{n_{w1} \bullet f_1(0)}, \qquad (4)$$

where the subscript 1 refers to parameters for the primary observers, subscript 2 refers to parameters for the conditionally independent observer, and n_w = the number of sightings within the truncation distance w used for estimating the line-transect parameter $f(0)$.

Sightings by the primary team were included in estimating n_1 and $f_1(0)$ only if a conditionally independent observer was also on duty. This estimator (Eq. 4) is positively biased (Barlow, 1995), which results in an overestimation of $g(0)$ for the primary observers. Fully independent observer methods (Buckland et al., 2004) are generally superior to this conditionally independent method (referred to as the "removal method" by Buckland et al. [2004]); however, such methods could not be used because of the need to approach groups to determine species and estimate group sizes. The line-transect parameter $f(0)$ was estimated independently for the primary and independent observers with the software program Distance 5.0 (available from Thomas[2]); half-normal models were fitted with cosine adjustments (Buckland et al., 2001), and the best-fit model was selected by AIC$_c$. Because of sample size limitations, species were pooled into three categories for estimating $g(0)$: 1) delphinids (excluding killer whales), 2) large whales (most baleen whales and killer whales), and 3) Dall's porpoises. Killer whales were included with large baleen whales because they are very conspicuous and are seen at greater distances than are other delphinids (Barlow et al., 2001). Because trackline detection probabilities may vary with the size of the group (Barlow, 1995) or observation conditions, the numbers of sightings made by primary and independent observers were tested with Fisher's exact test to determine if the proportion varied with group size or Beaufort sea state. Delphinids and large whales were stratified into large and small groups with cutpoints at 20 and 3 individuals, respectively. Because of sample size limitations, a single detection function was fitted to large and small groups of delphinids seen by the independent observer. Estimates of $g(0)$ were stratified if this test was significant for either factor. Data for estimating $g(0)$ included transects covered on the preplanned survey grid and during more opportunistic survey periods, such as transits from a port to the starting point on the survey grid. Coefficients of variation for $g(0)$ estimates from the conditionally independent method were based on Equation 9 in Barlow (1995).

The above conditionally independent observer method for estimating $g(0)$ requires that all animals be available to be seen by the primary observer team. This approach does not work with long-diving species that may be submerged for the entire time that the ship is within visual range. Values of $g(0)$ for sperm whales, dwarf sperm whales, pygmy sperm whales, and all beaked whales were taken from a model of their diving behavior, detection distances, and the searching behavior of observers (Barlow, 1999).

Trackline detection probabilities for minke whales posed a special problem. Insufficient sightings were made to estimate $g(0)$ from the conditionally independent observer method (only one conditionally independent sighting was made) and insufficient information exists on their diving behavior to use the modeling approach. Here we assumed that $g(0)$ for minke whales was similar to that for small groups of delphinids (but see "Discussion" section).

Results

Surveys

Survey effort in Beaufort sea states from 0 to 5 covered the study areas fairly uniformly (Fig. 1). Although not all the planned transects were surveyed (because of inclement weather and mechanical breakdowns), the holes in the survey grid were small in relation to the entire study area, and all areas appeared to be well represented. Survey effort in calm sea conditions (Beaufort states 0–2) was not as uniformly distributed (Fig. 1) and was particularly poor in the Oregon-Washington region. Survey effort varied among years because of the availability of ship time.

---

[2] Thomas, L. 2005. Research Unit for Wildlife Population Assessment, University of St. Andrews, Scotland, UK. Website: http://www.ruwpa.st-and.ac.uk/distance/ (accessed 26 June 2007).

Table 2

Numbers of sightings (n) and mean group sizes for all species in the four geographic regions. For each group, size was estimated as the geometric mean of the observers' individual estimates and therefore is not necessarily an integer. The mean for each region is an arithmetic mean over all groups used in the abundance estimation. The overall mean group size is an average of all regions weighted by the number of sightings in each region.

	Southern California		Central California		Northern California		Oregon–Washington		All regions
Species	n	Mean group size	n	Mean group size	n	Mean group size	n	Mean group size	Mean group size
Short-beaked common dolphin	239	168.0	165	142.7	52	210.2	3	238.3	164.1
Long-beaked common dolphin	16	286.6	3	465.8	0	—	0	—	314.9
Unclassified common dolphin	17	67.6	11	19.8	1	8.0	0	—	47.4
Striped dolphin	37	67.2	22	28.6	13	33.8	1	2.2	48.7
Pacific white-sided dolphin	15	33.7	19	153.8	18	59.0	19	57.0	78.5
Northern right whale dolphin	12	13.9	13	45.0	17	20.9	18	35.4	29.1
Bottlenose dolphin	31	13.4	4	4.0	3	10.0	0	—	12.2
Risso's dolphin	50	15.1	25	32.1	13	16.4	22	29.7	22.0
Short-finned pilot whale	1	31.6	1	9.6	3	16.3	0	—	18.0
Killer whale	2	4.1	6	4.9	5	8.1	10	7.5	6.6
Dall's porpoise	5	2.5	27	3.8	115	3.6	67	3.7	3.6
Mesoplodon spp.	1	2.3	4	1.3	4	2.4	2	2.2	2.0
Cuvier's beaked whale	3	2.7	10	2.5	4	2.8	0	—	2.6
Baird's beaked whale	1	7.0	3	14.5	3	13.8	8	5.9	9.3
Kogia spp.	0	—	3	1.5	1	1.0	1	1.0	1.3
Sperm whale	19	8.1	5	7.2	22	8.5	9	7.6	8.1
Minke whale	4	1.6	7	1.1	4	1.1	3	1.0	1.2
Bryde's whale	0	—	1	2.1	0	—	0	—	2.1
Sei whale	0	—	2	1.0	3	1.8	2	1.3	1.4
Sei or Bryde's whale	2	1.0	2	1.0	0	—	0	—	1.0
Fin whale	35	2.4	100	2.4	51	2.1	28	1.3	2.2
Blue whale	106	1.8	67	1.8	18	1.5	7	1.0	1.8
Humpback whale	5	2.1	83	2.0	16	1.7	25	1.7	1.9
Unidentified delphinoid	14	44.9	18	13.6	10	5.4	4	4.8	20.6
Unidentified ziphiid whale	2	1.7	1	1.0	3	1.3	0	—	1.4
Unidentified small whale	7	1.5	1	1.1	3	1.4	1	1.0	1.4
Unidentified roqual whale	4	2.4	26	1.4	7	1.0	7	1.0	1.4
Unidentified large whale	12	1.5	8	1.7	7	1.4	3	1.4	1.5

The number of sightings of most species varied among geographic regions (Table 2). Short- and long-beaked common dolphins and striped dolphins were seen much more frequently in central and southern California. Dall's porpoises were seen much more commonly in the northern California and Oregon-Washington regions. The number of sightings of other dolphin species (including Risso's dolphins, Pacific white-sided dolphins, northern right whale dolphins, and killer whales) showed no clear pattern with geographic region. Dolphin group sizes were generally largest for the two species of common dolphin, but Pacific white-sided dolphins were consistently found in large groups in the central California region (Table 2). Blue whales were the most commonly seen baleen whale in the southern region, but were replaced by fin whales and humpback whales as the most common baleen whale in the northern regions (Table 2). The sighting locations are illustrated in Figure 2 for some common species. Locations of sightings of all species have been provided in the reports for each survey (Hill and Barlow, 1992; Mangels and Gerrodette, 1994; Von Saunder and Barlow, 1999; Appler et al., 2004; Forney, 2007).

Cetaceans were often found in mixed species assemblages. In some cases, species were obviously traveling together in close association; in other cases, the individual species may have been in the same area because they were feeding on the same resource or were there by coincidence. Some species (striped dolphins, bottle-

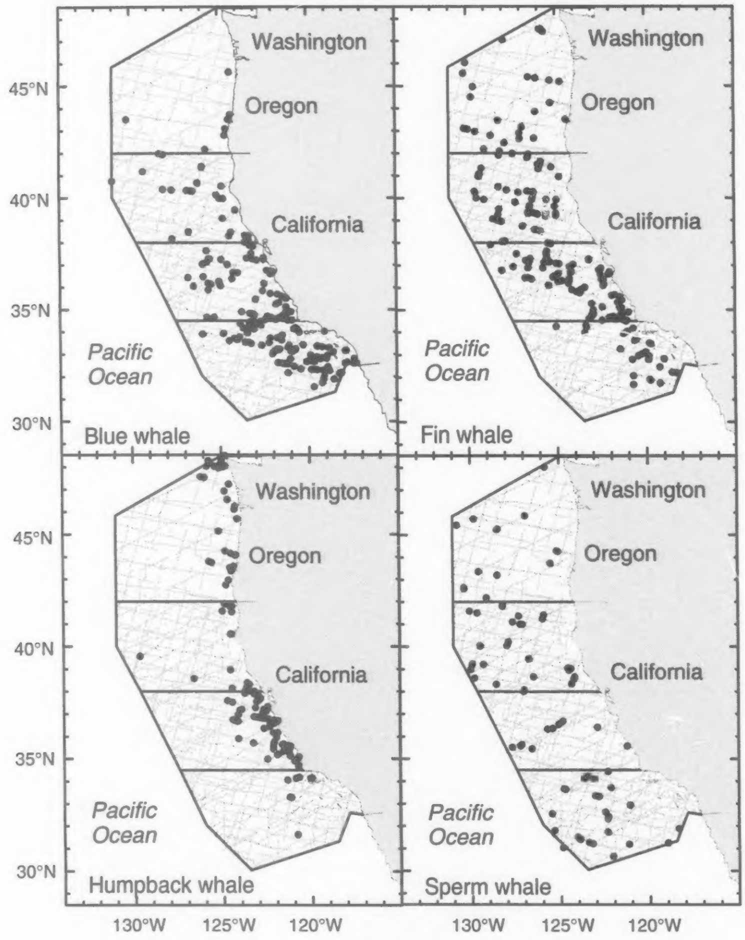

Figure 2

Sighting locations (•) for the species most commonly seen on the 1991–2005 surveys. Light gray lines indicate transects surveyed, and black lines indicate the four geographic regions.

nose dolphins, and Pacific white-sided dolphins) were found with other species more often than they were found alone, indicating that these associations were not coincidental.

Calibration of group size

Most regression coefficients for the indirect method of group-size calibration were less than one, indicating that observers were more likely to underestimate group size. For all groups and all species in this study, the ratio of the sum of all uncalibrated group sizes divided by the sum of all calibrated group sizes was 0.79. The mean ratio of calibrated to uncalibrated group size estimates was 0.92. This difference implies that proportionately larger corrections were applied to larger groups.

Probability of detection along the trackline

New trackline detection probabilities, $g(0)$, were estimated from sightings that were made by the independent observers but missed by the primary observers (Table 3). Beaufort sea state was not a significant factor in the numbers of delphinids or large whales seen by the independent observers (Fisher's exact test, $P=0.60$ and 0.87, respectively). Group size was a significant factor for delphinids ($P<0.0001$), but not for large whales ($P=0.79$). Consequently, estimates of $g(0)$ for delphinids were stratified by group size. The number of Dall's porpoise sightings by independent observers ($n=12$) was insufficient to stratify estimates of $g(0)$ for this species. Values of $g(0)$ from the literature that were used for other long-diving species are given in Table 4.

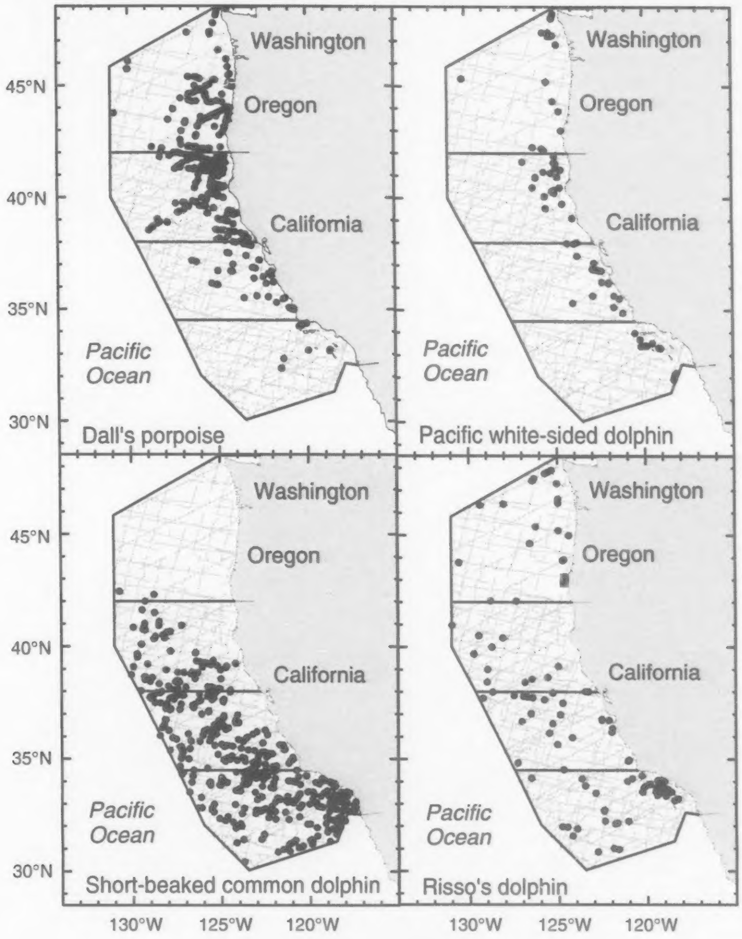

Figure 2 (continued)

Estimation of abundance from line-transect data

Short-beaked common dolphins dominated the abundance estimates for all regions except Oregon-Washington (Table 5), both because of the large number of sightings and the large group sizes for this species. Dall's porpoise was, by far, the most abundant small cetacean in the Oregon-Washington region (Table 5). Short-beaked common dolphins and Dall's porpoises together represented approximately 81% of all delphinoids and 79% of all cetaceans, and baleen whales (mysticetes) represented only about 1% of the total estimated cetacean individuals along the U.S. west coast (Table 6).

The estimated abundance of most species varied considerably among years (Tables 7 and 8). In large part, the year-to-year variation in abundance for most species could be attributed to low sample size and sampling variation; however, the distributions of all species extended beyond the boundaries of the study area and some of the annual variation was likely due to a different portion of a larger population being in the study area within a given year (Forney and Barlow, 1998). Because all years and all regions were pooled for estimating the line-transect parameters, the abundance estimates for different regions (Table 5) and for different years (Tables 7 and 8) were correlated and these estimates cannot be used in standard statistical tests of difference among regions or among years.

The most important covariates, z, for estimating line-transect function $f(0|z)$ varied among species and species groups (Table 4). Covariates appearing in more than one model were *Bino*, *Beauf*, *LnTotGS*, *Ship*, and *RainFog*. In addition to these, a covariate that coded for difference among species within a group (*SppGrp*) was chosen in the model for delphinids (large vs. small delphinids) and for small whales (beaked whales vs. *Kogia* spp. vs. minke whales). The mean ESWs for most

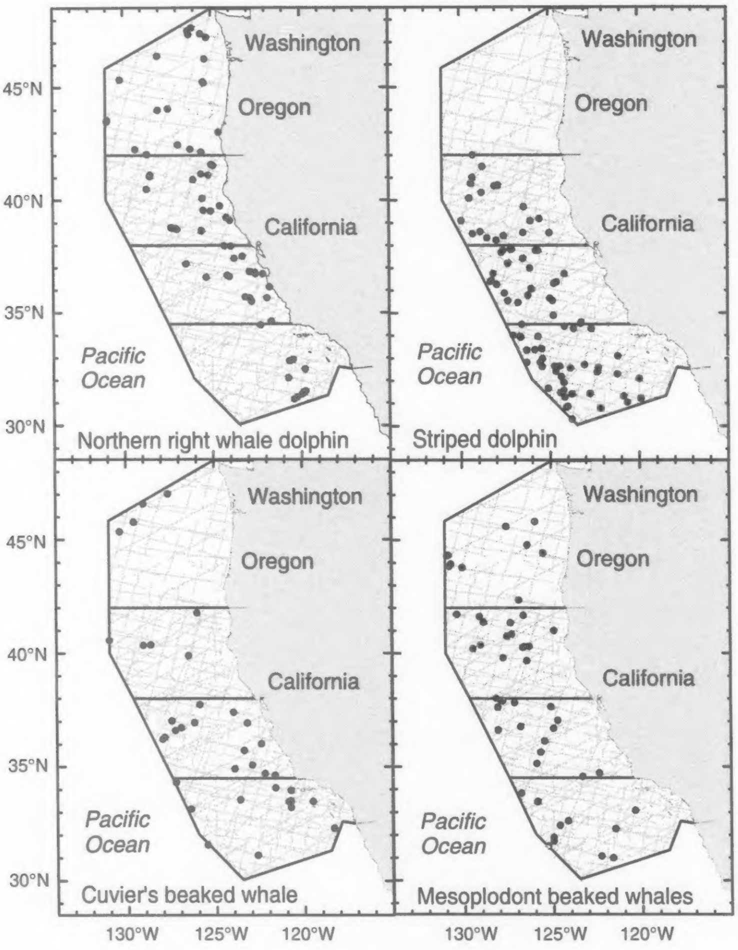
Northern right whale dolphin

Striped dolphin

Cuvier's beaked whale

Mesoplodont beaked whales

Figure 2 (continued)

species were between 2 and 3 km (Table 1). Dall's porpoise and *Kogia* species had the narrowest effective strip widths (~1 km), and humpback whales had the greatest values (~3.2 km).

Discussion

Abundance and density of cetaceans

Delphinidae Delphinids off the U.S. west coast can be classified as warm-temperate (short- and long-beaked common dolphins, striped dolphins, and short-finned pilot whales), cold-temperate (Pacific white-sided dolphins and northern right whale dolphins), or cosmopolitan (Risso's dolphin, bottlenose dolphins, and killer whales). The warm temperate species are generally more common in southern and central California, and the cold-temperate species are more common in the northern California and Oregon-Washington regions. In 1996, when waters were relatively cool off California, the abundance of striped dolphins (the most tropical species) was lower than average and the abundance of the two cold-temperate species was higher. Four of the five sightings of short-finned pilot whales were in 1993, a warm year. All four species have distributions that extend outside our study area. These changes in abundance are consistent with shifts in the distribution of these species into and out of our study area with changes in water temperature. The tendency for these species to change distribution with water temperature is also seen in seasonal distribution changes (Forney and Barlow, 1998). The abundance of common dolphins and the cosmopolitan species did not vary consistently with warm and cold years (Table 7).

Table 3

Trackline detection probabilities, $g(0)$, estimated with the conditionally independent observer method for delphinids, large whales, and Dall's porpoises. Values of $g(0)$ were derived from the estimated probability density functions evaluated at zero distance, $f(0)$, for sightings made by primary observers (n_1) and independent observers (n_2) (Eq. 4). Coefficients of variation (CV) are given for $f(0)$ and $g(0)$ values. Delphinids include all species except killer whales and are stratified into small (≤20) and large (>20) groups. Large whales include killer whales and all baleen whales, except minke whales.

	Primary observers			Independent observers				
Species groups and group size strata	n_1	$f(0)$	CV $f(0)$	n_2	$f(0)$	CV $f(0)$	$g(0)$	CV $g(0)$
Delphinids (truncation distance=1 km)								
Group size ≤20	141	2.74	0.13	25	2.23	0.21	0.856	0.056
Group size >20	188	1.60	0.11	4	2.23	0.21	0.970	0.017
Large whales (truncation distance=2.5 km)								
All group sizes	296	0.58	0.05	32	0.42	0.19	0.921	0.023
Dall's porpoises (truncation distance=1 km)								
All group sizes	115	1.34	0.09	12	2.30	0.34	0.822	0.101

Table 4

The covariates selected for the best-fit line-transect models and the trackline detection probabilities ($g(0)$ and its coefficient of variation, CV, in parentheses) for each of the species and species groups used for abundance estimates. Covariates in parentheses were not included in all of the models that were averaged. The species group (*SppGrp*) covariate allowed variation in the scale factor of the detection function for different subgroups within a species group for delphinids (small delphinids vs. large delphinids—see Table 1) and small whales (small ziphiids vs. *Kogia* spp. vs. minke whales). Other selected covariates included binocular type (*Bino*), total group size (*TotGS*), the logarithm of total group size (*LnTotGS*), Beaufort sea state (*Beauf*), survey vessel (*Ship*), initial sighting event (*Cue*), the presence of rain or fog (*RainFog*), visibility (*Vis*), and geographic region (*Region*). Values of $g(0)$ are from Table 3, Barlow (1999), and Barlow and Taylor (2005).

Species Species group	Best-fit line-transect model	Small groups $g(0)$	Small groups CV $g(0)$	Large groups $g(0)$	Large groups CV $g(0)$
Delphinids	*Bino+Beauf+LnTotGS+Cue+SppGrp+Ship*	0.856	(0.056)	0.970	(0.017)
Dall's porpoise	*Bino+Ship (+LnTotGS+RainFog)*	0.822	(0.101)	0.822	(0.101)
Small whales	*SppGrp (+LnTotGS+TotGS+Ship+Beauf)*				
Mesoplodon spp.		0.450	(0.230)	0.450	(0.230)
Cuvier's beaked whale		0.230	(0.350)	0.230	(0.350)
Unidentified ziphiid whale		0.340	(0.290)	0.340	(0.290)
Kogia spp.		0.350	(0.290)	0.350	(0.290)
Minke whale		0.856	(0.056)	0.856	(0.056)
Unidentified small whale		0.856	(0.056)	0.856	(0.056)
Medium-size whales	*Vis+Beauf (+LnTotGS+TotGS+Ship)*				
Baird's beaked whales		0.960	(0.230)	0.960	(0.230)
Bryde's and sei whales		0.921	(0.023)	0.921	(0.023)
Fin, blue, and killer whales	*Bino+RainFog+Region (+Ship)*	0.921	(0.023)	0.921	(0.023)
Humpback whale	*Null model*	0.921	(0.023)	0.921	(0.023)
Sperm whale	*Null model (+LnTotGS+Ship+Vis)*	0.870	(0.090)	0.870	(0.090)
Unidentified rorqual	*Bino+RainFog+LnTotGS*	0.921	(0.023)	0.921	(0.023)
Unidentified large whale	*Bino+RainFog+LnTotGS (+Ship)*	0.921	(0.023)	0.921	(0.023)

Table 5

Estimated abundances (*N*) and coefficients of variation (CV) for each species in each of the four geographic regions. Data from 1991 to 2005 were pooled. CVs were not available (NA) if no sightings were made. Variances were assumed to be additive in estimating the CVs of the column totals. Unidentified large whales and small whales were not sufficiently specified to be included in the subtotals.

	Southern California		Central California		Northern California		Oregon–Washington	
Species	Abundance *N*	CV(*N*)	Abundance *N*	CV(*N*)	Abundance *N*	CV(*N*)	Abundance *N*	CV(*N*)
Short-beaked common dolphin	165,400	0.19	115,200	0.21	66,940	0.42	4555	0.77
Long-beaked common dolphin	17,530	0.57	4375	1.03	0	NA	0	NA
Unclassified common dolphin	4281	0.85	1313	0.49	35	1.00	0	NA
Striped dolphin	12,529	0.28	2389	0.42	4040	0.76	16	1.07
Pacific white-sided dolphin	2196	0.71	9486	0.74	4137	0.54	7998	0.37
Northern right whale dolphin	1172	0.52	2032	0.55	1652	0.46	6242	0.42
Bottlenose dolphin (offshore)	1831	0.47	61	0.77	133	0.68	0	NA
Risso's dolphin	3418	0.31	3197	0.30	1036	0.41	4260	0.52
Short-finned pilot whale	118	1.04	48	1.02	184	0.60	0	NA
Killer whale	30	0.73	116	0.47	142	0.47	521	0.37
Dall's porpoise	727	0.99	8870	0.64	27,410	0.26	48,950	0.71
Mesoplodon spp.	132	0.96	269	0.53	341	0.78	435	0.70
Cuvier's beaked whale	911	0.68	2647	0.74	784	1.18	0	NA
Baird's beaked whale	127	1.14	159	1.02	200	0.74	520	0.54
Kogia spp.	0	NA	710	0.58	130	1.25	397	1.25
Sperm whale	607	0.57	143	0.66	736	0.40	448	0.63
Minke whale	226	1.02	284	0.74	102	1.56	211	0.84
Bryde's whale	0	NA	7	1.01	0	NA	0	NA
Sei whale	0	NA	14	0.78	47	0.68	37	1.14
Sei or Bryde's whale	7	1.07	11	0.79	0	NA	0	NA
Fin whale	359	0.40	992	0.27	448	0.43	299	0.33
Blue whale	842	0.20	528	0.27	115	0.37	63	0.51
Humpback whale	36	0.51	586	0.38	90	0.47	231	0.36
Unidentified delphinoid	2845	0.53	1609	0.54	299	0.47	214	0.58
Unidentified ziphiid whale	226	0.86	65	1.11	172	0.65	0	NA
Unidentified small whale	357	0.66	27	1.44	73	0.60	72	1.14
Unidentified roqual whale	34	0.53	147	0.31	30	0.42	59	0.37
Unidentified large whale	72	0.33	54	0.61	35	0.44	28	0.82
Subtotal: Delphinoids	212,077	0.16	148,695	0.18	106,007	0.27	72,756	0.49
Subtotal: Ziphiidae	1396	0.49	3140	0.63	1497	0.66	955	0.43
Subtotal: Physeteridae	607	0.57	853	0.49	866	0.39	845	0.68
Subtotal: Balaenopteridae	1504	0.21	2568	0.17	831	0.31	900	0.25
Total	216,014	0.15	155,336	0.17	109,309	0.27	75,556	0.47

Dall's porpoise Abundance estimation for Dall's porpoise is difficult because of their attraction to vessels (Turnock and Quinn, 1991). To obtain unbiased estimates, these animals must be detected before they react to the survey vessel. Our data indicate that the behavior of the vast majority of Dall's porpoise seen at low sea states is "slow rolling." This contrasts with the "roostertailing" or fast swimming behavior seen by animals that are approaching the ship. However, when effort is limited to calm conditions (Beaufort states 0–2), the amount of search effort is greatly reduced (Fig. 1). As a result, the coefficients of variation for Dall's porpoise abundance are greater than would be expected for such a common species. Off California, the temporal pattern shows higher Dall's porpoise abundance in 1996 (Table 7), mirroring the higher abundance that year of cold-temperate delphinids. Forney (2000) found that sea surface temperature was a very good predictor of Dall's porpoise distribution. In their 12 year time series of surveys off central California, Keiper et al. (2005) also found that

Table 6

Total numbers of sightings (n), estimated cetacean abundance (N), and density per 1000 km^2 within the entire study area. Data from 1991 to 2005 were pooled within geographic regions, and estimates of abundance for each region were summed to give total abundance. Coefficients of variation (CV) apply to both abundance and density estimates. CVs and 95% confidence intervals (CI) were based on a bootstrap calculation. Variances were assumed to be additive in estimating the CVs of the subtotals and totals. Unidentified large whales and small whales were not sufficiently specified to be included in the subtotals.

Species	n	Abundance N	CV(N)	Lower 95% CI	Upper 95% CI	Density per 1000 km^2
Short-beaked common dolphin	459	352,069	0.18	234,430	489,826	309.35
Long-beaked common dolphin	19	21,902	0.50	4833	43,765	19.24
Unclassified common dolphin	29	5629	0.64	1127	14,231	4.95
Striped dolphin	73	18,976	0.28	9286	29,038	16.67
Pacific white-sided dolphin	71	23,817	0.36	9991	40,760	20.93
Northern right whale dolphin	60	11,097	0.26	5654	16,712	9.75
Bottlenose dolphin (offshore)	38	2026	0.44	743	4443	1.78
Risso's dolphin	110	11,910	0.24	7501	19,255	10.46
Short-finned pilot whale	5	350	0.48	68	708	0.31
Killer whale	23	810	0.27	408	1157	0.71
Dall's porpoise	214	85,955	0.45	42,318	211,118	75.53
Mesoplodon spp.	11	1177	0.40	311	1648	1.03
Cuvier's beaked whale	17	4342	0.58	1636	11,555	3.82
Baird's beaked whale	15	1005	0.37	382	1821	0.88
Kogia spp.	5	1237	0.45	0	4981	1.09
Sperm whale	55	1934	0.31	991	3163	1.70
Minke whale	18	823	0.56	403	2874	0.72
Bryde's whale	1	7	1.01	0	21	0.01
Sei whale	7	98	0.57	15	227	0.09
Sei or Bryde's whale	4	18	0.65	0	46	0.02
Fin whale	214	2099	0.18	1448	2934	1.84
Blue whale	198	1548	0.16	1138	2087	1.36
Humpback whale	129	942	0.26	584	1411	0.83
Unidentified delphinoid	46	4968	0.36	2044	8585	4.37
Unidentified ziphiid whale	6	463	0.50	115	986	0.41
Unidentified small whale	12	528	0.50	209	1370	0.46
Unidentified roqual whale	44	270	0.20	170	373	0.24
Unidentified large whale	30	189	0.25	107	292	0.17
Subtotal: Delphinoids	1147	539,509	0.14			474.05
Subtotal: Ziphiidae	49	6987	0.37			6.14
Subtotal: Physeteridae	60	3171	0.26			2.79
Subtotal: Balaenopteridae	615	5805	0.12			5.10
Total	1913	556,189	0.14			488.71

Dall's porpoise abundance was inversely related to sea surface temperature.

Balaenopteridae The common baleen whales in California waters were blue, fin, and humpback whales. The abundance of these species was consistently high during the summer and fall study period. Our estimates of humpback whale abundance increased from 1991 to 1996 and decreased slightly in 2001 and 2005; however, humpback whales were observed to be highly concentrated in productive nearshore waters off California and northern Washington during 2005 that were not well sampled during our surveys. A more comprehensive and precise abundance estimate of 1769 humpback whales (CV=0.16) was obtained when additional survey effort was included within these areas (Forney, 2007). More precise estimates from mark-recapture studies also indicate an increase in abundance from 1991 to 1997 (Calambokidis and Barlow, 2004), a decrease in 1999–2000 and in 2000–2001, and a subsequent increase to about 1400

Table 7

Number of sightings (n) and estimated abundance (N) for each species in the three California regions for the years 1991, 1993, 1996, 2001, and 2005. The total lengths of transects surveyed were 9893, 6287, 10,251, 6438, and 7779 km for these years, respectively, in Beaufort sea states of 5 or less and were 2160, 1521, 1556, 852, and 1055 km, respectively, in Beaufort sea states of 2 or less. Unidentified large whales and small whales were not sufficiently specified to be included in the subtotals.

	1991		1993		1996		2001		2005	
Species	n	Abundance N	n	Abundance N	n	Abundance N	n	Abundance N	n	Abundance N
Short-beaked common dolphin	119	249,044	94	397,813	103	313,994	64	335,365	76	483,353
Long-beaked common dolphin	5	16,714	0	0	6	49,431	2	20,076	6	11,191
Unclassified common dolphin	8	4568	3	1454	10	2768	1	383	7	18,968
Striped dolphin	21	32,370	14	14,622	13	4796	6	12,570	18	29,037
Pacific white-sided dolphin	11	4843	10	4222	19	37,762	9	9209	3	13,677
Northern right whale dolphin	14	4554	6	2554	9	7950	12	6337	1	897
Bottlenose dolphin (offshore)	14	2165	2	1058	7	382	9	5375	6	2066
Risso's dolphin	28	10,746	15	7510	15	5083	17	8521	13	7036
Short-finned pilot whale	0	0	4	1506	0	0	0	0	1	639
Killer whale	3	193	2	385	4	380	2	270	2	203
Dall's porpoise	57	59,112	1	206	50	54,501	23	18,125	16	45,373
Mesoplodon spp.	3	697	5	2116	1	202	0	0	0	0
Cuvier's beaked whale	9	9546	4	5137	2	1152	1	3217	1	2615
Baird's beaked whale	2	99	3	1591	2	913	0	0	0	0
Kogia spp.	2	1970	2	1345	0	0	0	0	0	0
Sperm whale	11	837	7	1335	6	593	9	2495	13	2795
Minke whale	4	502	0	0	4	522	2	486	5	236
Bryde's whale	1	28	0	0	0	0	0	0	0	0
Sei whale	0	0	2	117	1	114	1	29	1	47
Sei or Bryde's whale	2	27	2	75	0	0	0	0	0	0
Fin whale	23	892	29	1514	55	1832	19	1784	60	3082
Blue whale	53	1908	39	1965	74	1927	9	516	16	665
Humpback whale	6	196	15	570	49	1282	14	765	20	662
Unidentified delphinoid	11	1237	5	7697	14	4890	3	587	9	9768
Unidentified ziphiid whale	0	0	2	652	2	615	0	0	2	1104
Unidentified small whale	6	582	0	0	2	482	2	825	1	483
Unidentified roqual whale	3	63	2	93	18	423	2	70	12	296
Unidentified large whale	9	221	1	23	9	246	3	75	5	143
Subtotal: Delphinoids	291	385,546	156	439,027	250	481,937	148	416,818	158	622,208
Subtotal: Ziphiidae	14	10,342	14	9496	7	2881	1	3217	3	3719
Subtotal: Physeteridae	13	2807	9	2680	6	593	9	2495	13	2795
Subtotal: Balaenopteridae	92	3616	89	4334	201	6100	47	3650	114	4988
Total	425	403,114	269	455,561	475	492,238	210	427,080	294	634,335

in 2002–2003 (Calambokidis[3]). Our estimates of blue whale abundance decreased markedly in 2001 and 2005 compared to previous estimates, and they were more widespread in offshore and northern waters than during the 1990s. The lower abundance estimates, rather than reflecting a true population decline, appear to be caused by a redistribution of animals outside of the study area. Mark-recapture estimates of blue whale abundance remained high (1781) in the period of 2000–2003, but blue whales have recently been seen off British Columbia (Calambokidis[3]) and in the Gulf of Alaska (J. Barlow, unpubl. data). The recruitment of krill off central and northern California was poor during 2005 (Peterson et al., 2006), and given that this is the sole food for blue whales, the redistribution may be a result of decreased food supplies. Fin whales appeared to be monotonically increasing in abundance during the three

---

[3] Calambokidis, J. 2005. Personal commun. Cascadia Research, 218½ W. 4th Avenue, Olympia, WA 98501.

Table 8

Number of sightings (n) and estimated abundance (N) for each species in the Oregon-Washington region for the years 1996, 2001, and 2005. The total lengths of transects surveyed were 4336, 3100, and 2525 km for these years, respectively, in Beaufort sea state of 5 or less and were 532, 380, and 292 km, respectively, for Beaufort sea state of 2 or less. Unidentified large whales and small whales were not sufficiently specified to be included in the subtotals.

	1996		2001		2005	
Species	*n*	Abundance N	*n*	Abundance N	*n*	Abundance N
Short-beaked common dolphin	1	3749	1	219	1	11,286
Long-beaked common dolphin	0	0	0	0	0	0
Unclassified common dolphin	0	0	0	0	0	0
Striped dolphin	1	37	0	0	0	0
Pacific white-sided dolphin	7	5812	7	8884	5	10,708
Northern right whale dolphin	5	3397	10	8600	3	8265
Bottlenose dolphin (offshore)	0	0	0	0	0	0
Risso's dolphin	11	5248	9	5584	1	549
Short-finned pilot whale	0	0	0	0	0	0
Killer whale	3	250	4	881	3	548
Dall's porpoise	46	79,479	12	17,315	8	28,806
Mesoplodon spp.	1	479	0	0	1	926
Cuvier's beaked whale	0	0	0	0	0	0
Baird's beaked whale	3	179	2	348	3	1319
Kogia spp.	1	899	0	0	0	0
Sperm whale	3	318	2	98	4	1103
Minke whale	2	340	1	194	0	0
Bryde's whale	0	0	0	0	0	0
Sei whale	0	0	0	0	2	147
Sei or Bryde's whale	0	0	0	0	0	0
Fin whale	8	210	10	334	10	409
Blue whale	0	0	3	87	4	141
Humpback whale	1	13	7	331	17	483
Unidentified delphinoid	2	292	1	126	1	189
Unidentified ziphiid whale	0	0	0	0	0	0
Unidentified small whale	1	162	0	0	0	0
Unidentified roqual whale	1	20	2	60	4	127
Unidentified large whale	1	14	0	0	2	85
Subtotal: Delphinoids	76	98,264	44	41,609	22	60,351
Subtotal: Ziphiidae	4	658	2	348	4	2245
Subtotal: Physeteridae	4	1217	2	98	4	1103
Subtotal: Balaenopteridae	12	583	23	1006	37	1307
Total	98	100,897	71	43,061	69	65,091

survey periods, and a more detailed study of trends in fin whale abundance is warranted.

Bryde's and sei whales are very rare off the U.S. west coast, and minke whales are not common, particularly in offshore waters. Bryde's whales are commonly viewed as tropical baleen whales and therefore their low abundance is expected. However, sei whales were previously harvested commercially along the west coast by coastal whaling stations, and their near absence is more of a mystery. Minke whales are known to be common in some nearshore areas (Stern, 1992), which were not well sampled during our broad-scale cruises, but overall densities were low. Minke whale densities may have been underestimated in the study area because trackline detection probabilities were not directly estimated. There are no previous estimates of $g(0)$ for minke whales based on observers searching with 25× binoculars. Skaug et al. (2004) used observers searching with naked eyes and estimated $g(0)$ values between approximately 0.7 in Beaufort 1 and

0.5 in Beaufort 2. We assumed that $g(0)$ for minke whales in Beaufort 0 to 2 would be the same as for small groups of delphinids (0.846), but minke whales are very difficult to detect and an overestimate of this parameter would lead to an underestimate of minke whale abundance.

Physeteridae The estimated abundance of sperm whales is temporally variable off California (Table 7), but the two most recent estimates (2001 and 2005) were markedly higher than the estimates for 1991–96. Following the 1997–98 Niño, giant squid (*Dosidicus gigas*) have been more frequently observed off northern California and Oregon, in particular beginning in 2002 (Pearcy, 2002; Field et al., in press). Sperm whales are known to forage on giant squid, and their increased abundance within our study area may have been related to the increased availability of this prey species in recent years. Compared to baleen whales, sperm whales are found in larger groups, and fewer groups were seen on each survey, both of which contribute to more variable estimates. Also, the sperm whale population is likely to extend outside the study area, at least during certain times of the year. Of 176 tags that were implanted in sperm whales off southern California in winter, only three were later recovered by whalers (Rice, 1974); of these three, one was recovered outside the study area (far west of British Columbia). It is likely that at least some fraction of the population is absent during part of the year, and that fraction may vary with oceanographic conditions. This pattern of distribution differs from the situation with humpback whales; the majority of the humpback population appeared to be feeding in U.S. west coast waters during the time of the surveys. The density of sperm whales estimated in our study for the California Current (1.7 per 1000 km^2) is similar to the worldwide global average for this species (1.4 per 1000 km^2; Whitehead, 2002) but is less than recent estimates for waters in the eastern temperate Pacific (3–5 per 1000 km^2; Barlow and Taylor, 2005) and around Hawaii (2.8 per 1000 km^2; Barlow, 2006).

Dwarf and pygmy sperm whales are seldom seen by people because of their offshore distribution and cryptic behavior. Nonetheless, the estimated number of individuals found off the U.S. west coast exceeds the number of some much more commonly seen species, such as killer whales.

Ziphiidae Although they are rarely seen, approximately 7000 beaked whales were found in west coast waters—a number that exceeds that documented for baleen whales. The absence of California sightings for two beaked whale genera (*Mesoplodon* and *Berardius*, Table 7) since 1996 is disconcerting, especially in light of recent discoveries about the susceptibility of this group to loud anthropogenic sounds (Simmonds and Lopez-Jurado, 1991; Cox et al., 2006); however, weather conditions were less favorable for the detection of beaked whales during the more recent surveys (Fig. 1) and it is unclear whether this may have played a role in their apparent decrease. The distributions of all beaked whale species extend outside the study area, and it is likely that some individuals move in to and out of the study area as habitat changes. An analysis of trends in beaked whale abundance should include consideration of these effects.

Previous abundance estimates

Estimates presented in this study differ, typically by a small amount, from previous estimates from the 1991 survey (Barlow, 1995) and preliminary estimates from the 1993 (Barlow and Gerrodette, 1996), 1996 and 2001 (Carretta et al., 2006), and 2005 (Forney, 2007) surveys. The differences are primarily due to differences in the stratification and in the use of multiple covariates in the line-transect modeling. Both modifications should result in more precise estimates of cetacean abundance. In addition, some of these previous estimates did not include group-size calibration for individual observers, and therefore our estimates corrected a small negative bias present in those earlier estimates. The principle weakness of the current analysis is the small sample size for several rare species. However, we believe it is better to include all species for completeness and to properly quantify uncertainty in the estimates for rare species.

Acknowledgments

We thank the marine mammal observers (W. Armstrong, L. Baraff, S. Benson, J. Cotton, A. Douglas, D. Everhardt, H. Fearnbach, G. Friedrichsen, J. Gilpatrick, J. Hall, N. Hedrick, K. Hough, D. Kinzey, E. LaBrecque, J. Larese, H. Lira, M. Lycan, S. Lyday, R. Mellon, S. Miller, L. Mitchell, L. Morse, S. Noren, S. Norman, C. Oedekoven, P. Olson, T. O'Toole, S. Perry, J. Peterson, B. Phillips, R. Pitman, T. Pusser, M. Richlen, J. Quan, C. Speck, K. Raum-Suryan, S. Rankin, J. Rivers, R. Rowlett, M. Rosales, J. C. Salinas, G. Serra-Valente, B. Smith, C. Stinchcomb, N. Spear, S. Tezak, L. Torres, B. Troutman, and E. Vasquez,), cruise leaders (E. Archer, L. Ballance, E. Bowlby, J. Carretta, S. Chivers, T. Gerrodette, P. S. Hill, M. Lowry, K. Mangels, S. Mesnick, R. Pitman, J. Redfern, B. Taylor, and P. Wade), survey coordinators (J. Appler, A. Henry, P. S. Hill, A. Lynch, K. Mangels, and A. VonSaunder), and officers and crew who dedicated many months of hard work collecting these data. T. Gerrodette was the chief scientist for the 1993 survey. J. Cubbage and R. Holland wrote the data entry software. Data were edited and archived by A. Jackson. Areas within the 20-m depth contour were calculated by R. Cosgrove. J. Laake provided his R-language code for fitting the multiple-covariate line-transect models. This article benefited from the reviews and comments by M. Ferguson, L. Thomas, and the Pacific Scientific Review Group. Funding was provided by National Oceanic and Atmospheric Administration and the Strategic Environmental Research and Development Program (SERDP). This work was supported in part by the Monterey Bay Sanctuary Foundation.

Literature cited

Appler, J., J. Barlow, and S. Rankin.

2004. Marine mammal data collected during the Oregon, California and Washington line-transect expeditions (ORCAWALE) conducted aboard the NOAA ships McArthur and David Starr Jordan, July–Dec 2001. NOAA Tech. Memo. NMFS-SWFSC-359, 28 p.

Barlow, J.

1995. The abundance of cetaceans in California waters. Part I: Ship surveys in summer and fall of 1991. Fish. Bull. 93:1–14.

1999. Trackline detection probability for long-diving whales. *In* Marine mammal survey and assessment methods (G. W. Garner, S. C. Amstrup, J. L. Laake, B. F. J. Manly, L. L. McDonald, and D. G. Robertson, eds.), p. 209–221. Balkema Press, Rotterdam, The Netherlands.

2006. Cetacean abundance in Hawaiian waters estimated from a summer/fall survey in 2002. Mar. Mamm. Sci. 22(2):446–464.

Barlow, J., and T. Gerrodette.

1996. Abundance of cetaceans in California waters based on 1991 and 1993 ship surveys. NOAA Tech. Memo. NMFS-SWFSC-233, 15 p.

Barlow, J., T. Gerrodette, and J. Forcada.

2001. Factors affecting perpendicular sighting distances on shipboard line-transect surveys for cetaceans. J. Cetacean Res. Manage. 3(2):201–212.

Barlow, J., and B. L. Taylor.

2005. Estimates of sperm whale abundance in the northeastern temperate Pacific from a combined acoustic and visual survey. Mar. Mamm. Sci. 21(3):429–445.

Buckland, S. T., D. R. Anderson, K. P. Burnham, J. L. Laake, D. L. Borchers, and L. Thomas.

2001. Introduction to Distance Sampling: Estimating abundance of biological populations, 432 p. Oxford Univ. Press, Oxford, England.

2004. Advanced Distance Sampling: Estimating abundance of biological populations, 416 p. Oxford Univ. Press, Oxford, England.

Calambokidis, J., and J. Barlow.

2004. Abundance of blue and humpback whales in the eastern North Pacific estimated by capture-recapture and line-transect methods. Mar. Mamm. Sci. 21(1):63–85.

Carretta, J. V., K. A. Forney, and J. L. Laake.

1998. Abundance of southern California coastal bottlenose dolphins estimated from tandem aerial surveys. Mar. Mamm. Sci. 14(4):655–675.

Carretta, J. V., K. A. Forney, M. M. Muto, J. Barlow, J. Baker, B. Hanson, and M. S. Lowry.

2006. U.S. Pacific Marine Mammal Stock Assessments: 2005. NOAA Tech. Memo. NMFS-SWFSC-388, 317 p.

Carretta, J. V., T. Price, D. Petersen, and R. Read.

2005. Estimates of marine mammal, sea turtle, and seabird mortality in the California drift gillnet fishery for swordfish and thresher shark, 1996–2002. Mar. Fish. Rev. 66(2):21–30.

Cox, T. M., T. J. Ragen, A. J. Read, E. Vos, R. W. Baird, K. Balcomb, J. Barlow, J. Caldwell, T. Cranford, L. Crum, A. D'Amico, G. D'Spain, A. Fernandez, J. Finneran, R. Gentry, W. Gerth, F. Gulland, J. Hildebrand, D. Houser, T. Hullar, P. D. Jepson, D. Ketten, C. D. MacLeod, P. Miller, S. Moore, D. C. Mountain, D. Palka, P. Ponganis, S. Rommel, T. Rowles, B. Taylor, P. Tyack, D. Wartzok, R. Gisiner, J. Mead, and L. Benner.

2006. Understanding the impacts of anthropogenic sound on beaked whales. J. Cetacean Res. Manage. 7(3):177–187.

Dohl, T. P., M. L. Bonnell, and R. G. Ford.

1986. Distribution and abundance of common dolphin, *Delphinus delphis*, in the Southern California Bight: A quantitative assessment based on aerial transect data. Fish. Bull. 84:333–343.

Efron, B., and G. Gong.

1983. A leisurely look at the bootstrap, the jackknife, and cross-validation. Am. Stat. 37(1):36–48.

Field, J. C., K. Baltz, A. J. Phillips, and W. A. Walker.

In press. Range expansion and trophic interactions of the jumbo squid, *Dosidicus gigas* in the California Current. Calif. Coop. Fish. Invest. Rep.

Forney, K. A.

2000. Environmental models of cetacean abundance: reducing uncertainty in population trends. Conserv. Biol. 14(5):1271–1286.

2007. Preliminary estimates of cetacean abundance along the U.S. West Coast and within four National Marine Sanctuaries during 2005. NOAA Tech. Memo. NMFS-SWFSC-TM-406, 27 p.

Forney, K. A., and J. Barlow.

1998. Seasonal patterns in the abundance and distribution of California cetaceans, 1991–92. Mar. Mamm. Sci. 14(3):460–489.

Gerrodette, T., and J. Forcada.

2005. Non-recovery of two spotted and spinner dolphin populations in the eastern tropical Pacific Ocean. Mar. Ecol. Prog. Ser. 291:1–21.

Hill, P. S., and J. Barlow.

1992. Report of a marine mammal survey of the California coast aboard the research vessel McARTHUR July 28–November 5, 1991. NOAA Tech. Memo. NMFS-SWFSC-169, 103 p.

Julian, F., and M. Beeson.

1998. Estimates of marine mammal, turtle, and seabird mortality for two California gillnet fisheries: 1990–95. Fish. Bull. 96:271–284.

Keiper, C. A., D. G. Ainley, S. G. Allen, and J. T. Harvey.

2005. Marine mammal occurance and ocean climate off central California, 1986 to 1994 and 1997 to 1999. Mar. Ecol. Prog. Ser. 289:285–306.

Mangels, K. F., and T. Gerrodette.

1994. Report of cetacean sightings during a marine mammal survey in the eastern Pacific Ocean and the Gulf of California aboard the NOAA ships *McArthur* and *David Starr Jordan* July 28–November 6, 1993. NOAA Tech. Memo. NMFS-SWFSC-211, 86 p.

Marques, F. C., and S. T. Buckland.

2003. Incorporating covariates into standard line transect analysis. Biometrics 59:924–935.

Pearcy, W. G.

2002. Marine nekton off Oregon and the 1997–98 El Niño. Prog. Oceanogr. 54: 399–403.

Peterson, W. T., R. Emmett, R. Goericke, E. Venrick, A. Mantyla, S. J. Bograd, F. B. Schwing, R. Hewitt, N. Lo, W. Watson, J. Barlow, M. Lowry, S. Ralston, K. A. Forney, B. E. Lavaniegos, W. J. Sydeman, D. Hyrenbach, R. W. Bradley, P. Warzybok, F. Chavez, K. Hunter, S. Benson, M. Weise, J. Harvey, G. Gaxiola-Castro, and R. Durazo.

2006. The state of the California Current, 2005–2006:

warm in the north, cool in the south. Calif. Coop. Fish. Invest. Rep. 47:30–74.

Rice, D. W.
1974. Whales and whale research in the eastern North Pacific. *In* The whale problem: a status report (W. E. Schevill, ed.), p. 170–195. Harvard Press, Cambridge, MA.

Rugh, D. J., R. C. Hobbs, J. A. Lerczak, and J. M. Breiwick.
2005. Estimates of abundance of the eastern North Pacific stock of gray whales 1997 to 2002. J. Cetacean Res. Manage. 7(1):1–12.

Simmonds, M. P., and L. F. Lopez-Jurado.
1991. Whales and the military. Nature 51:448.

Skaug, H. J., N. Øien, T. Schweder, and G. Bøthun.
2004. Abundance of minke whales (*Balaenoptera acutorostrata*) in the Northeast Atlantic: variability in time and space. Can. J. Fish. Aquat. Sci. 61:870–886.

Stern, J. S.
1992. Surfacing rates and surfacing patterns of minke whales (*Balaenoptera acutorostrata*) off central California, and the probability of a whale surfacing within visual range. Reports of the International Whaling Commission 42:379–385.

Trites, A. W., V. Christensen, and D. Pauly.
1997. Competition between fisheries and marine mammals for prey and primary production in the Pacific Ocean. J. Northwest Atl. Fish. Sci. 22:173–187.

Turnock, B. J., and T. J. Quinn, II.
1991. The effect of responsive movement on abundance estimation using line transect sampling. Biometrics 47: 701–715.

Von Saunder, A., and J. Barlow.
1999. A report of the Oregon, California and Washington Line-transect Experiment (ORCAWALE) conducted in west coast waters during summer/fall 1996. NOAA Tech. Memo. NMFS-SWFSC-264, 40 p.

Whitehead, H.
2002. Estimates of the current global population size and historical trajectory for sperm whales. Mar. Ecol. Prog. Ser. 242:295–304.

Abstract—Does adult spillover (movement out of marine protected areas [MPAs]) of fish create a net export of fish biomass from MPAs to adjacent fished reefs? Biomass of five commercial reef fish species was estimated by visual census within and outside three MPAs in Guam, Micronesia. For most species and sites, biomass was significantly higher within the MPAs than in adjacent fished sites. Movement of fishes into and out of the MPAs was determined by mark-recapture experiments, in which fishes were tagged both inside and outside of MPAs. Four out of five species studied showed little or no net movement out of MPAs. However, the orangespine surgeonfish (*Naso lituratus*) showed a net spillover of biomass from all three MPAs; 21.5% of tagged individuals and 29% of the tagged biomass emigrated from MPAs. Patterns of spillover were strongly influenced by physical habitat barriers, such as channels, headlands, or other topographic features. MPAs that are physically connected by contiguous reef structures will likely provide more spillover to adjacent fished sites than those that are separated by habitat barriers. This study demonstrates that MPAs can enhance export of fish biomass to fished areas, but spillover is species-specific and depends on factors such as species size and mobility.

Manuscript submitted 21 November 2005 to the Scientific Editor's Office.

Manuscript approved for publication 2 July 20007 by the Scientific Editor.

Fish. Bull. 105:527–537 (2007).

Spillover of commercially valuable reef fishes from marine protected areas in Guam, Micronesia

Mark H. Tupper

Email address: m.tupper@cgiar.org

The WorldFish Center (address for correspondence)
Jalan Batu Maung, Batu Maung
11960 Bayan Lepas
Penang, Malaysia

and

Marine Laboratory
University of Guam, UOG Station
Mangilao, Guam 96923

Over the past two decades, marine protected areas (MPAs) have been increasingly adopted as an important fisheries management tool. The primary goals for MPAs are to protect critical habitat and biodiversity, to sustain or enhance fisheries by preventing spawning stock collapse, and to provide recruitment to fished areas (Gell and Roberts, 2003; Halpern, 2003). Enhancement of fished areas may occur through transport of larvae from spawning stock within the MPA (Gerber et al., 2005) or by a net emigration of adult fish to adjacent fished areas—a movement that is commonly known as "spillover" (e.g., Alcala et al., 2005; Abesamis et al., 2006; Goni et al., 2006).

The role of spillover in determining MPA effectiveness has been addressed in both theoretical modeling studies (e.g., DeMartini, 1993; Kramer and Chapman, 1999; Gerber et al., 2005) and in empirical studies. The latter involve indirect documentation of spillover inferred from increases in fish biomass or catch per unit of effort (CPUE) in adjacent fished areas (e.g., Russ and Alcala, 1996; Roberts et al., 2001; Tupper and Rudd, 2002; Alcala et al., 2005), and direct documentation of fish movement through mark-recapture or sonic tracking experiments (e.g., Chapman and Kramer, 2000; Meyer et al., 2000; Kaunda-Arara and Rose, 2004; Meyer and Holland, 2005). There are a number of ways in which movement across MPA boundaries may occur; these include random movements of fish during their routine activities (sometimes referred to as diffusion), emigration in response to density dependence (e.g., Tupper and Juanes, 1999; Abesamis and Russ, 2005), directed dispersal due to migration, and ontogenetic habitat shifts (Gerber et al., 2005). In order for spillover to effectively enhance adjacent fisheries, the net direction of these movements, and the number and size of fishes moving, must result in a net flow of biomass out of the MPA. Measuring the movement of biomass into the MPA should therefore be equally important to measuring outward movements. However, few studies have measured immigration, and therefore net spillover, and those that do address bidirectional movements have reported conflicting results, depending on the species or life history stage, the habitat, and the size and placement of the MPA (e.g., Kelly and MacDiarmid, 2003; Zeller et al., 2003; Tremain et al., 2004; Goni et al., 2006).

The degree of spillover from MPAs depends on the rate of fish migration across MPA boundaries (DeMartini, 1993; Gerber et al., 2005). Larger or more mobile species with large home ranges may spend too much time outside of the MPAs to be effectively protected, whereas smaller, more sedentary species with small home ranges may not cross MPA boundaries in sufficient numbers to enhance adjacent fisheries by spillover (DeMartini, 1993; Tupper and Rudd, 2002). If the goal of a MPA is to enhance local fisheries by spillover in addition to conserving spawning biomass, then it must be designed and situated so that net movement of fishes from the MPA to fished areas can take place. In most tropical island nations, enhancement of local fisheries by adult spillover may be critical for continued support of the preserve system by the local fishing community (Russ and Alcala, 1999; Galal et al., 2002). In general, arguments for larval spillover carry little weight with fishermen because dispersal may not occur on spatiotemporal or "visual" scales that are meaningful to them (Russ and Alcala, 1996; Russ, 2002; Abesamis et al., 2006). This situation is doubtless the case in Guam, where little is known about the movement of fishes on coral reefs.

One characteristic of heavily exploited reefs is the very low abundance (in some cases virtual absence) of large carnivorous fishes, particularly groupers (Serranidae) and snappers (Lutjanidae) (Russ, 1991, 2002; Medley et al., 1993). In Guam, grouper biomass is noticeably lower than at the less heavily populated islands in Micronesia (e.g., Palau). Much research has therefore been directed at determining the effects of implementing MPAs on populations of large predatory fishes (e.g., Russ and Alcala, 1996, 2004). In Micronesia, however, herbivorous fishes, particularly surgeonfishes and unicornfishes (Acanthuridae) and parrotfishes (Scaridae) are equally important to local fisheries, and in many areas they have dominated the catch (Amesbury et al., 1986). Thus, it is important to understand the effects of MPAs on herbivorous and carnivorous fishes.

To address whether MPAs in Guam can increase fish biomass and provide spillover to adjacent reef areas, biomass of five important reef fish species inside three MPAs in Guam and on adjacent exploited reefs was determined by using underwater visual census. Net movements of both herbivorous and carnivorous reef fish across MPA boundaries were determined by using mark-recapture experiments.

Materials and methods

Study sites

In May of 1997, the Guam Department of Aquatic and Wildlife Resources (DAWR) established a network of five MPAs, termed "marine preserves," around the island, which accounted for 11.8% of Guam's shoreline and 15.3% of Guam's reef area. Fishing within these MPAs is restricted to shore-based cast netting and hook-and-line fishing for select reef species, except for the Piti Bomb Holes Marine Preserve, where no reef fishing (i.e., fishing from the shore to the reef margin) is allowed. Trolling seaward of the reef margin for pelagic fish is allowed in all preserves. Despite being implemented in 1997, the marine preserves did not become enforced until October 1999. Even then, only warnings were issued until January 2001, at which time the regulations became fully enforced, and all violators were subject to any or all penalties applicable under the law. This study was conducted in 2003–04 at three MPA sites (Achang Reef Flat Marine Preserve, Piti Bomb Holes Marine Preserve, and Tumon Bay Marine Preserve—hereafter referred to as Achang, Piti, and Tumon, respectively) on the western and southern coasts of Guam, Micronesia (Fig. 1). All three sites consist of shallow reef flats that lead seaward to a reef crest and then drop off to a reef slope. The two remaining marine preserves, Sasa Bay and Pati Point, were not surveyed. Sasa Bay is a mangrove swamp with no coral reefs within its boundaries, and Pati Point is located within a restricted military area (Anderson Air Force Base).

The Achang preserve is the largest of the three preserves (4.8 km^2). It includes a wide variety of habitats: mangroves, seagrass, sand, coral, and three channels that cut through the fringing reef from the outer reef slope to the reef flat. The largest of these, Manell Channel, separates Achang reef flat from Cocos Lagoon, to the west of Achang Reef Flat. To the west, the reef flat narrows and is interrupted by a rocky headland. Reference fished sites for the Achang Preserve were located in Cocos Lagoon. Seasonal traditional fishing is permitted in the Achang Preserve for juvenile streamlined spinefoot (*Siganus argenteus*), juvenile fusiliers (*Pterocaesio tile*), and big eye scad (*Selar crumenophthalmus*) under special permit.

The Piti preserve covers 3.6 km^2 and consists of a broad reef flat (1.4 km^2) in Piti Bay bordered by Tepungan Channel to the west. The fringing reef is continuous from Piti Bay eastward to the fished sites at Asan Bay. The reef flat includes unique features known as "bomb holes," which provide sheltered areas of deeper water. The deepest of these sinkholes were 9–10 m deep and were densely populated by a variety of hard and soft coral species. They host rich soft coral communities and fish and invertebrate assemblages not often found within the reef margin. The main sinkhole is occupied by an 11-m in diameter underwater observatory that was completed in 1996. It is also frequented by commercial scuba divers during diving tours (up to 200 divers a day). Fish feeding is a common practice around the observatory; therefore, our survey sites were located away from the sinkholes in order to minimize possible confounding effects of fish feeding and diver presence.

The Tumon preserve lies adjacent to the central tourist district on Guam. It is 4.5 km^2 in total area and consists of extensive reef flats (2.7 km^2), a gently sloping fore reef slope, and a broad shelf habitat. The reef flat is dominated by coral patch reefs. The Tumon MPA is bordered by headlands to the east and west, which interrupt the reef flat, although there is contiguous fringing reef which links Tumon with Tanguisson to the east. However, there is a sewage outfall at Tanguisson which may reduce movement of fish to the east. Because of the distance from the reef flat at the western boundary of the Tumon MPA to the reef flat at East Agana Bay (approximately 3 km), Tanguisson was the location chosen for the fished sites. Limited traditional fishing with hook-and-line or cast net from shore is allowed in the Tumon Bay preserve for four types of fish: convict surgeonfish (*Acanthurus triostegus*), spinefeet (*Siganus* spp., known regionally as rabbitfish), juvenile jacks and trevallies (*Caranx* spp.), and juvenile goatfishes (Mullidae). Cast nets are sometimes used for convict surgeonfish and spinefeet along the reef margin.

At each site, visual census and tagging were performed as near to the geometric center of the MPA as possible. The closest distance to the MPA boundary was measured, and census sites on adjacent fished reefs were chosen at this same distance outside the MPA. All transects were surveyed and tagging was conducted in habitats as similar as possible, generally on the seaward edge of the reef flat at a 2–3 m depth, where the substrate typically consisted of sand, rubble, and scattered patch reefs (mainly *Porites* spp.), and where seagrass beds are nearer to shore (except in Tumon, where seagrass is scarce). This experimental design served to minimize bias due to among-site variation in distance from the reserve boundary and habitat type.

Estimation of biomass in MPAs and adjacent fished areas

Underwater visual census was used to estimate biomass of five exploited reef fishes at three MPAs and adjacent fished sites. These included three herbivores: convict surgeonfish (*Acanthurus triostegus*), orangespine unicornfish (*Naso lituratus*), and little spinefoot (*Siganus spinus*), and two carnivores: yellowstripe goatfish (*Mulloidichthys flavolineatus*), and honeycomb grouper (*Epinephelus merra*). These five species were chosen because of their great abundance and prevalence in the Guam nearshore reef fishery and because they are relatively easy to capture and tag. At each study site, four 50 m×5 m transects were laid haphazardly. Divers swam each transect slowly, counting all commercially important species and estimating their lengths to the nearest cm. All divers were trained in fish size estimation for one month before this study. Biomass estimates were conducted biweekly from May through August 2003. In total, 32 transects were completed at each MPA and adjacent reference sites (8 census days×4 transects at each site). Biomass was estimated by substituting the length of each fish on the transect into length-weight regressions for that species. The total weight of all fish by species was then used as an estimate of biomass.

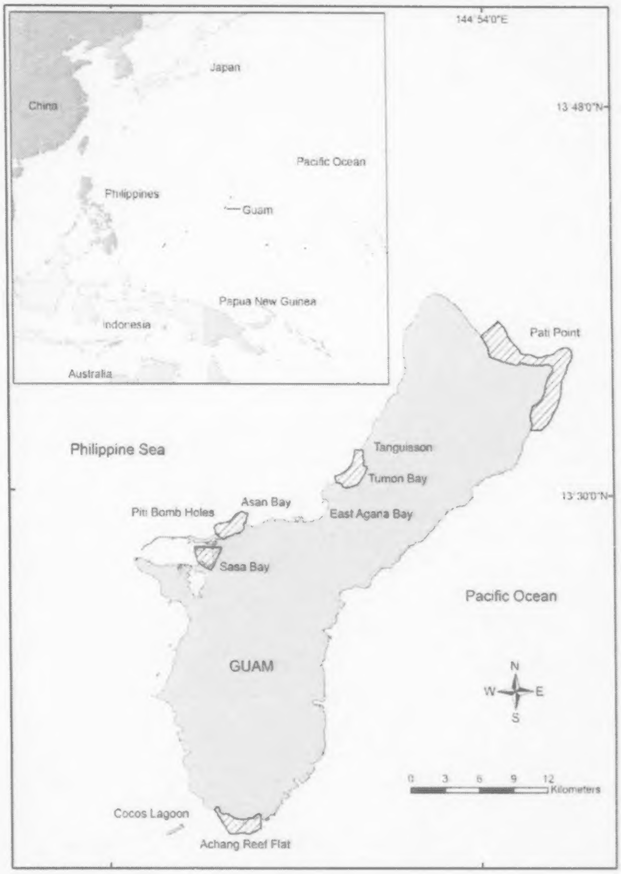

Figure 1

Map of Guam showing the locations of the three marine protected areas (MPAs) and three reference sites. MPAs (hatched areas) are Achang Reef Flat Marine Preserve, Piti Bomb Holes Marine Preserve, and Tumon Bay Marine Preserve. Reference sites are Cocos Lagoon, Asan Bay, and Tanguisson. Inset shows the location of Guam within the Western Pacific region.

Mark-recapture study

The five study species were collected from three preserves and from surrounding areas of reference sites. Within each preserve, six permanent quadrats, each 20 × 20 m in planar area, were located at a distance of 800 m from the boundary of the MPA and reference site. The perimeter of each study site was marked at 1-m intervals by tying flagging tape to a dead coral. Another six quadrats were marked on fished reefs at the reference site, also at a distance of 800 m from the MPA boundary. This distance was chosen because it allowed the location of the study sites to fall into appropriate and similar habitats at all MPAs and fish sites. This distance also ensured that all tagged fish had an equal distance to move in order to enter or leave the MPA. It also represented sufficient distance from the MPAs to encompass a large area of fished reef. A square area was chosen for the mark-recapture study because it was easier to deploy surround nets and to quantify fishing effort in a large square than in a typical narrow rectangle used for belt transects. Within each permanent quadrat, fish were captured by squirting an anesthetic (10% solution of Quinaldine sulfate in seawater) into the water where the fish were hiding and by casting a surround net (for smaller and more sedentary fishes) around corals heads or small patch reefs. For each species, an attempt was made to tag the same number of individuals at each MPA and reference site. Because target species density was generally lower at the fished sites (see "Results" section), fish were captured and tagged first at the fished sites by exhaustively fishing each 20×20 m quadrat. The same numbers of fish were then tagged in quadrats within the MPAs. This procedure ensured that tagging effort was equal across all sites, although fishing effort was often lower in the MPAs because sufficient fish could be captured in a shorter time. For recaptures of tagged fish, all permanent quadrats were fished exhaustively and all tagged individuals were recorded.

Tagging took place biweekly from May through July 2003 and from January through March 2004. Recaptured fish were collected weekly from May through August 2003 and January through April 2004 (n=32 total recapture attempts per site), allowing 1 week to 6 months between tagging and recapture. Captured fish were identified, measured, and tagged with visible implant elastomer (VIE) tags (Northwest Marine Technologies, Inc., Shaw Island, WA), and immediately released at the site of capture. The VIE tag was implanted under a fish's skin and thus would not become entangled, scraped off, or fouled with algae. Tag loss can lead to underestimates of recapture rates if a fish is recaptured after losing its tag. Past studies with several reef fish families (Labridae, Scaridae, Acanthuridae, and Serranidae) showed high (>90%) retention of elastomer implants, particularly for individuals greater than 150 mm standard length (Tupper, 2007). The effective life of the VIE tag in most reef fish is about 6 months, after which the tissue surrounding the tag generally has overgrown and obscured the tag (Tupper, 2007). The use of surround nets allowed for capture of resighted tagged fish. This approach enabled much higher recapture rates than those in more conventional studies where external tags and nonselective gears (such as traps) are solely used.

Analysis of data

To calculate spillover (S) for a given species, the numbers and biomass of tagged fish emigrating or immigrating across an MPA boundary were estimated. Spillover was calculated as the number (or biomass) of emigrants minus the number (or biomass) of immigrants. Percent spillover was calculated as the proportion of tagged fish (numbers and biomass) exported to adjacent fished areas minus the proportion of tagged biomass imported to the MPA:

$$S = (B_e/B_P - B_i/B_R) \times 100,$$

where S = percent spillover;
B_e = biomass emigrating from the preserve;
B_P = biomass remaining in the preserve;
B_i = biomass immigrating into the preserve; and
B_R = biomass remaining in the reference site.

A positive value would indicate net spillover; a negative value would indicate net influx of biomass to the MPA. Thus, a positive value indicates that the MPA is a source of biomass for adjacent fished areas, where a negative value indicates that the MPA is a biomass sink and perhaps better suited to conserving biomass of a given species than to enhancing local fisheries.

Before analysis, all raw data were tested for normality by using the Shapiro-Wilk W test and for homogeneity of variance by using Levene's test (Sokal and Rohlf, 1995). Because raw density and raw spillover data did not initially meet these assumptions, they were square-root transformed. Percent spillover data were arc-sin transformed. All transformed data met the assumptions of parametric analysis of variance (ANOVA). Variation in mean fish biomass between locations and between MPAs and fish sites was determined with 2-way ANOVA. For this analysis, each MPA was paired with its adjacent fished site and this grouping resulted in three pairs: North (Tumon and Tanguisson), central (Piti and Asan Bay), and south (Achang and Cocos Lagoon). The ANOVA design was crossed, with location (north vs. central vs. south) as one factor and protection status (MPA vs. fished site) as a second factor. Variation in mean spillover between locations and between species was also analyzed bby using 2-way ANOVA. Tukey's honestly significant difference (HSD) was used as a *post hoc* comparison test to determine pairwise differences in mean biomass and mean spillover in MPAs and reference sites. Linear regression was used to explore the relationship between density (expressed as biomass) of fish within the MPAs and the spillover rate from the MPAs.

Results

Biomass estimates

Mean biomass of the three herbivorous species was higher in MPAs than in the fished sites (Fig. 2). Mean biomass of convict surgeonfish did not differ between locations (i.e., between south, central, and north, 2-way ANOVA, F=0.79, P=0.46) but was significantly higher in MPAs than in fished sites at all locations (F=13.47, P<0.001; Tukey's HSD, P<0.05 for all paired comparisons). There was no significant interaction between location and protective status. Mean biomass of orangespine unicornfish also did not differ between locations (2-way ANOVA, F =0.90, P=0.42) but was significantly higher in MPAs than in fished sites (F=12.02, P<0.0001). There was a significant interaction (F=9.4, P<0.01) between location and protective status because biomass

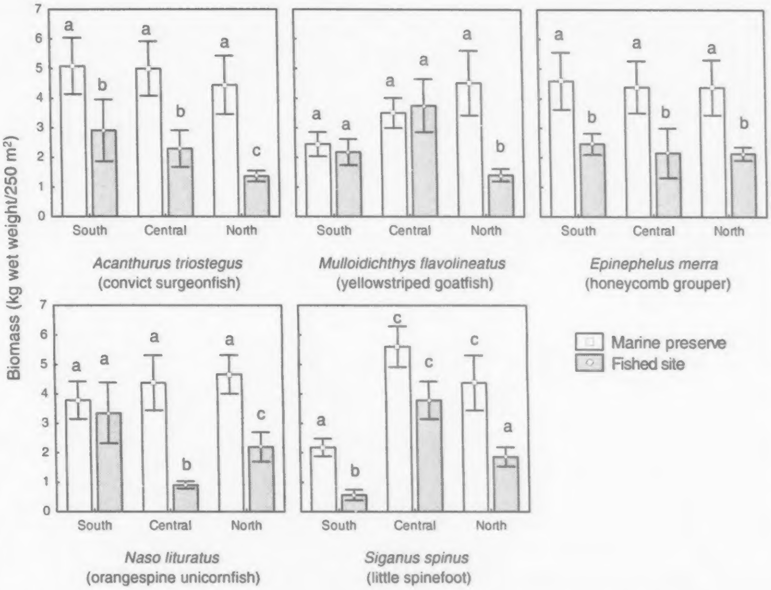

Acanthurus triostegus (convict surgeonfish)

Mulloidichthys flavolineatus (yellowstriped goatfish)

Epinephelus merra (honeycomb grouper)

Naso lituratus (orangespine unicornfish)

Siganus spinus (little spinefoot)

Figure 2

Mean biomass of five exploited reef fishes in three marine protected areas (MPAs) and three reference sites at Guam, Micronesia. South = Achang Marine Preserve and Cocos Lagoon reference site. Central = Piti Bomb Holes Marine Preserve and Asan Bay reference site. North = Tumon Bay Marine Preserve and Tanguisson reference site. Error bars represent ± 1 standard deviation; $n = 32$ censuses per site. Letters indicate groups of no significant difference among MPAs and reference sites, according to pairwise comparisons (Tukey's HSD).

of orangespine unicornfish was significantly higher in the Piti and Tumon MPAs than in adjacent fished sites (Tukey's HSD, $P<0.05$), but there was no significant difference in biomass between Achang and Cocos Lagoon (Tukey's HSD, $P<0.05$). Mean biomass of little spinefoot differed significantly between locations (2-way ANOVA, $F=15.02$, $P<0.0001$) and was significantly higher in the north and central locations than in the south (Tukey's HSD, $P<0.05$). Mean biomass of little spinefoot was also significantly higher on protected reefs ($F=16.01$, $P<0.0001$) at all locations (Tukey's HSD, $P<0.05$ for all paired comparisons).

For carnivorous species, mean biomass of yellowstripe goatfish (Fig. 2) did not differ between locations (2-way ANOVA, $F=1.76$, $P=0.18$). There was a nonsignificant higher abundance in MPAs than in reference sites ($F=3.30$, $P=0.076$). There was a significant interaction between location and protective status ($F=3.32$, $P<0.05$), which occurred because biomass of yellowstripe goatfish was higher in the Tumon MPA than at Tanguisson, but did not differ between MPAs and reference sites at the central and south locations. Mean biomass of honeycomb grouper (Fig. 2) did not differ between locations (2-way ANOVA, $F=0.07$, $P=0.93$) but was significantly higher in MPAs than at fished sites ($F=11.33$, $P=0.002$) at all locations.

Spillover

A total of 2674 fishes were tagged; of these 935 (35%) were recaptured (Table 1). The species with the highest recapture rate (78%) was the honeycomb grouper; a solitary, benthic predator. Mobile, schooling species such as yellowstripe goatfish and little spinefoot had lower recapture rates (25–35%) but were abundant enough to allow relatively large numbers of returns.

Most recaptured fish did not cross the MPA boundaries. The overall grand mean spillover (i.e., over all species at all sites) was 5.9% of individuals and 8.0% of biomass from the MPAs. Table 2 shows biomass and mean number of tagged fish remaining within each MPA and fished site, immigrating to each MPA, and emigrating to each fished site. The difference between emigration and immigration is shown in Table 2 as the net flux in biomass and as the net flux in numbers. Spillover (the proportion of tagged fish exported to adjacent fished areas minus the proportion of tagged fish imported to the MPA) is also presented as spillover in

Table 1

Number of fish tagged and recaptured at three marine protected areas (MPAs) and three fished sites in Guam, Micronesia. Study species were convict surgeonfish (*Acanthurus triostegus*), honeycomb grouper (*Epinephelus merra*), yellowstripe goatfish (*Mulloidichthys flavolineatus*), orangespine unicornfish (*Naso lituratus*), and little spinefoot (*Siganus spinus*).

Species	Achang MPA	Cocos Lagoon	Piti MPA	Asan Bay	Tumon MPA	Tanguisson	Total	Recaptures	% Recaptured
Convict surgeonfish	135	134	135	130	132	130	796	247	31.0
Orangespine unicornfish	50	47	48	45	50	44	284	112	39.4
Yellowstrip goatfish	65	62	65	65	70	63	390	137	35.1
Honeycomb grouper	40	40	41	40	40	39	240	188	78.3
Little spinefoot	162	157	165	158	164	158	964	251	26.0
Total	452	440	454	438	456	434	2674	935	35.0

biomass and in numbers. For both net flux and spillover, a positive value indicates net movement out of the MPA; a negative value indicates net movement into the MPA. For the combination of all species, overall spillover was lowest at the Tumon MPA, where only 1.7% of all tagged biomass was exported (two-way ANOVA, F=17.12, P<0.01, Tukey's HSD, P<0.05). Spillover did not differ between the other two MPAs (20.3% at Piti and 16.7% at Achang, Tukey's HSD, P<0.05).

A significant interaction between species and location (two-way ANOVA, F=7.73, P<0.0001) warranted a closer inspection of fish movements at each location. Orangespine unicornfish was the only species exported from all three MPAs. The overall mean spillover for orangespine unicornfish was 29.4% of biomass (Table 2) and 21.5% of individuals (Table 2). This was significantly higher than the other four species (2-way ANOVA, F=6.27, P<0.0001). There was no significant difference in spillover of orangespine unicornfish between MPAs (2-way ANOVA, F=2.71, P=0.34). Although yellowstripe goatfish showed low overall mean spillover (1.1% of individuals imported to MPAs but 16.4% of biomass exported), it was actually very mobile; 34% of its tagged biomass moved into the Achang MPA, and 31% of its tagged biomass moved out of the Piti MPA. These net inward and outward movements at different locations cancelled each other in the calculation of overall mean spillover for this species. No movement of this species occurred across the Tumon MPA boundaries. In contrast, net export of convict surgeonfish occurred at Achang and Piti MPAs, but there was a net import of surgeonfish biomass to the Tumon MPA (Table 2). Spillover of convict surgeonfish did not differ between the Achang and Piti MPAs (Tukey's HSD, P>0.05). Honeycomb grouper showed an overall mean outward movement of 3.3% of tagged biomass (Table 2). However, there was no net movement of individuals across MPA boundaries at all sites (Table 2); this result indicated that primarily larger individuals moved out of the MPAs.

In general, for most species, the percentage of biomass exported from the MPAs was greater than the percentage of individuals exported. The exception was that of yellowstripe goatfish at the Achang MPA, which showed a net outward movement of 15.6% of individuals (Table 2) but a net inward movement that was 34.2% of biomass (Table 2), indicating that the fish moving into Achang MPA were much larger than the fish moving out. In contrast, at Piti there was a net outward movement of 15.6% of individuals and 30.8% of the biomass for yellowstripe goatfish, indicating that larger fish were primarily exported. The effect of resident biomass on spillover of each species was examined by plotting spillover (in biomass) against the biomass ratio of each species at each MPA, measured as biomass inside the MPA divided by the biomass at the fished site. The variation in density between censuses rendered it impossible to create separate regressions for each species or MPA. Thus, the overall mean biomass ratio and mean spillover were pooled for all species and MPAs into a single regression. No relationship was found between the biomass ratio and mean spillover (r^2=0.1, P=0.34; Fig. 3).

Discussion

One of the primary effects of protection from fishing is an increase in size and abundance of fishes, and therefore in biomass, in MPAs (Russ, 2002; Halpern, 2003). Biomass of reef fish was greater in marine reserve areas than in fished areas after about six years of effective no-take protection at Sumilon and Apo Islands in the Philippines (Alcala et al., 2005). Moreover, these differences became larger with increased duration of protection up to 19 years. Russ and Alcala (2004) concluded that the time required for full recovery of reef fish populations at the Sumilon and Apo Island MPAs would be 15 and 40 years, respectively. Biomass of leopard coralgrouper (*Plectropomus leopardus*) and spotted coralgrouper (*P. maculatus*), two large roving grouper species, was five times higher in no-fishing zones than in fished zones of the Great Barrier Reef Marine Park, after 14 years of protection (Evans and Russ, 2004). Numerous other studies had found no difference in biomass of *Plectro-*

Table 2

Summary of mean numbers and biomass of recaptured fish that remained resident in the marine protected areas (MPAs) and fished sites, or that moved into or out of the MPAs. Spillover is the difference between emigration from and immigration to the MPAs. Percent spillover is the proportion of tagged fish emigrating from the MPAs minus the proportion of tagged fish immigrating to the MPAs. Data are presented as biomass of fish and number of fish. All data are means ±1 standard deviation; $n = 32$ recapture events for each site. Superscripts ($^{a, b}$) indicate significant differences among MPAs according to pairwise comparisons (Tukey's honestly significant difference [HSD] test). Fished sites for Achang, Piti, and Tumon were Cocos Lagoon, Asan Bay, and Tanguisson, respectively (see Fig. 1). Study species were convict surgeonfish (*Acanthurus triostegus*), honeycomb grouper (*Epinephelus merra*), yellowstripe goatfish (*Mulloidichthys flavolineatus*), orangespine unicornfish (*Naso lituratus*), and little spinefoot (*Siganus spinus*).

Biomass of fish

Species	Location	Fish biomass (MPA) 250 m^2	Fish biomass (fished site) g wet wt/ 250 m^2	Biomass immigrants g wet wt/ 250 m^2	Biomass emigrants g wet wt/ 250 m^2	Spillover (biomass) g wet wt/ 250 m^2	Spillover (%)
Convict surgeonfish	Achang	2207 ±408	2742 ±777	407 ±316	1232 ±658	825 ±742	22.1 ±19.8^a
	Piti	4051 ±1684	4806 ±1376	1137 ±666	1848 ±791	711 ±1055	14.1 ±15.9^a
	Tumon	2720 ±1757	2969 ±1841	2018 ±682	1109 ±326	–910 ±564	–19.8 ±18.0^b
Honeycomb grouper	Achang	3206 ±863	3206 ±862	141 ±283	184 ±367	42 ±85	1.4 ±2.7
	Piti	1886 ±304	1716 ±463	530 ±398	749 ±59	220 ±358	7.5 ±12.4
	Tumon	2494 ±362	2588 ±285	141 ±283	168 ±336	27 ±53	0.9 ±1.9
Yellowstripe goatfish	Achang	2514 ±759	2524 ±791	1647 ±551	523 ±1045	–1125 ±561	–34.2 ±19.7^a
	Piti	2005 ±986	2752 ±1517	209 ±246	1227 ±472	1016 ±720	30.8 ±31.4^b
	Tumon	2267 ±396	2267 ±396	0	0	0	0^b
Orangespine unicornfish	Achang	1872 ±1248	2932 ±1682	291 ±346	1351 ±379	1060 ±450	33.6 ±5.2
	Piti	4546 ±689	6459 ±592	1321 ±995	3234 ±1139	1914 ±630	25.4 ±9.3
	Tumon	2563 ±1353	4046 ±2543	341 ±404	1824 ±1437	1483 ±1614	29.2 ±35.5
Little spinefoot	Achang	4097 ±1434	3824 ±1599	1476 ±334	1203 ±417	–272 ±311	–6.2 ±5.6^a
	Piti	2629 ±994	4357 ±1624	547 ±271	2275 ±405	1728 ±639	23.7 ±6.3^b
	Tumon	3524 ±1530	3169 ±1526	806 ±678	451 ±302	–644 ±228	–8.6 ±19.5^a

Number of fish

Species	Location	Number of fish (MPA)	Number of fish (reference site)	Number of immigrants	Number of emigrants	Spillover (numbers)	Spillover (%)
Convict surgeonfish	Achang	6.5 ±0.58	7.8 ±0.96	1.0 ±0.82	2.3 ±0.96	1.3 ±0.96	13.9 ±10.6^a
	Piti	9.3 ±3.30	9.8 ±1.71	2.8 ±1.50	3.3 ±1.50	0.5 ±1.73	6.0 ±13.1^a
	Tumon	7.8 ±1.89	6.8 ±3.20	3.3 ±0.96	1.5 ±0.58	–1.8 ±0.96	–20.0 ±20.2^b
Honeycomb grouper	Achang	5.0 ±1.41	5.0 ±1.41	0.3 ±0.50	0.3 ±0.50	0	0
	Piti	3.0 ±0.82	3.0 ±0.82	1.0 ±0.82	1.0 ±0.00	0.0 ±0.82	0.0 ±16.3
	Tumon	4.5 ±0.58	4.5 ±0.58	0.3 ±0.50	0.3 ±0.50	0	0
Yellowstripe goatfish	Achang	4.8 ±1.50	4.8 ±2.06	3.0 ±0.82	1.3 ±2.50	–1.8 ±1.89	1.5 ±5.8
	Piti	4.5 ±1.73	5.0 ±2.71	0.5 ±0.58	1.5 ±0.58	1.0 ±1.15	15.6 ±19.4
	Tumon	4.5 ±0.58	4.5 ±0.58	0	0	0	0
Orangespine unicornfish	Achang	3.5 ±1.73	4.8 ±2.22	0.5 ±0.58	1.8 ±0.50	1.3 ±0.50	23.8 ±2.5
	Piti	9.0 ±4.08	9.5 ±1.73	1.8 ±1.26	3.8 ±1.71	2.0 ±0.82	17.2 ±6.5
	Tumon	4.0 ±1.63	5.8 ±3.10	0.5 ±0.58	2.3 ±1.71	1.8 ±2.06	23.4 ±33.4
Little spinefoot	Achang	9.8 ±2.22	9.3 ±2.99	2.8 ±0.50	2.3 ±1.26	–0.5 ±1.00	–5.8 ±8.3^a
	Piti	6.8 ±2.22	9.5 ±3.32	1.3 ±0.50	4.0 ±0.82	2.8 ±1.26	24.5 ±7.7^b
	Tumon	7.8 ±1.50	7.0 ±2.58	1.8 ±1.71	0.8 ±0.50	–1.0 ±1.63	–11.6 ±20.5^a

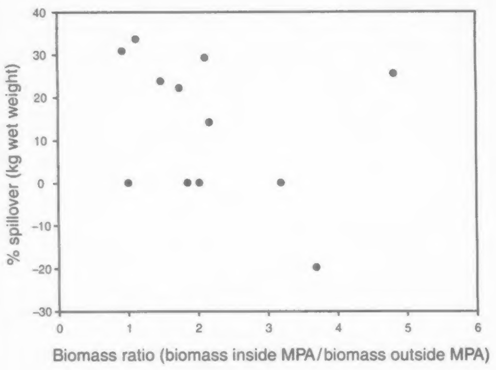

Figure 3

Effect of biomass ratio (biomass in marine protected area/ biomass in reference site) on spillover of reef fishes from marine protected areas in Guam, Micronesia. Points represent the level of spillover for a given biomass ratio. Data are pooled for five species and three MPAs. Study species are convict surgeonfish (*Acanthurus triostegus*), honeycomb grouper (*Epinephelus merra*), yellowstripe goatfish (*Mulloidichthys flavolineatus*), orangespine unicornfish (*Naso lituratus*), and little spinefoot (*Siganus spinus*).

pomus spp. after <10 years of protection (reviewed in Evans and Russ, 2004). In Kenyan MPAs, complete recovery of fish populations was estimated to take 22 years (McClanahan and Graham, 2005). Other studies have reported more rapid buildup of biomass. Biomass of five commercially exploited fish families tripled within three years of implementation of the Soufriere Marine Management Area in St. Lucia (Roberts et al., 2001). Biomass of reef fish in another MPA in St. Lucia, Anse Chastanet Reserve, doubled within two years of effective protection (Roberts and Hawkins, 1997) and a similar, rapid buildup of biomass was observed in a small MPA in Saba (Roberts, 1995). Rates of biomass buildup inside MPAs should generally be consistent with life history characteristics of the fish (Russ and Alcala, 1996; Mosquera et al., 2000; Alcala et al., 2005). Large predators (e.g., epinepheline serranids [large groupers], Lutjanidae, Lethrinidae, and Carangidae) and many Acanthuridae (surgeonfish) are long-lived, often with low rates of natural mortality and recruitment. Such characteristics would indicate that recovery rates would be gradual, as observed by Evans and Russ (2004) and Alcala et al. (2005).

In this study, it was not possible to determine the rate of biomass buildup because data were not collected at the initial implementation of the MPAs or at the initiation of full enforcement. After approximately 2.5 years of protection, biomass of all five study species of reef fish was higher within the MPAs than in fished sites, although the difference was not statistically significant at the 95% confidence level for yellowstripe goatfish. A longer period of protection may result in greater biomass differentials between the marine preserves and fished sites. Biomass of all three species of herbivores was significantly higher within the MPAs, indicating that fishing pressure on herbivores in Guam is sufficient to show a biomass increase within no-fishing zones. Thus, increasing herbivore biomass on exploited reefs through spillover from MPAs may have the potential to reduce algal overgrowth, at least within a limited area adjacent to the MPA.

Given rapid population turnover, coupled with high fishing effort in the reference areas, significantly higher biomass in the MPAs may be evident after only 2–3 years of protection. All the species in this study are small to medium-size fishes with rapid growth and maturation rates (Choat and Robertson, 2002). What is somewhat surprising is that the densities of convict surgeonfish, yellowstripe goatfish, and little spinefoot were all significantly higher in the Tumon MPA than at the adjacent fished site, given that these species were legally targeted by subsistence fishermen within the MPA. However, the regulations stipulate that fishing with hook-and-line or cast net only and from shore or the exposed reef margin only. Moreover, fishermen in Tumon would have to contend with large numbers of tourists in the immediate vicinity, and fishing effort appeared low throughout the course of this study.

Several studies indicate that MPAs connected to fished areas by continuous reef will have higher rates of spillover (e.g., Kaunda-Arara and Rose, 2004). In this study, the highest overall spillover to surrounding fished reefs occurred from Piti, where the MPA and fished site are connected by a continuous reef flat. This was the only site at which no net inward movement of any species occurred. Fishermen were often seen along the boundary of the marine preserve, no doubt "fishing the line" in hopes of catching larger fish emigrating from the Piti MPA. When species were combined, the lowest rate of net flux occurred at Tumon. The fished site to the east of Tumon was at Tanguisson. These two bays are divided by a high, rocky headland (Punta Dos Amantes) with no reef flat. A sewage outfall just north of Punta Dos Amantes also separates the MPA and fished site. However, three of the five study species appeared to move freely between Tumon and Tanguisson—only yellowstripe goatfish and honeycomb grouper did not. Thus, the low overall rate of net flux was caused by the net import of convict surgeonfish and little spinefoot that balanced the net export of orangespine unicornfish. The overall spillover from Achang to Cocos Lagoon was also low, perhaps partly because these areas are separated by a wide tidal channel to the west of the Achang reef flat. However, the low mean spillover from Achang occurred because of the large number of adult yellowstripe goatfish moving into the MPA. These results demonstrate the importance of determining spillover at the species level. Because different species can vary in their market value, the mean spillover of all fishes from an MPA may not be indicative of the net value of fish moving from MPAs to fished reefs.

The results of this study demonstrate that large, mobile herbivores like orangespine unicornfish may be exported from MPAs. The high rates of spillover for this species may result in part from its larger size in relation to the other species. In general larger fish have larger home ranges (Kramer and Chapman, 1999). In this study, the percentage of biomass exported from a given MPA tended to be higher than the percentage of individuals exported, indicating that spillover was primarily accomplished by larger fish. However, some acanthurids are known to be very site attached (e.g. Bell and Kramer, 2000; Meyer and Holland, 2005). For example, the larger congener (*N. unicornis*) is very site attached, and Meyer and Holland (2005) found little evidence for spillover of this species from a small (0.34 km^2) no-take marine reserve in Waikiki, Hawaii. Movements of adult *N. vlamingii* across the boundaries of Apo Island marine reserve are rare, but density-dependent interactions within the reserve are sufficient to displace smaller fish from the reserve (Abesamis and Russ, 2005). In a separate study, no cross-boundary migration was found for three other acanthurids: *Acanthurus nigricans*, *Ctenochaetus striatus*, and *N. unicornis* (M. Tupper, unpubl. data). Convict surgeonfish showed notable spillover (14–22% of tagged biomass) at Achang and Piti, but showed a net import of 20% of tagged biomass into Tumon. Similarly, yellowstripe goatfish showed net import to Achang and net spillover from Piti. These species tended to form large, mobile foraging schools at all locations. The spatial variation in movement of these two species may be a function of foraging or spawning movements constrained or modified by natural physical barriers (channels or headlands) and possibly anthropogenic barriers (e.g., the sewer outfall south of Tanguisson). For example, net inward movement of yellowstripe goatfish to Achang may be related to a spawning aggregation of this species located in Asgadao Channel, in the center of the Achang MPA (M. Tupper, unpubl. data). Alternatively, the disparity in direction of net movement at different sites may be simply explained by large ranging schools that happened to be tagged inside but recaptured outside the MPA at one location and vice versa at another. As might be expected, the honeycomb grouper, a small, sedentary, ambush predator, showed very low rates of spillover; no net movement in either direction was found at any of the study sites.

Movement across MPA boundaries may occur as a result of random dispersal of fish during their routine activities, directed dispersal due to migration or ontogenetic habitat shifts (Gerber et al., 2005), or emigration in response to density dependence. High densities of conspecifics in MPAs may lead to increased juvenile mortality (Goeden, 1979; Tupper and Juanes, 1999), decreased growth (Béné and Tewfik, 2003; Tewfik and Béné, 2003), or increased emigration, or to a combination of all three (Tupper and Juanes, 1999; Abesamis and Russ, 2005). In this study, there was no relation between density and spillover of reef fish. This may have been due to fact that the density of fish in Guam's MPAs has not yet reached carrying capacity, i.e., the biomass within the MPAs is not yet representative of virgin, unfished stocks. It should be noted that pooled species and locations were used in the regression analysis. More data on individual species and locations would result in a more powerful test.

In conclusion, rates of adult import or export from MPAs appear to result from a combination of foraging behavior, potential spawning movements, and random daily movements across MPA boundaries. These movements were influenced by reef topography. Spillover was highest in areas joined by continuous fringing reef systems and lowest where reefs where separated by a headland barrier. Knowledge of fish movement patterns with respect to reef topography may be useful for choosing MPA boundaries in order to maximize the spillover of target species. The herbivorous orangespine unicornfish showed the highest rate of spillover from MPAs, which indicates that MPAs have the potential to provide herbivore biomass to adjacent fished areas which may be suffering from algal overgrowth due to fishing of herbivores and from nutrient input due to agricultural activities. However, given the declines in density of exploited fishes at the fished sites since the implementation of the MPAs (Gutierrez[1]), it is evident that overall spillover has not yet been sufficient to increase fish biomass on adjacent reefs. This is not surprising, given the relatively short time since the implementation of these MPAs and the displacement of fishing effort from the MPAs to adjacent fished areas. Although spillover rates of four out of five study species were quite low, adult migration is only one process that may benefit fisheries. Further research is needed to determine the role of MPAs in enhancing larval supply and the transport of recruits from Guam's MPAs to adjacent fished areas.

Acknowledgments

I am grateful to J. Castro and J. Cruz for their invaluable assistance in collecting and tagging fishes. I thank G. Davis, C. Leberer, and J. Gutierrez of the Guam Division of Aquatic and Wildlife Resources for permitting me to collect fishes at the marine preserves. I am also grateful to D. Burdick and S. J. Teoh for assistance with the map shown as Figure 1. Funding for data collection was provided by grants to the University of Guam from the National Oceanic and Atmospheric Administration's Coral Reef Ecosystems Studies Program, the National Oceanic and Atmospheric Administration State and Territorial Coral Reef Management program and from the U.S. Department of Fish and Wildlife. Funding for data analysis and for manuscript writing was provided by the WorldFish Center.

---

[1] Gutierrez, J. 2004. Personal commun. Division of Aquatic and Wildlife Resources, 163 Dairy Road, Mangilao, Guam 96910.

Literature cited

Abesamis, R. A., and G. R. Russ.
2005. Density-dependent spillover from a marine reserve: long-term evidence. Ecol. Appl. 15(5):1798–1812.

Abesamis, R. A., A. C. Alcala, and G. R. Russ.
2006. How much does the fishery at Apo Island benefit from spillover of adult fish from the adjacent marine reserve? Fish. Bull. 104:360–375.

Alcala, A .C., G. R. Russ, A. E. Maypa, and H. P. Calumpong.
2005. A long-term, spatially replicated experimental test of the effects of marine reserves on local fish yields. Can. J. Fish. Aquat. Sci. 62:98–108.

Amesbury, S. S., F. A. Cushing, and R. K. Sakamoto.
1986. Fishing on Guam, 110 p. Univ. Guam Press, Mangilao, Guam.

Bell, T., and D. L. Kramer.
2000. Territoriality and habitat use by juvenile blue tangs, *Acanthurus coeruleus*. Environ. Biol. Fishes 58:401–409.

Béné, C., and A. Tewfik.
2003. Biological evaluation of a Marine Protected Area: evidence of crowding effect on a protected population of queen conch in the Caribbean. Mar. Ecol. 24(1) 45–58.

Chapman, M. R., and D. L. Kramer.
2000. Movements of fishes within and among fringing coral reefs in Barbados. Environ. Biol. Fishes 57:11–24.

Choat, J. H., and D. R. Robertson.
2002. Age-based studies. *In* Coral reef fishes: dynamics and diversity in a complex ecosystem (P. F. Sale, ed.), p. 57–80. Academic Press, San Diego, CA.

DeMartini, E. E.
1993. Modelling the potential of fishery reserves for managing Pacific coral reef fishes. Fish. Bull. 91: 414–427.

Evans, R. D., and G. R. Russ.
2004. Larger biomass of targeted reef fish in no-take marine reserves on the Great Barrier Reef, Australia. Aquatic Conserv: Mar. Freshw. Ecosyst. 14: 505–519.

Galal, N., R. F. G. Ormond, and O. Hassan.
2002. Effect of a network of no-take reserves in increasing catch per unit effort and stocks of exploited reef fish at Nabq, South Sinai, Egypt. Mar. Freshw. Res. 53:199–205.

Gell, F., and C. M. Roberts.
2003. Benefits beyond boundaries: the fishery effects of marine reserves. Trends Ecol. Evol. 18: 448–455

Gerber, L. R., S. S. Heppell, F. Ballantyne, and E. Sala.
2005. The role of dispersal and demography in determining the efficacy of marine reserves. Can. J. Fish. Aquat. Sci. 62:863–871.

Goeden, G. B.
1979. Is the Great Barrier Reef being overfished? Aust. Fish. 1979:18–20.

Goni, R., A. Quetglas, and O. Reñones.
2006. Spillover of spiny lobsters *Palinurus elephas* from a marine reserve to an adjoining fishery. Mar. Ecol. Prog. Ser. 308:207–219.

Halpern, B. S.
2003. The impact of marine reserves: do reserves work and does reserve size matter? Ecol. Appl. 13(1):S117–S137.

Kaunda-Arara, B., and G. A. Rose.
2004. Out-migration of tagged fishes from marine reef National Parks to fisheries in coastal Kenya. Environ. Biol. Fishes 70:363–372.

Kelly, S., and A. B. MacDiarmid.
2003. Movement patterns of mature spiny lobsters, *Jasus edwadsii*, from a marine reserve. N. Z. J. Mar. Freshw. Res. 37:149–158.

Kramer, D. L., and M. R. Chapman.
1999. Implications of fish home range size and relocation for marine reserve function. Environ. Biol. Fishes 55:65–79.

McClanahan, T. R., and N. A. J. Graham.
2005. Recovery trajectories of coral reef fish assemblages within Kenyan marine protected areas. Mar. Ecol. Prog. Ser. 294:241–248.

Medley, P. A., G. Guadian, and S. Wells.
1993. Coral reef fisheries stock assessment. Rev. Fish Biol. Fish. 3:242–285.

Meyer, C. G., and K. N. Holland.
2005. Movement patterns, home range size and habitat utilization of the bluespine unicornfish, *Naso unicornis* (Acanthuridae) in a Hawaiian marine reserve. Environ. Biol. Fishes 73:201–210.

Meyer, C. G., K. N. Holland, B. M. Wetherbee, and C. G. Lowe.
2000. Movement patterns, habitat utilization, home range size and site fidelity of whitesaddle goatfish, *Parupeneus porphyreus*, in a marine reserve. Environ. Biol. Fishes 59:235–242.

Mosquera, I., I. M. Côté, S. Jennings, and J. D. Reynolds.
2000. Conservation benefits of marine reserves for fish populations. Anim. Conserv. 4:321–332.

Roberts, C. M.
1995. Rapid buildup of fish biomass in a Caribbean marine reserve. Conserv. Biol. 9: 815–826.

Roberts, C. M., J. A. Bohnsack, F. Gell, J. P. Hawkins, and R. Goodridge.
2001. Effects of marine reserves on adjacent fisheries. Science 294:1920–1923.

Roberts, C. M., and J. Hawkins
1997. How small can a marine reserve be and still be effective? Coral Reefs 16:150.

Russ, G. R.
1991. Coral reef fisheries: effects and yields. *In* The ecology of fishes on coral reefs (P. F. Sale, ed.), p. 601–635. Academic Press, San Diego, CA.
2002. Yet another review of marine reserves as reef fisheries management tools. *In* Coral reef fishes: dynamics and diversity in a complex ecosystem (P. F. Sale, ed.), p. 421–443. Academic Press, San Diego, CA.

Russ, G. R., and A. C. Alcala.
1996. Do marine reserves export adult fish biomass? Evidence from Apo Island, central Philippines. Mar. Ecol. Prog. Ser. 132:1–9.
1999. Management histories of Sumilon and Apo Marine Reserves, Philippines, and their influence on national marine resource policy. Coral Reefs 18:307–319.
2004. Marine reserves: long-term protection is required for full recovery of predatory fish populations. Oecologia 138:622–627.

Sokal, R. R., and F. J. Rohlf.
1995. Biometry: the principles and practice of statistics in biological research, 3rd ed., 887 p. W. H. Freeman and Co., New York, NY.

Tewfik, A., and C. Béné.
2003. Effects of natural barriers on the spillover of

a marine mollusk: implications for fisheries reserves. Aquatic Conserv: Mar. Freshw. Ecosyst. 13:473–488.

Tremain, D. M., C. W. Harnden, and D. H. Adams.
2004. Multidirectional movements of sportfish species between an estuarine no-take zone and surrounding waters of the Indian River Lagoon, Florida. Fish. Bull. 102:533–544

Tupper, M.
2007. Identification of nursery habitats for commercially valuable humphead wrasse (*Cheilinus undulatus*) and large groupers (Pisces: Serranidae) in Palau. Mar. Ecol. Prog. Ser. 332:189–199.

Tupper, M., and F. Juanes.
1999. Effects of a marine reserve on recruitment of grunts (Pisces: Haemulidae) at Barbados, West Indies. Environ. Biol. Fishes 55:53–63.

Tupper, M., and M. A. Rudd.
2002. Species-specific impacts of a small marine reserve on reef fish production and fishing productivity in the Turks and Caicos Islands. Environ. Cons. 29(4):484–492.

Zeller, D. C., S. L. Stoute, and G. R. Russ.
2003. Movements of reef fishes across marine reserve boundaries: effects of manipulating a density gradient. Mar. Ecol. Prog. Ser. 254:269–280.

Species-specific effects of four preservative treatments on oocytes and ovarian material of Atlantic cod (*Gadus morhua*), haddock (*Melanogrammus aeglefinus*), and American plaice (*Hippoglossoides platessoides*)

Nikolai Klibansky

Francis Juanes (contact author)

Email address for F. Juanes: juanes@forwild.umass.edu

Department of Natural Resources Conservation
University of Massachusetts
160 Holdsworth Way
Amherst, Massachusetts 01003

Abstract—The lack of information concerning the preservation of ovarian material of fish species inhibits its standardization of methods for determining fecundity and measuring oocytes. The effects of four preservatives (10% phosphate-buffered formalin, modified Gilson's solution, 70% ethanol, and freezing) on ovarian material weight and oocyte size were quantified for prespawning Atlantic cod (*Gadus morhua*), haddock (*Melanogrammus aeglefinus*), and American plaice (*Hippoglossoides platessoides*). Effects of preservation were similar between Atlantic cod and haddock but different between Atlantic cod and American plaice for nearly all comparisons. Although all treatments affected the weight of ovarian material, freezing caused the most change and formalin caused the least. Such significant species-specific effects should be quantified in the calculation of life history characteristics, such as fecundity, to minimize error. This is one of few studies dedicated to evaluating the effects of preservation on oocytes and ovarian material and is the first to evaluate multiple preservatives on species.

Manuscript submitted 17 October 2006 to the Scientific Editor's Office.

Manuscript approved for publication 5 July 2007 by the Scientific Editor.

Fish. Bull. 105:538–547 (2007).

Because of the weak relationship between spawning stock biomass and stock reproductive potential (Marshall et al., 1998, 2003), stock assessment scientists recommend incorporating basic reproductive biology (such as fecundity) into estimates of stock reproductive potential. Estimating fecundity and other reproductive biological parameters often requires oocytes or ovarian material, preserved chemically or by freezing. Ovaries can sometimes be weighed fresh, but often, as when they are collected aboard ships where special marine scales are not available, they must be preserved until they are weighed in the laboratory.

Common preservatives can affect the size and weight of oocytes differently among species. Formalin can increase the mean diameter of catfish eggs by 4–11% (Tan-Fermin, 1991), and the mean diameter of cod eggs by 3.5% (Svaasand et al., 1996), but does not affect the weight of salmon eggs (Fleming and Ng, 1987). Common preservatives have also been shown to affect oocyte size of the same species differently in different studies. Schaefer and Orange (1956) found that standard Gilson's solution and formalin had the same effect on oocyte diameter of yellowfin (*Neothunnus macropterus*) and skipjack (*Katsuwonus pelamis*). In contrast, Joseph (1963) found the mean diameter of oocytes of these same tuna species preserved in standard Gilson's solution to be 24% smaller than the mean diameter of oocytes preserved in formalin.

To enable accurate comparisons of fecundity information among populations and years, data should be collected and analyzed by a standard method and a standard preservative should be used for storing oocytes and ovarian material. But because little research has been conducted on the effects of preservatives on oocyte size, the selection of a preservative is usually based more on popular use than empirical knowledge—a process that may perpetuate the use of inferior preservatives and unnecessary toxins. Preservatives that have been used in past fecundity research may be adequate for determining fecundity but may not preserve ovarian material well enough for related analyses, particularly histology.

The three most commonly employed chemical treatments for ovarian material are 10% buffered formalin (3.7% formaldehyde), standard Gilson's solution, and freezing. Formalin and freezing are best used for short-term preservation (up to two years) of ovarian material; however, formalin is ideally employed as a fixative. Standard Gilson's solution also preserves ovarian material but was developed to dissolve the interstitial material that holds oocytes together

Table 1

Summary information for all Atlantic cod (*Gadus morhua*), haddock (*Melanogrammus aeglefinus*), and American plaice (*Hippoglossoides platessoides*) sampled on Georges Bank (GB) and in the Gulf of Maine (GOM). Maturity stage is based on Tomkiewicz et al. (2003a). Month = month of sampling; Jan = January, Feb = February, Mar = March, etc. n = number of individuals sampled.

Species	Month	Region	Spawning season (peak)	Maturity stage	n
Atlantic cod	Feb 04	GB	Nov–May (Feb–Mar)	Ripening, stage IV	19
Haddock	Feb 04	GB	Jan–May (Mar–Apr)	Ripening, stage IV	16
Atlantic cod	May 04	GOM	Nov–May (Mar–May)	Ripening, stage IV	23
American plaice	May 04	GOM	Feb–Jun (Apr–May)	Ripening, stage IV	16

so they could then be counted and measured more easily (Simpson, 1951).

In this analysis, the effects of four preservatives on ovarian material weight and oocyte diameter of three species of commercially important Northwest Atlantic groundfish are evaluated. The preservatives are formalin (0.037 formaldehyde, 0.015 methyl alcohol, <0.01 sodium phosphate dibasic, <0.01 sodium phosphate monobasic, 0.93 deionized water), modified Gilson's solution (0.10 60% ethanol, 0.015 nitric acid, 0.008 glacial acetic acid, 0.88 distilled water), 70% ethanol, and freezing and are hereafter referred to simply as formalin, Gilson's, ethanol, and freezing. The three species used in this project included two gadids, Atlantic cod (*Gadus morhua*) and haddock (*Melanogrammus aeglefinus*), and one pleuronectid, American plaice (*Hippoglossoides platessoides*). These species are hereafter referred to as cod, haddock, and plaice. All are historically important groundfish species in the Northwest Atlantic that have been reduced to low numbers over the past century (Boreman et al., 1997) and are now managed together in the Northeast multispecies fishery. Reproductive biology and ecology are similar among these species: they are all iteroparous, determinate, batch spawners exhibiting group-synchronous ovarian organization (Murua and Saborido-Rey, 2003). Although data are abundant for these species on many characteristics used to predict stock reproductive potential, such as maturity and sex-ratio, data on fecundity and oocyte size remain very limited (Tomkiewicz et al., 2003b).

Materials and methods

Ovary collection

All ovarian specimens were taken from fish caught in bottom trawls in the Northwest Atlantic during peak spawning (Table 1). In February 2004 the ovaries of 19 ripening (classified as stage IV by the maturity key developed by Tomkiewicz et al. [2003a]) cod and 16 haddock were collected by bottom trawling in the western portion of Georges Bank (GB). In May 2004 the ovaries of 23 ripening cod and 16 ripening plaice were collected by bottom trawling in the inshore waters of the Gulf of Maine (GOM).

Preservation and measurement

For all specimens collected on GB (cod and haddock), fresh weight of the left ovary was measured at sea, to the nearest 1.0 g, with a Marel marine balance (Marel Food Systems, Gardabaer, Iceland). These ovaries were then preserved in formalin. Specimens collected in the GOM (cod and plaice) could not be weighed at sea and therefore were packed in ice until they could be weighed to the nearest 0.001 g in the laboratory 24 hours later. The left ovarian lobes of 17 cod caught in the GOM were reweighed after 48 hours on ice to determine if time on ice affected ovary weight.

Within minutes of weighing, the entire left lobe of most specimens was placed in a 1-L jar containing a volume of formalin approximately equal to four times the volume of the ovary. When the left lobe was too large (>250 g) to fit through the opening of the jar, a large portion weighing 250 g or less was cut off and weighed and preserved as above. These whole lobes and lobe portions of ovarian material remained in formalin for 158–175 (mean=169) days and were then reweighed to the nearest 0.001 g. These are hereafter referred to as lobe-formalin samples.

From the center of the right ovary of each fish, four 1.5-mL subsamples of ovarian material (i.e., one subsample per fish for each of four treatments: formalin, Gilson's, ethanol, and freezing) almost entirely comprising vitellogenic oocytes, were removed with a 3-mL plastic syringe tube, the end of which was cut off at the zero mark. The collection of subsamples from fresh ovaries in this way was very easy, gave no evidence of damaged oocytes, and repeatedly produced subsamples with a mean of 1.54 g (n=155, coefficient of variation [CV]=3.70). Across fish species, differences in oocyte size and density within and between left and right ovarian lobes are uncommon (West, 1990), and oocyte size tends not to vary among different locations in cod ovaries (Kjesbu and Holm, 1994). Still, in this study ovarian material was always taken from the same part of each ovary in order to ensure that subsamples of oocytes removed from the same localized population of oocytes all had the same mean size and density. Each of these subsamples was then preserved in one of four ways, such that one subsample from each fish was placed in each treatment (i.e., one replicate per fish within a treatment). Only subsamples from specimens collected in May in the GOM (i.e., 23 cod and all 16 plaice) were weighed to the nearest 0.001 g before preservation.

In the formalin treatment (termed the sub-formalin treatment in weight comparisons to distinguish it from the lobe-formalin treatment), a subsample of ovarian material was placed in a vial (10-mL plastic vial with screw cap) containing 5 mL of formalin. Similarly in the Gilson's treatment, a subsample of ovarian material was placed in a vial containing 5 mL of modified Gilson's solution. This modified form of Gilson's solution was employed because it does not contain mercuric chloride, and is thus not toxic, but still effectively preserves and separates oocytes (Friedland et al., 2005). These samples were capped and shaken to ensure oocytes were all thoroughly immersed in the preservative, and were then stored upright in a rack at room temperature. In the ethanol treatment, a subsample of ovarian material was placed in a vial and immersed in 4 mL of 95% ethanol for approximately 15 seconds, before 1.5 mL of distilled water was added to the sample through a graduated pipette, before the solution was diluted to 70% ethanol. Samples in this treatment were also shaken and stored at room temperature. Briefly submerging the material in 95% ethanol is meant to act as a fixative, whereas 70% ethanol is better for long-term preservation (Black and Dodson, 2003). In the freezing treatment a subsample of ovarian material was immersed in a vial of distilled water. Because of our concern that the expansion with freezing too much water might crack the vials, 3 mL of water was used rather than 5 mL as in the other treatments. These samples were also shaken, but then placed (upright) in the freezer so that the ovarian material would be frozen solid in ice. The samples were frozen in this way to preserve the shape of the oocytes and to stop them from drying out or becoming freezer damaged.

Subsamples that were weighed fresh (i.e., those collected in May) were reweighed after 97–111 (mean=102) days of preservation and then returned to their preservative vials. To weigh a preserved subsample, the entire content of a vial was poured into a 40-μ mesh, nylon cell-strainer fitted atop a hand operated vacuum pump. Excess fluid was then removed from each sample by repeatedly squeezing the handle of the hand pump until preserved ovarian material was all that remained in the strainer. The strainer and its contents were then weighed to the nearest 0.001 g, and the known weight of the strainer was subtracted to find the preserved subsample weight.

In addition to the four treatments mentioned above, a fifth split-formalin treatment (so termed because preservation was split into two phases described below) was used for the left ovarian lobes. After 91–131 (mean=111) days of preservation in formalin, each left lobe was removed from its jar and a 1.5-mL subsample was removed from its center and placed in a vial containing 5 mL of formalin. Because they were not preweighed, these subsamples were used only for examining preservative effects on oocyte size. These subsamples remained in vials for another 33–92 (mean=63) days before they were analyzed. Including the total time that split-formalin samples were preserved, the time that samples from all treatments were preserved was 117–164 (mean=145) days before the mean oocyte diameter of each sample was estimated.

The method used here for measuring oocytes is largely based on the work of Thorsen and Kjesbu (2001) but is described here because of differences in details. To start, a vial was shaken vigorously for 30–60 seconds to break apart any oocytes still connected. Samples in modified Gilson's solution did not require shaking because the oocytes were already chemically separated. Most other samples broke apart very well from this shaking, especially those with larger oocytes. Samples in ethanol and samples containing the smallest oocytes were more difficult to break apart and required more shaking. After the vial was shaken, a transfer pipette was used to agitate the oocytes by the action of drawing in and expelling the solution rapidly, so that all oocytes were effectively mixed randomly in suspension and would not settle out by size. While the suspension was being agitated, a portion of the vial's contents was drawn and quickly emptied into a Petri dish containing ≈2 mm of the respective preservative and a drop of 5% Palmolive soap solution which helped the oocytes spread out in the dish and kept them from floating. Oocytes were then added to the Petri dish until the bottom of the dish was filled but so that the oocytes could still be spread out without clumping. A black lid was then placed on the dish to serve as a contrasting background, and an image of the sample was captured with a flatbed scanner. Each sample was scanned at 1200 dpi in 16-bit gray scale and a contrast setting of 18 with the use of an Epson Perfection 1670 scanner (Epson, Long Beach, CA). The same selection marquis was used for each sample so that all images were exactly the same size: 3688×3671 pixels, within a 12.9 MB uncompressed TIFF file.

Because samples in most treatments were stored at room temperature, no temperature adjustment was needed before they were scanned. For samples in the freezing treatment, however, care was taken to be sure that vials were thawed one hour before they were scanned out of concern that oocyte diameter may be affected by how much time thawed samples were left in water.

Once scanned, each image was analyzed in the freeware program Scion Image (Scion Image, version beta 4.0.2, Scion Corporation, Frederick, MD) by first setting the scale of each image to 1200 pixels per inch (472 pixels per cm), and the measurements to micrometers. The lower limit of the density slice tool was then set to 40 and the upper limit ranged from 180 to 205, and was typically 195. The upper limit varied because the grey value of the oocyte margins varied between samples depending on how dark the oocytes were. The Scion

Image software used those grey values to determine the perimeter of the particles; therefore standardizing the upper limit of the density slice among samples would result in less accurate measurements. Then the "analyze particles" command was run on particles from 150 to 1500 pixels in area. The process was also set to include interior holes and to ignore particles touching the perimeter as the oocytes were measured.

The output of this process produced four columns of data: area, perimeter, major axis length, and minor axis length for each particle. These data were then transferred to a Microsoft Excel spread sheet (Microsoft® Office Excel 2003, Microsoft Corporation, Redmond, WA), where a macro was run to filter out measurements of non-oocytes by accepting only particles within a narrow range of roundess values. The macro then calculated the mean oocyte diameter of each sample, as well as other descriptive statistics, and produced a percent frequency histogram for the sample of roundness-filtered particles.

Ideally all samples would have been analyzed after the same amount of time that they had been preserved, although it was not practical to do so. Thus time (days) preserved was recorded for each sample and the average time that the sample was preserved was compared between groups where appropriate.

Statistical analyses

The preserved weight of a lobe or subsample of ovarian material was compared to its fresh weight. Percent change in weight was calculated with Equation 1:

$$\%\Delta_{Wt} = \left((Wt_{Preserved} - Wt_{Fresh}) / Wt_{Fresh}\right) \times 100, \qquad (1)$$

where $\%\Delta_{Wt}$ = the percent change between $Wt_{Preserved}$ and Wt_{Fresh};
$Wt_{Preserved}$ = preserved weight of a sample of ovarian material; and
Wt_{Fresh} = fresh weight of that sample.

A positive $\%\Delta_{Wt}$ indicated an increase in weight due to preservation.

It was not logistically possible to measure the diameters of fresh oocytes; therefore it was necessary to use one of the preservative treatments as a control treatment. The formalin treatment was chosen for this purpose, because it is a standard preservation method and thus was expected to have the most consistent effect on oocyte size. In this experiment, the other four treatments (Gilson's, ethanol, freezing, and split-formalin) were considered experimental treatments. Change in mean oocyte diameter due to preservation in the experimental treatments was quantified by using Equation 2:

$$\%\Delta_{OD} = \left((OD_{Experimental} - OD_{Control}) / OD_{Control}\right) \times 100, \qquad (2)$$

where $\%\Delta_{OD}$ = the percent difference in mean oocyte diameter between $OD_{Experimental}$ and $OD_{Control}$;
$OD_{Experimental}$ = the mean oocyte diameter of a subsample of an ovary preserved in one of the four experimental treatments; and
$OD_{Control}$ = the mean oocyte diameter of a subsample of the same ovary preserved in the formalin treatment.

A positive $\%\Delta_{OD}$ indicates that the mean oocyte diameter of a subsample in the experimental treatment is larger than in the formalin treatment.

For examining $\%\Delta_{Wt}$ and $\%\Delta_{OD}$, samples were grouped by experimental treatment within species, and then in the case of cod where samples were collected from two regions, the samples were further grouped by region. *T*-tests were conducted within these groups to test the null hypothesis (H_0) that $\%\Delta = 0$ for each experimental treatment. Assessment of normality of each group by examining boxplots and histograms indicated that data did not require transformation. Statistical analyses were performed with SAS (version 9.1, SAS Institute Inc., Cary, NC). Each test had $n_1 + n_2 - 2$ degrees of freedom (Tables 2 and 3) where n_1 and n_2 were the total numbers of observations from each group. Where t-tests were conducted in groups, significance (α) levels were adjusted by the sequential Bonferroni procedure (Quinn and Keough, 2002), to minimize family-wise type-I error rate.

When a significant difference in $\%\Delta_{OD}$ was found between two groups, time preserved was investigated as a confounding factor, although any major change in oocyte size due to preservation typically happens within one day (Kjesbu et al., 1990). A *t*-test of time preserved between the groups was conducted in which the ratio of time preserved in experimental treatment to time preserved in control treatment was used as a metric of time preserved, because the calculation for $\%\Delta_{OD}$ includes $OD_{Control}$ in the denominator (see Eq. 2). If no significant difference was found, we concluded that the difference in $\%\Delta_{OD}$ was not due to time preserved. If a significant difference was found, a one-tailed *t*-test of $\%\Delta_{OD}$ between these groups was conducted. Assuming that the sign of the slope of the relationship between time preserved and oocyte diameter is constant after the initial changes that occur within days of preservation, the group with a higher time preserved value should have exhibited a greater $|\%\Delta_{OD}|$. Thus the H_0 for each one-tailed *t*-test was: $|\text{mean } \%\Delta_{OD}|$ of group preserved for more time $\leq$ $|\text{mean } \%\Delta_{OD}|$ of group preserved for less time. If this analysis implicated time preserved as a likely cause of a significant difference in $\%\Delta_{OD}$, then the effect of the experimental treatment would be considered confounded.

In situations where there was a significant difference in $\%\Delta_{OD}$ and time preserved, but the sign of $\%\Delta_{OD}$ was different between the groups, no such test was performed. Instead it was concluded that the difference in $\%\Delta_{OD}$ was not due to time preserved, based on the assumption that the sign of the slope of the relationship between time preserved and oocyte diameter is constant.

Table 2

The effects of method and treatment on ovary weight among the species Atlantic cod (*Gadus morhua*), haddock (*Melanogrammus aeglefinus*), and American plaice (*Hippoglossoides platessoides*), within the region Georges Bank (GB), the Gulf of Maine (GOM) or within both regions combined (Combined), and between regions for Atlantic cod. *T*-tests compare percent change in fresh weight among species within each treatment group. The methods column designates whether ovaries were used as 1.5-mL subsamples (Sub) or as entire lobes (Lobe). df = degrees of freedom, t = t-statistic, * = statistically significant at the appropriate Bonferroni adjusted α-value.

Species	Method	Region	Treatment	t	df	P-value	α-value[1]
Atlantic cod	Sub	GOM	Formalin	−0.24	38	0.81	0.05
American plaice	Sub	GOM	Gilson's	3.05	37	0.0042*	0.025
			Ethanol	−9.61	37	<0.001*	0.013
			Freezing	7.47	32	<0.001*	0.017
Atlantic cod	Lobe	GB	Formalin	−3.73	40	<0.001*	0.05
Atlantic cod	Lobe	GOM					
Atlantic cod	Sub	GOM	Formalin	6.06	44	<0.001*	0.05
Atlantic cod	Lobe	GOM					
Atlantic cod	Lobe	GB	Formalin	−1.19	36	0.24	0.05
Haddock	Lobe	GB					
Atlantic cod	Lobe	Combined	Formalin	1.33	59	0.19	0.05
Haddock	Lobe	GB					

[1] α-values lower than 0.05 were adjusted by the sequential Bonferroni procedure for multiple comparisons (Quinn and Keough, 2002).

Similar analyses were conducted when a significant difference in $\%\Delta_{Wt}$ was identified between two groups. For these comparisons, however, days preserved was used as the metric of time preserved, since fresh weights were taken for all these samples.

Results

Effect of preservation on weight of ovarian material

All four experimental treatments had significant effects on subsample weight for cod and plaice (Fig. 1), except for plaice samples in the freezing treatment (P=0.12), which also had the highest standard error (SE) of $\%\Delta_{Wt}$ (SE=4.93). For cod, standard error of $\%\Delta_{Wt}$ was also highest in the freezing treatment (SE=3.37) along with mean $\%\Delta_{Wt}$ (mean=51.32). Mean $\%\Delta_{Wt}$ was lowest for cod in the ethanol treatment (mean=−4.21) but highest for plaice (mean=25.3). In the lobe-formalin treatment there was a significant difference in $\%\Delta_{Wt}$ for GB cod (P=0.036), GOM cod (P<0.001), all cod combined (P<0.001), and haddock (P=0.002). These data were not available for plaice.

Mean $\%\Delta_{Wt}$ was not significantly different between cod and haddock in the lobe-formalin treatment regardless of whether haddock was compared with cod samples restricted to GB (P=0.24, α=0.03) or when all cod were combined (P=0.28, α=0.05). Mean $\%\Delta_{Wt}$ of subsamples was significantly different between cod and plaice for the ethanol (P<0.001), freezing (P<0.001), and Gilson's (P=0.0042) treatments (Table 2). There was no difference in $\%\Delta_{Wt}$ between cod and plaice in the subformalin treatment (P=0.81). This test marks the only comparison between cod and plaice where no difference was found. There was a significant difference in mean $\%\Delta_{Wt}$ (P<0.001) for cod between GB (mean=1.41) and the GOM (mean=6.79) in the lobe-formalin treatment. For cod from the GOM, there was a significant (P<0.001) and nearly threefold difference in mean $\%\Delta_{Wt}$ between lobe-formalin (mean=6.79) and sub-formalin (mean=19.32) treatments.

For the 17 ovaries collected from cod caught in the GOM, all of which were weighed after 24 and then 48 hours on ice (fresh weights were not available), mean percent change in weight during this interval was significantly different from zero (P=0.02). However this change was very slight (mean=−0.32, SE=0.11).

Effect of preservation on oocyte diameter

Oocyte diameter in the experimental treatment was significantly different from that of the control treatment (Fig. 2), in all but three comparisons. Significant differences were not detected for plaice (P=0.22) in the ethanol treatment or for GB cod (P=0.59) or haddock (P=0.37) in the split-formalin treatment. Of the four experimental treatments, the freezing treatment produced the highest mean $\%\Delta_{OD}$ for GB cod (mean=18.81), GOM cod (mean=26.99), GB and GOM cod combined (mean=23.29), and haddock (mean=28.88). Plaice samples in the freezing treatment also exhibited a significant positive change (P<0.001, mean=9.90), but a larger change was exhibited in the Gilson's treatment

Table 3

The effects of experimental treatment (Gilson's, ethanol, freezing, and split-formalin) on oocyte diameter among the species Atlantic cod (*Gadus morhua*), haddock (*Melanogrammus aeglefinus*), and American plaice (*Hippoglossoides platessoides*) within the regions of Georges Bank (GB), the Gulf of Maine (GOM), or within both regions combined (Combined), and between regions for Atlantic cod. *T*-tests were used to compare mean percent difference[1] in oocyte diameter between experimental and control (formalin) treatments among species. t = t-statistic, df = degrees of freedom, * = statistically significant at the appropriate Bonferroni adjusted α-value.

Species	Region	Treatment	t	df	P-value	α-value[2]
Atlantic cod	GB	Gilson's	5.19	40	<0.001*	0.013
Atlantic cod	GOM	Ethanol	–1.79	40	0.082	0.05
		Freezing	–3.91	37	<0.001*	0.025
		Split-Formalin	–4.21	39	0.001*	0.017
Atlantic cod	GB	Gilson's	2.49	33	0.018	0.017
Haddock	GB	Ethanol	–2.09	33	0.045	0.025
		Freezing	–2.62	33	0.013	0.013
		Split-Formalin	–1.11	32	0.28	0.05
Atlantic cod	Combined	Gilson's	0.36	56	0.72	0.05
Haddock	GB	Ethanol	–1.75	56	0.085	0.017
		Freezing	–1.92	53	0.06	0.013
		Split-Formalin	0.72	54	0.48	0.025
Atlantic cod	GOM	Gilson's	2.84	37	0.0073*	0.05
American plaice	GOM	Ethanol	–5.39	37	<0.001*	0.017
		Freezing	11.40	32	<0.001*	0.013
		Split-Formalin	3.41	36	0.002*	0.025
Atlantic cod	Combined	Gilson's	4.33	56	<0.001*	0.013
American plaice	GOM	Ethanol	–5.74	56	<0.001*	0.025
		Freezing	6.18	51	<0.001*	0.017
		Split-Formalin	2.98	55	0.0043*	0.05

[1] Defined by the following: (*TreatmentDiameter–FormalinDiameter*) × 100), where *TreatmentDiameter* = the mean oocyte diameter of a subsample of an ovary preserved in one of the experimental treatments and *FormalinDiameter* = the mean oocyte diameter of a subsample of the same ovary preserved in the formalin treatment.

[2] α-values lower than 0.05 were adjusted by the sequential Bonferroni procedure for multiple comparisons (Quinn and Keough, 2002).

(mean=–18.43). Of the four experimental treatments, the split-formalin treatment produced the smallest mean $\%\Delta_{OD}$ for GB cod (mean=–0.31), GOM cod (mean=2.90), GB and GOM cod combined (mean=1.41), and haddock (mean=0.77). Plaice samples in the split-formalin treatment also exhibited only a small change (mean=–2.59), but the smallest change (mean=0.94) was in the ethanol treatment.

Mean $\%\Delta_{OD}$ was not significantly different between cod and haddock for any treatment (Table 3), regardless of whether haddock samples were compared with cod samples restricted to GB or when cod from GB and GOM were combined. Mean $\%\Delta_{OD}$ was significantly different between cod and plaice for all treatments, also regardless of whether cod samples were restricted to GB or when all cod were combined. There was a significant difference in mean $\%\Delta_{OD}$ for cod from GB and cod from the GOM in the Gilson's ($P<0.001$, $\alpha=0.013$), freezing ($P<0.001$, $\alpha=0.025$), and split-formalin ($P=0.001$, $\alpha=0.017$) treatments, but not the ethanol treatment ($P=0.08$, $\alpha=0.05$).

In the comparison between lobe-formalin and subformalin samples, analyses showed time preserved could not have caused the difference in preserved weight between these groups. Although significant differences in $\%\Delta_{Wt}$ of subsamples were detected between cod and plaice in the Gilson's, ethanol, and freezing treatments, time preserved between species was consistent for all treatments.

There were only five comparisons where it was appropriate to investigate time preserved as a possible cause for differences in $\%\Delta_{OD}$ between two groups. These comparisons were the following: cod from GB and GOM in the Gilson's, freezing, and split-formalin treatments, and cod (GB and GOM combined) and plaice, in the Gilson's and freezing treatments. The H_0 that mean $\%\Delta_{OD}$ of group preserved longer ≤ mean $\%\Delta_{OD}$ of group preserved shorter was only rejected in the comparison between cod (GM and GOM combined) and plaice in the freezing treatment ($P<0.001$).

For four haddock samples in the freezing treatment, mean oocyte diameter was measured immediately after the sample was freshly thawed, and then again after 48 hours of refrigeration. Mean oocyte diameter of the samples decreased by 3–10% after refrigeration, although the average decrease of 4.4% was not significantly different from zero ($P=0.11$), perhaps because of the small sample size.

Discussion

Of the preservatives tested in this study, the results with formalin were most similar among individuals and species, and the results from freezing were the least consistent among individuals within and among species. In terms of image quality, samples preserved in formalin were clearest and contained the least debris. In weight comparisons between cod and plaice, the subformalin treatment was the only one where no significant difference between the two species was found. Of the tested preservatives, the best option for a standard preservative was formalin, especially when samples might be used for histology, where postovulatory follicles and fine cellular structures must be preserved.

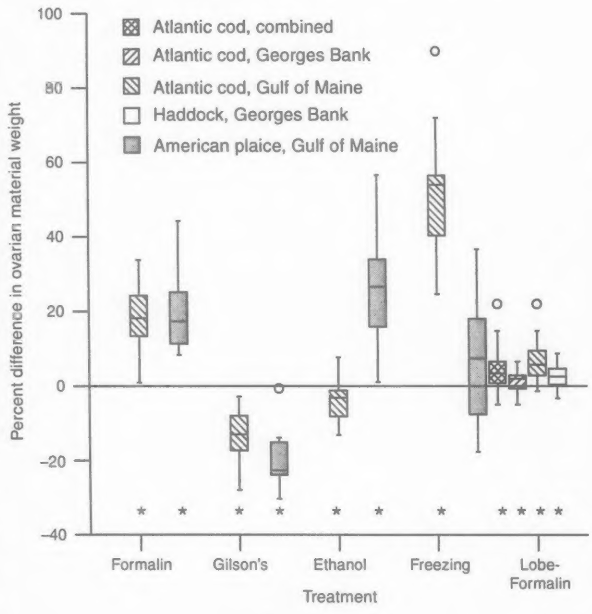

Figure 1

Percent difference in ovarian material weight (%Δ_{Wt}) for each species (Atlantic cod [*Gadus morhua*]), haddock [*Melanogrammus aeglefinus*], and American plaice [*Hippoglossoides platessoides*]) and region, grouped by treatment. For Atlantic cod, observations are displayed together in the combined group and are then displayed separately by region (i.e., Georges Bank or the Gulf of Maine). The horizontal line at zero on the vertical axis indicates values where the percent difference in weight between preserved and fresh ovarian material was equal to zero. Circles indicate outliers. Asterisks indicate that mean %Δ_{Wt} was significantly different from zero at the appropriate Bonferroni adjusted α-value. Box length is equal to the interquartile range which contains the central 50% of the observations (25% above and below the median). Whiskers extend 1.5 box-lengths above and below the limits of the box.

When realized fecundity is estimated from total potential fecundity, estimates may be biased if samples are collected too late in the season and spawning has already begun, or if atresia is likely to occur between sampling and the time of spawning. Both of these biases are quantified through histological analysis. In species or stocks where the developing stage is difficult to identify or where high rates of atresia are expected, histological analysis is necessary to assure that estimates of realized fecundity are accurate. Although Gilson's solution and ethanol may be used for fecundity research and may be superior in certain situations for particular species, they do not preserve tissue well enough for histological analysis, and thus they are undesirable in many situations.

Formalin is a common preservative for ovarian material and is widely used to fix and preserve animal tissue. Although our results show differences between formalin samples and Gilson's and frozen samples that contrast with results of studies on other species, the effects of formalin preservation were very consistent among the species we studied. Formalin preservation resulted in an increase in sample weight in all species, and when compared between species these changes were similar.

The differences between the formalin and split-formalin treatments for all species (Fig. 2), although significant for GB and GOM cod combined, GOM cod, and plaice, were quite small and therefore indicated that formalin preserves oocyte size similarly whether ovarian material is in large membrane-bound lobes or in 1.5-mL subsamples. However, the large and significant difference in %Δ_{Wt} of samples of GOM cod ovarian material between the lobe-formalin and subformalin treatments indicates a conflict because oocyte diameter and ovarian material weight are inherently related. If ovarian material weight increases much more in one treatment than another, oocyte size should as well. The reason for this disagreement may lie in the fact that after subsamples in the split-formalin treatment were removed from whole preserved lobes, they were preserved as subsamples for several weeks before the oocytes were measured. During that time, swelling that was inhibited by the dense packing of oocytes in the ovarian lobe may have occurred; therefore by the time they were measured, oocytes were very similar in size to those preserved in the sub-formalin treatment.

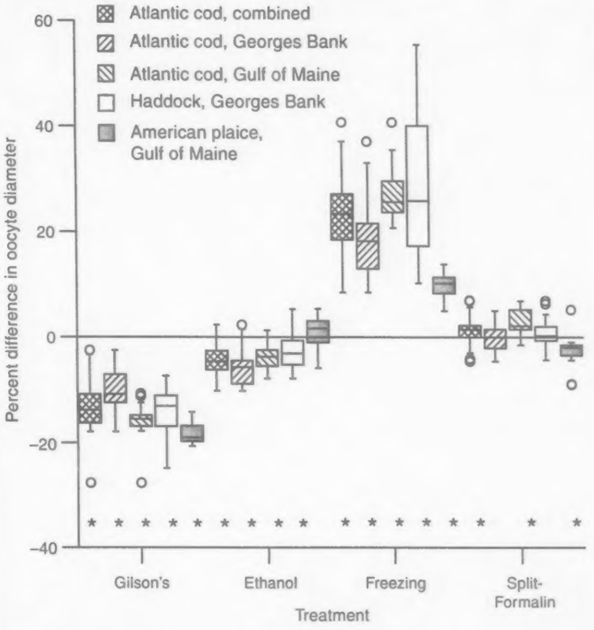

Figure 2

Percent difference in mean oocyte diameter ($\%\Delta_{OD}$) for each species (Atlantic cod [*Gadus morhua*], haddock [*Melanogrammus aeglefinus*], and American plaice [*Hippoglossoides platessoides*]) and region, grouped by treatment. For Atlantic cod, observations are displayed together in the combined group and are then displayed separately by region (i.e., Georges Bank or the Gulf of Maine). The horizontal line at zero on the vertical axis indicates values where the $\%\Delta_{OD}$ between experimental treatments and the control treatment (formalin) was equal to zero. Circles indicate outliers. Asterisks indicate mean $\%\Delta_{OD}$ was significantly different from zero at the appropriate Bonferroni adjusted α-value. Box length is equal to the interquartile range containing the central 50% of the observations (25% above and below the median). Whiskers extend 1.5 box-lengths above and below the box.

Standard Gilson's solution has been a common oocyte preservative since it was developed. Joseph (1963) found that tuna oocytes preserved in standard Gilson's solution were 24% smaller than those preserved in 4% formalin. In contrast Schaefer and Orange (1956) concluded that mean diameters of oocytes from the same tuna species, preserved in standard Gilson's solution and formalin (concentration not specified) were similar, although they did not present statistical evidence to support this conclusion. Cod, haddock, and plaice oocytes preserved in modified Gilson's solution were 13.28%, 13.77%, and 18.43% smaller, respectively, than those preserved in 10% formalin. These results were all significant, and are similar to Joseph's (1963) results. The discrepancy between our results and those of Joseph (1963) could be attributed to interspecies variation. Although differences were identified, we consider the effects of modified Gilson's solution to be fairly consistent among species.

Ethanol is rarely used to preserve ovarian material used in fecundity studies, but because Black and Dodson (2003) used ethanol to successfully fix and preserve water fleas (*Daphnia pulex*) and their eggs, and ethanol caused less distortion and change in body size than a solution of sucrose and 4% formalin, it was evaluated in this study. Oocytes preserved in this treatment were of sufficient quality for use in digital image analysis. Ethanol also had a bleaching effect on oocytes, which resulted in greater contrast between oocytes and the black background. The ethanol treatment tended to cause smaller changes to oocyte size and ovarian material weight than other treatments, except for the large increase in subsample weight in plaice. In ethanol, $\%\Delta_{Wt}$ was negative for cod, $\%\Delta_{OD}$ was negative for cod and haddock, and both were positive for plaice. Such results make it difficult to generalize about the effects of ethanol on ovarian material across taxa and may make this treatment less desirable than others.

Freezing is one of the most common methods of ovary preservation, but this treatment has not been used to preserve oocytes for digital image analysis. Although freezing was expected to result in many ruptured oocytes, oocytes in the frozen treatment maintained a very round shape and rarely broke even after vigorous shaking and agitation. Freezing the oocytes solid in distilled water may have improved the ultimate quality of the samples by limiting the exposure of oocytes to the oxidizing and desiccating effects of air. Although the quality of the images obtained from these samples was high enough for measurement and counting, percent change in ovarian material weight and oocyte diameter of frozen specimens proved to be very variable and often very high (Figs. 1 and 2).

Although the mean diameter of cod, haddock, and plaice oocytes preserved in the freezing treatment was 23.29%, 28.88%, and 9.90% larger, respectively, than the mean diameter of oocytes in the formalin treatment, Ramon and Bartoo (1997) found that the mean diameter of tuna eggs in 10% buffered formalin was generally 5–10% larger than the mean diameter of oocytes from frozen ovaries. It may not be surprising to find a difference between the species we studied and the tunas, but such a substantial difference showing an opposite trend is somewhat surprising and is probably largely due to the difference in freezing methods. Although freezing ovarian material in water may improve the quality of the preserved oocytes, it is probably responsible for the large and variable changes that we observed. Because ovarian material is placed in hypotonic distilled water, it will absorb the water, thus increasing the size and weight of the oocytes. If it takes a long time for ovarian material in water to become isotonic, the material may not be osmotically stable by the time it is frozen and even by the time the oocytes are measured, which could cause the observed changes and variation in size and weight. In future research ovarian material should be frozen in an isotonic solution to prevent oocytes from swelling.

The initial reason ovary samples were preserved in a variety of treatments was to determine if oocytes preserved by these methods could be used in digital image analysis. The only studies we are aware of that employ digital image analysis to count and measure fish oocytes preserve them in either formalin (Thorsen and Kjesbu, 2001; Yoneda and Wright, 2004) or modified Gilson's solution (Friedland et al., 2005). All treatments in our study preserved ovarian material of cod, haddock, and plaice well enough to permit easy identifcation and measurements of oocytes. Clumping was a factor for many samples in all but the Gilson's treatment, but most clumps could be broken up well by shaking the vial for 30–60 seconds. Very tight clumps could be broken apart by rapidly drawing in and expelling oocytes and solution for 30–120 seconds with a 10-mL glass pipette with an ~1 mm diameter and a plastic, thumb-wheel pipette pump. A glass pipette worked better than a plastic transfer pipette, probably because its rigidity allows more suction to be created as fluid is quickly drawn into it. With simple, albeit occasionally time-consuming (up to five minutes) mechanical separation, all clumps could be sufficiently broken up so that the oocytes could be measured and counted.

Considering all comparisons for all three species, cod and haddock oocytes and ovarian material are affected similarly by a given type of preservative, whereas effect on plaice tends to differ with different preservatives. This is not unexpected because cod and haddock are in the same family, Gadidae, whereas the narrowest taxonomic group common to cod and plaice is the subdivision Euteleostei. One would expect tissues of closely related species would have similar chemical properties, and should thus be affected similarly by preservatives. Although it could be inferred from results among studies that differences in preservation exist among fish species, specific differences have not been reported before the present study.

A difference in the effect of preservation between cod samples from GB and those from GOM is also reported. This difference is unexpected but is supported by the results of comparisons of oocyte size in the Gilson's, freezing, and split-formalin treatments, and by the comparison of ovarian material weight in the lobe-formalin treatment. Samples from GB were collected in February, whereas samples from the GOM were collected in May, which may somehow contribute to this difference. Still, it is unclear why time of year or region of sample collection would affect preservation and we suggest this as an area worthy of future research.

We successfully evaluated and quantified the effects of several preservatives on the ovarian material of several fish species, but perhaps more importantly we demonstrated how preservation can add variation to seemingly simple measurements like ovary weight and oocyte size, and can have different effects between species. Thus we stress the importance of consistent experimental methods and suggest that in studies of preserved ovarian material it should not be assumed that the effects of different preservatives and preservation treatments are consistent.

Acknowledgments

We thank R. Brown, J. Ford, R. Sherman, B. Hoffman, M. Russo and T. Ligenza for providing us with access to ovary samples. We also thank K. Friedland, E. Garcia-Vazquez, O. S. Kjesbu, two anonymous reviewers, A. Moles, and E. Calvert for their suggestions and comments. Funding for this study was provided through the Cooperative Marine Education and Research Program (CMER) at the University of Massachusetts, Amherst and a Hatch grant. Writing was completed while F. Juanes was a Center Fellow at the National Center for Ecological Analysis and Synthesis, funded by NSF (Grant #DEB-0553768), the University of California, Santa Barbara, and the State of California.

Literature cited

Black, R., and S. I. Dodson.
2003. Ethanol: a better preservation technique for *Daphnia*. Limnol. Oceanogr. Methods. 1:45–50.

Boreman, J. L., B. S. Nakashima, J. A. Wilson, and R. L. Kendall.
1997. Northwest Atlantic groundfish: perspectives on a fishery collapse, 242 p. Am. Fish. Soc., Bethesda, MD.

Fleming, I. A., and S. Ng.
1987. Evaluation of techniques for fixing, preserving and measuring salmon eggs. Can. J. Fish. Aquat. Sci. 44:1957–1962.

Friedland, K. D., D. Ama-Abasi, M. Manning, L. Clarke, G. Kligys, and R. C. Chambers.
2005. Automated egg counting and sizing from scanned images: Rapid sample processing and large data volumes for fecundity estimates. J. Sea Res. 54:307–316.

Joseph, J.
1963. Fecundity of yellowfin tuna (*Thunnus albacares*) and skipjack (*Katsuwonus pelamis*) from the eastern Pacific Ocean. Inter-Am. Trop. Tuna Comm. Bull. 7:255–292.

Kjesbu, O. S., and J. C. Holm.
1994. Oocyte recruitment in first-time spawning Atlantic

cod (*Gadus morhua*) in relation to feeding regime. Can. J. Fish. Aquat. Sci. 51:1893–1898.

Kjesbu, O. S., P. R. Witthames, P. Solemdal, and M. Greer Walker.
1990. Ovulatory rhythm and a method to determine the stage of spawning in Atlantic cod (*Gadus morhua*). Can. J. Fish. Aquat. Sci. 47:1185–1193.

Marshall, C. T., O. S. Kjesbu, N. A. Yaragina, P. Solemdal, and O. Ulltang.
1998. Is spawner biomass a sensitive measure of the reproductive and recruitment potential of Northeast Arctic cod? Can. J. Fish. Aquat. Sci. 55:1766–1783.

Marshall, C. T., L. O'Brien, J. Tomkiewicz, F. W. Koster, G. Kraus, G. Marteinsdottir, M. J. Morgan, F. Saborido-Rey, J. L. Blanchard, D. H. Secor, P. J. Wright, N. V. Mukhima, and H. Bjornsson.
2003. Developing alternative indices of reproductive potential for use in fisheries management: case studies for stocks spanning an information gradient. J. Northw. Atl. Fish. Sci. 33:161–190.

Murua, H., and F. Saborido-Rey.
2003. Female reproductive strategies of marine fish species of the North Atlantic. J. Northw. Atl. Fish. Sci. 33:23–31.

Quinn, G. P., and M. J. Keough.
2002. Experimental design and data analysis for biologists, 520 p. Cambridge Univ. Press, Cambridge, UK; New York, NY.

Ramon, D., and N. Bartoo.
1997. The effects of formalin and freezing on ovaries of albacore, *Thunnus alalunga*. Fish. Bull. 95:869–872.

Schaefer, M. B., and C. J. Orange.
1956. Studies of the sexual development and spawning of yellowfin tuna (*Neothunnus macropterus*) and skipjack (*Katsuwonas pelamis*) in three areas of the eastern Pacific Ocean, by examination of gonads. Inter-Am. Trop. Tuna Comm. Bull. 1:283–320.

Simpson, A. C.
1951. The fecundity of the plaice. Fish. Invest. II. 17:1–27.

Svaasand, T., K. E. Jorstad, H. Otteraa, and O. S. Kjesbu.
1996. Differences in growth performance between Arcto-Norwegian and Norwegian coastal cod reared under identical conditions. J. Fish Biol. 49:108–119.

Tan-Fermin, J. D.
1991. Suitability of different formalin-containing fixatives for the eggs of freshwater Asian catfish *Clarias macrocephalus* (Gunther). Isr. J. Aquacult.-Bamid. 43:57–61.

Thorsen, A., and O. S. Kjesbu.
2001. A rapid method for estimation of oocyte size and potential fecundity in Atlantic cod using a computer-aided particle analysis system. J. Sea Res. 46:295–308.

Tomkiewicz, J., M. J. Morgan, J. Burnett, and F. Saborido-Rey.
2003b. Available information for estimating reproductive potential of Northwest Atlantic groundfish stocks. J. Northw. Atl. Fish. Sci. 33:1–21.

Tomkiewicz, J., L. Tybjerg, and A. Jespersen.
2003a. Micro- and macroscopic characteristics to stage gonadal maturation of female Baltic cod. J. Fish Biol. 62:253–275.

West, G.
1990. Methods of assessing ovarian development in fishes: a review. Aust. J. Mar. Freshw. Res. 41:199–222.

Yoneda, M., and P. J. Wright.
2004. Temporal and spatial variation in reproductive investment of Atlantic cod *Gadus morhua* in the northern North Sea and Scottish west coast. Mar. Ecol. Prog. Ser. 276:237–248.

Diets of and trophic relationships among dominant marine nekton within the northern California Current ecosystem

Todd W. Miller (contact author)[1]
Richard D. Brodeur[2]
Email address for T. W. Miller: millertw@dpc.ehime-u.ac.jp

[1] Cooperative Institute for Marine Resources Studies
Oregon State University
Newport, Oregon 97365
Present address: Center for Marine Environmental Studies (CMES)
Ehime University, 2-5 Bunkyo-cho, Matsuyama
Ehime, 790-8577, Japan

[2] National Oceanic and Atmospheric Administration
National Marine Fisheries Service, Northwest Fisheries Science Center
Hatfield Marine Science Center
Newport, Oregon 97365

Abstract—In this study we analyzed the diets of 26 nekton species collected from two years (2000 and 2002) off Oregon and northern California to describe dominant nekton trophic groups of the northern California Current (NCC) pelagic ecosystem. We also examined interannual variation in the diets of three nekton species. Cluster analysis of predator diets resulted in nekton trophic groups based on the consumption of copepods, euphausiids, brachyuran larvae, larval-juvenile fishes, and adult nekton. However, many fish within trophic groups consumed prey from multiple trophic levels—euphausiids being the most widely consumed. Comparison of diets between years showed that most variation occurred with changes in the contribution of euphausiids and brachyuran larvae to nekton diets. The importance of euphausiids and other crustacean prey to nekton indicates that omnivory is an important characteristic of the NCC food web; however it may change during periods of lower or higher upwelling and ecosystem production.

Eastern Pacific boundary upwelling zones, such as the California Current, are generally highly productive and support major fisheries, yet these ecosystems also exhibit substantial temporal fluctuations in primary and higher-level production (Francis and Hare, 1994; Carr, 2002; Chavez et al., 2003). This variation has been attributed to variability in abiotic forcing through relatively short-term (interannual) El Niño and La Niña events (Pearcy and Schoener, 1987), as well as long-term (decadal) environmental forcing (Francis and Hare, 1994; Mantua et al., 1997). This apparent link between abiotic forcing and the ecosystem has led to considerable discussion regarding energy flow through large marine ecosystems (Jackson et al., 2001). However, few studies have comprehensively examined multispecies trophic patterns within a system. Understanding trophic patterns and temporal changes between species across multiple trophic groups is essential in understanding energy transfer within a system and mechanisms behind ecosystem stability (Worm and Duffy, 2003).

The northern California Current (NCC) system encompasses the northern region of the California Current production zone (approximately 41–49° N) along the continental shelf and shelf break between northern California and Washington. This system is a major upwelling region, where Pacific sardine (*Sardinops sagax*), northern anchovy (*Engraulis mordax*), jack mackerel (*Trachurus symmetricus*), market squid (*Loligo opalescens*), and Pacific hake (*Merluccius productus*) are the dominant nektonic species (Brodeur and Pearcy, 1986; Brodeur et al., 2005). Between April and September, strong but episodic coastal upwelling is the dominant hydrographic feature of the NCC. This upwelling provides cool nutrient-rich water to the euphotic zone across the shelf (Huyer, 1983), allowing for high levels of primary production (Hood et al., 1991). Interannual variation in coastal upwelling, particularly between El Niño and La Niña events, greatly influences primary production (Corwith and Wheeler, 2002) and higher trophic levels (Ainley et al., 1996). On an interdecadal scale, the California Current also experiences production regimes of 30 years or more, which have been linked to salmon survival (Mantua et al., 1997) and variation in NCC zooplankton biomass (McGowan et al., 1998).

The diets of multiple species within the NCC pelagic ecosystem have been examined in only a few studies, and these studies were mostly performed on single or a few closely related spe-

Manuscript submitted 23 February 2007 to the Scientific Editor's Office.

Manuscript approved for publication 5 July 2007 by the Scientific Editor.

Fish. Bull. 105:548–559 (2007).

cies (e.g., Brodeur and Pearcy, 1990; Robinson, 2000). During the 1980s, Brodeur et al. (1987) analyzed the diets from a diverse assemblage of pelagic nekton from the NCC, but since that time, the NCC system has exhibited major shifts in the abiotic environment and in community composition (Peterson and Schwing, 2003) and a concomitant change in nekton species composition (Emmett and Brodeur, 2000). Observed environmental shifts and changes in the NCC pelagic community are undoubtedly conveyed in-part through trophic interactions. Description of the NCC in the context of the current ocean environment and nekton community is therefore important in determining the mechanisms linking climate change and pelagic ecosystem response. In this study we analyzed the diets of 26 nekton species collected during two separate years (2000 and 2002) from coastal northern California to central Oregon, applied cluster analysis to diet data to delineate trophic groups based on dominant prey taxa, and compared the importance of these prey between the two years for several species.

Materials and methods

Field collections

Nekton were collected for diet analyses from Northeast Pacific Global Ocean Ecosystems Dynamics (GLOBEC) cruises during 29 May–18 June and 29 July–12 August 2000, and 29 May–18 June and 31 July–19 August 2002. Sampling occurred along nine transects across the shelf between Crescent City, CA (41°54′N), and Newport, OR (44°39′N) (for station locations see Brodeur et al. [2004] and Reese and Brodeur [2006]), during daylight hours. At each station, nekton were collected with a Nordic-264 (Nor'Eastern Trawl Systems, Bainbridge Island, WA) rope trawl (30 m wide × 18 m deep) that was towed for 30 minutes. Up to 30 individuals per species were collected per tow for diet analysis. Nekton were immediately frozen on ship (–20°C) after removal from the net and then processed at a later date in the laboratory.

Laboratory analysis

Laboratory processing of nekton involved measurement of individuals and extraction of stomachs for diet analysis. Lengths of fish and squid were measured (±1.0 mm) for either fork length, standard length, or dorsal mantle length. Stomachs were extracted and immediately placed in 10% buffered formalin for 10 days, rinsed with tap water, and transferred to 70% ethanol. Diet analyses were performed by assessing fullness, digestive condition, and identification and quantification of prey taxa in each stomach. Fullness was assessed on a scale of 0–5, with 0 being empty and 5 being distended. Condition of individual digested prey was assessed by using a 0–4 scale, with 0 being unrecognizable and 4 being fresh. Prey taxa were identified to the lowest possible taxon, enumerated, and wet weighed (±0.1 mg) after excess water was removed with blotting paper. When individual prey items were too numerous to enumerate, individual weights were estimated by obtaining the damp weight of a known number of animals and regressing this number on the total weight of the prey. For Pacific sardine, diets comprised large amounts of phytoplankton mixed with small zooplankton and euphausiid eggs that required a subsampling method for diet analysis (Emmett et al., 2005). Chinook salmon (*Oncorhynchus tshawytscha*) were divided into subyearlings, yearlings, and adults, and coho salmon (*O. kisutch*) were separated into yearlings and adults (Brodeur et al., 2004).

Data analysis

Trophic relationships of nekton were examined by using agglomerative hierarchical cluster analysis (AHCA) to form cluster dendrograms. The percent wet weight contribution of prey to predator diets were arranged in a simple predator (row) × prey (column) matrix. For AHCA we used the Sørensen (Bray-Curtis) distance measure and Ward's linkage method. Trophic groups from cluster analysis were established by choosing a cutoff level with biological meaning while maintaining a reasonable level (at least 40%) of information explained in the cluster dendrogram. The significance of trophic groups was examined using a multiresponse permutation procedure (MRPP), which tests for the null hypothesis of no difference between groups. MRPP gauges within and between group differences using an A-statistic that ranges between 0 and 1, with 0 being no agreement within a group and 1 being complete agreement. All AHCA and MRPP analyses were performed with PC-ORD software (version 4, MjM Software, Gleneden Beach, OR).

Before nonparametric analyses of diets, certain modifications to the data were performed. Nekton species that were found in <5% of the tows within a cruise were excluded from analyses, although these species were retained in the general description of diets. This level of exclusion was somewhat arbitrary; however exclusion of nekton species that were found in 5–10% of tows would have removed many predator species from analyses. Prey taxa modifications involved removal of rare species and aggregation of certain groups. Larval-juvenile fishes, hyperiid amphipods, brachyuran and decapod larvae, and adult fish prey were combined into higher taxonomic categories and life history stages. This arrangement was required to retain important species groups for multivariate analyses. Adjustments for all data involved the removal of rare prey that were only present in ≤10% of the nekton diets (rows) in the main matrix. Removal of rarer species reduced noise in the data and allowed for comparisons of important prey between nekton predators.

Trophic relationships were also analyzed by calculating the degree of diet similarity between nekton species pairs by using Schoener's similarity index (Schoener, 1974), modified as a percent similarity index (PSI) of the diets of paired nekton:

$$PSI = \left[1 - 0.5\sum_{i=1}^{n}\left|p_{ik} - p_{jk}\right|\right] \times 100, \qquad (1)$$

where p = the proportion of biomass (wet weight) of the kth prey species consumed by predator species i and j.

Diet overlap values $\geq 60\%$ were considered biologically significant (Wallace and Ramsay, 1983). As in the AHCA, prey items of unidentified material, and fish and crustacean tissue, were eliminated from the calculation of PSI.

Diets (percent wet weight of major prey taxa) from selected species were compared with respect to interannual differences. Comparisons between 2000 and 2002 were limited to species and life history stages of nekton that were found in $\geq 5\%$ of the total number of hauls within a cruise, which left only yearling and adult chinook and coho salmon, and juvenile steelhead trout (*O. mykiss*). Comparisons between years were undertaken by visual inspection of plotted diet data.

Results

Trophic groups

A total of 3161 stomachs from 26 species of marine nekton were analyzed for diet composition from the June and August 2000 and 2002 cruises. A species-specific summary of number of stomachs analyzed, nekton percent frequency of occurrence, nekton size (mean and standard deviation), and mean stomach fullness and condition are presented in Table 1. A more detailed description of specific prey species consumed by nonsalmonids can be found in Miller (2006). Results from cluster analysis and MRPP showed major trophic groups for both years based on nekton diet (percent wet weight) of the following general prey groups: adult fish, larval-juvenile fish, euphausiids (*Thysanoessa spinifera* and *Euphausia pacifica*), decapod larvae, copepods, and other mixed zooplankton groups (predominantly hyperiid amphipods, gelatinous zooplankton, and phytoplankton). For 2000 and 2002, five significant trophic groups (2000 MRPP, A statistic=0.37, $P \ll 0.001$; 2002 MRPP, A statistic=0.31, $P \ll 0.001$) were observed at the cutoff level of 60% and 52% information remaining, respectively (Fig. 1).

From AHCA of nekton diets for the year 2000, trophic group A (blue shark [*Prionace glauca*] and adult coho salmon, Figs. 1 and 2) had diets that consisted (62% and 80%, respectively) of adult Osteichthyes (Clupeidae and unidentifiable fish tissue), and to a lesser extent of larval-juvenile Osteichthyes (for adult coho salmon) and euphausiids (for blue shark). Trophic group B (juvenile and adult salmon) had diets comprising >90% larval-juvenile fish and adult euphausiids for each age class. Of the euphausiids consumed, *T. spinifera* contributed the highest proportion by wet weight to salmonid diets. Trophic group C (jack mackerel, Pacific saury [*Cololabis saira*], and Pacific sardine) had diets of 86%, 93%, and 90% euphausiids, respectively; most euphausiids consumed by this group were identified as *E. pacifica*. Trophic group D (market squid and surf smelt [*Hypomesus pretiosus*] had the most diverse diet of all nekton: mixed species of crustacean zooplankton (brachyuran larvae, euphausiids, hyperiid amphipods) accounted for most of the diet by wet weight. Trophic group E (Pacific herring [*Clupea pallasi*], whitebait smelt [*Allosmerus elongates*], and juvenile sablefish [*Anoplopoma fimbria*]), consumed euphausiids that contributed 77%, 96%, and 97% to the wet weight of their diets, respectively. Except for *E. pacifica*, which was consumed most by juvenile steelhead trout, *T. spinifera* was the dominant euphausiid species consumed by nekton within this group. The remaining nekton not included in the cluster analysis generally consumed a mix of crustacean zooplankton or crustacean zooplankton and larval-juvenile Osteichthyes (Fig. 2).

There was a similar trend in 2002 nekton diets based on the consumption of adult and larval-juvenile Osteichthyes, euphausiids, and brachyuran larvae (Figs. 1 and 3). As in 2000, blue shark and adult coho salmon (trophic group A, Figs. 1 and 3) diets consisted mainly of adult Osteichthyes (81% and 30%, respectively); blue shark diets consisted secondarily of osteichthyean tissue (16%), and adult coho salmon diet consisted secondarily of brachyuran larvae (69% of which were Dungeness crab [*Cancer magister*] megalopae). Pacific hake and adult chinook salmon, also in this group, consumed adult Osteichthyes (predominantly Clupeidae), larval-juvenile Osteichthyes (chinook salmon only), euphausiids (Pacific hake only), and brachyuran larvae (adult chinook and coho salmon). Trophic group B (Fig. 1) consisted of jack mackerel, northern anchovy, Pacific herring, juvenile sablefish, and whitebait smelt, whose diets consisted mostly of euphausiids (predominantly *T. spinifera*) and various other zooplankton and larval-juvenile Osteichthyes (Fig. 3). Juvenile chinook, coho, and chum salmon (*O. keta*), and juvenile steelhead trout formed a trophic group (C, Fig. 1), where larval-juvenile Osteichthyes represented >50% of wet weight of diet for all species (Fig. 3). Euphausiids were important in only juvenile steelhead trout (35%). Trophic group D (Fig. 1) consisted of market squid, surf smelt, spiny dogfish (*Squalus acanthias*), and Pacific sand lance (*Ammodytes hexapterus*) which consumed a mix of crustacean zooplankton (euphausiids, brachyuran larvae, hyperiids) and in the case of spiny dogfish, gelatinous zooplankton. Pacific sardine, juvenile widow rockfish (*Sebastes entomelas*), and Pacific saury clustered into a group (trophic group E, Fig. 1) that had mixed zooplankton diets of copepods, euphausiid eggs, and euphausiids. The remaining nekton not included in the cluster analysis were juvenile rockfish (*Sebastes* spp.) species and juvenile lingcod (*Ophiodon elongatus*). Juvenile lingcod diets consisted mostly of large copepods (68%, *Calanus* spp.), and larval-juvenile Osteichthyes (30%). Juvenile rockfish consumed a combination of euphausiids, copepods, hyperiid amphipods, and gelatinous zooplankton or material (Fig. 3).

Table 1

Summary of nekton species analyzed for stomach contents from June and August 2000 and 2002 GLOBEC cruises in the northern California Current ecosystem. Percent frequency of occurrence (FO) of individual species is the occurrence of a species from 163 and 212 net tows in 2000 and 2002, respectively. Length denotes fork length with the exception of *Loligo opalescens*, which was measured in dorsal mantle length, and *Prionace glauca*, *Merluccius productus*, and *Squalus acanthias* measured in total length. Standard deviation of length is denoted as SD.

	2000				2002			
			Length (mm)				Length (mm)	
Nekton taxa	n	FO (%)	Mean	SD	n	FO (%)	Mean	SD
Market squid (*Loligo opalescens*)	38	4.8	72	17	178	5.8	84	25
Blue shark (*Prionace glauca*)	9	6.3	1331	136	13	3.3	1607	234
Spiny dogfish (*Squalus acanthias*)				128	6.3	263	34	
Northern anchovy (*Engraulis mordax*)	4	2.5	152	6	177	12.7	157	16
Pacific herring (*Clupea pallasi*)	134	8.3	146	11	152	5.8	192	24
Pacific sardine (*Sardinops sagax*)	160	13.4	221	27	108	4.1	198	24
Surf smelt (*Hypomesus pretiosus*)				87	2.5	137	11	
Whitebait smelt (*Allosmerus elongatus*)	89	4.2	100	9	69	2.0	109	7
Chinook salmon (subyearling) (*Oncorhynchus tshawytscha*)	56	3.8	137	14	29	15.3	283	29
(yearling)	100	18.1	225	30	100	22.4	281	33
(adult)	32	12.6	378	43	100	24.3	378	108
Coho salmon (yearling) (*O. kisutch*)	84	19.7	261	48	38	25.0	25	182
(juvenile)				148	10.6	114	11	
(adult)	13	7.1	594	71	56	8.7	9	514
Chum salmon (juvenile) (*O. keta*)	147	10.6	113	11				
Cutthroat trout (adult) (*O. clarki*)	4	2.2	297	19	7	5.9	321	28
Steelhead trout (juvenile) (*O. mykiss*)	55	13.4	284	29	15	5.5	268	30
(adult)	1	1	430					
Pacific hake (*Merluccius productus*)				72	1.9	252	51	
Pacific saury (*Cololabis saira*)	40	5.1	157	22	140	5.8	214	38
Bank rockfish (juvenile) (*Sebastes rufus*)				9	1.0	84	25	
Canary rockfish (juvenile) (*S. pinniger*)				16	2.9	27	3	
Darkblotched rockfish (juvenile) (*S. crameri*)	7	1.2	47	4	11	2.9	29	2
Yellowtail rockfish (juvenile) (*S. flavidus*)	26	2.4	49	4				
Rockfish (juvenile) (*Sebastes* spp.)	4	1.2	48	2	19	2.9	37	7
Widow rockfish (juvenile) (*Sebastes entomelas*)				41	4.8	53	4	
Lingcod (juvenile) (*Ophiodon elongatus*)	10	4.8	74	4	1	1.0	64	
Sablefish (*Anoplopoma fimbria*)	6	2.5	157	22	15	5.0	181	9
Jack mackerel (*Trachurus symmetricus*)	74	11.4	497	75	242	13.1	505	54
Pacific mackerel (*Scomber japonicus*)	24	1.3	325	19				
Pacific sand lance (juvenile) (*Ammodytes hexapterus*)				73	5.8	57	5	
Total	1117				2044			

Percent similarity of diets between nekton species varied by year (Tables 2 and 3). During 2000 (Table 2), highest similarity values were found between yearling chinook and yearling coho salmon (94%), yearling and adult chinook salmon (88%), and yearling coho salmon and adult chinook salmon (88%). Trophic groups B (yearling and adult chinook salmon and yearling coho salmon) and C (jack mackerel, Pacific saury, and Pacific sardine) had the highest similarities in diet (mean 90% and 58%, respectively). For trophic group B, larval-juvenile Osteichthyes and adult euphausiids together accounted for over 80% of the total percent similarity in diets among the three nekton, and larval-juvenile Osteichthyes accounted for 60% of the overlap. Other nekton that had significant (>60%) percent similarity in diets (Table 2) were 1) jack mackerel and juvenile steelhead trout and 2) juvenile steelhead trout and Pacific herring; and the similarities were primarily due to euphausiids, or to species that fed on euphausiids and other mixed zooplankton, or in the case of adult coho

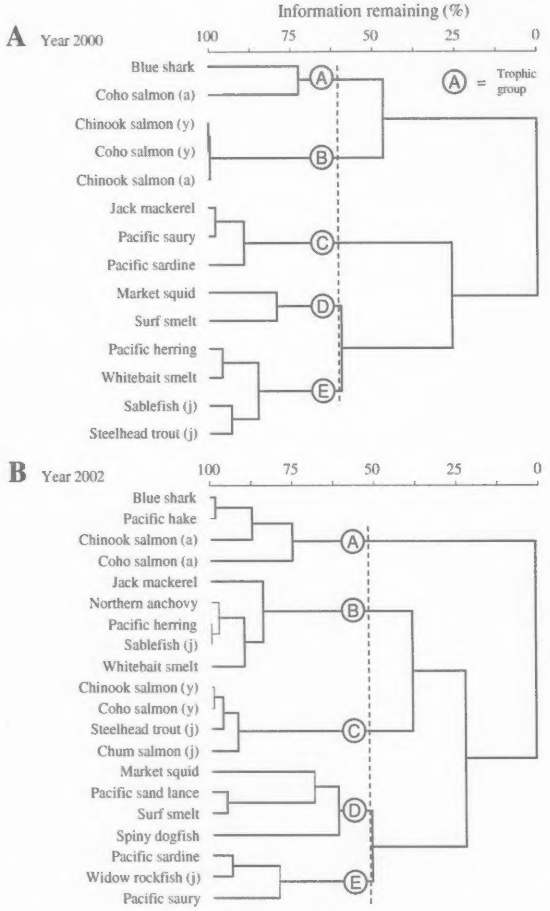

Figure 1

Dendrograms of nekton based on diet (percent wet weight contribution of prey) as determined by agglomerative hierarchical cluster analysis of nekton collected from the northern California Current during June and August 2000 and 2002 GLOBEC (GLOBal ocean ECosystems dynamics) cruises. Dashed line denotes the level (percent information remaining) at which trophic groups were established in the dendrogram. The percent information remaining is a function of the amount of information lost at each step of hierarchical cluster analysis. Scientific names of the species in the order they appear in the figure (from top to bottom) are the following: blue shark (*Prionace glauca*), coho salmon (*Oncorhynchus kisutch*), chinook salmon (*O. tshawytscha*), jack mackerel (*Trachurus symmetricus*), Pacific saury (*Cololabis saira*), Pacific sardine (*Sardinops sagax*), market squid (*Loligo opalescens*), surf smelt (*Hypomesus pretiosus*), Pacific herring (*Clupea pallasi*), whitebait smelt (*Allosmerus elongatus*), sablefish (*Anoplopoma fimbria*), steelhead trout (*O. mykiss*), Pacific hake (*Merluccius productus*), northern anchovy (*Engraulis mordax*), chum salmon (*O. keta*), Pacific sand lance (*Ammodytes hexapterus*), spiny dogfish (*Squalus acanthias*), and widow rockfish (*Sebastes entomelas*). Life history stages of nekton are shown in parentheses: j = juvenile, y= yearling, and a = adult; nekton and prey with no indication of life history stage are adult.

salmon and blue shark, to adult Osteichthyes (Fig. 2).

In 2002, trophic group C containing yearling chinook and coho salmon, juvenile chum salmon, and steelhead trout had the highest overall mean percent similarity (63%); and the highest similarity (78%) was between yearling chinook and yearling coho salmon (Table 3) . Most of the similarity in diet within this trophic group was due to larval-juvenile Osteichthyes (70% of total similarity). Trophic groups B and A had the next highest similarities in diet (mean 61% and 46%, respectively). Similarities in diet within these two groups were primarily attributed to euphausiids (that represented 68% of total similarity) for trophic group B, and adult Osteichthyes (that represented 58% of total similarity) for trophic group A. The remaining trophic groups D and E had percent similarities <30%.

Interannual variation

Adult coho salmon and juvenile steelhead trout displayed the largest contrast in diet between 2000 and 2002. For adult coho salmon, adult and larval-juvenile Osteichthyes contributed >95% of the diet in 2000, and brachyuran larvae contributed approximately 50% of the diet in 2002 (Fig. 4). Steelhead trout had a greater proportion of its diet from euphausiids (84%) in 2000, whereas larval-juvenile Osteichthyes were more important in 2002 (57%). The remaining nekton displayed relatively similar diets between years, although differences were observed in the contribution of euphausiids and brachyuran larvae. Yearling coho and chinook salmon showed that larval-juvenile fishes contributed >70% of their diet for both years. Euphausiids contributed more to diets of both species during 2000 (≥18%) compared to 2002 (>5%), whereas in 2002 brachyuran larvae were more prominent in the diets (Fig. 4). The trend of higher proportions of euphausiids in diets in 2000 and of brachyuran larvae in 2002 was also observed in adult coho and chinook salmon.

Discussion

Trophic groups

Diet analysis of 26 nekton species of the northern California Current ecosystem

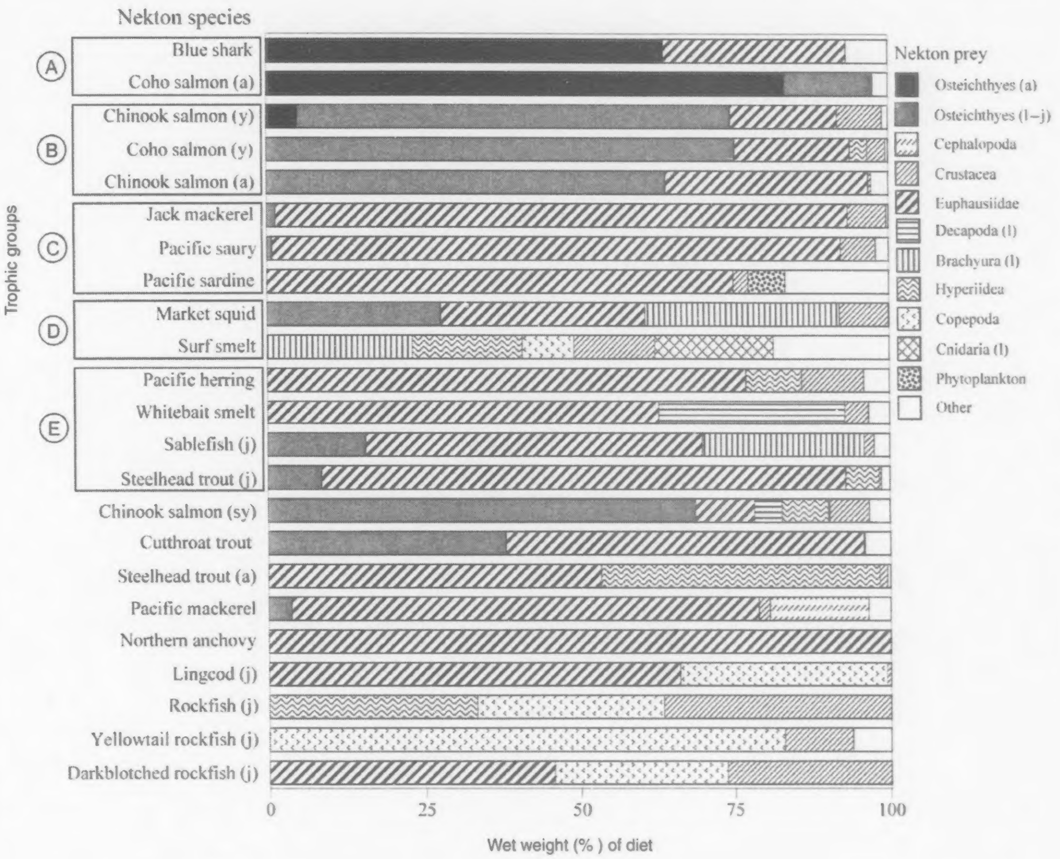

Figure 2

Summary of nekton diets analyzed from June and August 2000 northern California Current GLOBEC (GLOBal ocean Ecosystems dynamics) cruises. Trophic groups based on cluster analysis of diets (percent wet weight) are blocked and labeled (**A**) to (**E**). Species not blocked lacked sufficient numbers and frequency of occurrence for analysis. Scientific names of species in the order they appear in the figure (from top to bottom) are the following: blue shark (*Prionace glauca*), coho salmon (*Oncorhynchus kisutch*), chinook salmon (*O. tshawytscha*), jack mackerel (*Trachurus symmetricus*), Pacific saury (*Cololabis saira*), Pacific sardine (*Sardinops sagax*), market squid (*Loligo opalescens*), surf smelt (*Hypomesus pretiosus*), Pacific herring (*Clupea pallasi*), whitebait smelt (*Allosmerus elongatus*), sablefish (*Anoplopoma fimbria*), steelhead trout (*O. mykiss*), cutthroat trout (*O. clarki*), Pacific mackerel (*Scomber japonicus*), northern anchovy (*Engraulis mordax*), lingcod (*Ophiodon elongatus*), rockfish (*Sebastes* spp.), yellowtail rockfish (*S. flavidus*), darkblotched rockfish (*S. crameri*). Life history stages of nekton are shown in parentheses: j = juvenile; sy = subyearling; y = yearling, and a = adult; nekton and prey with no indication of life history stage are adult.

revealed general trophic groups that primarily consumed adult Osteichthyes, larval-juvenile Osteichthyes, euphausiids, mixed zooplankton, and copepods; however, in each trophic group omnivory was expressed and actually predominated in some nekton trophic groups. The importance of omnivory in the higher trophic group of blue shark and adult coho salmon indicated that the typical mid-trophic level taxa, such as anchovy and Pacific sardine, were sometimes bypassed for direct feeding on large zooplankton, in particular adult euphausiids. Previous studies from the NCC system have also shown that blue shark (Brodeur et al., 1987; Harvey, 1989), adult coho (Brodeur et al., 1987), and adult chinook (Hunt et al., 1999) salmon feed on adult nekton and euphausiids. With the exception of Pacific hake, top-down trophic pressure from fish may be less influential in the NCC because top nekton predators are not as abundant in this system as nekton prey such as euphausiids (Ressler

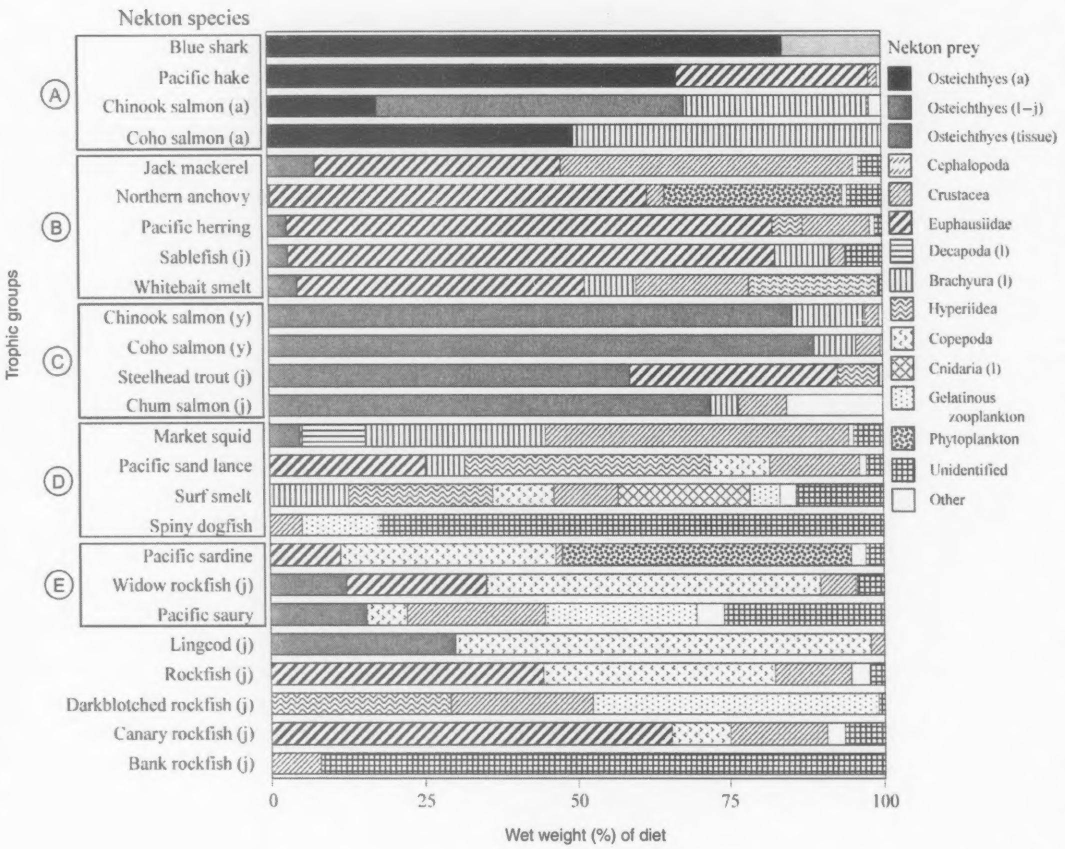

Figure 3

Summary of nekton diets analyzed from June and August 2002 northern California Current GLOBEC (GLOBal ocean ECosystems dynamics) cruises. Trophic groups based on cluster analysis of diets (percent wet weight) are blocked and labeled (**A**) to (E). Species not blocked lacked sufficient numbers and frequency of occurrence for analysis. Scientific names of species in the order they appear in the figure are the following: blue shark (*Prionace glauca*), Pacific hake (*Merluccius productus*), chinook salmon (*Oncorhynchus tshawytscha*), coho salmon (*O. kisutch*), jack mackerel (*Trachurus symmetricus*), northern anchovy (*Engraulis mordax*), Pacific herring (*Clupea pallasi*), sablefish (*Anoplopoma fimbria*), whitebait smelt (*Allosmerus elongatus*), steelhead trout (*O. mykiss*), chum salmon (*O. keta*), market squid (*Loligo opalescens*), Pacific sand lance (*Ammodytes hexapterus*), surf smelt (*Hypomesus pretiosus*), spiny dogfish (*Squalus acanthias*), Pacific sardine (*Sardinops sagax*), widow rockfish (*Sebastes entomelas*), Pacific saury (*Cololabis saira*), lingcod (*Ophiodon elongatus*), rockfish (*Sebastes* sp.), darkblotched rockfish (*S. crameri*), canary rockfish (*S. pinniger*), and bank rockfish (*S. rufus*). Life history stages of nekton are shown in parentheses: j = juvenile, y = yearling, and a = adult; nekton and prey with no indication of life history stage are adult.

et al., 2005). Pacific hake likely represent the largest predatory biomass off the west coast of North America (Methot and Dorn, 1995). They feed on adult nekton (Brodeur et al., 1987; Emmett and Krutzikowsky, in press) but also extensively on euphausiids (Brodeur et al., 1987; Tanasichuk, 2002) and give evidence that as omnivores they may not impose direct and intensive trophic pressures upon adjacent trophic species in this upwelling ecosystem, as would be implied by the classical theory of top-down control.

Euphausiids were also observed as important prey of many middle-trophic-level nekton species. Three trophic groups were evident at this trophic level: 1) a group of species that consumed predominantly larval-juvenile fish and to a lesser degree euphausiids, 2) a group of species that consumed mostly euphausiids, and 3) a group of species that fed on euphausiids and other mixed zooplankton. Although these trophic groups were formed for both years, trophic group membership changed, and many of nekton shifted between the consumption of euphausiids and other zooplankton prey. The importance of euphausiids in the diets of mid-trophic nekton species agreed with observations by Brodeur et al. (1987), and with results that showed the importance of larval-juvenile fishes in diet studies of jack mackerel (Brodeur et al., 1987) and juvenile salmonids (Brodeur and Pearcy, 1990). Nekton secondary consumers, those feeding on copepods, euphausiid eggs and furcilia, consisted of juvenile rockfishes (*Sebastes* spp.) and Pacific sardine. However, some species of juvenile rockfish (widow and darkblotched) and juvenile lingcod also consumed larger prey, such as adult euphausiids, and other larval-juvenile fishes (Reilly et al., 1992). Pacific sardine have been observed to be highly euryphagous, feeding on phytoplankton, copepods, and euphausiids (Hand and Berner, 1959). Little information is available on the diets of juvenile rockfish species and juvenile lingcod; many of these species also showed a diverse size-range of prey, consuming copepods, egg-adult stages of euphausiids and, as in juvenile lingcod, other larval-juvenile fishes. Various life stages of euphausiids and larval-juvenile fishes therefore played an important role in the diets of many nekton at the time of this study, indicating that most nekton were feeding at or near the secondary consumer level.

The substantial contribution of euphausiids to many nekton species may have been due to recent increases in euphausiid abundance after 1999 within the NCC pelagic ecosystem. Feinberg and Peterson (2003) observed an extension in the season of euphausiid spawning and multiple peaks in egg density starting in 1999, presumably when there was a regime shift to higher upwelling and primary and secondary production (Peterson and Schwing, 2003). In a trophic study of the NCC system during the 1980s, Brodeur and Pearcy (1992) also observed higher dietary overlap among different nekton species during high upwelling years, and that much of the overlap was attributed to euphausiids. Moreover, they observed that nekton showed lower dietary overlap and increased foodweb complexity during the 1983 El Niño, a period of low upwelling and primary and secondary production.

Table 2

Percent similarity index (PSI) of nekton diets for fish collected from the northern California Current during the June and August 2000 GLOBEC cruises. Trophic groups were derived from agglomerative hierarchical cluster analysis (AHCA) of percent wet weight of diet. Blocked PSI values denote within-trophic group comparisons. PSI values >60% are shown in bold. Life history stages of nekton are shown in parentheses and represent juvenile (j), yearling (y), and adult (a); nekton with no indication of life history stage are adult.

Trophic group	Nekton species	*Prionace glauca*	*Oncorhynchus kisutch* (a)	*O. tshawytscha* (a)	*O. kisutch* (y)	*O. tshawytscha* (y)	*Trachurus symmetricus*	*Cololabis saira*	*Sardinops sagax*	*Loligo opalescens*	*Hypomesus pretiosus*	*Clupea pallasi*	*Allosmerus elongatus*	*Anoplopoma fimbria* (j)	*O. mykiss* (j)
A	*Prionace glauca*	X													
	Oncorhynchus kisutch (a)	**61**	X												
B	*O. tshawytscha* (a)	26	15	X											
	O. kisutch (y)	29	15	**94**	X										
	O. tshawytscha (a)	33	14	**88**	**88**	X									
C	*Trachurus symmetricus*	28	9	20	25	28	X								
	Cololabis saira	27	5	17	15	18	**69**	X							
	Sardinops sagax	8	6	12	19	14	**65**	40	X						
D	*Loligo opalescens*	0	3	16	12	19	9	0	6	X					
	Hypomesus pretiosus	7	9	18	18	10	13	9	21	28	X				
E	*Clupea pallasi*	28	10	32	30	34	44	34	19	37	30	X			
	Allosmerus elongatus	25	11	35	30	36	34	24	20	32	23	60	X		
	Anaplopoma fimbria	38	13	37	39	48	33	24	10	32	8	58	50	X	
	O. mykiss (j)	36	14	35	40	44	**69**	51	53	34	23	**67**	57	60	X

Table 3

Percent similarity index (PSI) of diets of nekton species collected from the northern California Current during June and August 2002 GLOBEC cruises. Trophic groups were derived from agglomerative hierarchical cluster analysis (AHCA) of percent wet weight of diet. Blocked PSI values denote within-trophic group comparisons. PSI values >60% are shown in bold. Life history stages of nekton are shown in parentheses and represent juvenile (j), yearling (y), and adult (a); nekton with no indication of life history stage are adult.

Trophic group	Nekton species	*Prionace glauca*	*Merluccius productus*	*Oncorhynchus tshawytscha* (a)	*O. kisutch* (a)	*Trachurus symmetricus*	*Engraulis mordax*	*Clupea pallasi*	*Anoplopoma fimbria* (j)	*Allosmerus elongatus*	*O. tshawytscha* (y)	*O. kisutch* (y)	*O. mykiss* (j)	*O. keta* (j)	*Loligo opalescens*	*Ammodytes hexapterus*	*Hypomesus pretiosus*	*Squalus acanthias*	*Sardinops sagax*	*Sebastes entomelas* (j)	*Cololabis saira*
A	*Prionace glauca*	X																			
	Merluccius productus	**67**	X																		
	Oncorhynchus tshawytscha (a)	41	**62**	X																	
	O. kisutch (a)	30	33	41	X																
B	*Trachurus symmetricus*	1	26	27	8	X															
	Engraulis mordax	0	30	31	2	33	X														
	Clupea pallasi	1	33	34	6	49	**63**	X													
	Anaplopoma fimbria (j)	0	32	34	10	39	**61**	**76**	X												
	Allosmerus elongatus	0	26	33	6	28	43	**62**	58	X											
C	*O. tshawytscha* (y)	0	41	35	5	38	24	40	28	34	X										
	O. kisutch (y)	1	27	**78**	27	37	34	44	38	28	**78**	X									
	O. mykiss (j)	0	31	53	5	39	38	49	40	36	54	**74**	X								
	O. keta (j)	0	4	34	4	15	9	19	9	19	71	57	45	X							
D	*Loligo opalescens*	1	5	7	2	7	4	8	4	13	8	7	3	9	X						
	Ammodytes hexapterus	0	14	19	5	12	33	44	30	38	19	27	21	10	6	X					
	Hypomesus pretiosus	0	7	14	6	13	13	29	10	24	15	19	11	21	15	50	X				
	Squalus acanthias	0	4	8	1	8	7	9	6	8	7	11	6	7	3	3	8	X			
E	*Sardinops sagax*	0	10	16	4	14	51	26	12	16	16	17	15	14	5	26	21	8	X		
	Sebastes entomelas (j)	0	3	19	2	13	11	17	9	13	19	18	18	21	3	17	18	4	49	X	
	Cololabis saira	0	3	16	6	16	11	17	10	15	13	19	16	18	3	15	18	5	17	23	X

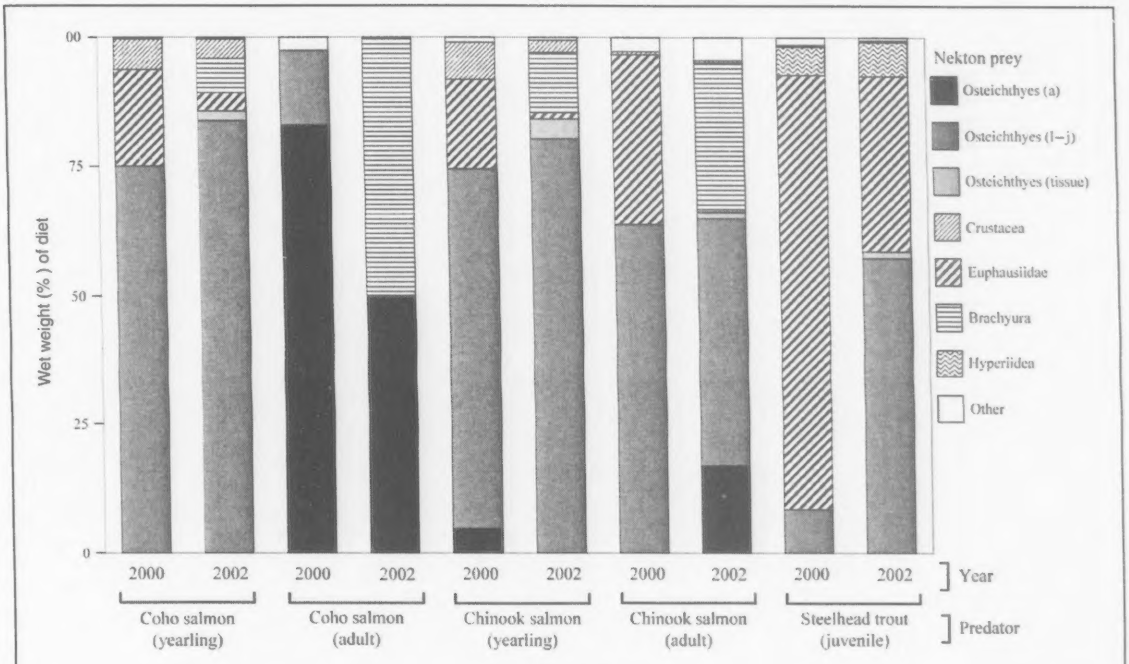

Figure 4

Comparison of 2000 and 2002 nekton diets (percent wet weight) analyzed from northern California Current GLOBEC (GLOBal ocean ECosystems dynamics) cruises. Scientific names of the species in the order they appear in the figure are the following: coho salmon (*Oncorhynchus kisutch*), chinook salmon (*O. tshawytscha*), and steelhead trout (*O. mykiss*).

Feeding by many nekton directly on phytophagous euphausiids results in more direct food webs and fewer trophic levels, and concomitant increases in food-web efficiency. Observations by Brodeur and Pearcy (1992) and by the authors of the present study thus indicate that trophic characteristics of the NCC system may have periods of high production when euphausiids are consumed across many trophic levels. Additional research of trophic relationships between dominant nekton and zooplankton within the NCC at varying levels of production would further clarify whether this pattern is an important characteristic of this ecosystem.

Interannual variation

Limited interannual variation in diets was observed; only juvenile steelhead trout and adult coho salmon expressed major differences between 2000 and 2002. Other nekton, particularly yearling coho and chinook salmon, showed relatively little variation in diet; only euphausiids and brachyuran larvae (which represent a small portion of nekton diet in general) varied most between the two years. Whether this variability was an artifact of sampling is uncertain; however, it is interesting to note that the higher prevalence of euphausiids in the 2000 diets and the higher prevalence of brachyuran larvae in 2002 diets indicated that variation between the two years may have been a result of the relative abundance of these prey. Other studies from the NCC have also indicated high temporal variation in zooplankton (Mackas et al., 2001, 2004) and in the diets of Pacific hake (Emmett and Krutzikowsky, in press) and juvenile salmonids (Brodeur and Pearcy, 1990). Although both 2000 and 2002 were years of high upwelling and high production, substantial interannual variability in the hydrographic environment was observed. During the summer of 2002, an intrusion of cold, nutrient-rich, subarctic bottom water resided on the Oregon shelf, resulting in high phytoplankton production in surface waters and in hypoxic conditions near the bottom (Thomas et al., 2003; Wheeler et al., 2003). Although it is possible that this nutrient-rich water may have influenced the prey field available to the different predators, no discernible effect on their diet was observed in our study.

The temporal variability in nekton diets reveals an important characteristic of the NCC system in that this variability reflects the duration of trophic interactions between predator and prey in relation to population-scale parameters. If variability in the time scale of trophic links is short compared to nekton population dynamics, then more short-lived species (such as market squid) or those exhibiting a critical ontogenetic shift (such as juvenile salmonids) will be more influenced by interannual variability in the availability and quality of prey. Species exhibiting extensive feeding migrations through the NCC system, such as Pacific hake and Pacific sardine, may be less influenced by localized prey limitation because critical feeding for recruitment success can occur in other regions with different physical and biological parameters.

Interannual and interdecadal comparisons of species distribution and community structure of pelagic nekton have demonstrated that the northern California Current ecosystem can vary between months and years (Brodeur et al., 2005). As fishery management shifts away from single-species towards multispecies or ecosystem-based fishery management (Pikitch et al., 2004), detailed information on the trophic interactions within this pelagic ecosystem as presented here will become indispensable for development of management plans and ecosystem models. Further analysis of the relationships between major nekton and their prey is warranted to elucidate differences in trophic relationships between major upwelling regions, especially those that are influenced by strong climatic variability.

Acknowledgments

We thank R. Emmett, J. Fisher, C. Bucher, P. Bentley, R. Baldwin, and S. Pool for field and laboratory support and the captains and crew of the FV Sea Eagle and FV Frosti for help with sampling. H. Li, B. Pearcy (both at Oregon State University), Ed Casillas (Northwest Fisheries Science Center, Seattle), and three anonymous reviewers provided valuable comments on earlier drafts of the manuscript. This work was funded in part by a Mamie Markham Fellowship, the U.S. GLOBEC Northeast Pacific Program, and the Bonneville Power Administration. This article is contribution number 540 of the U.S. GLOBEC Program.

Literature cited

Ainley, D. G., L. B. Spear, and S. G. Allen.
1996. Variation in the diet of Cassin's auklet reveals spatial, seasonal, and decadal occurrence patterns of euphausiids off California, USA. Mar. Ecol. Prog. Ser. 137:1–10.

Brodeur, R. D., J. P. Fisher, R. L. Emmett, C. A. Morgan, and E. Casillas.
2005. Species composition and community structure of pelagic nekton off Oregon and Washington under variable oceanographic conditions. Mar. Ecol. Prog. Ser. 298:41–57.

Brodeur, R. D., J. P. Fisher, D. J. Teel, R. L. Emmett, E. Casillas, and T. W. Miller.
2004. Juvenile salmonid distribution, growth, condition, origin, and environmental and species associations in the northern California Current. Fish. Bull. 102:25–46.

Brodeur, R. D., H. V. Lorz, and W. G. Pearcy.
1987. Food habits and dietary variability of pelagic nekton off Oregon and Washington, 1979–1984. NOAA Tech. Rep. NMFS 57:1–32.

Brodeur, R. D., and W. G. Pearcy.
1986. Distribution and relative abundance of pelagic nonsalmonid nekton off Oregon and Washington, 1979–84. NOAA Tech. Rep. NMFS 46, 85 p.
1990. Trophic relations of juvenile Pacific salmon off the Oregon and Washington coast. Fish. Bull. 88:617–636.
1992. Effects of environmental variability on trophic interactions and food web structure in a pelagic upwelling ecosystem. Mar. Ecol. Prog. Ser. 84:101–119.

Carr, M. E.
2002. Estimation of potential productivity in eastern boundary currents using remote sensing. Deep-Sea Res. II 49:59–80.

Chavez, F. P., J. Ryan, S. E. Lluch-Cota, and M. C. Ñiquen.
2003. From anchovies to sardines and back: multidecadal change in the Pacific Ocean. Science 299:217–221.

Corwith, H. L., and P. A. Wheeler.
2002. El Niño related variations in nutrient and chlorophyll distributions off Oregon. Prog. Oceanogr. 54:361–380.

Emmett, R. L., and R. D. Brodeur.
2000. Recent changes in the pelagic nekton community off Oregon and Washington in relation to some physical oceanographic conditions. Bull. North Pac. Anadrom. Fish. Comm. 2:11–20.

Emmett, R. L., R. D. Brodeur, T. M. Miller, S. S. Pool, P. J. Bentley, G. K. Krutzikowsky, and J. McCrae.
2005. Pacific sardine *(Sardinops sagax)* abundance, distribution and ecological relationships in the Pacific Northwest. Calif. Coop. Oceanic Fish. Invest. Rep. 46:122–143.

Emmett, R. L., and G. R. Krutzikowsky.
In press. Nocturnal feeding by Pacific hake (*Merluccius productus*) and jack mackerel (*Trachurus symmetricus*) off the mouth of the Columbia River, 1999–2004: implications for juvenile salmon predation. Trans. Am. Fish. Soc.

Feinberg, L. R., and W. T. Peterson.
2003. Variability in duration and intensity of euphausiid spawning off central Oregon, 1996–2001. Prog. Oceanogr. 57:363–379.

Francis, R. C., and S. R. Hare.
1994. Decadal-scale regime shifts in the large marine ecosystems of the North-east Pacific: a case for historical science. Fish. Oceanogr. 3:279–291.

Hand, C. H., and L. Berner.
1959. Food of the Pacific sardine (*Sardinops caerulea*). Fish. Bull. 164:175–184.

Harvey, J. T.
1989. Food habits, seasonal abundance, size, and sex of the blue shark, *Prionace glauca*, in Monterey Bay, California. Cal. Fish Game. 75:33–44.

Hood, R. R., M. R. Abbott, and A. Huyer.
1991. Phytoplankton and photosynthetic light response in the coastal transition zone off northern California in June 1987. J. Geophys. Res. 96(C8):14769–14780.

Hunt, S. L., T. J. Mulligan, and K. Komori.
1999. Oceanic feeding habits of chinook salmon, *On-*

corhynchus tshawytscha, off northern California. Fish. Bull. 97:717–721.

Huyer, A.
1983. Coastal upwelling in the California Current system. Prog. Oceanogr. 12:259–284.

Jackson, J. B., M. X. Kirby, W. H. Berger, K. A. Bjorndal, L. W. Botsford, B. J. Bourque, R. H. Bradbury, R. Cooke, J. Erlandson, J. A. Estes, T. P. Hughes, S. Kidwell, C. B. Lange, H. S. Lenihan, J. M. Pandolfi, C. H. Peterson, R. S. Steneck, M. J. Tegner, and R. R. Warner.
2001. Historical overfishing and the recent collapse of coastal ecosystems. Science 293:629–637.

Mackas, D. L., W. T. Peterson, and J. E. Zamon.
2004. Comparisons of interannual biomass anomalies of zooplankton communities along the continental margins of British Columbia and Oregon. Deep Sea Res. II 51:875–896.

Mackas, D. L., R. E. Thomson, and M. Galbraith.
2001. Changes in the zooplankton community of the British Columbia continental margin, 1985–1999, and their covariation with oceanographic conditions. Can. J. Fish. Aquat. Sci. 58:685–702.

Mantua, N. J., S. R. Hare, Y. Zhang, J. M. Wallace, and R. C. Francis.
1997. A Pacific decadal climate oscillation with impacts on salmon. Bull. Am. Meteorol. Soc. 78:1069–1079.

McGowan, J. A., D. R. Cayan, and L. M. Dorman.
1998. Climate-ocean variability and ecosystem response in the northeast Pacific. Science 281:210–217.

Methot, R. D., and M. W. Dorn.
1995. Biology and fisheries of North Pacific hake (*M. productus*). *In* Hake: biology, fisheries and markets (J. Alheit, and T. J. Pitcher, eds.), p. 389–414. Chapman and Hall, London.

Miller, T. W.
2006. Trophic dynamics of marine nekton and zooplankton in the northern California Current pelagic ecosystem. Ph. D. diss., 212 p. Oregon State Univ., Corvallis, OR.

Pearcy, W. G., and A. Schoener.
1987. Changes in the marine biota coincident with the 1982–1983 El Niño in the northeastern subarctic Pacific Ocean. J. Geophys. Res. 92(C13):14,417–14,428.

Peterson, W. T., and F. B. Schwing.
2003. A new climate regime in northeast pacific ecosystems. Geophys. Res. Lett. 30(17):1896.

Pikitch, E. K., C. Santora, E. A. Babcock, A. Bakun, R. Bonfil, D. O. Conover, P. Dayton, P. Doukakis, D. Fluharty, B. Heneman, E. D. Houde, J. Link, P. A. Livingston, M. Mangel, M. K. McAllister, J. Pope, and K. J. Sainsbury.
2004. Ecosystem-based fishery management. Science 305:346–347.

Reese, D. C., and R. D. Brodeur.
2006. Identifying and characterizing biological hot spots in the Northern California Current. Deep Sea Res. II 53:291–314.

Reilly, C. A., T. W. Echeverria, and S. Ralston.
1992. Interannual variation and overlap in the diets of pelagic juvenile rockfish (Genus: *Sebastes*) off central California. Fish. Bull. 90:505–515.

Ressler, P. H., R. D. Brodeur, W. T. Peterson, S. K. Pierce, P. M. Vance, A. R. Røstad, and J. A. Barth.
2005. The spatial distribution of euphausiid aggregations in the northern California Current during August 2000. Deep Sea Res. II 52:89–108.

Robinson, C. L. K.
2000. The consumption of euphausiids by the pelagic fish community off southwestern Vancouver Island, British Columbia. J. Plankton Res. 22(9):1649–1662.

Schoener, T. W.
1974. Resource partitioning in ecological communities. Science 185:27–39.

Tanasichuk, R. W.
2002. Implications of interannual variability in euphausiid population biology for fish production along the southwest coast of Vancouver Island: a synthesis. Fish. Oceanogr. 11:18–30.

Thomas, A. C., P. T. Strub, and P. Brickley.
2003. Anomalous satellite-measured chlorophyll concentrations in the northern California Current in 2001–2002 spring 2005 in the California Current. Geophys. Res. Lett. 30(15), 8022.

Wallace, H., and J. S. Ramsay.
1983. Reliability in measuring diet overlap. Can. J. Fish. Aquat. Sci. 40:347–351.

Wheeler, P. A., A. Huyer, and J. Fleischbein.
2003. Cold halocline, increased nutrients and higher chlorophyll off Oregon in 2002. Geophys. Res. Lett. 30(15), 8021.

Worm, B., and J. E. Duffy.
2003. Biodiversity, productivity and stability in real food webs. Trends Ecol. Evol. 18:628–632.

Timing and duration of mating and brooding periods of Atka mackerel (*Pleurogrammus monopterygius*) in the North Pacific Ocean

Robert R. Lauth[1] **(contact author)**
Jared Guthridge[2,3]
Dan Nichol[1]
Scott W. McEntire[1]
Nicola Hillgruber[3]

Email address for R. R. Lauth: Bob.Lauth@noaa.gov

[1] National Oceanic and Atmospheric Administration
National Marine Fisheries Service
Alaska Fisheries Science Center
Resource Assessment and Conservation Engineering Division
7600 Sand Point Way NE
Seattle, Washington 98115

[2] Alaska SeaLife Center
301 Railway Avenue
Seward, Alaska 99664

[3] School of Fisheries and Ocean Sciences
University of Alaska Fairbanks
11120 Glacier Highway
Juneau, Alaska 99801

Abstract—The timing and duration of the reproductive cycle of Atka mackerel (*Pleurogrammus monopterygius*) was validated by using observations from time-lapse video and data from archival tags, and the start, peak, and end of spawning and hatching were determined from an incubation model with aged egg samples and empirical incubation times ranging from 44 days at a water temperature of 9.85°C to 100 days at 3.89°C. From June to July, males ceased diel vertical movements, aggregated in nesting colonies, and established territories. Spawning began in late July, ended in mid-October, and peaked in early September. The male egg-brooding period that followed continued from late November to mid-January and duration was highly dependent on embryonic development as affected by ambient water temperature. Males exhibited brooding behavior for protracted periods at water depths from 23 to 117 m where average daily water temperatures ranged from 4.0° to 6.2°C. Knowledge about the timing of the reproductive cycle provides a framework for conserving Atka mackerel populations and investigating the physical and biological processes influencing recruitment.

Manuscript submitted 23 February 2007 to the Scientific Editor's Office.

Manuscript approved for publication 24 July 2007 by the Scientific Editor.

Fish. Bull. 105:560–570 (2007).

Atka mackerel (*Pleurogrammus monopterygius*) is distributed along the edges of the North Pacific Ocean and adjoining basins in rocky shelf regions near landmasses and archipelagos, and in rocky reefs atop prominent bathymetric features rising from the sea floor (Rutenberg, 1962; Allen and Smith, 1988). Atka mackerel is one of the most abundant groundfish in the central and western North Pacific Ocean (Zenger, 2004) where it is a key prey item for marine fishes, birds, and mammals (Murie, 1959; Kenyon, 1965; Sinclair and Zeppelin, 2002). Modern large-scale commercial trawling by U.S. and foreign fishing vessels began during the latter half of the twentieth century, and since the end of the joint venture fishing in 1989, total landings of U.S. fishing vessels have averaged 54,000 metric tons annually (Lowe et al., 2006).

Knowledge about the timing of the reproductive cycle and temporal use of nesting habitat is essential for understanding processes affecting the recruitment and population dynamics of Atka mackerel, and for making management decisions regarding commercial fishing activity. Despite Atka mackerel's relatively high abundance and value to the ecosystem, surprisingly little is known about its life history and ecology. Access to Atka mackerel is difficult and costly because the species inhabits a vast and remote region that is notorious for inclement weather and rough seas. Studies on the reproductive biology of Atka mackerel are further limited by a general lack of knowledge about the location of spawning and nesting sites in these remote areas. In the eastern North Pacific Ocean off the coast of Kamchatka Peninsula, there are only a handful of known spawning and nesting sites (Zolotov, 1993), and in the central and eastern North Pacific Ocean, the geographic and bathymetric distribution of spawning and nesting sites was completely unknown until recently (Lauth et al., in press).

Previously published studies have used ovarian condition to determine the start and end of the spawning period (Gorbunova, 1962; Zolotov, 1993; McDermott and Lowe, 1997), but very little has been done to investigate the time spent by males in either establishing nesting territories before spawning or in brooding eggs afterwards. Only from the western North Pacific Ocean is there published information on the nesting period from beginning to end, but methods and results have been vague and have relied on catch data from various nonstandardized fishing gears and methods (Gorbunova, 1962; Zolotov, 1993). Egg incubation times are useful for approximating the end of the male nest brooding period (Gorbunova, 1962; Lauth and Blood, 2007), however, controlled rearing experiments at a wider range of water temperatures are needed to accurately determine how the rate of embryonic development is affected (Lauth and Blood, 2007).

The objective of this study was to clarify Atka mackerel's temporal use of breeding habitat by investigating the timing and duration of nesting, spawning, and brooding phases in the North Pacific Ocean. This study makes use of *in situ* visual and behavioral observations of male Atka mackerel and an incubation model that synthesizes data from laboratory incubation experiments, egg mass collections from three different nesting sites, and descriptions of embryonic development from a companion manuscript (Lauth and Blood, 2007).

Materials and methods

Direct observation of nesting behavior

Visual and behavioral observations from time-lapse video and data from archival tags were used for determining the beginning and end of the nesting period (i.e., the duration of male territoriality), and to document nesting behaviors before the onset of spawning. Sexual dichromatism (Medveditsyna, 1962; Rutenberg, 1962) and behavioral changes in males (Nichol and Somerton, 2002; Lauth et al., in press) are primary indications of nesting activity. Nest guarding males are distinguished by their bright yellow or orange color and dark black vertical stripes. When males are breeding, they defend a nesting territory for long periods and refrain from vertical migrations. Sexually mature females or nonspawning Atka mackerel of both sexes are bluish-green or gray and typically undergo diel vertical migrations year round (Nichol and Somerton, 2002).

Time-lapse camera Diving operations to deploy and retrieve underwater camera equipment were conducted from the National Atmospheric and Oceanic Administration (NOAA) National Marine Fisheries Service (NMFS) charter vessels FV *Morning Star* (May 2002), FV *Sea Storm* (July 2002), and the United States Fish and Wildlife Service RV *Tîglâx* (August 2002). A Sony Hi8 (Sony Electronics, Inc., San Diego, CA) video camera was placed inside a Plexiglas housing and secured to a mooring on the seafloor at 23 m by a diver at a known nesting site at Seguam Island, Alaska (52 22.10°N, 172 20.26°W) on 31 May 2002. The video camera had a time-lapse controller that could be set by the user to record video images at periodic intervals. The camera was attached to a tripod frame made of welded steel. On the initial deployment, the time-lapse controller was set to record 1 minute of video each day. It was recovered on 28 July 2002 (60 days later) and reset at the same location to record 1 minute of video every hour until 7 August 2002 (a 10-day period). The camera was recovered and reset a final time to record 15 sec/h until 31 August 2002 (a 24-day period) when the camera was recovered.

Archival tags Archival tag data from a previously published study on Atka mackerel diel behavior (Nichol and Somerton, 2002) were used to infer nest-guarding behavior and to corroborate nesting periods. In July 2000, 117 Atka mackerel were captured by trawl, tagged, and released in Seguam Pass with archival tags that recorded the time, depth, and temperature once each minute (Nichol and Somerton, 2002). Commercial trawlers recovered 14 Atka mackerel with tags. Data from four of the tags were from males that showed no vertical movement for extended periods, which is consistent with nesting. Data from two of the four tags were also reported in Nichol and Somerton (2002).

Laboratory incubation experiments

Results from laboratory rearing experiments were used to develop parameters for an incubation model to determine how Atka mackerel incubation time varies between nesting sites. Laboratory experiments were conducted at the Alaska Sealife Center (ASLC) with egg masses spawned by captive Atka mackerel. In October 2002, a commercial fishing vessel with a bottom trawl collected 20 live Atka mackerel from Seguam and Tanaga Passes. The fish were kept live in tanks on board the fishing vessel and transported to the ASLC. After acclimation, antibiotic treatment, and a one-month quarantine at the ASLC, 14 Atka mackerel were transferred to ASLC exhibit tanks equipped with a submersible video camera for documenting spawning and nesting behavior. Each time an egg mass was discovered, the videotape was reviewed to determine the time of egg mass deposition. Fertilized egg masses were transferred to one of four closed-system incubation tanks consisting of a 150-L tank, recirculation pump, and a 1/3 hp inline chiller controlled by an electronic thermostat. The configuration of the system provided stable temperatures with very little fluctuation. Temperatures for the incubation chambers were chosen on the basis of *in situ* observations at nesting sites in the Aleutian Islands (Lauth et al., in press). Ten incubation experiments were conducted at four different water temperatures: three each at 4°, 5°, and 7°C, and two at 10°C. The light cycle in the aquaria was regulated with an electronic timer set at 12 h light and 12 h dark.

For all incubation experiments, hatching day for an egg mass was defined as the first day larvae hatched from the egg mass. A scatter plot of incubation temperature versus total days to first hatching was constructed for all incubation temperature trial data, and regression analysis (Zar, 1999) was used to determine how total days to hatching varied as a function of temperature.

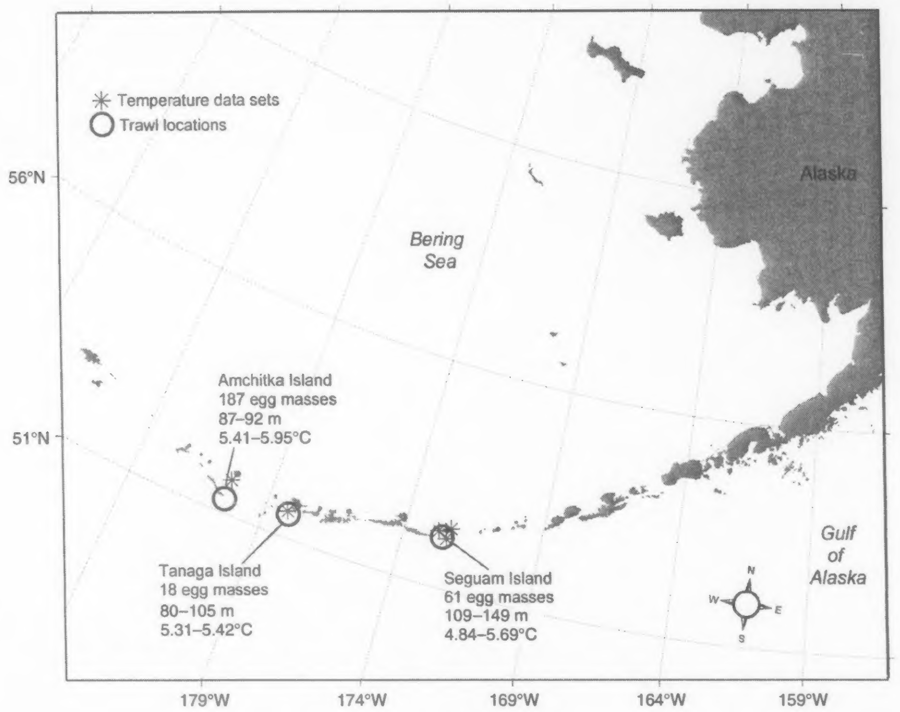
Temperature data sets
Trawl locations
56°N
51°N
Bering Sea
Alaska
Gulf of Alaska
Amchitka Island
187 egg masses
87–92 m
5.41–5.95°C
Tanaga Island
18 egg masses
80–105 m
5.31–5.42°C
Seguam Island
61 egg masses
109–149 m
4.84–5.69°C
N
W
E
S
179°W
174°W
169°W
164°W
159°W

Figure 1

Map showing collection sites for water temperature data sets (asterisks; also see Table 1) and trawl locations where Atka mackerel (*Pleurogrammus monopterygius*) egg masses were collected (open circles). The number of egg masses collected and the range of water depth and temperature are listed beneath each trawling location.

Incubation model

An incubation model was used for extrapolating spawning and hatching dates for egg mass samples collected from three different Atka mackerel nesting sites. During the period 7–23 October 2004, egg masses were collected from trawl hauls aboard the commercial stern-trawler FV *Seafisher* and samples were preserved in 10% phosphate-buffered formalin. The October collection period was chosen because histological studies have indicated it is the month when spawning ends in Alaska (McDermott and Lowe, 1997). A total of 266 egg masses were collected: 187 from the Amchitka Island area, 18 from near Tanaga Island, and 61 from the waters surrounding Seguam Island (Fig. 1). In the laboratory, egg mass samples were placed underneath a stereo dissecting microscope and aged to the nearest day by using the the descriptions of embryonic development from the incubation experiment described by Lauth and Blood (2007).

The calculation of spawning and hatching dates was based on the assumption that the effect of temperature on incubation rate for any given development stage was nearly a constant linear relationship for the entire incubation period. The constant relationship is generally true for temperatures normally encountered by eggs in their habitat (Ahlstrom, 1943; Riley, 1974; Hempel, 1979). Spawning and hatching dates were estimated by using the following relationship:

$$d_t = \frac{D_t s_{6^\circ C}}{S_{6^\circ C}}$$

where d_t = age of the egg mass (days) at temperature t;
D_t = total incubation time (days) at temperature t;
$s_{6^\circ C}$ = estimated age of the collected egg mass (days) using the descriptions of embryonic development from Lauth and Blood (2007);
$S_{6^\circ C}$ = total number of days for first egg to first hatching:

Spawning date = *Egg mass collection date* − d_t, and
Hatching date = (*Egg mass collection date* − d_t) + D_t.

Table 1

Source, latitude, longitude, depth, and time periods for water temperature data sets from sites surrounding Amchitka/Tanaga and Seguam Islands (also see Fig. 1). PMEL EPIC = Pacific Marine Environmental Laboratory Eastern Pacific Investigation of Climate Processes.

Source	Latitude (N)	Longitude (W)	Depth (m)	Time period
Amchitka and Tanaga sslands				
PMEL EPIC buoy data	51°46.12′	179°30.70′	39	08 June 1987 to 18 June 1988
PMEL EPIC buoy data	51°35.40′	178°12.60′	142	03 May 2002 to 11 May 2003
Seguam Island				
PMEL EPIC buoy data	52°08.08′	172°25.57′	109	03 May 2002 to 01 Oct 2002
PMEL EPIC buoy data	52°08.08′	172°25.57′	109	01 Oct 2002 to 03 Nov 2002
PMEL EPIC buoy data	52°16.00′	172°45.10′	147	02 May 2002 to 10 May 2003
PMEL EPIC buoy data	52°16.00′	172°45.10′	147	19 May 2001 to 13 Oct 2001
PMEL EPIC buoy data	52°16.00′	172°45.10′	139	13 Oct 2001 to 13 Feb 2001
Atka mackerel archival tag	Exact location unknown		92	23 July 2000 to 21 Jan 2001
Nearshore current meter[1]	52°22.09′	172°20.26′	22	01 June 2002 to 01 Sept 2002

[1] The current meter was anchored to substrate within an Atka mackerel nesting site.

Values for the total incubation time of a collected egg mass (D_t) were calculated with a best-fit regression equation derived from the laboratory incubation experiments.

Temperature data sets used for determining a low and high range of D_t were obtained from buoys operated by the Eastern Pacific Investigation of Climate Processes (EPIC) program of the NOAA Pacific Marine Environmental Laboratory (PMEL; Table 1; Fig. 1). There were two EPIC temperature data sets available for the Amchitka and Tanaga Island area and five for the Seguam Island area (Table 1). The depths for the EPIC buoy data ranged from 39 to 147 m, which are close to the depth limits where Atka mackerel nesting sites were observed (Lauth et al., in press). In addition to the EPIC data sets for the Seguam Island area, two more temperature data sets were available from a shallow (22 m) and deep (92 m) Atka mackerel nesting site (Table 1). The temperature data from the shallow nesting site were collected from the data logger attached to the time-lapse camera and the data from the deep nesting site were collected from an archival tag on a male that exhibited nesting behavior. Daily water temperatures were pooled by area for calculating an average daily water temperature and standard deviation. The minimum and maximum average daily water temperatures from each area for the period 1 July to 15 January were used in the incubation model for the low and high D_t.

Egg mass spawning and hatching dates were pooled by week and ogives of the pooled data were made for a low and high range of D_t for each egg collection area. To estimate the timing of spawning and nesting periods across the entire geographical region, pooled data for both low and high temperatures from all three areas were proportioned equally, combined, and plotted by relative frequency over time.

Results

Direct observation of nesting behavior

Time-lapse camera The time-lapse camera was used for documenting the arrival of male Atka mackerel at a nesting site near Seguam Island in 2002 (Fig. 1). Divers at the site observed no males or Atka mackerel egg masses when the camera was deployed on 31 May, nor were males observed in the camera footage for the first five days. On 5 June, a bright yellow male with black vertical stripes (male nesting coloration) swam across the screen during a 10-second period. There was a similar observation on 6 June. Neither of these males exhibited territorial behavior toward a specific patch of rocky substrate. On 9 June, two males hovered close to the bottom at mid-screen in the background for the entire minute, and on 10 June, one male pursued another Atka mackerel of unknown sex, followed it (off screen), and then returned to mid-screen and hovered for the remainder of the minute. Atka mackerel were not observed with the time-lapse camera for the next two days. On 13 June, a group of three males swam across the screen in the distance. On 14, 15, and 17 June, males were observed hovering in the distance or swimming across the screen. On 18 June, a bright yellow male with dark black vertical bands was positioned in front of the camera. The same male was observed in the same area in front of the camera every day after that through 31 August (74 days). Between 18 June and 31 August, other males were periodically observed in the background exhibiting nesting behavior. During all three recoveries of the time-lapse camera, divers observed two egg masses within a 1 m radius of the camera mooring.

Archival tags Two archival tags were retrieved from Seguam Pass in September 2000, and one each in September 2001 and January 2001. It was evident from the depth data of two tags that Atka mackerel males made regular diel vertical movements during the nonbreeding season from mid-December through May (Fig. 2, A and B). During the breeding season from June to December, the behavior of all four tagged males was characterized by an extended period of time on the bottom and very limited or no vertical movement (Fig. 2). It was assumed that these periods corresponded with nesting behavior. The earliest date within a year that such nesting behavior was observed was 4 June (Fig. 2A) and the latest was 12 December (Fig. 2B). The male in Fig. 2A was at liberty for 406 days and exhibited 89 days of limited vertical movement before being captured. The male in Fig. 2B displayed nesting behavior for 141 consecutive days,—the longest uninterrupted time period for all tagged males. Also unique to the male in Figure 2B was a depth shift from 125 to 92 m on 14 September followed by a continuation of nesting behavior until 14 December (89 days). Three of the four males displayed nesting behavior shortly after being released (Fig. 2, B–D), but two of these males (Fig. 2, C and D) abandoned the behavior after only 33 days, whereas the other male (Fig. 2B) shifted depth and continued nesting behavior. Males in Figures 2B and 2D also showed unexplained and periodic ascents and descents during periods of presumed nesting behavior.

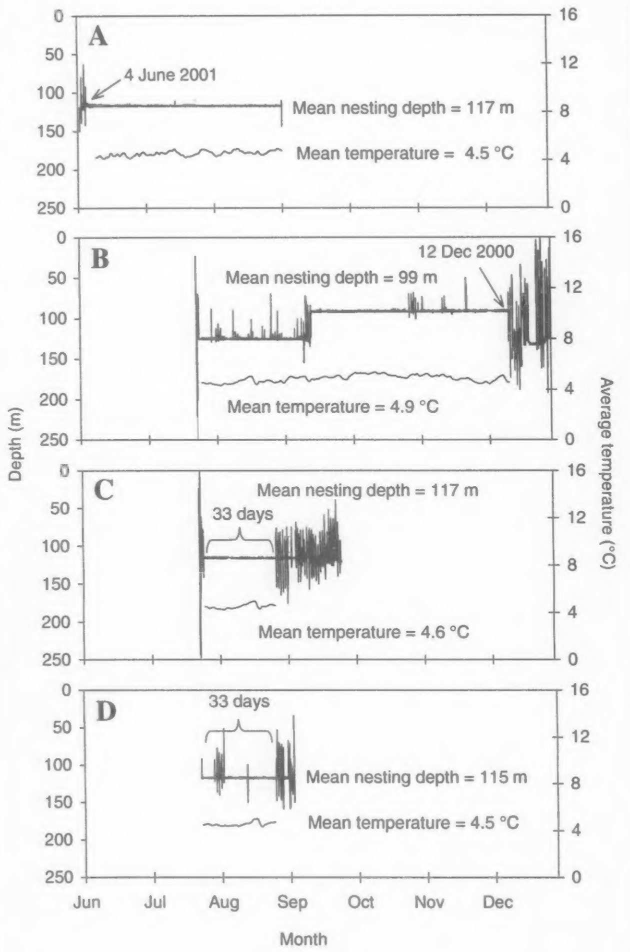

Figure 2

Plots **A–D** show the depth and temperature data of archival tags from four captured male Atka mackerel (*Pleurogrammus monopterygius*) that were originally tagged and released in July 2000. The calendar year for plot A is 2001, and for plots B–D is 2000. All four males exhibited periods of limited vertical movement consistent with nesting behavior. An arrow points to the start of nesting behavior in plot A and the end of nesting behavior in plot B, and plots C and D have brackets delineating the nesting periods and the length of nesting behavior (days) is indicated above the brackets. Mean water depth and temperature of nesting behavior periods are also presented along with average daily water temperature represented by the lower black line in each plot. Periods with frequent and repeated diel vertical migrations outside the arrows and brackets are consistent with non-nesting behavior.

The average depths where male nesting behavior was displayed ranged from 92 to 117 m and the water temperatures at those locations ranged from 4.5° to 4.9°C. Water temperatures varied by a maximum of 2.6°C during these periods.

Laboratory incubation experiments

In 2004, ten egg masses were fertilized and all were incubated successfully at the ASLC. The first spawning event for the captive Atka mackerel was recorded on 27 July, and the last was on 13 October. For 2005, the first and last spawning dates were 13 July and 12 October. The average temperature for each of the four treatments was 3.89°, 5.04°, 7.03°, and 9.85°C. The incubation time of 74 days at 6.15°C from Lauth and Blood (2007) was also used in the analysis. The best fit of the data was a logarithmic function with a negative slope (Fig. 3). Total incubation time (D_t) was a function of the natural logarithm of incubation temperature (t) with days to first hatching ranging from 44 days at 9.85°C to 100 days at 3.89°C (Fig. 3).

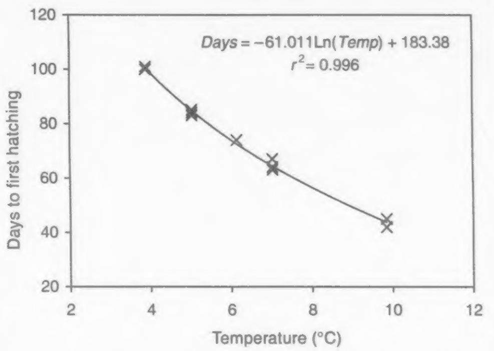

Figure 3

Plot of results from laboratory experiments in which Atka mackerel (*Pleurogrammus monopterygius*) eggs were incubated in a series of controlled incubation temperatures. The best fit relationship of days to first hatching as a function of temperature (°C) is represented by the equation, coefficient of determination (r^2), and the line drawn through the data points.

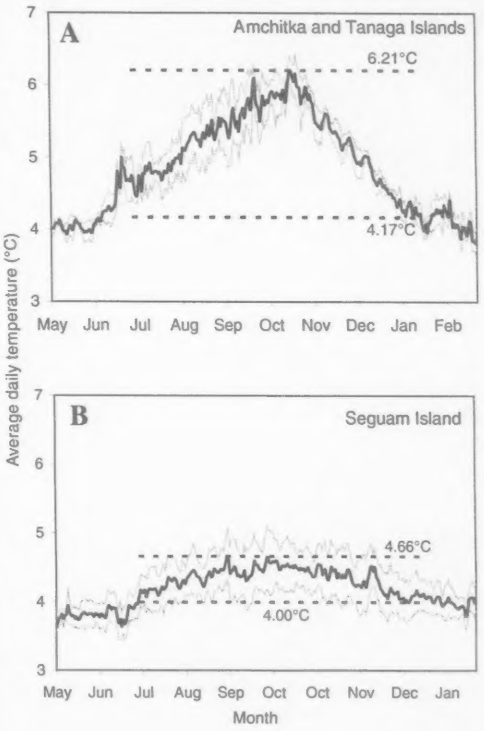

Figure 4

Pooled average daily temperatures (°C) from historical time series data collected from (**A**) Amchitka and Tanaga islands, and (**B**) Seguam Island. The dark lines represent the average daily water temperature and the lighter lines, the standard deviation. The dashed lines represent the low and high average daily water temperatures chosen for the incubation model.

Incubation model

Water temperatures varied by area and time of year; daily averages were generally highest during the spawning and hatching periods from late summer to early winter, and higher near Amchitka and Tanaga Islands compared to Seguam Island (Fig. 4). During the period 1 July to 15 January, average daily water temperatures from Amchitka and Tanaga Islands reached a maximum of 6.21°C during October and a minimum of 4.17°C in January (Fig. 4A). Average daily water temperatures were generally lower and more variable for the same period at Seguam Island, ranging from 4.00°C in June and January to 4.66°C in August (Fig. 4B). The mean and standard deviation for all daily average water temperatures for the period 1 July to 15 January was 5.22 ±0.16°C for Amchitka Island and 4.34 ±0.50°C for Seguam Island.

Amchitka Island Spawning started from late-July to early August, peaked from mid-August to early September, and ended in late September (Fig. 5). Some of the egg masses collected at Amchitka Island were at an advanced stage of development; therefore hatching began about the same time that egg masses were collected in mid-October and was completed by early to mid-December.

Tanaga Island Assuming the same incubation temperatures as Amchitka Island, calculated spawning and hatching dates for Tanaga Island were about a half-month later than Amchitka Island (Fig. 5). Spawning commenced from early to mid-August and ended in late September or early October. Hatching began in early November and ended by late December or early January.

Seguam Island Spawning and hatching dates for Seguam Island were the latest among the three areas sampled (Fig. 5). Spawning began in mid-August, peaked in mid-September, and ended in early-October. Hatching commenced in mid-November and ended from early to mid-January.

All areas and temperatures combined For all areas combined, spawning began in mid-July, peaked in early September, and ended mid-October (Fig. 6). Hatching immediately followed the end of spawning, peaked in early December, and continued until late January.

Discussion

The mating and brooding cycle (i.e., reproductive cycle) of Atka mackerel lasts from June to January. The mating phase begins with males aggregating in nesting colonies where they establish individual nesting territories. Time-lapse camera footage and archival tag data show that male Atka mackerel begin aggregating and establishing nesting territories in early June, 1.5 months before spawning commences. The reason for the lengthy nest-establishment period is unknown, but fishes that provide male parental care of eggs typically put considerable effort into choosing and preparing an optimal nesting territory because it can be an important determinant for maximizing reproductive success (e.g., Sargent, 1982; Sikkel, 1988; Bisazza et al., 1989; Östlund-Nilsson, 2000).

The second phase of mating consists of courtship and spawning, during which time a territorial male can mate with multiple females. Spawning begins mid-July and ends in mid-October. A July to October spawning period has been corroborated by a histological study of 978 Atka mackerel ovaries from collections made across the entire North American geographical range (McDermott and Lowe, 1997), and from observations of captive spawning Atka mackerel used in the incubation experiments from the present study. Because such a high proportion of egg masses were found in later stages of development at Amchitka, it is possible that some hatching occurred before the egg mass collections. This would have the effect of shifting the onset of the spawning and hatching period at Amchitka to an earlier time. Because egg masses collected from Tanaga and Seguam Islands were much younger at the time they were collected, it is not likely that some earlier hatching took place, especially given the low water temperatures characteristic of each nesting site.

Detailed analysis of spawning times by area, with the use of aged egg masses, indicated a later onset of and peak in spawning as spawning activity moved from west to east. Female Atka mackerel spawn an average of 4.6 separate batches of eggs during the 12-week spawning period (McDermott et al., 2007), but uncertainty about precise ambient temperatures precludes conclusions regarding the periodicity of separate spawning events and whether these events were continuous or episodic.

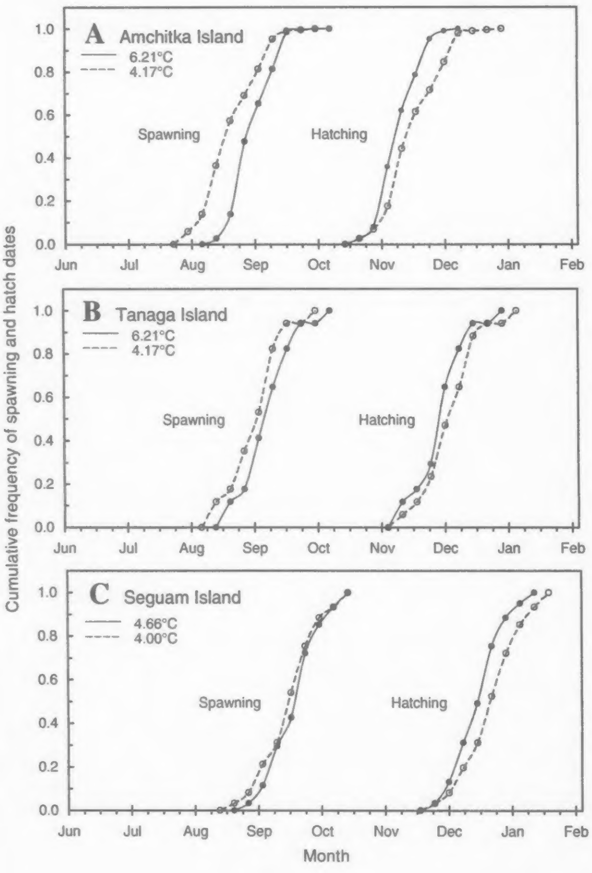

Figure 5

Ogive plots of incubation model results for Atka mackerel (*Pleurogrammus monopterygius*) egg masses collected from (**A**) Amchitka Island, (**B**) Tanaga Island, and (**C**) Seguam Island. The *y*-axis is the cumulative frequency of egg mass spawning and hatching dates by week for low (dashed line) and high (solid line) average daily water temperatures for each area (see Fig. 4).

During the brooding phase, spawning has ended and males guard the incubating egg masses within their territory until all the eggs hatch. The duration of the male brooding phase is highly dependent on water temperature. The average water temperature of 106 nesting sites covering a broad temporal, bathymetric, and geographic range in the Aleutian archipelago was 5.4°C (Lauth et al., in press). If this water temperature represented a true mean for the entire range of Atka mackerel, the average male brooding period would be 11.5 weeks. Using a video drop camera on 30 November 2005, the principal author verified that males were still aggregated and exhibiting nesting behavior at a nesting site near Dutch Harbor, AK. Considering that egg masses are spawned until late October and that *in situ* water temperatures as low as 3.99°C are observed at nesting sites, it is plausible that some males brood eggs at nesting sites until January.

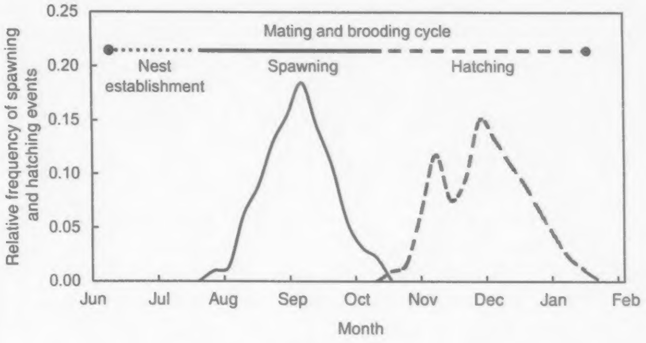

Figure 6

Plot of incubation model results for Atka mackerel (*Pleurogrammus monopterygius*) egg masses collected from Amchitka, Tanaga, and Seguam islands combined. The *y*-axis is the relative frequency of egg mass spawning (solid line) and hatching events (dashed line) by week for pooled low and high average daily water temperatures. The horizontal line at top represents the duration of the mating and brooding cycle and identifies the periods of nest establishment (dotted line), spawning (solid black line), and hatching (dashed line).

There may be several reasons for the 2-month difference in the duration of the reproductive cycle between Alaska (7+ months) and the western Pacific Ocean (5+ months; Gorbunova, 1962; Zolotov, 1993). First, all the western Pacific Ocean nesting sites were located in coastal areas in water depths <32 m where water temperatures were likely higher and the length of the brooding period shorter than those in Alaskan waters. Second, no distinction was made between the onset of the nesting and spawning periods; that is, Gorbunova (1962) and Zolotov (1993) assumed both periods commenced in June. In Alaska, males aggregate and prepare nesting territories 1–2 months before spawning. Without a direct means for observing males at a nesting site with such tools as archival tags and time-lapse cameras, it is difficult to determine when males first arrive. Assuming a 1-month nest establishment period during May and longer incubation times for the western Pacific Ocean population, the duration of the reproductive cycle for Atka mackerel is similar to the duration of the cycle for other parts of the North Pacific Ocean.

The timing of the Atka mackerel reproductive cycle is unusual because fishes in temperate and subarctic waters typically synchronize the hatching time of larvae with periods of high zooplankton abundance in the spring or early summer (Cushing, 1990; Haldorson et al., 1993). The possible adaptive significance of hatching during the late fall and early winter may be predator avoidance, dispersal, or availability of specific prey. Atka mackerel larvae are neustonic after hatching (Kendall and Dunn, 1985) and have large mouths (Gorbunova, 1962) capable of feeding on larger planktonic prey.

The temporal, geographic, and bathymetric distribution of sampling for this study was relatively limited given the temporally and spatially complex marine environment that Atka mackerel inhabit (Ladd et al., 2005; Ohshima et al., 2005). Large-scale climate changes to the ecosystem (Rodionov et al., 2005) can cause alterations in recruitment dynamics that may affect population structure (Bailey, 2000; Ciannelli et al., 2005) and ultimately change the timing of the reproductive cycle (Hutchings and Myers, 1994; Wieland et al., 2000; Ojaveer and Kalejs, 2005). We did not investigate how water temperature or other environmental factors vary over larger scales, or how such variability influences the timing of the Atka mackerel's reproductive cycle. This study does, however, provide a framework for process-oriented investigations of stock dynamics, recruitment, and distribution of Atka mackerel populations. Time of hatching, geographic location, and hydrographic features can all affect the dispersal of larvae and play a significant role, along with biological processes, in determining recruitment success and population structure (Napp et al., 2000).

For unknown reasons, nest fidelity varied among the tagged male Atka mackerel. Given a late July onset of spawning and relatively low ambient water temperatures at nesting sites, it is unlikely that males are able to successfully tend, from start to end, more than one brood of egg masses per season. Nests are commonly composed of eggs from multiple females (Lauth et al., in press) deposited over the 3-month spawning period and by the time the first batch of eggs hatches, the spawning period is nearing completion or has ended.

It appears that none of the four archival tags contained data from a nesting male for the duration of one complete mating and brooding cycle. All four males were captured, tagged, and released while the breeding season was underway in late July. The first male (Fig. 2A) did not exhibit nesting behavior until June of the following year. The other three males (Fig. 2, B–D) resumed nesting behavior shortly after being released; and their behavior may indicate that they were defending nesting territories before they were captured and tagged. Two of the males ended nesting behavior after one month, and the third appeared to abandon one nesting territory and establish a second when it abruptly started exhibiting nesting behavior at a shallower depth on 14 September 2000 (Fig. 2B). It appears that the male that changed depths may have established a new nest, spawned, and successfully brooded eggs because nesting behavior ended 89 days later, which is a few days longer than the period needed for eggs to incubate and hatch at the water temperatures recorded by the archival tag (mean=4.9°C). If one considers that this male may have already spent 2 months establishing a nest before being captured and tagged, the total nesting period would be 6.5 months. Given the ambient water temperature and late July start of spawning, there was insufficient time for the other three male Atka mackerel to brood a new or existing batch of eggs. Being displaced from an original nesting territory or failing to attract a female to spawn may be reasons for changing a nesting site or for abandoning it altogether. Nesting colonies can have a broad depth range, cover areas over many square kilometers, and be physically and biologically diverse (Lauth et al., in press); therefore the quality of some territories within a nesting colony may be more suitable for attracting females to spawn.

In addition to males changing the depth and location of their nesting territory, there is evidence to suggest that some male Atka mackerel adopt already existing nesting territories containing eggs. In the exhibit tank at the ASLC, a non-nesting male displaced a territorial nest-guarding male and adopted the egg masses already present on the nest. Adoptive nest behavior is also thought to be a characteristic of another hexagrammid, lingcod (*Ophiodon elongates*) (Withler et al., 2004). Abandoning nests or allowing another fish to assume nest-guarding responsibilities is a common behavior in males that provide parental care of eggs (Gozlan et al., 2003). Male fish that guard territories containing eggs are more reproductively successful because females prefer to mate with males that already have eggs (e.g., Marconato and Bisazza, 1986; DeMartini, 1987; Pruett-Jones, 1992).

There is a high energetic cost to male parental care (Marconato et al., 1993; Gillooly and Baylis, 1999; Steinhart et al., 2005), and protracted nest-guarding severely restricts feeding opportunities for males. Egg cannibalism by males is common in Atka mackerel (Zolotov, 1993; Yang, 1999) and may serve as a means for nest-guarding males to sustain themselves during the protracted nesting season (Zolotov, 1993). Cannibalism of eggs within a male's own nesting territory (filial cannibalism) is considered an adaptive behavior in marine fishes that provide paternal care of eggs and it is especially common in species with protracted breeding cycles (Rowher, 1978; Kondoh and Okuda, 2002).

Commercial trawling on nesting habitat during the spawning and breeding periods would probably result in high mortality of both nest-guarding males and developing embryos. Atka mackerel aggregate for spawning and nesting (Lauth et al., in press), and aggregating behavior is generally predictable and makes a population easier to target and more vulnerable to fishing (Colin et al., 2003). The reproductive success of a fish species is also negatively impacted by alterations to the structural habitat and the benthic community—alternations that are caused by fishing gears (Auster and Langton, 1999). There is some spatial and temporal overlap of commercial trawling and nesting sites in the Aleutian archipelago (Fritz and Lowe, 1998; Lauth et al., in press), but it is difficult to assess the impacts of the fishery on the reproductive success of Atka mackerel without knowing the total distribution of nesting habitat. Knowledge of the temporal use of breeding habitat can be used as a management tool for minimizing negative impacts of the commercial fishery during crucial periods of Atka mackerel life history.

Conclusions

This study provides detailed information about the timing and duration of three specific phases of the Atka mackerel's reproductive cycle: 1) establishment of a nest, 2) spawning, and 3) egg brooding. An accurate incubation rate from controlled laboratory experiments, egg mass collections from nesting sites, and water temperatures characteristic of those observed at nesting sites were used in an incubation model that showed that nest-guarding males use nesting habitat for more protracted periods than previously known. Model results for the start and end of the reproductive cycle were validated with observations from a time-lapse video camera and archival tags. The duration of the reproductive cycle appears to be affected most by the length of the male brooding phase, which can double in duration within the range of ambient water temperatures observed in our laboratory incubation experiments. Knowledge about the timing and duration of the reproductive cycle is essential for conserving Atka mackerel populations and for providing a solid framework for investigations into the physical and biological processes influencing recruitment and population dynamics.

Acknowledgments

This project was funded by grants from the North Pacific Research Board (# F0417) and the National Marine Fisheries Service (NMFS) Essential Fish Habitat (EFH) fund. Rearing experiments at the Alaska Sealife Center (ASLC) by J. Guthridge were part of the requirements for his Master of Science thesis at the University of Alaska, Fairbanks. R. Lauth thanks the skippers and crew from the FV *Morning Star,* FV *Sea Storm,* FV *Seafisher*, and RV *Tîglâx*, especially K. Bell, S. Branstiter, P. Deng, T. Meintz, and S. Clark for field support of this research. Many thanks to S. Atkinson from ASLC for assisting with the proposal and those who helped with field support, scuba diving, or reviewing this manuscript including D. Cooper, G. Duker, G. Hoff, J. Lee, L. Logerwell, S. Lowe, S. McDermott, R. Nelson, K. Rand, C. Rilling, D. Somerton, G. Stauffer, S. VanSant, and two anonymous reviewers.

Literature cited

Ahlstrom, E. H.
1943. Studies on the Pacific pilchard or sardine (*Sardinops caerulea*). 4. Influence of temperature on the rate of development of pilchard eggs in nature. U.S. Fish Wildl. Serv. Spec. Sci. Rep. No. 23:1–26.

Allen, M. J., and G. B. Smith.
1988. Atlas and zoogeography of common fishes in the Bering Sea and Northeastern Pacific. NOAA Tech. Rep. NMFS 66, 151 p.

Auster, P. J., and R. W. Langton.
1999. The effects of fishing on fish habitat. *In* Fish habitat: essential fish habitat and rehabilitation (L. Benaka, ed.), p. 150–187. Am. Fish. Soc., Symposium 22, Bethesda, MD.

Bailey, K. M.
2000. Shifting control of recruitment of walleye pollock *Theragra chalcogramma* after a major climatic and ecosystem change. Mar. Ecol. Prog. Ser. 198:215–244.

Bisazza, A., A. Marconato, and G. Marin.
1989. Male competition and female choice in *Padogobius martensi* (Pisces, Gobiidae). Anim. Behav. 38:406–413.

Ciannelli, L., K. M. Bailey, K.-S. Chan, A. Belgrano, and N. C. Stenseth.
2005. Climate change causing phase transitions of walleye pollock (*Theragra chalcogramma*) recruitment dynamics. Proc. R. Soc. B 272:1735–1743.

Colin, P. L., Y. J. Sadovy, and M. L. Domeier.
2003. Manual for the study and conservation of reef fish spawning aggregations, 98 p. Society for the Conservation of Reef Fish Aggregations Special Publication no. 1 (version 1.0), Oceanside, CA.

Cushing, D. H.
1990. Plankton production and year-class strength in fish populations: an update of the match/mismatch hypothesis. Adv. Mar. Biol. 26:249–293.

DeMartini, E. E.
1987. Paternal defense, cannibalism and polygamy: factors influencing the reproductive success of painted greenling (Pisces, Hexagrammidae). Anim. Behav. 35:1145–1158.

Fritz, L. W., and S. A. Lowe.
1998. Seasonal distributions of Atka mackerel (*Pleurogrammus monopterygius*) in commercially-fished areas of the Aleutian Islands and Gulf of Alaska. U. S. Dep. Commer., NOAA Tech. Memo. NMFS-AFSC-92, 29 p.

Gillooly, J. F., and J. R. Baylis.
1999. Reproductive success and the energetic cost of parental care in male smallmouth bass. J. Fish Biol. 54:573–584.

Gorbunova, N. N.
1962. Spawning and development of greenlings (family Hexagrammidae). *In* Greenlings: taxonomy, biology, interoceanic transplantation (T. S. Rass, ed.), p. 121–185. Tr. Inst. Okeanol., Akad. Nauk. SSSR 59:118–182. [In Russian.] (translated by Isr. Program. Sci. Trans., 1970). [Available from Natl. Tech. Inf. Serv., Springfield, VA, as TT 69-55097 S.]

Gozlan, R. E., C. J. Flower, and A. C. Pinder.
2003. Reproductive success in male sunbleak, a recent invasive fish species in the U.K. J. Fish Biol. 63:131–143.

Haldorson, L., M. Pritchett, D. Sterritt, and J. Watts.
1993. Abundance patterns of marine fish larvae during spring in a southeastern Alaskan bay. Fish. Bull. 91:36–44.

Hempel, G.
1979. Early life history of marine fish: the egg stage, 70 p. Washington Sea Grant, Seattle, WA.

Hutchings, J. A., and R. A. Myers.
1994. Timing of cod reproduction: interannual variability and the influence of temperature. Mar. Ecol. Prog. Ser., 108:21–31

Kendall, A. W., and J. R. Dunn.
1985. Ichthyoplankton of the continental shelf near Kodiak Island, Alaska. U.S. Dep. Commer., NOAA Tech. Memo. NMFS-20, 89 p.

Kenyon, K. W.
1965. Food of harbor seals at Amchitka. J. Mamm. 46:103–104.

Kondoh, M., and N. Okuda.
2002. Mate availability influences filial cannibalism in fish with paternal care. Anim. Behav. 63:227–233.

Ladd, C., G. L. Hunt, Jr., C. W. Mordy, S. Salo, and P. Stabeno.
2005. Marine environment of the eastern and central Aleutian Islands. Fish. Oceanogr., 14(Suppl. 1): 22–38.

Lauth, R. R., S. W. McEntire, and H. H. Zenger.
In press. Geographic distribution, depth range, and description of Atka mackerel (*Pleurogrammus monopterygius*) nesting habitat in Alaska. Alaska Fish. Res. Bull.

Lauth, R. R., and D. M. Blood.
2007. Description of embryonic development of Atka mackerel (*Pleurogrammus monopterygius*). Fish. Bull. 105:571–576.

Lowe, S., J. Ianelli, M. Wilkins, K. Aydin, R. Lauth, and I. Spies.
2006. Stock assessment of Aleutian Islands Atka mackerel. *In* Stock assessment and fishery evaluation eeport for the groundfish resources of the Bering Sea/Aleutian Islands regions, p. 949–1016. North Pacific Fishery Management Council, Anchorage, AK.

Marconato, A., and A. Bisazza.
1986. Males whose nests contain eggs are preferred by female *Cottus gobio* L. (Pisces: Cottidae). Anim. Behav. 34:1580–1582.

Marconato, A., A. Bisazza, and M. Fabris.
1993. The cost of parental care and egg cannibalism in the river bullhead, *Cottus gobio* L. (Pisces: Cottidae). Behav. Ecol. Sociobiol. 32:229–237.

McDermott, S. F., and S. A. Lowe.
1997. The reproductive cycle of Atka mackerel, *Pleurogrammus monopterygius*, in Alaska waters. Fish. Bull. 95:321–333.

McDermott, S. F., K. Pearson, and D. Gunderson.
2007. Annual fecundity, batch fecundity, and oocyte atresia of Atka mackerel (*Pleurogrammus monopterygius*) in Alaska waters. Fish. Bull. 105:19–29.

Medveditsyna, A. V.
1962. Data on the Atka mackerel (*Pleurogrammus monopterygius* (Pallas)). *In* Greenlings: taxonomy, biology, interoceanic transplantation (T. S. Rass, ed.), p.104–106. Tr. Inst. Okeanol., Akad. Nauk. SSSR 59:101–103. In Russian (translated by Isr. Program. Sci. Trans., 1970). [Available from Natl. Tech. Inf. Serv., Springfield,VA, as TT 69-55097 S.]

Murie, O. J.
1959. Fauna of the Aleutian Islands and Alaska Pen-

insula. U.S. Fish Wildl. Serv., North American Fauna 61:395–406

Napp, J. M., A. W. Kendall Jr., and J. D. Schumacher.
2000. A synthesis of biological and physical processes affecting the feeding environment of larval walleye pollock (*Theragra chalcogramma*) in the eastern Bering Sea. Fish. Oceanogr. 9:147–162

Nichol, D. G., and D. A. Somerton.
2002. Diurnal vertical migration of the Atka mackerel *Pleurogrammus monopterygius* as shown by archival tags. Mar. Ecol. Prog. Ser. 239:193–207.

Ohshima, K. I., Y. Fukamachi, T. Mutoh, and M. Wakatsuchi.
2005. A generation mechanism for mesoscale eddies in the Kuril Basin of the Okhotsk Sea: baroclinic instability caused by enhanced tidal mixing. J. Oceanogr. 61:247–260.

Ojaveer, E., and M. Kalejs.
2005. The impact of climate change on the adaptation of marine fish in the Baltic Sea. ICES J. Mar. Sci. 62:1492–1500.

Östlund-Nilsson, S.
2000. Are nest characters of importance when choosing a male in the fifteen-spined stickleback (*Spinachia spinachia*)? Behav. Ecol. Sociobiol. 48(3):229–235.

Pruett-Jones, S.
1992. Independent versus nonindependent mate choice: do females copy each other? Am. Nat. 140:1000–1009.

Riley, J. D.
1974. The distribution and mortality of sole eggs (*Solea solea* L.) in inshore areas. *In* The early life history of fish (J. H. S. Blaxter, ed.) p. 39–52. Springer, Heidelberg, Germany.

Rodionov, S. N., J. E. Overland, and N. A. Bond.
2005. Spatial and temporal variability of the Aleutian climate. Fish. Oceanogr, 14 (suppl.) 1:3–21.

Rohwer, S.
1978. Parent cannibalism of offspring and egg raiding as a courtship strategy. Am. Nat. 112:429–440.

Rutenberg, E. P.
1962. Survey of the fishes family Hexagrammidae. *In* Greenlings: taxonomy, biology, interoceanic transplantation (T. S. Rass, ed.), p.1–103. Tr. Inst. Okeanol., Akad. Nauk. SSSR 59:3-100. In Russian (translated by Isr. Program. Sci. Trans., 1970). [Available from Natl. Tech. Inf. Serv., Springfield,VA, as TT 69-55097 S.]

Sargent, R. C.
1982. Territory quality, male quality, courtship intrusion and female nest-choice in the three-spined stickleback, *Gasterosteous aculeatus*. Anim. Behav. 30:364–374.

Sikkel, P. C.
1988. Factors influencing spawning site choice by female garibaldi, *Hypsypops rubicundus* (Pisces: Pomacentridae). Copeia 1988:710–718.

Sinclair E. H., and T. K. Zeppelin.
2002. Seasonal and spatial differences in diet in the western stock of Steller sea lions (*Eumetopias jubatus*). J. Mamm. 83:973–990.

Steinhart, G. B., M. E. Sandreneb, S. Weavera, R. A. Steina, and E. A. Marschalla.
2005. Increased parental care cost for nest-guarding fish in a lake with hyperabundant nest predators. Behav. Ecol. 2005 16(2):427–434.

Wieland, K., A. Jarre-Teichmann, and K. Horbowa.
2000. Changes in the timing of spawning Baltic cod: possible causes and implications for recruitment. ICES J. Mar. Sci. 57:452–464.

Withler R. E., J. R. King, and J. B. Marliave.
2004. Polygamous mating and high levels of genetic variation in lingcod (*Ophiodon elongatus*) of the Strait of Georgia, British Columbia. Environ. Biol. Fishes (69):345–357.

Yang, M-S.
1999. The trophic role of Atka mackerel, *Pleurogrammus monopterygius*, in the Aleutian Islands area. Fish. Bull. 97(4):1047–1057.

Zar, J. H.
1999. Biostatistical analysis, 4th ed., 663 p. Prentice-Hall, Inc., Englewood Cliffs, NJ.

Zenger, H. H., Jr.
2004. Data report: 2002 Aleutian Islands bottom trawl survey. U.S. Dep. Commer., NOAA Tech. Memo. NMFS-AFSC-143, 247 p.

Zolotov, O. G.
1993. Notes on the reproductive biology of *Pleurogrammus monopterygius* in Kamchatkan waters. J. Ichthyol. 4:25–37.

Description of embryonic development of Atka mackerel (*Pleurogrammus monopterygius*)

Robert R. Lauth (contact author)

Deborah M. Blood

Email address for R.R. Lauth: Bob.Lauth@noaa.gov

National Oceanic and Atmospheric Administration
National Marine Fisheries Service
Alaska Fisheries Science Center
Resource Assessment and Conservation Engineering Division
7600 Sand Point Way NE
Seattle, Washington 98115

Atka mackerel (*Pleurogrammus monopterygius*) is a hexagrammid fish that inhabits the temperate and subarctic North Pacific Ocean and neighboring seas (Fig. 1). This highly abundant fish is a critically important prey species (Sinclair and Zeppelin, 2002; Zenger, 2004) that supports a directed commercial trawl fishery (Lowe et al., 2006). Atka mackerel is a demersal spawner and males provide parental care to eggs (Zolotov, 1993). During breeding periods, sexually mature males aggregate on the bottom at nesting sites where they establish territories (Lauth et al., in press). Sexually mature females periodically visit male nesting territories from July to October to spawn batches of demersal egg masses (McDermott and Lowe, 1997; McDermott et al., 2007). Individual nests may consist of multiple egg masses deposited by different females, and males defend nesting territories for a protracted period lasting from the time territories are being established until all eggs within the territory are completely hatched (Lauth et al., 2007). Knowledge about the timing of the reproductive cycle and the use of spawning habitat are important for understanding population structure and the dynamics of stock recruitment, which in turn are important factors in the management of Atka mackerel populations.

The male brooding phase of the reproductive cycle has not been a focus of studies despite its critical importance in the propagation and survival of Atka mackerel. The incubation period from fertilization to hatching is a good proxy for determining the time that nest-guarding males stay at nesting sites once spawning has ended. There is one published study describing embryonic development of Atka mackerel at 11°C (Gorbunova, 1962); however the results are incomplete and provide only a partial description of embryonic development. An accurate and complete timetable of embryonic development is essential for determining how temperature affects the incubation period and the timing of the reproductive cycle in the North Pacific Ocean (Lauth et al., 2007). The objective of this study was to determine the incubation period of Atka mackerel embryos by using a controlled water temperature, and to construct a complete embryonic development series, from fertilization to first hatching, with particular reference to morphological features and pigmentation for categorizing preserved egg specimens.

Materials and methods

Eggs used to construct the embryonic development series were obtained by scuba divers from a nearshore Atka mackerel nesting site at Seguam Island in the Aleutian archipelago (Fig. 1) on 7 August 2002. The *in situ* egg mass was deposited and fertilized on a nest at an unknown time between two scuba dives at 1115 and 1720 Alaska Daylight Time (ADT). For the purpose of this experiment, the time of egg fertilization was assumed to be 6 hours before egg mass collection. The bottom water temperature at the time of the collection dive was 4.1°C

The egg mass was brought to the surface, separated into two halves, and each half was placed in a four-liter glass jar with seawater and an air stone. The jars with incubating egg masses were secured in a refrigerator set at 6.0°C and water temperature was monitored with a Tidbit Datalogger (Onset Computers, Bourne, MA) that recorded temperature once every minute. On 16 August 2004, eggs were transported inside thermoses and coolers with ice by air to the Alaska Fisheries Science Center (AFSC) in Seattle, WA. Upon arrival, the egg masses were placed in two 38-L aquaria housed in a temperature-controlled room maintained at 6.0°C. Each aquarium was equipped with air pumps, air stones, and a water circulation pump and water flow directed at the eggs. Seawater for the aquaria was pumped from Puget Sound, WA, run through 1-μm filters, sterilized with ultraviolet light, and stored in 200-L plastic barrels. The seawater in the barrels was adjusted to 32–33 ppt by using aquarium salt, and the barrels were kept inside the temperature-controlled room at the AFSC to maintain the same water temperature as that of the aquaria. Half the water volume in the aquaria was changed on a daily basis and incandescent lights were set on automatic timers to simulate daylight from 0600 to 1800 Pacific Daylight Time (PDT). Five to ten eggs were sampled every 1–3 days from 16 August to hatching and preserved in phosphate-buffered 5% formalin solution. Chorions were removed from eggs to facilitate examination of development with a stereo dissecting microscope. Descriptions of obvious morphological features or pigmentation were recorded for each

Manuscript submitted 31 May 2007
to the Scientific Editor's Office.

Manuscript approved for publication
29 July 2007 by the Scientific Editor.

Fish. Bull. 105:571–576 (2007).

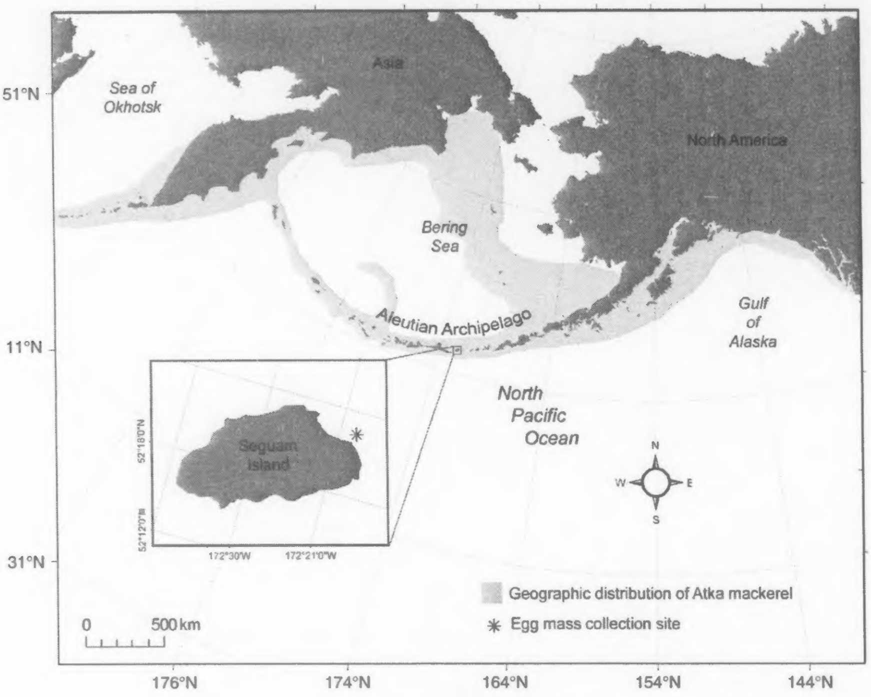

Figure 1

Map showing the geographic distribution of Atka mackerel (*Pleurogrammus monopterygius*; light gray shading) in the North Pacific Ocean and adjoining seas. Also shown is the location (✱) near Seguam Island where a newly fertilized Atka mackerel egg mass was obtained for an incubation experiment.

preserved embryo and the observations from the entire progression were used to construct a chronological series describing embryonic development at 6.0°C.

Results

The newly fertilized eggs were collected from a nest containing several separate egg masses. The eggs were light green and were relatively soft and loosely clumped, in contrast to their character in the following days when they became more firm, rubbery, and tightly attached to one another. As the eggs aged, their color turned reddish brown. The original egg mass had approximately 1500 eggs that ranged in diameter from 2.5 to 2.8 mm. The average daily water temperature during the incubation ranged from 5.42° to 6.57°C and the mean and standard deviation were 6.2° and ±0.3°C, respectively. Incubated eggs began hatching on day 74 and preserved length of yolksac larvae was 9.4–10.9 mm SL.

Embryonic development

The description of embryonic development was divided into two sections: the first section is a description of the development of morphological features, and the second is a description of the development of pigmentation. For brevity, each paragraph in the pigmentation section describes one or more pigment type from the time they first appear until they are fully developed. Table 1 provides descriptive summaries for the progression of both morphological features and pigmentation.

Morphological features

Preserved eggs from the day of collection (fertilization) had a single blastomere sitting on a yolk containing a group of >50 oil globules varying in size (0.08–0.20 mm). After 72 hours of meroblastic cleavage, a blastodermal cap formed on top of the yolk. Over the next four days, the blastodermal cap flattened and increased in diameter as the edge began folding under (gastrulation) to form a germ ring that started moving downward over the yolk (epiboly; Table 1). The embryonic shield formed as the germ ring advanced over the yolk. The blastopore closed on day 15 when the germ ring completely enveloped the yolk. During days 17–21, the optic capsule and eye lenses formed, the head and anterior body became thick and more defined, and the notochord, myomeres, and Kupffer's vesicle became visible (Table 1).

Table 1

Description of embryonic development by day for Atka mackerel (*Pleurogrammus monopterygius*) eggs incubated at 6.2°C.

Day	Description
0	Single blastomere; yolk contains group of >50 oil globules; meroblastic clevage begins
1	4 blastomeres
2	32 blastomeres
3	64–28 blastomeres
4	Blastodermal cap; individual cells indistinguishable and begin to flatten
7	Gastrulation, epiboly, and formation of embryonic shield begin
9	25% epiboly
11	50% epiboly
12	75% epiboly
15	Blastopore closed
17	Optic vesicles begin to form
18	Myomeres visible on anterior body behind nape
19	Kupffer's vesicle visible; optic vesicles formed; myomeres visible on central 60% of body
21	Posterior 50% of body thick and raised from surface of yolk; eye lenses are formed
22	Midbrain enlarges to form bump; tail region lifts away from yolk
23	Midbrain differentiates and forms a bump behind eyes
24	Embryo arches over 50% of the yolk
25	Tail curves away from longitudinal axis
26–27	Otic capsules formed
28	Dorsal finfold on posterior 1/3 of body extends anteriorly to 60% BL
29	Dorsal finfold extends anteriorly to nape; embryo 75% of the way around yolk
31	Pigmentation first appears in eye and along dorsal midline, posterior dorsolateral nape, and dorsal gut
35	Pectoral fin buds formed
36	Head pigment on snout, midbrain and nape; embryo tail touches snout
40	Nares visible; embryo tail extends past anterior edge of eye
41	Nares formed
42	Lower jaw beginning to form
48	Embryo tail extends past posterior edge of head
51	Postanal ventral midline pigment appears
55	Nape enlarges to form hump
58	Opercular pigment; lower jaw fully formed
62	Internal notochord pigment visible
64	Embryo tail length is 1.75× circumference of yolk
65	External lateral pigment visible
71	Pigmentation indistinguishable between embyros and hatched larvae
74	First hatching

One week after blastopore closure (day 22), the tail region began lifting away from the yolk, and within two days, the length of the embryo was 50% of the circumference of the yolk. As the tail grew longer, it curved further away from its longitudinal axis, causing the embryo to curl around the top quarter of the yolk rather than at the equator. The tail was 75% of its way around the yolk by day 29 and touched the snout by day 36. Lengthening further, the tail extended past the anterior edge of the eye (day 40) and past the posterior edge of the head (day 48); the maximum length was reached on day 64 when it was 1.75 times the circumference of the yolk.

Pigmentation

Embryo pigmentation first appeared on day 31. Sparse melanophores appeared in the eye surrounding the lens and along the dorsal midline, nape, and gut (Table 1; Fig. 2). The eye became completely pigmented and much darker by day 38. The beginning of the dorsal midline series was observed as scattered melanophores in the area between 20% body length (BL) and 50% BL. By day 44 the dorsal midline series extended as a double row anterior to the nape and posterior to 50% BL where it joined to form a single row of irregularly spaced melanophores that continued to 70% BL. On day 49, the single row of dorsal midline pigment extended to 5–6 myomeres anterior to the caudal peduncle. At hatching, the dorsal midline series was a double row of continuous pigment extending from the nape to three myomeres anterior of the caudal peduncle (Fig. 3). Dorsal gut pigment first appeared halfway along the gut where the pigment progressively spread posteriorly toward the anus, and then anteriorly toward the head. On day 42, the dorsal gut pigment extended the full length of the gut, excluding the anus. During subsequent development, a few melanophores migrated ventrally onto the lateral gut wall and others moved close to the newly developed pectoral fin buds. By the last week of development (day 71), there was heavy dorsal gut pigment, moderate pigment on the lateral gut, and no pigment on the ventral gut or anus (Fig. 3).

The head remained unpigmented until day 36 when melanophores appeared on the snout, forebrain, midbrain, and nape (Fig. 2). Initially, head pigment was scattered lightly across the dorsal surface except where it outlined the posterior edge of both lobes of the nape. The nape pigment converged toward the double row of melanophores extending anteriorly from the dorsal midline series. During days 37–61, the dorsal midbrain and nape pigment increased, leaving an unpigmented area along the midline (Fig. 2) and several melanophores also became visible on the opercle between the eye and pectoral-fin base. By day 61, opercular pigment concentrated into one dark spot and a second smaller spot appeared on the opercle below the right lower quadrant of the eye (Fig. 3). Head pigmentation was complete by day 64; stellate melanophores coalesced on the midbrain and nape and heavy pigment covered the nape and midbrain except for an unpigmented midline through the midbrain and anterior half of the nape. Internal pigment was also visible at the base of the midbrain near the nape and external pigment increased slightly on the forebrain and disappeared on the snout (Fig. 2).

Postanal ventral melanophores (pvm) became visible late during the embryonic development (day 51) along the ventral midline at 80% BL. By day 65, the pvm series extended anteriorly to 50% BL. At time of hatching, the completed series consisted of a light irregular line of melanophores at 50% BL, larger and more closely spaced melanophores at 60–80% BL, and ended 1–2 myomeres anterior to the terminus of the dorsal midline series (Fig. 3).

The internal and external lateral pigment series were the last two pigments to appear. On day 62, internal

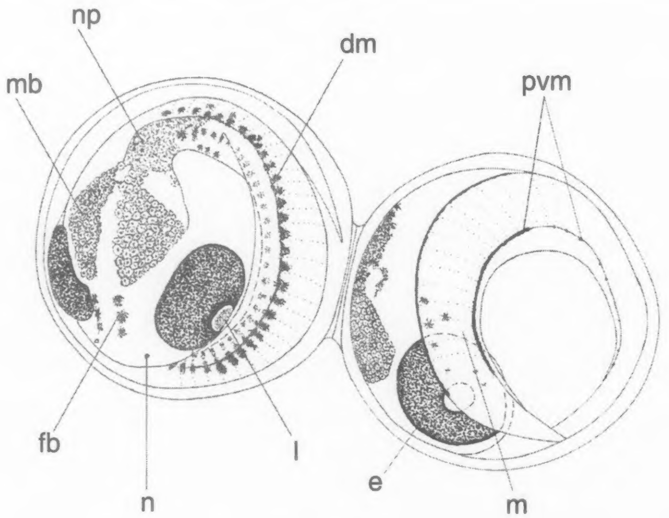

Figure 2

Drawing of two Atka mackerel (*Pleurogrammus monopterygius*) embryos with egg diameters of 2.5–2.8 mm after 11 weeks of development at 6.15°C (areas of pigment: fb = forebrain, mb = midbrain, np = nape, dm = dorsal midline, and pvm = postanal ventral melanophores; morphological features: n = nares, l = lens, e = eye, and m = myomere).

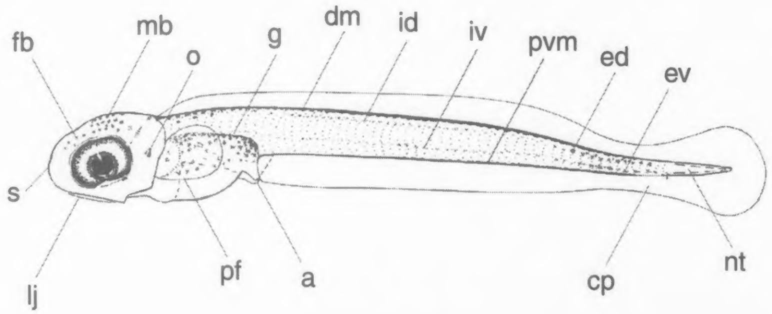

Figure 3

Drawing of a 10.9 mm Atka mackerel (*Pleurogrammus monopterygius*) larva one day after hatching (areas of pigment: fb = forebrain, mb = midbrain, o = opercular, g = gut, dm = dorsal midline, id = internal dorsal, iv = internal ventrolateral, pvm = postanal ventral melanophores, ed = external dorsolateral, and ev = external ventrolateral; morphological features: s = snout, lj = lower jaw, pf = pectoral fin, a = anus, cp = caudal peduncle, and nt = notochord).

pigment was observed above and below the notochord, posterior to the anus, and extending toward the tail; the ventrolateral series began 2–5 myomeres posterior to the start of the dorsolateral series. On day 65, the external lateral pigment appeared on the posterior 20% of the body above and below the notochord and on the ventrolateral caudal body. From day 71 to 74, there were no appreciable differences between hatched and unhatched embryos (Fig. 3). The internal dorsolateral series began just anterior to the anus and was spaced regularly with about one melanophore per myomere until termination at a point even with the dorsal midline series. The internal ventrolateral series began 10–12 myomeres posterior to the anus with similar spacing until 80% BL, where it became irregular until terminating three myomeres before the end of the pvm (postanal ventral melanophore) series. The external dorsolateral and ventrolateral pigment covered the posterior 25% of the body; dorsolateral pigment ended even with the dorsal midline series and the ventrolateral series extended halfway onto the caudal peduncle. Some larvae had one melanophore on the caudal peduncle midway between the last myomere and notochord tip.

Discussion and conclusions

This study provides a complete description of embryonic development that details the progression of morphological features and pigmentation in Atka mackerel embryos from fertilization to first hatching. Daily egg development did not deviate from known fish embryology, and the incubation period was 74 days at an average daily water temperature of 6.2°C. The formerly published incubation period of 40–45 days at an average water temperature of 11°C was based on a 19-day rearing experiment supplemented with data from *in situ* egg samples collected from nesting sites (Gorbunova, 1962). Additional imprecision may have been introduced by unregulated and widely varying water temperatures used during the incubation experiment (8–15°C; Gorbunova, 1962). Comparing our study with that of Gorbunova (1962), we found that incubation time was inversely related to temperature, which is commonly known to be true for fishes (Hempel, 1979).

A review of the scientific literature on near-bottom water temperatures at North Pacific Ocean nesting sites shows that temperatures are generally within several degrees of the incubation temperature used in our study (6.2°C). At western North Pacific Ocean nesting sites, water temperatures ranged from 2.5° to 8.2°C in 1958 (Gorbunova, 1962), and from 4.84° to 8.30°C in 1985 and 1992 (Zolotov, 1993). Similarly, across the central and eastern North Pacific Ocean, the mean and standard deviation of water temperature at 106 nesting sites was 5.4°±1.2°C and was as low as 3.9°C (Lauth et al., in press). It is apparent from our study that the use of nesting substrate by males increases substantially with the longer incubation periods caused by lower water temperatures. In such cases where males are guarding multiple egg masses at varying developmental stages, the brooding phase will be more protracted than that where there is only a single egg mass.

Additional controlled rearing experiments at a wider range of water temperatures are needed to determine more accurately how the rate of embryonic development, and hence male brooding period, is affected. The complete embryonic development series from this study and an empirically derived incubation rate can be used for modeling the relative spawning and hatching dates of egg masses collected from different nesting sites (Lauth et al., 2007). Such an incubation model would be useful for investigating the variability in timing of the reproductive cycle across the broad longitudinal range of Atka mackerel, which is important for conserving and managing Atka mackerel populations and nesting habitat.

Acknowledgments

This project was funded by a grant from the National Marine Fisheries Service (NMFS) Essential Fish Habitat (EFH) fund. This work would not have been possible without the help of S. Porter and A. Dougherty who taught R. Lauth incubation techniques and let him use their wet lab. B. Vinter drew the illustrations of the Atka mackerel egg and larva. R. Lauth thanks S. Branstitter and the crew from the FV *Sea Storm* for field support of this research. Many thanks to those who helped with field support, scuba diving, or reviewing this manuscript: B. Dixon, G. Duker, J. Lee, L. Logerwell, S. Lowe, S. McDermott, R. Nelson, C. Rilling, D. Somerton, G. Stauffer, J. Watson, and two anonymous reviewers.

Literature cited

Gorbunova, N. N.
1962. Spawning and development of greenlings (family Hexagrammidae). *In* Greenlings: taxonomy, biology, interoceanic transplantation (T. S. Rass, ed.), p.121–185. Tr. Inst. Okeanol., Akad. Nauk. SSSR 59:118–182. In Russian (translated by Isr. Program. Sci. Trans., 1970). [Available from Natl. Tech. Inf. Serv., Springfield, VA, as TT 69-55097 S.]

Hempel, G.
1979. Early life history of marine fish: the egg stage, 70 p. Washington Sea Grant, Seattle, WA.

Lauth, R. R., J. Guthridge, D. Nichol, S. W. McEntire, and N. Hillgruber.
2007. Timing of mating and brooding periods of Atka mackerel (*Pleurogrammus monopterygius*) in the North Pacific Ocean. Fish. Bull. 105:**560–571**.

Lauth, R. R., S. W. McEntire, and H. H. Zenger.
In press. Geographic distribution, depth range, and description of Atka mackerel (*Pleurogrammus monopterygius*) nesting habitat in Alaska. Alaska Fish. Res. Bull.

Lowe, S., J. Ianelli, M. Wilkins, K. Aydin, R. Lauth, and I. Spies.
2006. Stock assessment of Aleutian Islands Atka

mackerel. *In* Stock assessment and fishery evaluation report for the groundfish resources of the Bering Sea/Aleutian Islands regions, p. 949–1016. North Pacific Fishery Management Council, Anchorage, AK.

McDermott, S. F., and S. A. Lowe.
1997. The reproductive cycle of Atka mackerel, *Pleurogrammus monopterygius*, in Alaska waters. Fish. Bull. 95:321–333.

McDermott, S. F., K. Pearson, and D. Gunderson.
2007. Batch spawning, atresia, and fecundity of Atka mackerel (*Pleurogrammus monopterygius*) in Alaska waters. Fish. Bull. 105:19–29.

Sinclair E. H., and T. K. Zeppelin.
2002. Seasonal and spatial differences in diet in the western stock of Steller sea lions (*Eumetopias jubatus*). J. Mamm. 83:973–990.

Zenger, H. H., Jr.
2004. Data report: 2002 Aleutian Islands bottom trawl survey. U.S. Dep. Commer., NOAA Tech. Memo. NMFS-AFSC-143, 247 p.

Zolotov, O. G.
1993. Notes on the reproductive biology of *Pleurogrammus monopterygius* in Kamchatkan waters. J. Ichthyol. 4:25–37.

Using the empirical Bayes method to estimate and evaluate bycatch rates of seabirds from individual fishing vessels

Daniel K. Kimura

E-mail address: dan.kimura@noaa.gov

Alaska Fisheries Science Center
National Marine Fisheries Service
National Oceanic and Atmospheric Administration
7600 Sand Point Way NE
Seattle, Washington 98115-6349

Minimizing bycatch of seabirds is a major goal of the U.S. National Marine Fisheries Service. In Alaska waters, the bycatch (i.e., inadvertent catches) of seabirds has been an incidental result of demersal groundfish longline fishery operations. Notably, the endangered short-tailed albatross (*Phoebastria albatrus*) has been taken in this groundfish fishery. Bycatch rates of seabirds from individual vessels may be of particular interest because vessels with high bycatch rates may not be functioning effectively with seabird avoidance gears, and there may be a need for suggestions on how to use these avoidance gears more effectively. Therefore, bycatch estimates are usually made on an individual vessel basis and then summed to obtain the total estimate for the entire fleet.

The empirical Bayes (EB) (Efron and Morris, 1975; Casella, 1985) method offers the possibility of improving within-vessel bycatch estimates, with the assumption that the individual vessel bycatch rate of seabirds has a gamma prior distribution. With the resulting Poisson-gamma EB model, it is assumed that each vessel's bycatch of seabirds has a Poisson distribution conditioned on the realized "true" bycatch rate. The basic principle of the EB method comes from the realization that the parameters for the gamma distribution can be estimated from individual vessel bycatches, and that the resulting EB estimators of individual vessel bycatch rates should provide estimates of individual bycatch rates that have smaller total mean squared error (*TMSE*) than the individual vessel bycatch rates estimated independently. The independently estimated individual vessel bycatch rate is simply the bycatch per thousand hooks fished for each vessel. A more complete introduction to the empirical Bayes method as it has been applied to different types of problems is provided by Ver Hoef (1996).

The goal of this note is to clearly describe empirical Bayes estimation and provide a detailed example of its application to the problem of estimating seabird bycatch. It is to be hoped that a better understanding of the theory underlying empirical Bayes methods will lead to more applications in the area of fisheries management.

Materials and methods

General theory

Mathematically, the empirical Bayes (EB) method can be described as a statistical procedure that has clearly defined steps (Carlin and Louis, 2000). Let the prior distribution of a parameter θ (the parameter of greatest interest) be $g(\theta \mid \eta)$, where the η are unknown parameters, and the sampling distribution for each stratum observation y is $f(y \mid \theta)$. From the joint distribution defined by $h(y,\theta \mid \eta)=f(y \mid \theta)g(\theta \mid \eta)$, the marginal distribution of the observed y can be derived by integrating out θ: $m(y \mid \eta)=\int h(y,\theta \mid \eta)d\theta$. The empirical Bayes method arises from the recognition that η can be estimated from $m(y \mid \eta)$ by using the marginal maximum likelihood (MML) estimators or related methods. Once $\hat{\eta}$ is estimated, the posterior distribution of θ can be obtained by using the Bayes rule, $p(\theta \mid y,\hat{\eta})=f(y \mid \theta)g(\theta \mid \hat{\eta})/m(y \mid \hat{\eta})$, and an EB estimate of θ can be made from this posterior distribution.

The Poisson-gamma empirical Bayes model

The Poisson-gamma model is ideal for illustrating how to calculate EB estimators from the general theory because the all the required integrals result in a gamma function. For this model, denote the gamma prior for the seabird bycatch rate of vessel i as $g(\lambda_i \mid \alpha,\beta)$, and the Poisson sampling distribution as $f(y_i \mid \lambda_i,\tau_i)$, where y_i is the number of seabirds observed, and τ_i are the number of hooks observed. The joint distribution of y_i and λ_i is then

$$h(y_i,\lambda_i \mid \alpha,\beta,\tau_i)=\frac{\exp(-\lambda_i\tau_i)(\lambda_i\tau_i)^{y_i}}{y_i!}\times \frac{\lambda_i^{\alpha-1}\exp(-\lambda_i/\beta)}{\Gamma(\alpha)\beta^{\alpha}}$$

$$\text{for } \alpha,\beta,\lambda_i>0, y_i\geq 0.$$

The marginal distribution is calculated by integrating out λ_i:

$$m(y_i \mid \alpha,\beta,\tau_i)= \frac{\tau_i^{y_i}}{y_i!\Gamma(\alpha)\beta^{\alpha}}\frac{\Gamma(y_i+\alpha)}{(\tau_i+1/\beta)^{y_i+\alpha}}.$$

Manuscript submitted 2 April 2007 to the Scientific Editor's Office.

Manuscript approved for publication 16 May 2007 by the Scientific Editor.

Fish. Bull. 105:577–581 (2007).

The probability for all vessels (i.e., strata) can then be written as

$$P[X_1 = y_1,\dots,X_n = y_n \mid \tau_1,\dots,\tau_n] = \prod_{i=1}^{n} \frac{\tau_i^{y_i}}{y_i!\Gamma(\alpha)\beta^{\alpha}} \frac{\Gamma(y_i+\alpha)}{(\tau_i+1/\beta)^{y_i+\alpha}}.$$

The parameters of the gamma prior, $g(\lambda_i \mid \alpha, \beta)$, can then be estimated by maximizing the marginal likelihood given above and arriving at MML estimates $(\hat{\alpha},\hat{\beta})$. Initial estimates for the gamma distribution can be provided by moment estimators (Carlin and Louis, 2000) where: $r_i=m_i/\tau_i$, and $\bar{r}$ and s_r^2 and the sample mean and variance of the$\{r_i\}$, and

$$\hat{\alpha}_0 = \bar{r}^2/(s_r^2 - \bar{r}\sum_{i=1}^{n}(1/\tau_i)/n) \text{ and } \hat{\beta}_0 = \bar{r}/\hat{\alpha}.$$

The gamma prior is the conjugate distribution (Patrick, 1972; Carlin and Louis, 2000) for the Poisson sampling distribution, which means that the posterior distribution is in the same family as the prior distribution for each stratum. The posterior distribution is $p(\lambda_i \mid y_i, \hat{\alpha}, \hat{\beta}, \tau_i)= f(y_i, \lambda_i \mid \hat{\alpha},\hat{\beta},\tau_i)/g(y_i \mid \hat{\alpha},\hat{\beta},\tau_i)$, which can be verified to have the gamma distribution $g(\lambda_i \mid \alpha'=y_i+\alpha,\beta'=1/(\tau_i+1/\beta))$. The mean of this posterior distribution, providing estimators for the λ_i, can be calculated from

$$\begin{aligned}\tilde{\lambda}_i &= E(\lambda_i)\\ &= \int_0^{\infty} \lambda_i p(\lambda_i \mid y_i,\hat{\alpha},\hat{\beta},\tau_i)d\lambda_i\\ &= (y_i+\hat{\alpha})/(\tau_i+1/\hat{\beta})\end{aligned}$$

or more simply can be recognized as the product of the parameters of the posterior distribution.

The conventional maximum likelihood (ML) estimator of λ_i for the Poisson strata is $\hat{\lambda}_i=y_i/\tau_i$. The EB estimator of λ_i based on the mean of the posterior distribution can be seen as the weighted average of the ML stratum estimator and the mean of the gamma prior $\hat{\alpha}\hat{\beta}$ and will lie between these two values.

Simulation methods

Simulation was performed on the Poisson-gamma EB model described above. Each replication simulated the seabird bycatch of 50 vessels, and was repeated 1000 times. Each replication assumed that the "true" bycatch rate for each vessel (λ_i) was distributed as an observation from the gamma distribution $g(\lambda_i \mid \alpha=0.603, \beta=0.030)$; whose parameters were estimated in the EB analysis which follows. The number of hooks that were "observed," in thousands, was distributed uniformly as $U(0, \tau_{\max})$, with $\tau_{\max} = \{200, 500, 1000, 2000, 5000\}$. For each of these simulations then, $\tau_{\text{ave}} = \{100, 250, 500, 1000, 2500\}$. Finally, the number of "observed" seabirds (y_i) was simulated using the Poisson distribution with $\lambda_i'=\lambda_i\tau_i$, where λ_i and τ_i were previously randomly generated as described.

For each replication, the simulated (y_i, τ_i) were analyzed by using the empirical Bayes method, by first estimating $(\hat{\alpha},\hat{\beta})$ using the MML, and then using these parameters to calculate the EB estimate $\hat{\lambda}_i=(y_i+\hat{\alpha})/(\tau_i+1/\hat{\beta})$. The ML estimator for each stratum was $\hat{\lambda}_i=y_i/\tau_i$, and the global unstratified (GU) estimator was $\lambda=\Sigma y_i/\Sigma\tau_i$. The performance of these estimators was measured by using

$$TMSE = \sum_{i=1}^{50}(X_i-\lambda_i)^2/50,$$

where X_i could be any of $\hat{\lambda}_i$, $\tilde{\lambda}_i$, or $\hat{\lambda}$. The simulation was repeated 1000 times, and the *TMSE* values were averaged to measure the overall performance of these estimators.

Analysis of bycatch data

In 2002, The North Pacific Longline Association, which has many longline vessel operators as members, voluntarily followed proposed regulations that required the use of effective seabird avoidance gear during fishing operations. These voluntary guidelines were implemented into formal regulations in February 2004.

EB analysis was performed on the bycatch of seabirds from individual longline vessels fishing in the eastern Bering Sea. The data were the annual observed bycatches of seabirds (y_i) and the total number of observed hooks in thousands (τ_i) of individual fishing vessels for 2002 and 2003. The 2002 data were used to fit the EB model, and resulting λ_i estimates were used to predict the λ_i for 2003. As a comparison, a similar analysis was performed on data collected from 1997 and 1998, a time when many vessels did not use bird-avoidance gear and when the bycatch rate of seabirds was much higher than in 2002 and 2003.

Results

Simulation results

All simulations consisted of 1000 replications as described above. When measured by *TMSE*, the EB estimator was clearly superior to both the maximum likelihood (ML) and global unstratified (GU) estimators (Table 1). This was true regardless of whatever value of $\tau_{\max}$ was used in the simulations. The ratio $R=TMSE(\hat{\lambda}_i)/TMSE(\tilde{\lambda}_i)$ increased as $\tau_{\max}$ increased, but the values of *TMSE* for GU remained constant. Note that the $(\hat{\alpha},\hat{\beta})$ appeared biased when $\tau_{\max} = 5000$ (Table 1).

Table 1

Simulation results from the Poisson-gamma empirical Bayes (EB) model with the assumption of 50 vessels (strata), and with random sample sizes (observed number of 1000 hooks) distributed as $U(0, \tau_{max})$ and replicated 1000 times. The gamma distribution prior was assumed to have parameters α=0.603, β=0.030 , as were estimated from the seabird bycatch analysis, and the average $\hat{\alpha}$ and $\hat{\beta}$ were calculated from the 1000 replications. The seabird bycatch rate for vessel i, λ_i, was estimated by the maximum likelihood (ML) estimator $\hat{\lambda}_i$, the empirical Bayes (EB) estimator $\tilde{\lambda}_i$, and the global unstratified (GU) estimator $\hat{\lambda}$. Performance of these estimators was measured by the total mean squared error (*TMSE*) averaged over the 1000 replications, and R was defined as the ratio of *TMSE* values calculated for ML and EB estimates.

Sample size τ_{max}	$TMSE(\hat{\lambda}_i)$ ML	$TMSE(\tilde{\lambda}_i)$ EB	$TMSE(\hat{\lambda}_i)$ GU	$R=\frac{TMSE(\hat{\lambda}_i)}{TMSE(\tilde{\lambda}_i)}$	Average $\hat{\alpha}$	Average $\hat{\beta}$
200	0.001390	0.000189	0.000542	7.4	0.712	0.029
500	0.001440	0.000103	0.000531	14.0	0.655	0.029
1000	0.001000	0.000063	0.000541	15.9	0.638	0.030
2000	0.000935	0.000038	0.000532	24.6	0.621	0.031
5000	0.000906	0.000018	0.000537	50.3	0.473	0.041

Results from fitting the Poisson-gamma model

The bycatch per thousand hooks in 1997–98, when bird avoidance gear was not as common, was 0.085 birds, compared with 0.013 birds in 2002–03 when seabird avoidance gear was voluntarily employed. Thus, the bycatch rate for all seabirds was reduced in 2002–03 to 15% of the 1997–98 value.

For the 2002 bycatch data, initial parameter estimates for the gamma distribution were made with the moment estimators described earlier. These initial estimates were refined by using the maximum of the marginal likelihood also described earlier. The final MML estimates were $\hat{\alpha}$=0.603 and $\hat{\beta}$=0.030.

For 2002, the resulting EB bycatch rate estimates per vessel, $\tilde{\lambda}_i$ (Table 2), differed little from conventional ML estimates per vessel. A similar result occurred in the 1997–98 analysis. However, vessel 28 (Table 2), showed a large adjustment between the ML and EB estimates. It is apparent from Table 2 that this vessel had unusually low effort (τ_{28}=34) and a relatively large seabird bycatch (y_{28}=8). This adjustment towards the aggregate mean is a predictable EB adjustment for situations where individual stratum data are weak. For vessel 28, the predicted EB estimate of seabird bycatch rate per thousand hooks was 4.4, whereas the actual observed bycatch rate was 8 (Table 2).

When the 2002 seabird bycatch rates were used to predict the 2003 seabird bycatch rates for individual vessels, neither the ML or EB estimates provided a significant correlation (ρ=0.036, n=38). In contrast, when the 1997 bycatch rates were used to predict the 1998 bycatch rates, there was a significant correlation for the one-tailed test ρ=0.324, n=33, P=0.033).

Discussion and conclusion

Empirical Bayes estimators are superior to Bayes estimators in the sense that prior distributions can be estimated rather than assumed. If one prefers the Bayes method, one would counter that noninformative priors make the assumption of priors relatively benign, whereas for the empirical Bayes model, the assumption of the family of priors may be quite critical.

The empirical Bayes method can be applied even when the marginal distribution is analytically intractable, by substituting numerical integration for analytical integrals. However, the computational intensity required by using numerical integration can appear daunting even with the current speed of desktop computers (Laslett et al., 2002).

Nevertheless, if the prior family is properly selected, the empirical Bayes method can provide very precise estimates. For our Poisson-gamma simulation, the empirical Bayes method provided uniformly superior estimates of the Poisson λ_i for a wide range of τ_{max} values. Although the ratio values in Table 1 indicate that the EB estimator is most useful when τ_{max} is large, the greatest benefit of the EB method is probably on the opposite end of the scale when individual stratum sampling is relatively weak. Note that the bias in $(\hat{\alpha},\hat{\beta})$ when τ_{max} = 5000 (Table 1) may be simply bias in marginal maximum likelihood estimates because maximum likelihood estimators are not generally unbiased. Another possibility is that bias was caused by computational error in calculating the marginal likelihood when the τ_i's were large, even though the marginal likelihood was calculated on the log-scale.

In the seabird bycatch analysis, results show that in almost all cases estimates of bycatch rates at the individual vessel level were not significantly affected by using the EB method. These results may indicate that individual vessel sampling levels (i.e., τ_i) are at a sufficiently high level that ML estimates are already precise estimates of seabird bycatch rates. For the prediction of the 2003 bycatch rate of seabirds from the 2002 analysis, the *TMSE* of the ML estimator of λ_i was reduced a minor amount from 0.0007904 to 0.0007339 by using the EB estimator of λ_i. However, the important issue is that neither the ML nor EB estimates for 2002 significantly correlated with the observed 2003 bycatch rates of seabirds. From the point of view of the EB method, this lack of correlation indicates that the Poisson catch rate, λ_i, was not a characteristic of individual fishing vessels, but is largely due to chance in any one year. Vessels 28 and 36 did not fish in 2003 and were excluded in the comparison. More detailed studies with current data should be carried out to determine if this is a valid conclusion.

As in 2002, the EB estimates for 1997 did not improve on stratum ML estimates for estimating seabird bycatch rates per vessel. However, ML and EB estimates of individual vessel bycatch rates in 1997 were found to be significantly positively correlated with observed bycatch rates for 1998. In this era of high bycatch rates of seabirds, bycatch rates were found to be more dependent on the practices of individual vessels.

Table 2

Bycatch of seabirds from the 2002 longline groundfish fishery in the eastern Bering Sea, where τ_i refers to the number of hooks observed, y_i is the observed number of birds caught, $\hat{\lambda}_i$ is the maximum likelihood (ML) estimate of the seabird bycatch rate, $\tilde{\lambda}_i$ is the empirical Bayes (EB) estimate of the seabird bycatch rate, and $\tilde{\lambda}_i\,\tau_i$ is the EB estimate of the expected observed number of birds caught.

Vessel number	Hooks (1000's) τ_i	Birds caught (numbers) y_i	ML vessel estimate $\hat{\lambda}_i$	EB estimate $\tilde{\lambda}_i$	EB estimate of birds caught $\tilde{\lambda}_i\,\tau_i$
1	1042	11	0.0106	0.0108	11.2
2	3895	22	0.0057	0.0058	22.4
3	917	16	0.0175	0.0175	16.0
4	1487	5	0.0034	0.0037	5.5
5	1272	12	0.0094	0.0097	12.3
6	2446	93	0.0380	0.0378	92.3
7	1477	0	0.0000	0.0004	0.6
8	1016	4	0.0039	0.0044	4.5
9	1758	6	0.0034	0.0037	6.5
10	253	0	0.0000	0.0021	0.5
11	1380	39	0.0283	0.0280	38.7
12	199	0	0.0000	0.0026	0.5
13	233	0	0.0000	0.0023	0.5
14	1212	13	0.0107	0.0109	13.2
15	2304	162	0.0703	0.0696	160.3
16	1408	30	0.0213	0.0212	29.9
17	2292	5	0.0022	0.0024	5.5
18	559	2	0.0036	0.0044	2.5
19	1332	26	0.0195	0.0195	26.0
20	753	17	0.0226	0.0224	16.9
21	2255	37	0.0164	0.0164	37.1
22	699	0	0.0000	0.0008	0.6
23	2907	5	0.0017	0.0019	5.5
24	3308	8	0.0024	0.0026	8.5
25	2221	10	0.0045	0.0047	10.4
26	1797	15	0.0084	0.0085	15.3
27	1413	13	0.0092	0.0094	13.3
28	34	8	0.2334	0.1271	4.4
29	659	101	0.1533	0.1468	96.7
30	1738	16	0.0092	0.0094	16.3
31	1527	4	0.0026	0.0030	4.5
32	2278	49	0.0215	0.0215	48.9
33	1332	19	0.0143	0.0144	19.1
34	2059	17	0.0083	0.0084	17.3
35	3089	2	0.0007	0.0008	2.6
36	1435	7	0.0049	0.0052	7.4
37	625	11	0.0176	0.0176	11.0
38	5447	14	0.0026	0.0027	14.5
39	1598	8	0.0050	0.0053	8.4
40	757	29	0.0383	0.0375	28.4

The empirical Bayes method indicates that sampling levels aboard individual vessels are sufficient to support individual vessel estimates of seabird bycatch rates. This seabird bycatch study was more an observational rather than a controlled study. It was not known which vessels used bird avoidance gear, or how this gear was deployed, or what other relevant onboard practices were taking place. Nevertheless, this seabird bycatch study illustrates how EB methods can provide alternative estimators and evaluation methods for a variety of sampling problems.

Acknowledgments

I thank S. Fitzgerald, J. Breiwick, P. Livingston, and three anonymous reviewers for comments that helped to improve the manuscript.

Literature cited

Carlin, B. P., and T. A. Louis.
2000. Bayes and Empirical Bayes Methods for Data Analysis, 419 p. Chapman and Hall/CRC, New York, NY.
Casella, G.
1985. An introduction to empirical Bayes data analysis. Am. Stat. 39(2):83–87.
Efron, B., and C. Morris.
1975. Data analysis using Stein's estimator and its generalizations. J. Am. Stat. Assoc. 70(350):311–319.
Laslett, G. M., J. P. Eveson, and T. Polacheck.
2002. A flexible maximum likelihood approach for fitting growth curves to tag-recapture data. Can. J. Fish. Aquat. Sci. 59:976–986.
Patrick, E. A.
1972. Fundamentals of pattern recognition, 504 p. Prentice-Hall, Englewood Cliffs, NJ.
Ver Hoef, J. M.
1996. Parametric empirical Bayes methods for ecological applications. Ecol. Appl 6(4):1047–1055.

No evidence of bias from fish behavior in the selectivity of size and sex of the protogynous red porgy (*Pagrus pagrus*, Sparidae) by hook-and-line gear

Douglas A. DeVries

Email address: doug.devries@noaa.gov

National Oceanic and Atmospheric Administration
National Marine Fisheries Service
Southeast Fisheries Science Center
Panama City Laboratory
3500 Delwood Beach Road
Panama City, Florida 32408

Most fisheries select the size of fish to be caught (are size selective), and many factors, including gear, market demands, species distributions, fishery laws, and the behavior of both fishermen and fish, can contribute to that selectivity. Most fishing gear is size-selective and some, such as gill nets, are more so than others. The targeting behavior of fishermen is another key reason commercial and recreational fisheries tend to be size-selective. The more successful fishermen constantly seek areas and methods that yield larger or more profitable sizes of fish. Fishery regulations, especially size limits, produce size-selective harvests. Another factor with the potential to cause selectivity in a hook-and-line fishery is the different behavioral responses of fish to the bait or lure, whether the different responses arise among different fish sizes or between the sexes.

There is reason for concern over the effect of size-selective fishing on protogynous species, i.e., sequential hermaphrodites, which begin life as females and later change sex to males. In one way, size-selective fishing affects gonochoristic (sexes separate) and protogynous species similarly: it not only reduces numbers, but also truncates size distributions. These effects can result in earlier maturation at smaller sizes and hence, at the very least, a reduction in individual fecundity (Jørgensen, 1990). Size-selective fishing can, however, uniquely affect protogynous species in at least two other ways. Because there is essentially a second maturation when sex change occurs, barring some compensatory response, size-selective fishing is sex-selective fishing. As exploitation removes the larger and primarily male members of the population, sperm limitation and decreased fertilization rates can occur. These effects could be caused by a reduction in the number of males or because rapidly skewed sex ratios disrupt the social cues for mating (Bannerot et al., 1987; Huntsman and Schaaf, 1994; Coleman et al., 1996). Naturally low sex ratios can decline precipitously in some heavily fished protogynous species, especially those that form large, temporally and spatially, predictable spawning aggregations (Coleman et al., 1996). The second potential effect of size-selective fishing that is unique to protogynous species is a decrease in population fecundity (Vincent and Sadovy, 1998), which could accompany a compensatory drop in size at sex change, because this drop in size would essentially equate to increased mortality on the largest, most fecund females (Shepard and Idoine, 1993). Such an effect, however, would only occur if at least some females were initially included in the exploited portion of the population.

The documented responses of protogynous species to fishing have varied. Significantly, fewer male daggerhead seabream (*Chrysoblephus cristiceps*) and Roman seabream (*C. laticeps*), both sparids, were found in areas open than in areas closed to fishing—a finding attributed to selective removal of larger size classes (Buxton, 1993). In contrast, the average size and age of male leopard coralgrouper (*Plectropomus leopardus*), a serranid, were not consistently smaller, nor was the sex ratio consistently more female-biased in areas open to fishing than in closed areas (Adams et al., 2000).

Recent significant declines in the modal sizes and proportions of males of gag (*Mycteroperca microlepis*) and scamp (*M. phenax*)—both serranids and protogynous species—in the Gulf of Mexico (GOM) were likely due to size-selective or sex-selective harvesting, or both, that was affected by fish behavior (Coleman et al., 1996). Among gag, the proportion of males fell from 17% during 1977–80 (Hood and Schlieder, 1992) to 1.3–2.7% during 1991–93 (Coleman et al., 1996) in the GOM, and from 19.6% during 1976–82 to 5.5% in 1995 in catches from U.S. Atlantic waters (McGovern et al., 1998). Coleman et al. (1996) cited Gilmore and Jones (1992) for their conclusions about behavior-related selectivity in scamp and personal observations by Gilmore for similar conclusions regarding gag. Gilmore and Jones (1992) speculated that the bias towards large males that they noted in hook-and-line collections of gag and scamp was related to the more aggressive behavior and greater movement of males, and the higher position of males in the water column. Even though these are the only protogynous species in which behavior-related size or sex selectivity has been documented (and only by observations, not experiments), the shift in size and sex ratio in gag has often been cited as an example of how a species with this kind of mating system responds to exploitation (Vincent and Sadovy, 1998).

The objective of the present study was to determine if there was any

Manuscript submitted 9 June 2006
to the Scientific Editor's office.

Manuscript approved for publication
15 July 2007 by the Scientific Editor.

Fish. Bull 105:582–587.

evidence that the behavior-related (as opposed to gear- or fishery-related) size or sex selectivity reported for gag and scamp also occurred in fishery-independent hook-and-line catches of the similarly protogynous, co-occurring red porgy (*Pagrus pagrus*) (Sparidae). In other words, at a given location, were males or larger individuals (more likely to be males in a protogynous species) more aggressive and more likely to bite a baited hook and be caught before females or smaller (more likely to be female) individuals? Such selectivity has never been experimentally demonstrated in any protogynous species.

The red porgy is found in warm temperate to subtropical waters on both sides of the N. Atlantic, including the northern GOM and Mediterranean Sea, and in the S.W. Atlantic from Venezuela to Argentina (Manooch and Hassler, 1978). This sparid is one of the most abundant, potentially exploitable reef fishes in the northeastern GOM but is only lightly fished there, entirely by hook-and-line gear. Red porgy are, however, often taken as bycatch by fishermen targeting other reef species. In contrast, the population(s) of red porgy in the Atlantic waters off the southeastern United States declined so steeply during the 1980s and 1990s (89% drop in spawning stock biomass and a two-orders-of-magnitude drop in recruitment to age 1), presumably because of overexploitation, that a one-year moratorium on their harvest and possession was enacted in 1999 (Vaughan and Prager, 2002).

It is important to establish whether behavior-related size or sex selectivity occurs in hook-and-line catches of red porgy. From a sampling (whether fishery-dependent or fishery-independent) and assessment standpoint, such selectivity could lead to very biased conclusions about population demographics and dynamics, life history traits, and stock status. In addition, the potential for this sort of selectivity to rapidly skew sex ratios, especially if it occurs in conjunction with size-selective harvesting caused by the gear and the targeting behavior of fishermen, could partly explain the apparent crash of the Atlantic population(s) of red porgy off the southeastern United States. Also, given the large number of exploited protogynous species among sparids and many other families, and the need to predict the effects of fishing, it is important to determine whether such behavior-related selectivity characterizes most fishes with this mating system or whether it is restricted to certain serranids. If demonstrated to occur in red porgy, this would be the first experimental evidence of selectivity caused by the behavior of a protogynous species other than a serranid.

Materials and methods

Red porgy were collected with standardized hook-and-line gear during February–November 2000 at seven low-relief (less than 0.5 m) hard (live) bottom sites at 41–67 m depths in the northeastern GOM, off Panama City, FL. The sites were a subset, and the deepest, of nine sites that had been regularly sampled for a larger study of small-scale spatial variation in population traits of red porgy (Fig. 3.1 in DeVries, 2006). Site selection was driven primarily by logistic constraints. Locations with the most consistently high catch rates were chosen to maximize the amount of information collected and to enable among-collection comparisons. Gear consisted of one or two size-1 Mustad j-style hooks (O. Mustad and Son (USA) Inc., Auburn, NY) attached to 5–10 cm droppers on a 27 kg test monofilament leader with a terminal lead sinker of varying (depending on current and wind conditions) weight. Bait consisted of squid and occasionally cut fish. All fishing was undertaken by two to four anglers (with varying levels of experience) during daytime hours and from an anchored boat.

Target sample size each time a site was fished was 25–30 red porgy, although for logistic reasons (primarily variable catch rates) that goal was not always met. For each collection, each fish was tagged with a unique sequential identification number indicating the order in which it was captured, and then placed on ice. The next day fish were measured to the nearest mm total length (TL) and sex was determined macroscopically, after which histological samples were taken from the gonads of any fish identified as female or transitional (DeVries, 2006). Final determination of sex was based on histological findings.

Nonparametric runs tests "above and below the median" and "up and down" (Sokal and Rohlf, 1981a; Zar, 1999) were used to look for evidence of behavior-related size selectivity in individual collections. Critical values for determining acceptance or rejection of the hypothesis that the order was random were obtained from statistical tables (Sokal and Rohlf, 1981b; Zar, 1999). Total length was the variable used in both tests. In general, runs tests are used to determine whether the order of a sequence of observations is random or whether each observation is independent of its predecessor. A run is defined as a sequence of one or more like elements preceded and followed by unlike elements (Sokal and Rohlf, 1981a). In the "above and below the median" test, observations above the median are labeled pluses and those below as minuses. The order of those pluses and minuses is then tested for randomness. If fish caught at the beginning of the collection tended to be larger, as would occur if larger individuals (more likely to be males) were more aggressive and tended to bite the hook before smaller ones (more likely females), there would be fewer runs than expected. The "up and down" test, particularly designed for trend data, examines the sequence of the signs of the difference from the previous value (Sokal and Rohlf, 1981a). Again, if larger fish tended to be caught before the smaller ones, the signs would be mostly negative and therefore there would be fewer changes in sign than if the sequence of lengths was random.

A runs test for dichotomized data (Sokal and Rohlf, 1981a; Zar, 1999) was used to determine if the order in which sexes were captured in a given collection was random. Because it was not known if transitional-stage

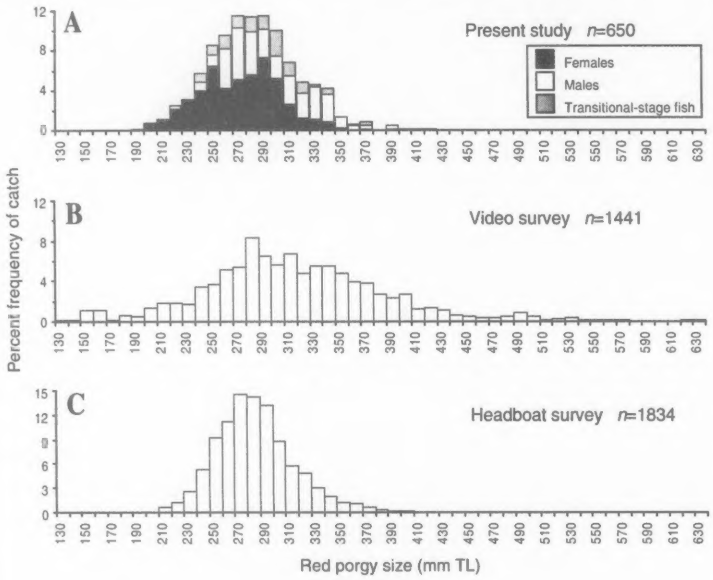

Figure 1

Percent length frequencies (mm total length) of red porgy (*Pagrus pagrus*) (**A**) collected by hook-and-line gear in the present study, (**B**) derived from laser measurements from the National Marine Fisheries Service Gulf of Mexico stationary video reef fish surveys, 1995–2002, and (**C**) in catches of recreational headboats from northwest Florida and Alabama during 1999–2001 sampled by the National Marine Fisheries Service headboat survey.

fish behave more like males or females, this test was run two ways: one in which transitional-stage fish were considered males and another in which they were considered females. Transitional gag and scamp may be as susceptible to behavior-related sex selectivity as fully transformed males if they adopt male behaviors before completing sex change (Coleman et al., 1996). The lyretail anthias (*Pseudanthias squamipinnis*) exhibits such a shift to male behavior before any visible morphological changes (Shapiro, 1979).

Results

A total of 27 collections of red porgy were made, both during and outside the spawning season, which runs November–March but peaks December–February (DeVries, 2006). Sample sizes were >20 in 21 of 27 instances (range: 10–31). Mean sizes and 95% confidence intervals (CI) of males, females, and transitional-stage fish were 296 ±4 mm, 270 ±3 mm, and 291 ±7 mm TL, respectively. The overall size distribution is shown in Figure 1. Mean proportion and 95% CI of males in 19 collections from five of the seven sites was 0.39 ±0.07, assuming transitional-stage fish were males, and 0.24 ±0.05, assuming transitional-stage fish were females. The two remaining sites were persistently and significantly more male-biased than the other sites (DeVries, 2006). Mean proportions of males at the eight collections from the two remaining sites were 0.66 ±0.10 (transitional fish as males) and 0.53 ±0.08 (transitional fish as females). For further details on the temporal and spatial distribution of the collections, see DeVries (2006).

The order in which red porgy were caught in each of 27 collections was random with respect to both size and sex, i.e., there was no evidence that larger fish or males were more likely to be caught before smaller individuals or females (Fig. 2). In both the "above and below the median" and "up and down" runs tests, the hypothesis that the sequence of lengths was random could not be rejected at $\alpha=0.05$ for any of the collections (Table 1.1 in DeVries, 2006). Whether transitional-stage fish were considered males or females, the hypothesis that the order in which sexes were caught was random could not be rejected at $\alpha=0.05$ for all but four of the collections (Table 1.2 in DeVries, 2006). In each of those four collections only one male was caught. The statistical table used for determining critical values (Table 28; Sokal and Rohlf, 1981b) required a minimum sample size of two for both of the dichotomous variables used (number of males and number of females); therefore these four collections could not be tested.

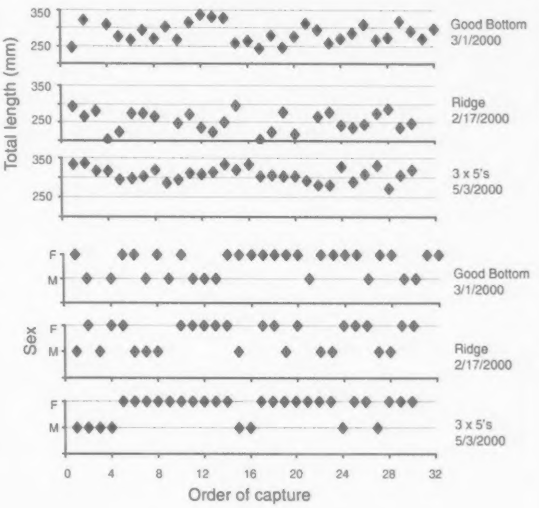

Figure 2

Plots of individual red porgy (*Pagrus pagrus*) size (upper 3 panels) and sex (lower three panels) in the order they were captured for three selected collections. The right hand column indicates the sampling site and date of capture. See Figure 3.1 in DeVries (2006) for site details. Transitional-stage fish were considered males. M = males, F = females.

Discussion

The absence of any evidence of behavior-related size or sex selectivity indicates that hook-and-line sampling can provide reasonably unbiased information on the population biology and stock status of red porgy. As hook size approaches the extremes, vulnerability will decrease and bias will increase, and therefore choice of hook size is critical. There is evidence in some reef fishes that, across at least a moderate range of hook sizes, selectivity can be relatively constant (Ralston, 1982; Dalzell, 1996). Size-1 Mustad j-style hooks were chosen for this study on the basis of considerable experience of the author in catching many species of reef fishes in the study area—experience that indicated that such hooks would readily catch all sizes of red porgy typically observed in both recreational and commercial catches in the GOM. During the study, red grouper (*Epinephelus morio*) that were much larger than the largest red porgy collected and that had considerably larger gapes were caught on the same hooks, as were many tomtates (*Haemulon aurolineatum*) which were similar in size and had similar gapes as the smallest red porgies caught.

A critical assumption of this study was that all sizes of red porgy present at a location when a given sample was collected were equally vulnerable to the gear. If, because of gear selectivity, smaller individuals were considerably less vulnerable than larger ones, and significant numbers of small fish were present at a site being sampled, then it would be possible for behavior-related selectivity for larger fish to occur undetected, or at least its magnitude would be underestimated.

Several lines of evidence indicate that the aforementioned scenario is very unlikely. Size data from the eastern GOM, collected during recent annual National Marine Fisheries Service (NMFS) reef fish surveys with the use of stationary video cameras equipped with laser measuring devices, showed no evidence of noticeably greater proportions of small fish than those seen in the hook-and-line samples of the present study (Fig. 1). Although the size distributions were statistically different (Kolmogorov-Smirnov 2-sample test, $P<0.001$)—not surprising given the very large sample sizes—the primary difference appeared to be that the distribution of red porgy sizes shown in the video data, which should have had little or at least much less bias, was shifted towards larger, not smaller fish. Although a few (3.6%) individuals in the video data were smaller than the smallest (193 mm TL) in the hook-and-line samples, it is important to note that the proportion of large fish (>360 mm) was almost 10-fold greater than in the hook-and-line samples, i.e., 21.6% versus 2.5%. Thus, if anything, the size distribution in the hook-and-line data is biased downwards, not upwards. The higher proportion of larger fish in the video data probably reflects spatial and bathymetric differences in the sampling more than different gear selectivities. The video survey focused on the hard bottom, high-relief habitat along the 73-m (40-fathom) isobath and inshore of that isobath in the Florida Middle Grounds. In contrast, all fish in the present study were caught between 41 and 67 m and on low-relief habitat. Larger red porgy have been found in deeper water and in the Florida Middle Grounds (Harris and McGovern, 1997; Hood and Johnson, 2000).

Red porgy size-structure data from the NMFS recreational headboat survey collected during 1999–2001 in northwest Florida and Alabama almost mirrored the data from this study (Fig. 1). The headboats regularly catch red snapper (*Lutjanus campechanus*) as large as or larger than the largest red porgy taken in this study, and their fishing grounds completely overlap the area, depths, and habitats sampled in the present study. If significant numbers of red porgy larger than those collected in the present study inhabited the area sampled in this study, it seems very unlikely they would not show up in the NMFS survey samples of headboat catches from the same region. Larger red porgy are in fact caught regularly by headboats fishing the Florida Middle Grounds off the central west coast of Florida (Hood and Johnson, 2000).

On many occasions over several years while scuba diving on hard-bottom habitat in the study area in depths from 25 to 30 m, I have observed red porgy of the size that dominated the distribution of those collected in the present study, but virtually none of the size in the left-hand tail (smaller fish) of the distribution from the NMFS video survey (Fig. 1). Similarly, individuals smaller than that typically seen in hook-and-line samples have rarely, if ever, been observed by personnel from the Panama City NMFS Laboratory, either from ROVs or stationary camera arrays at many sites in the N.E. Gulf of Mexico.

Lastly, juvenile red porgy have been found primarily on sandy bottom and typically in shallower waters than those inhabited by adults (Manooch and Hassler, 1978; Labropoulou et al., 1999). These findings, together with the scuba and video observations, support the validity of the assumption that the range of sizes of red porgy in a given collection in this study were the same or at least very similar to those actually present at the site at the time the sample was taken.

If the size structure of the hook-and-line samples in this study accurately reflect the true size distribution at the site at the time of the collection, then the sex ratios of those samples should also accurately reflect true values, and hence the finding of no evidence of sex selectivity is also valid. The absence of behavior-related size or sex selectivity in hook-and-line samples means that any evidence of truncation in size structure or skewing of sex ratios in exploited red porgy populations should not be attributed to greater aggression or "hook attraction" in males. Instead, such size truncation or skewing of sex ratios can be easily explained as the result of simple size-selective harvesting caused by the targeting behavior of fishermen, not by the behavior of the fish, and is a common phenomenon not unique to protogynous fishes.

Although there is historic evidence of such size-selective harvesting in red porgy fisheries off the southeastern United States, there is none indicating that behavior-related selectivity contributed to the crash of those fisheries in the 1980s. From the late 1970s through the mid 1990s, annual mean weights of red porgy in the southeastern United States were roughly 20–30% less in the recreational headboat fishery than in the commercial hook-and-line fishery (Fig. 2 in Vaughan and Prager, 2002). Such size-selective harvesting (taking larger individuals more likely to be male) may have skewed sex ratios temporarily, but there was no evidence of a long-term effect, i.e., an increasingly female-biased sex ratio. Males composed 15.8% 13.3%, and 20.4% of red porgy taken in a fishery-independent survey in U.S. Atlantic waters during 1979–81, 1988–90, and 1991–94, respectively (Harris and McGovern, 1997). The increasingly female-biased sex ratios observed in gag catches in the 1980s and 1990s have been attributed to behavior-related selectivity (Coleman et al., 1996; McGovern et al., 1998). An increasing trend in the proportion of males in smaller size classes off the southeastern United States indicates that red porgy compensated for the effects of fishery-driven selectivity for size by changing sex at smaller sizes (Harris and McGovern, 1997).

The targeting behavior of fishermen has produced selectivity in red porgy fisheries in the GOM, as well. Mean lengths of recreationally and commercially caught red porgy from the Florida Middle Grounds and off west central Florida have differed significantly (321 vs. 350 mm TL) (Hood and Johnson, 2000), in a manner similar to the pattern in weight differences in the Atlantic fisheries noted by Vaughan and Prager (2002). It is unlikely these length differences are related to fish behavior. More likely they reflect gear selectivity as well as spatial differences in areas fished. DeVries (2006) found persistent, significant, small-scale (<10 km) spatial differences in size structure and many other demographics and life history traits of red porgy in the N.E. GOM—differences that indicate that the species has a complex subpopulation or metapopulation structure. Further analysis of data from Hood and Johnson's (2000) study indicated that sex ratios also differed between the two fisheries: males composed 40.5% of the recreational and 49% of the commercial samples, although the sex of 78 of the 274 fish collected from the latter samples was not determined and these 78 fish were not included in the calculations. These differences in sex ratios likely reflect, and are consistent with, the differences in size structure. Additionally, as in the Atlantic, there was no evidence that sex ratios have become increasingly female biased. In 1978 and 1979 males composed 30% and 38%, respectively, of red porgy sampled from charter boat and headboat catches in northwest Florida (Salomon and Fable, 1981). Two decades later Hood and Johnson (2000) found that males composed 40.5% of recreational and 49% of the commercial samples, and in the present study the percentage of males averaged 39% from five of the sites and 66% at the remaining two sites.

Size or sex selectivity resulting from fish behavior does not appear to characterize the hook-and-line fisheries of all exploited protogynous species. Besides the apparent absence, in the case of red porgy, of selection for males with the use of hook-and-line gear, there is also no indication of such selection in the hook-and-line fishery for the red hind (*Epinephelus guttatus*), a serranid (Shapiro et al., 1993; Coleman et al., 1996). It may be that rapid skewing of sex ratios in protogynous fishes caused by behavior-related size or sex selectivity is the exception rather than the rule. The evidence that aggressive behavior in large, primarily male scamp and gag can lead to sex selection in their fisheries and rapidly skew sex ratios (Gilmore and Jones, 1992; Coleman et al., 1996) is primarily circumstantial or observational and there have been no controls or statistical tests. Although the case for behaviorally caused sex selectivity in gag is fairly convincing, more statistically rigorous and direct testing of the hypothesis would strengthen these conclusions. Until more studies, like the present one, are conducted on other species, the prevalence of this phenomenon and whether it is unique to serranids will remain unknown.

Acknowledgments

Thanks to C. Palmer and B. Walling for invaluable help in the field and lab. J. Brusher, J. Mikulas, C. Mangum, D. Harris, and many other coworkers, interns, and volunteers also helped collect and process samples. C. Gledhill provided size data from the National Marine Fisheries Service (NMFS) reef fish video survey. R. Dixon provided data from the NMFS headboat survey. P. Hood provided raw data from his Marine Fisheries Initiative study on red porgy. J. Travis, C. Grimes, C. Koenig, and D. Levitan provided helpful review and comments.

Literature cited

Adams, S., B. D. Mapstone, G. R. Russ, and C. R. Davies.
2000. Geographic variation in the sex ratio, sex specific size, and age structure of *Plectropomus leopardus* (Serranidae) between reefs open and closed to fishing on the Great Barrier Reef. Can. J. Fish. Aquat. Sci. 57:1448–1458.

Bannerot, S. W., W. Fox Jr., and J. E. Powers.
1987. Reproductive strategies and the management of snappers and groupers in the Gulf of Mexico and Caribbean. *In* Tropical snappers and groupers: biology and fisheries management (J. J. Polovina, and S. Ralston, eds.), p. 561–603. Westview Press, Boulder, CO.

Buxton, C. D.
1993. Life-history changes in exploited reef fishes on the east coast of South Africa. Environ. Biol. Fish. 36:47–63.

Coleman, F. C., C. C. Koenig, and L. A. Collins.
1996. Reproductive styles of shallow-water groupers (Pisces: Serranidae) in the eastern Gulf of Mexico and the consequences of fishing spawning aggregations. Environ. Biol. Fish. 47:129–141.

Dalzell, P.
1996. Catch rates, selectivity and yields of reef fishing. *In* Reef fisheries (N. V. C. Polunin, and C. M. Roberts, eds.), p. 161–192. Chapman and Hall, London.

DeVries, D. A.
2006. The life history, reproductive ecology, and demography of the red porgy, *Pagrus pagrus*, in the northeastern Gulf of Mexico. Ph.D. diss, 160 p. Florida State Univ., Tallahassee, FL.

Gilmore, R. G., and R. J. Jones.
1992. Color variation and associated behavior in the epinepheline groupers, *Mycteroperca microlepis* (Goode and Bean) and *M. phenax* Jordan and Swain. Bull. Mar. Sci. 51:83–103.

Harris, P. J., and J. C. McGovern.
1997. Changes in the life history of red porgy, *Pagrus pagrus*, from the southeastern United States, 1972–1994. Fish. Bull. 95:732–747.

Hood, P. B., and A. K. Johnson.
2000. Age, growth, mortality, and reproduction of red porgy, *Pagrus pagrus*, from the eastern Gulf of Mexico. Fish. Bull. 98:723–735.

Hood, P. B., and R. A. Schlieder.
1992. Age, growth, and reproduction of gag *Mycteroperca microlepis*, (Pisces: Serranidae), in the eastern Gulf of Mexico. Bull. Mar. Sci. 51:337–352.

Huntsman, G. R., and W. E. Schaaf.
1994. Simulation of the impact of fishing on reproduction of a protogynous grouper, the graysby. N. Am. J. Fish. Manage. 14:41–52.

Jørgensen, T.
1990. Long-term changes in age at sexual maturity of Northeast Arctic cod (*Gadus morhua* L.). J. Cons. Int. Explor. Mer 46(3):235–248.

Labropoulou, M., A. Machias, and N. Tsimenides.
1999. Habitat selection and diet of juvenile red porgy, *Pagrus pagrus* (Linnaeus, 1758). Fish. Bull. 97:495–507.

Manooch, C. S., and W. W. Hassler.
1978. Synopsis of biological data on the red porgy, *Pagrus pagrus* (Linnaeus). NOAA Tech. Rep. NMFS Circ. 412, 19 p.

McGovern, J. C., D. M. Wyanski, O. Pashuk, C. S. Manooch II, and G. R. Sedberry.
1998. Changes in the sex ratio and size at maturity of gag, *Mycteroperca microlepis*, from the Atlantic coast of the southeastern United States during 1976–1995. Fish. Bull. 96:797–807.

Ralston, S.
1982. Influence of hook size in the Hawaiian deep-sea handline fishery. Can. J. Fish. Aquat. Sci. 39: 1297–1302.

Saloman, C. H., and W. A. Fable Jr.
1981. Length-frequency distributions of recreationally caught reef fishes from Panama City, Florida in 1978 and 1979. NOAA Tech. Memo. NMFS-SEFC-61, 22 p.

Shapiro, D. Y.
1979. Social behavior, group structure, and the control of sex reversal in hermaphroditic fish. Adv. Study Behav. 10:43–102.

Shapiro, D. Y., Y. Sadovy, and M. A. McGehee.
1993. Size, composition, and spatial structure of the annual spawning aggregation of the red hind, *Epinephelus guttatus*, (Pisces: Serranidae). Copeia 1993:399–406.

Shepard, G. R., and J. S. Idoine.
1993. Length-based analyses of yield and spawning biomass per recruit for black sea bass, *Centropristis striata*, a protogynous hermaphrodite. Fish. Bull. 91: 328–337.

Sokal, R. R., and F. J. Rohlf.
1981a. Biometry, 2nd ed., 776 p. W. H. Freeman and Company, New York, NY.
1981b. Statistical tables, 2nd ed., 219 p. W. H. Freeman and Company, New York, NY.

Vaughan, D. S., and M. H. Prager.
2002. Severe decline in abundance of the red porgy (*Pagrus pagrus*) population off the southeastern United States. Fish. Bull. 100:351–375.

Vincent, A., and Y. Sadovy.
1998. Reproductive ecology in the conservation and management of fishes. *In* Behavioral ecology and conservation biology (T. Caro, ed.), p. 209–245. Oxford Univ. Press, New York, NY.

Zar, J. H.
1999. Biostatistical analysis, 4th ed., 663 p. Prentice Hall, Upper Saddle River, NJ.

Acknowledgment of reviewers

The editorial staff of Fishery Bulletin would like to acknowledge the scientists who reviewed articles published in 2006–2007. Their contributions have helped ensure the publication of quality science.

Dr. M. Shiham Adam
Dr. Robyn P. Angliss
Dr. Alexander I. Arkhipkin
Dr. Michael P. Armstrong
Dr. Peter J. Auster

Ms. Julia K. Baum
Dr. Richard J. Beamish
Dr. David A. Bengston
Dr. Paul Bentzen
Dr. Steve A. Berkeley
Dr. Jim Berkson
Dr. Barbara Block
Dr. James A. Bohnsack
Dr. John Boreman
Dr. Brian W. Bowen
Dr. Richard W. Brill
Mr. Michael Burton

Dr. John Calambokidis
Dr. John Caprio
Dr. James Carretta
Dr. Jennifer Caselle
Dr. Michael Castellini
Dr. R. Christopher Chambers
Dr. Edward J. Chesney, Jr.
Dr. Bruce B. Collette
Mr. L. Alan Collins

Dr. Gary E. Davis
Ms. Michelle L. Davis
Dr. Joseph T. DeAlteris
Dr. Edward E. DeMartini
Dr. Douglas DeMaster
Dr. Charles Derby
Mr. Edward J. Dick
Dr. Marlis Douglas
Dr. Miriam J. Doyle
Dr. Edward G. Durbin

Dr. Scott Eckert
Dr. Lisa Eisner
Dr. Karim Erzini

Dr. John Field
Dr. Alan M. Friedlander
Dr. Jean-Marc Fromentin
Dr. Kathryn J. Frost

Dr. Daniel Gaertner
Dr. Lance P. Garrison
Dr. Daniel J. Gaughan
Dr. Stephen R. Goldberg
Dr. Churchill B. Grimes

Dr. Steven L. Haeseker
Dr. Dana Haggarty
Dr. Richard G. Hartnoll
Dr. Euan Sinclair Harvey
Dr. James T. Harvey
Dr. Dan Hennen
Dr. Alexander Hesp
Dr. John Hess
Dr. Joseph E. Hightower
Dr. Nicola Hillgruber
Dr. Michael H. Hoff
Dr. Kim N. Holland
Dr. Simon Hoyle
Dr. Michelle Huepel
Dr. John R. Hunter

Dr. Kym Jacobson
Ms. Pamela C. Jensen
Dr. Donna L. Johnson
Dr. Francis Juanes

Dr. Constantina Karlou-Riga
Dr. Arthur W. Kendall
Dr. William Kiene
Dr. Michael C. S. Kingsley
Dr. Olav S. Kjesbu
Ms. Chris Kondzela

Dr. Han-Lin Lai
Dr. Craig Landry
Dr. Ralph J. Larson
Dr. Robert J. Latour
Dr. Mark A. Lazzari
Dr. Cheng-Shen Lee
Dr. James B. Lindholm
Dr. Jason S. Link
Dr. Phillip S. Lobel
Dr. Thomas Loughlin
Dr. Susan K. Lowerre-Barbieri
Mr. Chris Lunsford
Dr. Joanne Lyczkowski-Shultz

Dr. Gavin Macaulay
Ms. Beverly J. Macewicz
Dr. Ken MacKenzie
Dr. Jeffrey B. Marliave
Dr. Takashi Matsuishi
Dr. Takayuki Matsumoto
Dr. Tim McClanahan
Dr. Duncan E. McGehee
Dr. Richard D. Methot
Dr. David A. Milton
Dr. Sally A. Mizroch
Dr. William Montevecchi
Dr. Beatriz Morales-Nin
Dr. Cheryl Morgan
Dr. Franz-Josef Mueter
Ms. Kristen Munk
Dr. John A. Musick

Dr. John D. Neilson
Dr. David L. Nieland
Dr. Paul Nitschke

Mr. Ranier Oeberst
Dr. Jeff Olsen

Dr. Debra Palka
Dr. Steve Parker
Dr. Frank A. Parrish
Dr. George R. Parsons
Mr. Grey Pendleton
Dr. Michael Pennington
Dr. Theodore W. Pietsch
Dr. Graham Pilling
Dr. Kenneth H. Pollock
Ms. Jennifer C. Potts

Dr. Terrance J. Quinn II

Dr. Carol Reeb
Dr. Vincent Ridoux
Dr. Christopher N. Rooper
Dr. Garry R. Russ

Dr. Marlowe Sabater
Dr. Fran Saborido-Rey
Dr. Yvonne Sadovy
Dr. Keith M. Sakuma
Dr. Robert Schroeder
Ms. Rebecca Schroepfer
Dr. Carl James Schwarz
Dr. David H. Secor
Mr. Jun Shoji
Dr. Michael F. Sigler
Dr. Michael A. Simpkins
Dr. Elizabeth H. Sinclair
Mr. Joseph W. Smith

Dr. Paul Spencer
Dr. Alan M. Springer
Dr. Kostas I. Stergiou
Dr. Colette St. Mary
Dr. Jan Straley
Dr. Chi-Lu Sun

Dr. David Tallmon
Dr. Clyde Tamaru
Dr. Len Thomas
Dr. Bruce A. Thompson
Dr. Juan Timi
Dr. James Tolan
Dr. Michael Tringali

Dr. Juan Guillermo Vaca-Rodriguez
Dr. Douglas S. Vaughan
Dr. Laurent Vigliola

Dr. Susan L. Waddy
Dr. John R. Waldman
Dr. Robert (Trey) Walker
Dr. Eric Ward
Dr. Robert D. Ward
Dr. Joseph D. Warren
Dr. John C. Whitehead
Dr. Terrie M. Williams
Dr. Peter R. Witthames
Dr. Mark Wuenschel

Dr. Yongshun Xiao

Dr. Orio Yamamura
Dr. Richard E. Young

Ms. Tonya K. Zeppelin

The index and/or tab
been removed an
separately within this

For roll film users, this
current volume year i
of the microfilm. For a
this information is a
microfilm.

For microfiche users,
contents is contained o

able of contents has
and photographed
is volume year.

is information for the
r is at the beginning
r a prior year volume,
s at the end of the

rs, the index and/or
d on a separate fiche.

Fishery Bulletin

Guidelines for authors

Content of manuscripts

Contributions published in *Fishery Bulletin* describe original research in marine fishery science, fishery engineering and economics, as well as the areas of marine environmental and ecological sciences (including modeling). Preference will be given to manuscripts that examine processes and underlying patterns. Descriptive reports, surveys, and observational papers may occasionally be published but should appeal to an audience outside the locale in which the study was conducted. Although all contributions are subject to peer review, responsibility for the contents of papers rests upon the authors and not on the editor or publisher. *Submission of an article implies that the article is original and is not being considered for publication elsewhere.* **Articles** may range from relatively short contributions (10–15 typed, double-spaced pages, tables and figures not included) to extensive contributions (20–30 typed pages). **Notes** are reports of 5 to 10 pages without an abstract and describe methods or results not supported by a large body of data. Manuscripts must be written in English; authors whose native language is not English are strongly advised to have their manuscripts checked by English-speaking colleagues before submission.

Manuscript Preparation

Title page should include authors' full names and mailing addresses and the senior author's telephone, fax number, and e-mail address, and a list of key words to describe the contents of the manuscript. **Abstract** should be limited to 200 words (one-half typed page), state the main scope of the research, and emphasize the author's conclusions and relevant findings. Do not review the methods of the study or list the contents of the paper. Because abstracts are circulated by abstracting agencies, it is important that they represent the research clearly and concisely. **Text** must be typed in 12 point Times New Roman font throughout. A brief introduction should convey the broad significance of the paper; the remainder of the paper should be divided into the following sections: **Materials and methods, Results, Discussion** (or **Conclusions**), and **Acknowledgments**. Headings within each section must be short, reflect a logical sequence, and follow the rules of multiple subdivision (i.e., there can be no subdivision without at least two items). The entire text should be intelligible to interdisciplinary readers; therefore, all acronyms, abbreviations, and technical terms should be written out in full the first time they are mentioned. Include FAO common names for species in the list of keywords and in the introduction. Regional common names may be used throughout the rest of the text if they are different from FAO common names which can be found at http://www.fishbase.org/search.html. Follow the U.S. Government Printing Office Style Manual (1984 ed.) and the CBE Style Manual (6th ed.) for editorial style; for fish nomenclature follow the most current issue of the American Fisheries Society's Common and Scientific Names of Fishes from the United States and Canada. Dates should be written as follows: 11 November 2000. Measurements should be expressed in metric units, e.g., 58 metric tons (t); if other units of measurement are used, please make this fact explicit to the reader. Write out the numbers zero through nine unless they form part of measurement units (e.g., nine fish but 9 mm). Refrain from using the shorthand slash (/), an ambiguous symbol, in the general text

Literature cited comprises published works and those accepted for publication in peer-reviewed literature (in press). Follow the name and year system for citation format in the "Literature cited" section (that is say, citations should be listed alphabetically by the authors' last names, and then by year if there is more than one citation with the same authorship). If there is a sequence of citations in the text, list chronologically: (Smith, 1932; Green, 1947; Smith and Jones, 1985). Abbreviations of serials should conform to abbreviations given in the Serial Sources for the BIOSIS Previews Database. Authors are responsible for the accuracy and completeness of all citations. Literature citation format: Author (last name, followed by first-name initials). Year. Title of report or manuscript. Abbreviated title of the series to which it belongs. Always include number of pages. Cite all software and special equipment or chemical solutions used in the study, not in a footnote but within parentheses in the text (e.g., SAS, vers. 6.03, SAS Inst., Inc., Cary, NC).

Tables and figures—general format

- Zeros should precede all decimal points for values less than one.
- Sample size, *n*, should be italicized.
- Capitalize the first letter of the first word in all labels within figures.
- Do not use overly large font sizes in maps and for units of measurements along axes in figures.
- Do not use bold fonts or bold lines in figures.
- Do not place outline rules around graphs.
- Do not use horizontal lines through graphs to indicate measurement units.
- Use a comma in numbers of five digits or more (e.g. 13,000 but 3000).
- Maps require a North arrow and degrees latitude-longitude (e.g., 170°E).

Tables are often overused in scientific papers; it is seldom necessary or even desirable to present all the data associated with a study. Tables should not be excessive in size and must be cited in numerical order in the text. Headings should be short but ample enough to allow the table to be intelligible on its own. All unusual symbols must be explained in the table legend. Other incidental comments may be footnoted with italic numeral footnote markers. Use asterisks to indicate probability in statistical data. Do not type table legends on a separate page; place them above the table data. *Do not submit tables in photo mode.*

Figures include line illustrations, photographs (or slides), and computer-generated graphs and must be cited in numerical order in the text. Graphics should aid in the comprehension of the text, but they should be limited to presenting patterns rather than raw data. Figures should not exceed one figure for every four pages of text. Figures must be labeled with author's name and number of the figure. Avoid placing labels vertically (except of y axis). Figure legends should explain all symbols and abbreviations and should be double-spaced on a separate page at the end of the manuscript. Please note that we do not print graphs in color.

Failure to follow these guidelines
and failure to correspond with editors
in a timely manner will delay
publication of a manuscript.

Copyright law does not apply to *Fishery Bulletin*, which falls within the public domain. However, if an author reproduces any part of an article from *Fishery Bulletin* in his or her work, reference to source is considered correct form (e.g., Source: Fish. Bull 97:105).

Submission

The Scientific Editorial Office encourages authors to submit their manuscripts as a *single* PDF (preferred) or Word (zipped) document by e-mail to Fishery.Bulletin@noaa.gov. Please use the subject heading, "Fishery Bulletin manuscript submission". *Do not* send encrypted files. For further details on electronic submission, please contact the Scientific Editorial Office directly (see address below). Or you may send your manuscript on a compact disc in one of the above formats along with four printed copies (one original plus three copies [stapled]) to the Scientific Editor, at the address shown below.

Dr. Adam Moles
Scientific Editor, *Fishery Bulletin*
NOAA/NMFS/AFSC
17109 Point Lena Loop Road
Juneau, AK 99801-8626

Once the manuscript has been accepted for publication, you will be asked to submit a final electronic copy of your manuscript. When requested, the text and tables should be submitted in Word or Word Rich Text Format. Figures should be sent as PDF files, Windows metafiles, tiff files, or EPS files. Send a copy of figures in the original software if conversion to any of these formats yields a degraded version.

Questions? If you have questions regarding these guidelines, please contact the Managing Editor, Sharyn Matriotti, at

Sharyn.Matriotti@noaa.gov

Questions regarding manuscripts under review should be addressed to Adam Moles, Scientific Editor, at Adam.Moles@noaa.gov

Superintendent of Documents Publications Order Form

*5178

☐ YES, please send me the following publications:

____ Subscriptions to *Fishery Bulletin*
for $36.00 per year ($50.40 foreign)

The total cost of my order is $ _______ . Prices include regular domestic postage and handling and are subject to change.

(Company or Personal Name) (Please type or print)

(Additional address/attention line)

(Street address)

(City, State, ZIP Code)

(Daytime phone including area code)

(Purchase Order No.)

Charge your order. IT'S EASY!

VISA

MasterCard

Please Choose Method of Payment:

☐ Check Payable to the Superintendent of Documents
☐ GPO Deposit Account ☐☐☐☐☐☐☐–☐
☐ VISA or MasterCard Account
☐☐☐☐☐☐☐☐☐☐☐☐☐☐☐☐☐☐☐☐
☐☐☐☐ (Credit card expiration date)

To fax your orders (202) 512-2250

(Authorizing Signature)

Mail To: Superintendent of Documents
P.O. Box 371954, Pittsburgh, PA 15250-7954

Thank you for your order!

This statement is required by the Act of August 12, 1970, Section 3685, Title 39, U.S. Code, showing ownership, management, and circulation of the *Fishery Bulletin*, publication number 366-370, and was filed on 3 October, 2007. The *Bulletin* is published quarterly (four issues annually) with an annual subscription price of $36.00 (sold by the Superintendent of Documents, U.S. Government Printing Office, Washington, DC 20402). The complete mailing address of the office of publication is NMFS Scientific Publications Office, NOAA, 7600 Sand Point Way NE, Seattle, WA 98115. The complete mailing address of the headquarters of the publishing agency is National Marine Fisheries Service, NOAA, Department of Commerce, 1315 East-West Highway, Silver Spring, MD 20910. The name of the publisher is Willis Hobart and the managing editor is Sharyn Matriotti; their mailing address is: NMFS Scientific Publications Office, 7600 Sand Point Way NE, Seattle, WA 98115. The owner is the U.S. Department of Commerce, 14th St. N.W., Washington, DC 20230; there are no bondholders, mortgages, or other security holders. The purpose, function, and nonprofit status of the organization (agency) and the exempt status for Federal income tax purposes has not changed during the preceding 12 months. The extent and nature of circulation is as follows: total number of copies (A) (average number of copies of each issue during the preceding 12 months) was 1056 and the actual number of copies of the single issue published nearest to the filing dates was 1043. Paid circulation (B) is handled by the U.S. Government Printing Office, Washington, DC 20402, and the total number printed for sales (mail subscriptions and individual sales) was 225 for the average number of copies each issue during the preceding 12 months and 225 the actual number of copies of the single issue published nearest to the filing date (C). Free distribution (D) by mail; samples, complimentary and other free copies (average number of copies each issue during the preceding 12 months) was 791 and the actual number of copies of the single issue published nearest to the filing date was 778. Free distribution outside the mail (E) by carriers or other means was 0 for both average number of copies and actual number of copies. Total free distribution (F) was 0 for both average number of copies and actual number of copies of the single issue published nearest the filing date. The total distribution (G: sum of D and B) (average number of copies each issue during the preceding 12 months) was 1016 and the actual number of copies of the single issue published nearest to the filing date was 1003. There were 40 copies (avg. annual) not distributed (H). The total (I: sum of G and H) is equal to the net press run figures shown in Item A: 1056 and 1043 copies, respectively. I certify that the statements made by me above are correct and complete: (Signed) Willis Hobart, Publisher.

Superintendent of Documents Publications Order Form

*5178

☐ **YES,** please send me the following publications:

____ Subscriptions to *Fishery Bulletin*
for $36.00 per year ($50.40 foreign)

The total cost of my order is $ _______ . Prices include regular domestic postage and handling and are subject to change.

(Company or Personal Name) (Please type or print)

(Additional address/attention line)

(Street address)

(City, State, ZIP Code)

(Daytime phone including area code)

(Purchase Order No.)

Charge your order. IT'S EASY!

VISA

MasterCard

Please Choose Method of Payment:

☐ Check Payable to the Superintendent of Documents

☐ GPO Deposit Account ☐☐☐☐☐☐☐–☐

☐ VISA or MasterCard Account

☐☐☐☐☐☐☐☐☐☐☐☐☐☐☐☐☐☐☐☐

☐☐☐☐ (Credit card expiration date)

To fax your orders (202) 512-2250

(Authorizing Signature)

Thank you for your order!

Mail To: Superintendent of Documents
P.O. Box 371954, Pittsburgh, PA 15250-7954

This statement is required by the Act of August 12, 1970, Section 3685, Title 39, U.S. Code, showing ownership, management, and circulation of the *Fishery Bulletin*, publication number 366-370, and was filed on 3 October, 2007. The *Bulletin* is published quarterly (four issues annually) with an annual subscription price of $36.00 (sold by the Superintendent of Documents, U.S. Government Printing Office, Washington, DC 20402). The complete mailing address of the office of publication is NMFS Scientific Publications Office, NOAA, 7600 Sand Point Way NE, Seattle, WA 98115. The complete mailing address of the headquarters of the publishing agency is National Marine Fisheries Service, NOAA, Department of Commerce, 1315 East-West Highway, Silver Spring, MD 20910. The name of the publisher is Willis Hobart and the managing editor is Sharyn Matriotti; their mailing address is: NMFS Scientific Publications Office, 7600 Sand Point Way NE, Seattle, WA 98115. The owner is the U.S. Department of Commerce, 14th St. N.W., Washington, DC 20230; there are no bondholders, mortgages, or other security holders. The purpose, function, and nonprofit status of the organization (agency) and the exempt status for Federal income tax purposes has not changed during the preceding 12 months. The extent and nature of circulation is as follows: total number of copies (A) (average number of copies of each issue during the preceding 12 months) was 1056 and the actual number of copies of the single issue published nearest to the filing dates was 1043. Paid circulation (B) is handled by the U.S. Government Printing Office, Washington, DC 20402, and the total number printed for sales (mail subscriptions and individual sales) was 225 for the average number of copies each issue during the preceding 12 months and 225 the actual number of copies of the single issue published nearest to the filing date (C). Free distribution (D) by mail; samples, complimentary and other free copies (average number of copies each issue during the preceding 12 months) was 791 and the actual number of copies of the single issue published nearest to the filing date was 778. Free distribution outside the mail (E) by carriers or other means was 0 for both average number of copies and actual number of copies. Total free distribution (F) was 0 for both average number of copies and actual number of copies of the single issue published nearest the filing date. The total distribution (G: sum of D and B) (average number of copies each issue during the preceding 12 months) was 1016 and the actual number of copies of the single issue published nearest to the filing date was 1003. There were 40 copies (avg. annual) not distributed (H). The total (I: sum of G and H) is equal to the net press run figures shown in Item A: 1056 and 1043 copies, respectively. I certify that the statements made by me above are correct and complete: (Signed) Willis Hobart, Publisher.

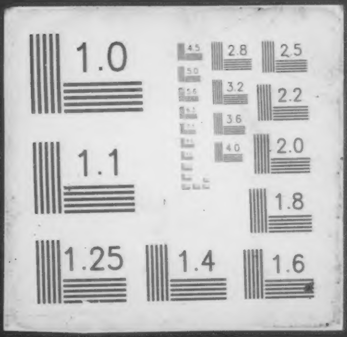
1.0
4.5
2.8
2.5
5.0
3.2
2.2
5.6
3.6
2.0
4.0
1.1
1.8
1.25
1.4
1.6